ACCUMULATION IN FED-BATCH REACTOR WITH MULTIPLE REACTION SCHEME

PAR

Charles Ibrahim GUINAND

EPFL

ÉCOLE POLYTECHNIQUE
FÉDÉRALE DE LAUSANNE

Suisse
2017

To my grandmother...

The ones who are crazy enough to think that they can change the world, are the ones who do.

Steve Jobs, 1955-2011

Acknowledgments

As always, after a long work and great collaborations, there are a million people to thank and only little brain power left to remember all of you. Of course, I will be forever grateful to have experienced and accomplished all that with you, along these last five years. I was lucky enough to be at the right place, at the right moment and with the right people to start such a great adventure. It did not come without any difficulties, but we made it.

First and foremost thank you to my family, especially my grandmother, my mother and father for their support and advises when times were hard. For the funny talks to change my mind but also the excellent dinners we shared (belly talk). There will always be a thought for you all, for pushing me toward a better version of myself and hope that I am making you proud by pursuing my passion as a scientist. I could continue with much more, but our journey is far from finished.

Thank you to all my professors and colleagues at the Haute Ecole d'Ingénierie et d'Architecture de Fribourg (HEAI-Fr), through the years who supported and helped me to achieve such significant research and discoveries. It truly was a crazy race which became possible through a brilliant collaboration between AKTS SA, the EPFL, and the HEIA-Fr. To you, Dr. Michal Dabros, Dr. Ennio Vanoli, Dr. Roger Marti, Dr. Richard Baltensperger and Olivier Naef, thank you for having made it possible as supervisors for the different things I had to manage during this five years trip at the HEIA-Fr.

Special thanks to everyone who has been a part of this team since day one and without your dedicated work I would not have been here. Thank you especially to my thesis Director, Prof. Francis Stoessel and Co-Director, MER Dr. Thierry Meyer, for their pieces of advice, patience and talks along this thesis.

I am very thankful to Prof. Albert Renken, Dr. Jean-Nicolas Aebischer and Prof. Jean-Michel Cabassud for being my jury members, and Prof. Jiri Vanicek, as jury president of this dissertation. I am grateful for their interest and their valuable feedback. The enlightening discussions, useful tips and hints they gave me brought out another

Regarding the lectures I had to teach, I would like to thank Dr. Ulrich Scholten and again Dr. Michal Dabros. It was a pleasure and honour to collaborate during four years to dispense, prepare and organise these courses at the HEIA-Fr and will remain one of my best professional experience.

Thank you to all the ones I did not include at this moment. There have been too many people to mention in one sitting that had an impact on me and my work in this school and I am sorry if I forget some of you.

A lot of good things filled my thesis path, but it has not come without its bumps. I have become an adult while growing as a real scientist and teacher, I have come to know myself better and realised that there is so much I want to accomplish with my life. I have strong interests in different fields, but there is so little time to explore them. I am grateful for all the opportunities, experiences and comforts this work has already given to me, and I will fight to continue this way.

Fribourg, April 2017   Charles Guinand

Abstract

Keywords: Calorimetry, Scale-up, Thermal Safety, Reaction Kinetics, Inherent safety, Reactor Dynamics, Modelling

Nowadays, the fine chemical industry requires increasingly faster time-to-market as well as economically efficient and safe processes. In addition, the growing product variety needs more versatile production plants able to produce from small amounts up to several hundred tons per year. As a consequence, the time devoted to development is limited, and the production often takes place in multipurpose plants. This implies that a given process can run in different reactors making the process development a long and complicated task. As a matter of fact, the behaviour of a reactive system changes with scale and also changes from one equipment to another which often leads to difficulties in controlling a reactor at the industrial scale.

In most cases, chemical incidents are caused by loss of control and wrong assessment of the thermal potential, resulting in runaway reactions or deviations in different units. These incidents could be foreseen and avoided or at least decreased with an appropriate process development and risk assessment. All processes should be optimised to achieve a fair productivity and still remain inherently safe.

Such process characterization aims at providing a better understanding of reaction pathways and thermal behaviour. To reach this goal, save resources and effort, the real system dynamics can be reproduced by models where parameters are estimated from experimental calorimetric data. The dynamic behaviour of the reaction system can be represented by two models: 1) The reaction kinetics, based on an assumption of the reaction scheme considering different reactions occurring along the process course and 2) The reactor dynamics highlighting how the heating/cooling system controls the reaction course by adjusting its temperature and the adopted feed profile strategy.

To acquire enough knowledge on the studied reaction system, several experiments have to be performed in a multiscale based approach to maximize the disturbances and explore the overall reaction kinetics. Nevertheless, even with this method, the

investigation can be very long due to the increasingly complex models, involving a large number of parameters and amount of experiments. Therefore, a new approach to solve these issues has to be developed.

The proposed approach is summarized in three steps:

1. Reaction Kinetic Investigation: Planning and minimize the number of experiments in a statistically optimal way to cover the experimental space efficiently and using a numerical method to extract the reaction kinetics based on the power rate law.

2. Reactor Dynamic Investigation: Planning the experiments in order to obtain information about the dynamic behaviour of the jacket together with its temperature controller and then use a numerical method to extract the parameters representing the reactor.

3. Risk assessment and Optimization: Combine the reaction kinetics and reactor dynamics to shape a Process Implementation model serving to predict the behaviour of the overall system and identify the optimal operating conditions the process inherently safe.

This research establishes a new process scale-up methodology, regarding the assessment of the thermal potential. The results demonstrate that a multiscale approach joined with modelling and inherent safety, lead to a better understanding of the system. This approach also notably helps to optimise the operating conditions making the process inherently safe and remaining economically favourable.

Zusammenfassung

Stichwörter: Kalorimetrie, Massstabvergrösserung, Thermische Sicherheit, Reaktionskinetik, Inhärente Sicherheit, Reaktordynamik, Modellierung

Heutzutage erfordert die Feinchemieindustrie einen schnellen und kurzen "Time-to-Market" als auch wirtschaftliche und sichere Prozesse. Darüber hinaus benötigt die wachsende Produktvielfalt geeignete Produktionsanlagen, die von kleinen Mengen bis zu mehreren hundert Tonnen pro Jahr produzieren können. Folglich ist die Entwicklungszeit sehr begrenzt und die Produktion findet häufig in Mehrzweckanlagen statt. Dies bedeutet, dass ein bestimmter Prozess in verschiedenen Reaktoren durchgeführt werden kann, was die Prozessentwicklung zu einer langen und komplexen Aufgabe macht. In der Tat ändert sich das Verhalten eines reagierenden Systems je nach Maßstab, sowie auch beim Wechsel von einer Anlage zur anderen. Einen Reaktor im industriellen Maßstab zuverlässsig zu steuern, führt daher oft zu Schwierigkeiten.

In den meisten Fällen werden chemische Vorfälle durch den Kontrollverlust und eine falsche Beurteilung des thermischen Potentials verursacht, was zu Durchlaufreaktionen oder Abweichungen in den verschiedenen Einheiten führen kann. Diese Vorfälle hätten vorhergesehen und vermieden werden können, oder zumindest mit einer entsprechenden Prozessentwicklung und Risikobewertung vermindert werden. Aus diesem Grund - um eine wirtschaftliche Produktivität erreichen und eine inhärente Sicherheit gewährleisten zu können - ist eine Optimierung aller Prozesse erforderlich.

Diese Prozesscharakterisierung richtet sich an ein besseres Verständnis der Reaktionswege und des thermischen Verhaltens. Um Ressourcen und Aufwand einzusparen, kann die reale Systemdynamik durch mathematische Modelle reproduziert werden, wobei die Parameter aus experimentellen kalorimetrischen Daten abgeschätzt werden.

Unter Annahme einer homogenen Lösung lässt sich das dynamische Verhalten des Reaktionssystems durch zwei mathematische Modelle, die auf Differentialgleichungen

Abstract (English/German)

basieren und deren Parameter unter Verwendung experimenteller Daten geschätzt werden, darstellen:

1. Das Reaktionskinetik Modell, das auf einem Reaktionsschema basiert, und unter Berücksichtigung unterschiedlicher Reaktionen, die während der Prozessdurchführung eintreten; sowie

2. Das Reaktordynamik Modell, das die Reaktortemperatur aufgrund der Temperatursteuerung durch die Regelung des Heiz-/Kühlsystems beschreibt.

Um das nötige und zusätzliche Wissen über das Reaktionssystem zu erwerben, müssen mehrere Experimente - basierend auf einem Multi-Scale-Ansatz – zur Maximierung der Systemanregungen sowie zur Erforschung der Gesamtreaktionskinetik, durchgeführt werden. Dennoch kann auch mit dieser Methode die Untersuchung aufgrund der zunehmend komplexen Modelle sehr lange dauern, da diese eine große Anzahl von Parametern beinhalten und eine Vielzahl von Experimenten benötigen. Zur Lösung dieser Probleme muss daher eine neue Vorgehensweise entwickelt werden.

Der vorgeschlagene Ansatz kann in drei Hauptschritten zusammengefasst werden:

1. Die Kinetische Untersuchung (eng: RKI= Reaction Kinetic Investigation): Planung der ersten Experimente in einem statistisch-optimalen Weg mithilfe einer numerischen Methode zur Bestimmung der Reaktionskinetik, die auf der Grundlage des Leistungsratengesetzes basiert, um den experimentellen Raum effizient und mit einer minimalen Anzahl von Experimenten abzudecken.

2. Die Untersuchung der Reaktordynamik (eng: RDI= Reactor Dynamic Investigation): Planung der Experimente, um Informationen über das dynamische Verhalten des Mantels zusammen mit dessen Temperaturreglers zu erhalten. Anschliessend ist die Anwendung einer numerischen Methode erforderlich, um die dynamischen Parameter des Reaktors zu bestimmen.

3. Die Risikobewertung (eng: Risk assessment): Kombination aus Reaktionskinetik und Reaktordynamik Modelle zur Gestaltung eines Prozess-Implementierungs-Modells, das dem Zweck dient, das Verhalten des betrachteten Gesamtsystems vorherzusagen und die optimalen Betriebsparameter zu identifizieren. Dabei wird die inhärente Sicherheit unter Beachtung der Sicherheitsbeschränkungen, gewährleistet.

Diese Forschungsarbeit hat zur Ausarbeitung einer neuen Prozess-Scale-up-Route, hinsichtlich der Beurteilung des thermischen Potentials, geführt. Die erworbenen Ergebnisse zeigen, dass ein Multi-Scale-Ansatz in Kombination mit Modellierung und inhärente Sicherheit, zu einem besseren Verständnis des Systems (Reaktionen

zusammen mit dem Reaktor) führen. Diese Vorgehensweise trägt hauptsächlich zur Optimierung der Betriebsbedingungen bei, die dem Prozess erlauben, innerhalb der Sicherheitsgrenzen - auch bei Kühlungsausfall -, zu laufen und wirtschaftlich attraktiv zu bleiben.

Preamble

The work presented in this thesis has been performed in the laboratories of ChemTech at the University of Applied Science in Fribourg (HEIA-Fr) directly supervised by Dr. Michal Dabros, in partnership with the Group of Chemical and Physical Safety from the Swiss Federal Institute of Technology in Lausanne (EPFL), under the supervision of Prof. Francis Stoessel and MER Dr. Thierry Meyer as thesis Director and Co-Director, respectively.

The supervisors Dr. Bertrand Roduit and Christophe Borgeat, from the industrial partner AKTS SA, supported and helped actively the development of methods and algorithms presented in this work.

Part of the work described in this dissertation has been published in peer-review journals or presented at conferences. Texts, figures or drawings have been adapted or reused from published materials (see Appendix B and C).

Contents

List of Symbols

Roman

Symbol	Description	Units
A	Heat exchange area	m^2
A, B	Chemical compounds	
C	Molar concentration	$mol \cdot g^{-1}$
c_p	Specific heat capacity	$J \cdot g^{-1} \cdot K^{-1}$
C^{ste}	Constant	$-$
C_w	Reactor heat capacity	$J \cdot K^{-1}$
D	Derivative time, Data set	$s, -$
d	Diameter, thickness or spacing	$m, -$
E_a	Activation energy	$J \cdot mol^{-1}$
f	Function	$-$
g	Acceleration of gravity	$m^2 \cdot s^{-1}$
H	Hessian	$-$
h	Film heat transfer coefficient	$W \cdot m^{-2} \cdot K^{-1}$
I	Reset time	s^{-1}
J	Jacobian	$-$
K	Proportional gain, proportionality constant	$-, -$
k	Rate constant	function of the rate law
k_0	Pre-exponential number	function of the rate law
M	Molar mass, Molar ratio	$g \cdot mol^{-1}, -$
m	Mass, number of points	$g, -$
$\dot{m}$	Mass flow rate	$g \cdot s^{-1}$
N	Mole, Normal distribution	$mol, -$
n	Revolution frequency, number of candidates	$rpm, -$

Acronyms

DSC	Differential Scanning Calorimetry
DTA	Differential Thermal Analysis
EGA	Evolved Gas Analysis
FBR	Fed-Batch Reactor
FTIR	Fourier Transform Infrared spectroscopy
GC	Gas Chromatography
GLMA	General Law of Mass Action
HPLC	High Performance Liquid Chromatography
LMA	Law of Mass Action
LOOCV	Leave-One-Out Cross-Validation
LPOCV	Leave-p-Out Cross-Validation
MAT	Maximum Allowable Temperature
MTSR	Maximum Temperature of Synthesis Reaction
NMR	Nuclear Magnetic Resonance
o-NCB	ortho- Nitrochlorobenzene
PFR	Plug Flow Reactor
PID	Proportional-Integral-Derivative
QFS	Quick start, Fair conversion and Smooth temperature profile
RC1e	Mettler-Toledo Reaction Calorimeter 1e
RC	Reaction Calorimetry
RDI	Reactor Dynamic Investigation
RKI	Reaction Kinetic Investigation
RMSE	Root Mean Square Error
RPO	Risk assessment and Process Optimisation
SFD	Space Filling Design
SSE	Sum of Squares of Errors
SSR	Sum of Square of Regression
SST	Sum of Square of Deviations
TA	Thermal Analysis
TG	Thermogravimetry
TMR	Time to Maximum Rate

List of Symbols

Greek

Symbol	Description	Units
α	Heat loss coefficient	$W \cdot K^{-1}$
Δ	Difference	$J \cdot mol^{-1}$
ΔH	Enthalpy	$J \cdot g^{-1}$
Δt	Check interval	s
ϵ	Error	$-$
γ	Material constant for heat transfer, minimal spacing	$W \cdot m^{-2} \cdot K^{-1}, -$
$\overline{\gamma}$	Mean distance	$-$
λ	Thermal conductivity	$W \cdot m^{-1} \cdot K^{-1}$
μ	Dynamic viscosity	$Pa \cdot s$
ν	Stoichiometric coefficient	$-$
Φ	Parameter space	$-$
Ψ	Correlation matrix	$-$
ρ	Density, correlation coefficient	$kg \cdot m^{-3}, -$
σ	Standard deviation	$-$
τ	Time constant	s
θ	Vector of parameters	$-$
φ	Heat transfer coefficient of equipment	$W \cdot m^{-2} \cdot K^{-1}$

Superscripts

Symbol	Description
a, b, c	Reactant order
exp	Experimental
sim	Simulation
$*$	Special situation

Subscripts

Symbol	Description
0	Zero, initial

a	Activation, Jacket side of the reactor wall
A, B	Reference to chemical compounds
acc	Accumulation
ad	Adiabatic
amb	Ambient
$batch$	Batch operation
c	Cooling
cf	Cooling failure
$crit$	Critical
$ctrl$	Control
dec	Decomposition
end	End
$event$	Event
ex	Exchange
f	Final
fd	Feed
fed	Fed
$fluid$	Internal fluid
g	Global
h	Heating
i	Component number, counter
in	Inputs
ind	Industrial
j	Reaction number, Jacket, counter
k	Counter
lab	Laboratory
lam	Laminar
lim	Limit
$loss$	Losses
m	Measurement point
max	Maximum
$mean$	Mean
min	Minimum
mix	Mix

List of Symbols

opt	Optimal
out	Outputs
p	Number of experiments, process
$pred$	prediction horizon
r	Reactor, reaction mixture
ref	Reference
reg	Regime
rx	Reaction
$rxtot$	All the reactions
s	Sample
set	Set point
st	Stirrer
sys	System
T	Training
th	Thermal
tot	Total
$trans$	Transitional
tur	Turbulent
V	Validation
w	Wall
x	Replacement variable

Specials

Symbol	Description
arg	Argument
CoM	Coverage Measure
Cov	Covariance
$diag$	Diagonalisation
$Dist$	Distance
$MinDist$	Minimal Euclidean distance
min	Minimization
R^2	Determination coefficient

Dimensionless Groups

Symbol	Description	Equation
Ne	Newton	$Ne = \dfrac{q_{st}}{d_{st}^5 \cdot n^3 \cdot \rho}$
Nu	Nusselt	$Nu = \dfrac{h_r \cdot d_r}{\lambda}$
Pr	Prandtl	$Pr = \dfrac{\mu \cdot c_{p,r}}{\lambda}$
Re	Reynold (stirred tank)	$Re = \dfrac{n \cdot d_s^2 \cdot \rho}{\mu}$
Th	Thermal potential	$Th = \dfrac{T_{cf}(t, t_{pred}) - T_r(t)}{\Delta T_{ad,batch}}$
Th_{crit}	Critical thermal potential	$Th_{crit} = \dfrac{MAT - T_r(t)}{\Delta T_{ad,batch}}$
θ_{Gu}	Normalised thermal potential	$\theta_{Gu} = \dfrac{T_{cf}(t, t_{pred}) - T_r(t)}{MAT - T_r(t)}$

1
Introduction

*Commit your blunders on a small
scale and make your profits on a
large scale.*

Leo H. Baekland - 1863-1944

1.1   Motivation and objectives

The process scale-up is usually defined as the way to design a pilot or industrial reactor to replicate the results obtained at laboratory scale through a standard methodology and conserving the same characteristics, namely the conversion, selectivity and product quality [1–3]. This terminology is somewhat unfortunate since experience has shown that process scale-up is not a straightforward task through process innovation but the result of favorable consecutive decisions, and sometimes of many mistakes [2]. Harmsen presents a complement to the latter definition, being more general and adding a valuable information toward an efficient scale-up: *"Process scale-up is generating knowledge to transfer ideas into successful implementations"* [4]. These words express the desire to acquire enough knowledge leading to an efficient risk assessment with the perspective of a safe and economically viable implementation.

An inaccurate process scale-up may lead to two main issues:

1. A small production capacity or deviation from the required product quality making the process economically unfavorable [4].

2. Erroneous operating conditions triggering secondary reactions resulting in a runaway and ultimately, lead to disastrous consequences [5].

The US Chemical Safety and Hazard Investigation Board (CSB) reported that 167 accidents occurred between 1980 and 2001 in the US were related to chemical reactivity [6, 7]. The root causes of these incidents were also analysed and studied by Verwijs who concluded that a majority of them could have been foreseen and avoided or at least decreased if an appropriate process development and risk assessment had been carried out [8]. In 2013, Kidam and Hurme investigated 394 chemical process accidents. Their analysis demonstrated that reactor equipment failure caused 14% of these accidents of which 71% were related to batch and fed-batch operations. This high percentage is due to the dynamic character of the reactions, variable product quality, materials handling and difficulties designing correct and efficient operating conditions [9–11].

Caygill et al. investigated the different problems occurring during the process scale-up and demonstrated that a clear lack of knowledge regarding thermochemistry for both, desired and undesired reactions was existing [12]. This last fact is one of the main reasons incidents occur. Atherton also reviewed extensively the issues encountered during the process scale-up and highlighted the most important points, as being [13]:

1. *The lack of knowledge:* the physicochemical, thermochemical as well as the reaction kinetics and reactor dynamics are valuable information to perform a correct scale-up. The problem encountered by a poor understanding of

the reaction system may lead to an underestimation of the heat evolution, unanticipated side reactions or unpredicted autocatalysis effects which may cause incidents [11, 12, 14].

2. *The heat transfer:* the decrease in heat transfer area compared to the volume with the increase of scale will lead to two major issues, namely:

   (a) if the heat transfer is limiting the reaction system progress, a significant increase in processing time can be expected or,

   (b) if the reaction is relatively fast and exothermic, the cooling system may be unable to control the progress course efficiently and trigger secondary reactions or gas formation.

3. *The mixing:* it is usually difficult to reproduce the same mixing state at laboratory as at large-scale. Indeed, the mixing time changes radically with the increment in circulation paths in larger reactor sizes [15]. In general and regardless the scale, poor mixing will result in less efficient mass transfer, especially for multiphase systems. It may lead to drastic changes in selectivity but also in the creation of dead zone leading to hotspot formation.

4. *The processing time:* by increasing the scale, several factors may increase, such as material handling, charging procedure (liquids and solids), waiting time for analytics or delays due to human resource availability. Such delays may affect the selectivity or yield but also material stability that may decompose (reactant and products) [11, 13].

These last obstacles have been reported as the leading root causes of many incidents over the past 50 years [12, 13, 16, 17]. Mannan et al. stated that: *"a deeper understanding of the substance behaviour under process conditions, as well as adequate computer-simulation process methods, is the key to reliable prediction of safe operation"* [18]. For a better process scale-up and safety, the current challenges are directed toward the determination of these behaviours in their whole, describing the considered system under many operating conditions.

The other factor to consider is the actual competitive environment due to the increasing product variety combined with the pressure to deliver in short time. This results in a requirement of more versatile production plants, capable of producing from small amounts up to several hundred tons per year. The European chemical industry council predicted by a long-term analysis that this situation is expected to continue for the next decade due to the strong contribution made by the fast and vigorous growth of the emerging regions. This last fact pushes the chemical industries to move toward more innovative and efficient processes and approaches [19–21].

Considering the scale-up of fed-batch reactors, a particular problem encountered is the thermal potential generated by the accumulation of unconverted reactants. Besides quality issues, such accumulation may lead to an uncontrolled temperature increase in case of process control malfunction or if the heat released by the reaction exceeds the heat removal capacity of the reactor for one of the following reasons:

- An undersized cooling system, e.g. due to low heat transfer coefficient or,

- A insufficiently fast cooling dynamics to control the heat released.

Therefore, mastering these aspects is one of the most challenging tasks in the development of safe and viable processes.

The traditional serial approach, focussing firstly on the feasibility regarding quality and yield, then assessing the process safety is disadvantageous in terms of time and cost involved. Therefore, there is a need for an innovative approach [22, 23]: the integrated process development combining quality optimisation with risk assessment and experiment-based modelling at different scales to control the accumulation of unconverted reactants.

1.2   Structure of the work

The key factor of success of a scale-up is the understanding of the physical phenomena governing the chemical processes to bring the different dynamics into real adequacy namely [12, 13]:

1. The chemical reaction dynamics described by the reaction kinetics,

2. The reactor dynamics described by the heat transfer with the cooling system, its control and inertia,

3. The mixing dynamics described by the mass transfer provoked by the stirrer motions.

Milewska and Molga studied the mixing dynamics extensively using Computational Fluid Dynamics. They stated that in the case of a perfectly mixed reactor, spatial non-uniformities of temperature and concentrations of the whole reaction mixture could be neglected. In many cases, this assumption is correct assuming that the mixing time is much shorter than the reaction time ($t_{mix} < t_r$) [24]. On the one hand, the reaction kinetics is mass-independent for a reaction system occurring in a homogeneous solution, and therefore independent of the scale. On the other hand, the reactor dynamics will drastically change with the increase of scale along with the heating/cooling unit and temperature control. This consequence is perfectly

recognizable through the definition of three time constants characterizing the reactor dynamics:

1. The reactor time constant (τ_r) describing the inertia of the exchange between the heat carrier and the reaction mixture,

2. The jacket heating time constant ($\tau_{j,h}$) describing the inertia of the heating system to provide the correct jacket temperature,

3. The jacket cooling time constant ($\tau_{j,c}$) describing the inertia of the cooling system to provide the right jacket temperature.

Therefore, a robust control of these two dynamics may lead to an economic and thermally safe process which results in the following thesis structure.

The combination of modelling and calorimetry is presented along Chapter 2 and afterwards applied to the study of reaction kinetics (Chapter 4) and reactor dynamics (Chapter 5). The resulting models are finally combined together to shape the process implementation model serving in the assessment of the thermal process safety (Chapter 6).

In practice, solving process development issues can be summarized in two fundamental questions:

1. How to design a reactor or use an existing one to be versatile enough and, at the same time, adapted to a particular reaction system?

2. How to find the optimal operating conditions to be inherently safe, focusing on an efficient control of thermal potential while remaining economically viable?

A full approach divided into three steps has been developed to answer these fundamental questions (Figure 1.1):

1. *Reaction Kinetic Investigation* (RKI): initial experiments are planned at different scales (milligram, gram and kilogram) to optimally cover the operating space while remaining at a minimum of tests. A reaction kinetic model is then developed based on a reaction scheme hypothesis where the kinetic parameters are estimated using the acquired data from different measurement techniques and by applying non-linear regression methods (Chapter 4).

2. *Reactor Dynamic Investigation* (RDI): the characterization of the physical and dynamic properties of the full-scale reactor to be used is performed using a strategically chosen set of heating and cooling experiments (Chapter 5) .

3. *Risk assessment and Process Optimisation* (RPO): determining the optimal operating conditions (feed and temperature profiles) by predicting the industrial

reactor behaviour working under constraints (safety and productivity) using the reaction kinetics and reactor dynamics models previously obtained (Chapter 6) .

The full strategy aims to purpose a way to handle the generated thermal potential due to the accumulation of unconverted reactants using experimentation and modelling. It is then applied to real cases as the Morton Inc. incident (Chapter 7) or the esterification of Acetic Anhydride using Methanol. As a conclusion, the general findings of this work are synthesized in Chapter 8 along with an outlook for possible improvements.
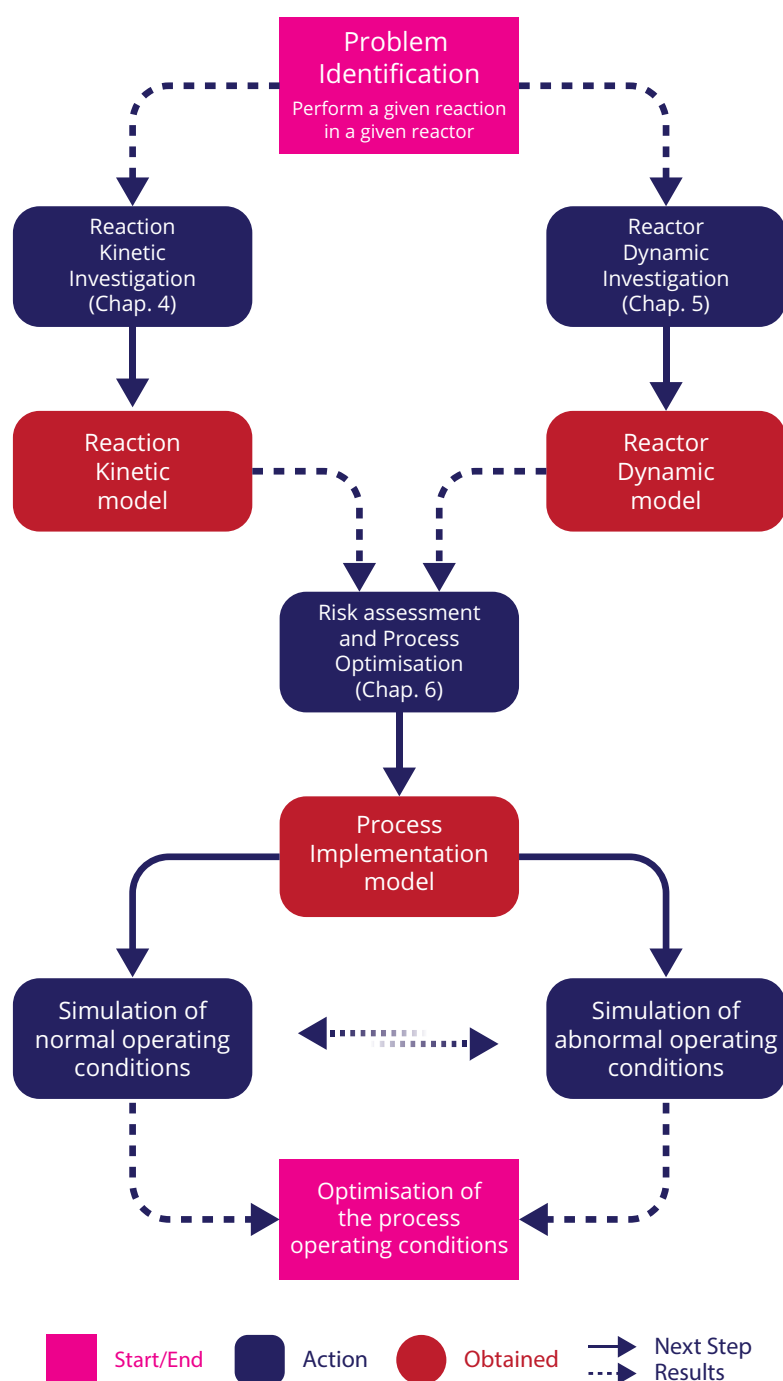
Figure 1.1 – Workflow of the different approaches and the resulting models interconnections: the reaction kinetic and reactor dynamic models are used to shape the process implementation model allowing to describe normal and abnormal operating conditions. The last model can be used to predict and evaluate operating conditions ensuring an inherently safe process.

2

Modelling Concepts & Parameter Estimation

As to methods there may be a million and then some, but principles are few. The man who grasps principles can successfully select his own methods. The man who tries methods, ignoring principles, is sure to have trouble.

Harrington Emerson, 1853-1931

In essence, the job of a chemical engineer is to understand the fundamental principles of physics and chemistry to ultimately cope with them in practical applications. These applications may appear to be very diverse as demonstrated by the following activities:

1. Design of installations or chemical plant operations such as reaction, separation or extraction,

2. Development of new technologies such as fuel cells, micro-reactors or new fuels and,

3. Improvement or maintenance of already existing processes.

The field that gathers all these activities is commonly named "*process development*" and mainly aims at extrapolating a reaction from the laboratory to industrial-scale regarding sustainability, economic, productivity and safety aspects [4, 25, 26]. The current economic environment pushes the chemical industry toward new approaches that bring the researches and developments to three primary advantages: cheaper and/or better and/or faster than the competitors [27]. Ultimately, the process development would result in a combination of only advantages, thus connected by a logical *AND* operator. However, this solution is often very difficult or impossible to achieve. A combination of logical *AND* and *OR* operators is often obtained.

An attractive asset in the recent chemical engineer portfolio is the availability of large and powerful modelling tools which might be of great help to optimise a process considering the previously mentioned objectives, reach the optimal combination of advantages and in the decision-making process for the scale-up. Primarily, the strength of such tools used for the simulation of different process conditions allows a deeper understanding of the process behaviour. Secondly, it gives access to conditions that would be difficult or risky to achieve experimentally, and finally reduces the number of experiments to determine the optimal operating conditions. These factors, if applied correctly, significantly assist in reducing implementation time and costs.

In such a case, a model is a simplified description of the considered system or process, aiming at enhancing our ability to understand, predict or possibly control its behaviour [28, 29]. Fundamentally, they help us to evaluate the outcome of an action in a real situation without actually performing it. In a similar way, in a chemical reactor, conditions leading to a runaway may be explored by numerical simulations. Many studies and authors mentioned the use of models and simulation as essential to the development of a productive and inherently safe process [2, 24, 30–32].

After gaining an overview of the process development, this chapter emphasizes the modelling and simulation techniques, both essential tools, which are presented in detail in the next sections. In order to answer all the unsolved industrial questions and problems involved in this part, the provided modelling techniques have to be applied.

2.1 Model creation

The main difficulty using such tools, is the development of a model that describes the studied system correctly and accurately. Actually, the creation of any model (dynamic or discrete) can be separated into five main steps (Figure 2.1) linked together as an iterative process [29, 33–35]:
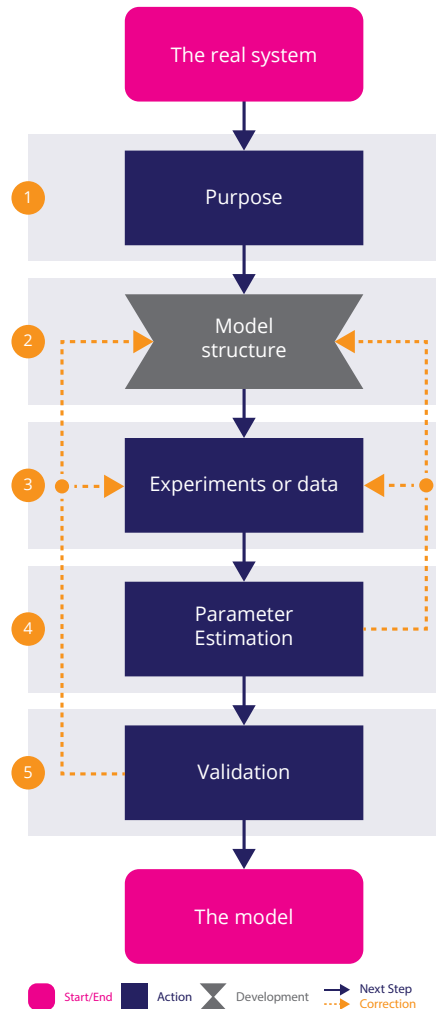
Figure 2.1 – Structure of the model creation process.

1. **The purpose** defines the very reason and necessity of a model. It will establish the bounds and the complexity of the modelling problem which will have a direct impact on all the subsequent steps. With the help of the following questions, it is easier to answer this point:

   (a) What should the model describe?

   (b) What questions should be answered by the model?

(c) What type of behaviour should the model be able to explain?

2. **The model structure** is dedicated to define the underlying equations or relations that describe the behaviour of the considered system. These relationships are generally based on physicochemical laws (first principle models) or stochastic approaches. During the model structure elaboration, the Ockam's razor principle should be applied: *"Among competing hypotheses, the one with the fewest assumptions should be selected"* [36]. The idea behind this quote is that the model structure should be kept as simple as possible and increase in complexity if necessary (after Step 4 or 5). This step allows identifying the output and the parameters requiring an evaluation.

3. **The Design of Experiment** (DoE) is directed toward the acquisition of experimental data or information describing the system behaviour on the studied experimental space. The experiments should be performed randomly as it may result in high costs, time consumption, and unnecessary or already existing information. Therefore, to optimally cover the experimental space, DoE methods are often used to plan them efficiently. The collected experimental data will serve as input for the parameter estimation.

4. **The parameter estimation** is mainly used to fit the model to the experimental data. Therefore, it allows the evaluation of the parameters describing the dynamic behaviour of the studied system. The findings of such estimation can also be used to evaluate the errors and quality of the model and its parameters [37]. If the parameter estimation fails, two possible reasons may emerge:

   (a) The structure of the model is too complicated or wrong;

   (b) The quantity of information available to describe the considered system is insufficient.

   As a result, an iterative process is implemented between, first, the model structure (Step 2) and then the parameter estimation (Step 3). However, if the model structure is not questioned, the number of experiments may have a considerable effect on the parameter estimation. Therefore, an iterative process is also existing between the experiments and parameter estimation.

5. **The validation** is mainly concerned by the verification of the model veracity toward the real system. As a matter of fact, the real studied system is never entirely known resulting in a model that is never a perfect representation but merely an approximation of the real system [29]. Therefore, this step allows evaluating if a model and its fitted parameters can predict the dynamic behaviour of the considered system with a good accuracy (can depend on the purpose of the model expressed in Step 1). Regarding different criteria, an iterative process

is implemented between:

(a) The validation and the model structure: the model may be oversimplified or too complicated which does not allow to describe a behaviour that was not accounted in the model.

(b) The validation and experiments: the number of experiments may be not sufficient to describe the overall system behaviour.

2.2   Model structures

The model creation brought out a number of steps necessary to develop relevant models that go beyond idealized systems. The consideration of experimental data allows to shape the model structure and making possible the description of real behaviour, an aspect primordial for the scale-up of productive and inherently safer processes.

As outlined in the introduction, a chemical process for a homogeneous mixture can be represented through the establishment of two specific dynamics (Figure 2.2):

1. *The reaction kinetics* which describes the reaction and transformation rates occurring in the reaction mixture and,

2. *The reactor behaviour* which describes how the latter controls the reaction course by adjusting the temperature of its cooling system and the adopted feed profile strategy.

The next section will, therefore, focus on the model structures that describe these two dynamics, starting by the reaction kinetics and following by the reactor dynamics.
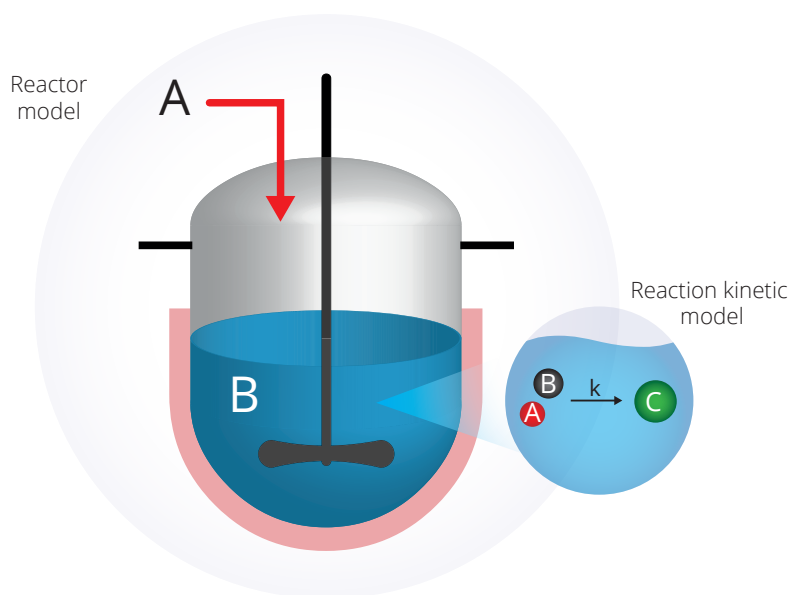
Figure 2.2 – Illustration of the model concepts to simulate a reactive system; The reaction kinetics is implemented into the reactor model to shape an overall model that represents the process.

2.2.1 Reaction kinetics

Most plants in the fine chemical industry contain units where reactions may take place. The goal is generally oriented toward producing with high yield, selectivity (for parallel reaction system), safely and efficiently. Therefore, a clear understanding of chemical interactions and transformations occurring along the process is a key requirement for a successful scale-up [38].

The field that investigates such behaviour is the reaction kinetics. It deals with the study of rates occurring along a process course and aims at answering two fundamental questions:

1. What changes/transformations are expected to occur?

2. How fast and at which temperature will they occur?

Considering these questions and the need to build a model structure that describes the different events occurring in a reaction mixture, the following section will be divided into four parts:

1. A state-of-the-art of the kinetic models available nowadays,

2. How to build a model based on the law of mass action?

3. How to obtain information on the reactive system?

4. How to analyze this information?

2.2.1.1 Reaction kinetic models

The last century observed a large number of developments in the field of reaction kinetics and its applications. It resulted in a large number of different models and demonstrated that a deep understanding of the reaction kinetics is important. Therefore, modelling such aspects involves different levels of knowledge: the micro-kinetics and the macro-kinetics. The micro-kinetics describe each individual pathway the different species of the reaction system will face while the macro-kinetics describe the mass transport phenomena. In many cases, due to complexity and insufficient information, the micro-kinetics is not available and the reaction system is approximated using the macro-kinetics. The latter can be approached based on:

1. Deterministic models: models in which outputs are precisely determined through known mathematical relationships among variables and events. The randomness or variability of the reality is avoided or not accounted [33].

2. Stochastic models: probabilistic models used to describe phenomena that evolve with the time or space in which ranges of values for each variable are used (probability distribution) to predict the randomness of the reality [39].

The next section describes three class of reaction kinetic models that may be useful for the development and scale-up of a safe and productive process.

Law of mass action
is certainly the most famous deterministic model to describe the reaction kinetics (detailed Section 2.2.1.2). It considers the reaction rate as a function of physical phenomena (mainly temperature and pressure) and reactant concentrations (in solution phase) or partial pressure (in gas phase).

$$A + B \rightarrow C \tag{2.1}$$

$$r = k \cdot C_A^a \cdot C_B^b \tag{2.2}$$

$$k = k_0 \cdot exp\left(\frac{-E_a}{RT}\right) \tag{2.3}$$

This model supposes that the activation energy (E_a), the pre-exponential factor (k_0) and the different reactant orders (a, b) are constants along the reaction course. Willson et al. demonstrated that this point may not be always respected. As a matter of fact, the orders may change along the reaction course [40, 41]. This model, however, has the advantage to describe the reaction system accurately when the reaction pathways are known. On contrary, such model requires many experiments to be established.

Isoconversional models

postulates that the activation energy and the pre-exponential factor are a function of the reaction progress X (2.5). The retrieved information are the apparent parameters E_a and k_0 during the reaction course as [42, 43]:

$$A \rightarrow B \tag{2.4}$$

$$\frac{dX}{dt} = k_0(X) \cdot \exp^{-\frac{E_a(X)}{RT}} \cdot f(X) \tag{2.5}$$

A wide variety of reaction models $f(X)$ is applied in solid-state kinetics [44]. They can be reduced to three major types when considering the dependency of the reaction progress on the time: decelerating, autocatalytic and accelerating. Such profiles are immediately recognized for isothermal data as shown in Figure 2.3.

This method does not need the knowledge of the reaction scheme or mechanism which makes the parameter estimation easier. In addition, the reaction progress is relatively simple to calculate from heat flow experiments (q) [44]:

$$X_{th} = \frac{\int_{t_0}^{t} q \, dt}{\int_{t_0}^{t_{end}} q \, dt} \tag{2.6}$$

The use of non-isothermal experiment imposes, in many cases, the reaction to proceed until completion, which can be very convenient. The use of isothermal data remains however valid as soon as different operating temperatures are available (a minimum of three experiments). On the one hand, this model is very useful when the whereabouts of the reaction sequence is not necessary or unknown as only the heat flow can be predicted. On the other hand, it cannot be used to improve the productivity, as the relationship between each reactant stays unknown for a reaction system made of
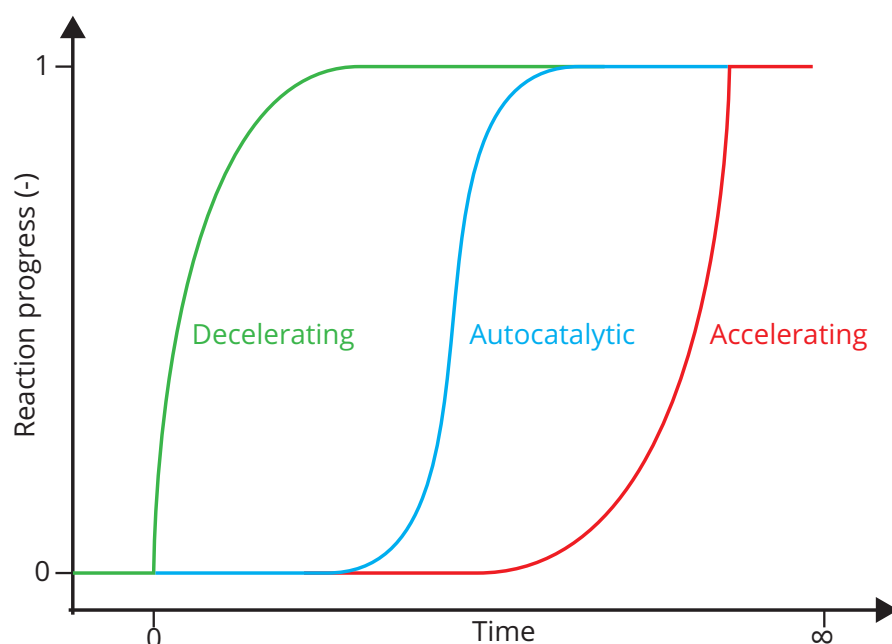
Figure 2.3 – Relationship of the reaction progress X versus time for decelerating, autocatalytic and accelerating isoconversional reaction models under isothermal conditions. Reproduced from [44].

several reaction types (consecutive, parallel, ...).

Many applications demonstrated the power of such model for storage and transportation evaluations [45]. It remains, however, that this kind of model is at the moment solely appropriate to closed systems namely batch systems. Hence, if a semi-closed system like fed-batch is considered (Section 2.2.2), other effects have to be accounted on the kinetics (feed, volume change,...) rending this approach inappropriate.

Stochastic models

A deterministic approach such as the Law of Mass Action (LMA) seems to be quite universal (Section 2.2.1.2). However, due to its entirely phenomenologycal character, it tends to use time-independent parameters. Such approach of the reaction kinetics will progressively lose its efficiency at low concentrations as demonstrated by Mira et al. in his educational examples [46]. The deterministic approach does not consider the randomness of chemical reactions, namely that each individual reaction is an unique event that occurs with a certain probability. Thus, the reaction system possesses a random character and may evolve in several ways [33, 47].

A large number of reactions fulfill the requirements for deterministic modelling.

However, when fluctuations in the reactant densities and presence of randomness are existing, such approach becomes limited [39]. Stochastic models provide a more detailed understanding of the reaction system behaviour, an aspect often necessary for the modelling of biological systems where small concentrations of chemical species or large fluctuations are encountered. Other examples present such characteristics, to only cite the most common: polymerizations, radical chain reaction or isomerization [39, 41, 48].

When comparing these models, it becomes logical that for an effective scale-up, the law of mass action is more appropriate. This model can account all the effects that may occur along the reaction course assuming that the reaction pathways are well-established. This model was chosen for the further developments for its large applicability.

2.2.1.2   Law of mass action

It all started in 1850 when Wilhelmy studied the inversion of sucrose in aqueous solution of acids [49]:

$$H_2O+ \qquad C_{12}H_{22}O_{11} \rightarrow \qquad C_6H_{12}O_6+ \qquad C_6H_{12}O_6 \qquad (2.7)$$
$$water \qquad\qquad sucrose \qquad\qquad glucose \qquad\qquad fructose$$
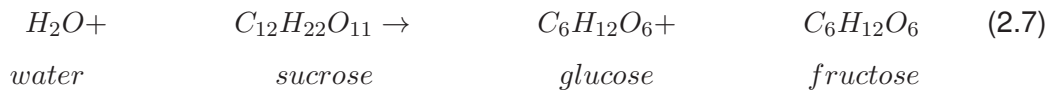
He found empirically that the rate of consumption of sucrose was proportional to the concentration of unconverted sucrose. Therefore, to introduce the *Law of Mass Action (LMA)*, let us assume an irreversible reaction occurring in a homogeneous phase which proceeds according to:

$$|\nu_A|A + |\nu_B|B + ... \rightarrow |\nu_P|P + |\nu_Q|Q + ... \qquad (2.8)$$

Where $A, B, ...$ are the reactants, $P, Q, ...$ the products and ν_i the respective stoichiometric coefficients. A stoichiometric coefficient is positive when a product appearance is observed and negative in the opposite case, namely a reactant disappearance.

In 1867, Guldberg and Waage formulated the exact law of mass action describing the reaction rate as a function of the reactant concentrations, a rate constant and reactant orders equal to their respective stoichiometric coefficients [50].

$$r = k \cdot C_A^{\nu_A} \cdot C_B^{\nu_B} \tag{2.9}$$

As the orders may not be equal to their respective stoichiometric coefficient [40], a *General Law of Mass Action* (GLMA) including the particular case of the exact LMA was considered. It becomes that the reaction rate r of the reaction (2.8), considering the influence of the temperature, composition and generalized reactant orders m is written as:

$$r = k \cdot C_A^{a} \cdot C_B^{b} \tag{2.10}$$

The reaction rate r is defined as the quantity of transformed material (usually in molar form) by unit of time and unit of an extensive variable (volume, mass, surface,...). This term is always positive.

In a generalized way, the reaction rate r of a reaction j involving several reactants is written as:

$$r_j = k_j \cdot \prod_{i=1}^{I} C_i^{a_{i,j}} \tag{2.11}$$

Where C is the concentration, k the rate constant and a the reaction order in respect to reactant i in reaction j.

In 1889, Arrhenius introduced the influence of temperature on a reaction j through the reaction rate constant k as:

$$k_j = k_{j,0} \cdot \exp\left(-\frac{E_{a,j}}{RT_r}\right) \tag{2.12}$$

In case of a complex reaction system, the transformation rate of a component cannot be described by a single stoichiometric equation. As example, a component i (reactants or products) can be involved simultaneously in several reaction j:

$$j = 1 : \qquad |\nu_{A,1}|A + |\nu_{B,1}|B \quad +|\nu_{C,1}|C \xrightarrow{k_1} \quad |\nu_{D,1}|D$$

$$j = 2 : \qquad |\nu_{A,2}|A \qquad +|\nu_{C,2}|C \xrightarrow{k_2} \qquad |\nu_{E,2}|E \qquad\qquad (2.13)$$

$$j = 3 : \qquad |\nu_{A,3}|A + |\nu_{B,3}|B \qquad \xrightarrow{k_3} \qquad\qquad |\nu_{F,3}|F$$
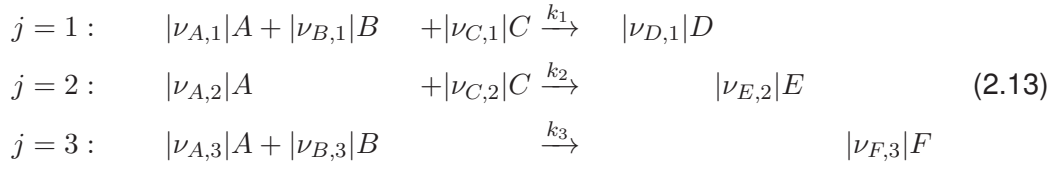
The transformation rate R of a component i considering all the reactions j, where i is involved, is written respectively to its stoechiometric coefficients as:

$$R_i = \sum_{j=1}^{J} \nu_{ij} r_j \qquad\qquad (2.14)$$

The transformation rate is defined as the quantity of transformed material (usually in molar form) by unit of time and by unit of an extensive variable (volume, mass, surface,...). It can be negative (reactant disappearance) or positive (product appearance) as it is proportional to the stoichiometric coefficients.

For example, the transformation rate of A in the reaction system previously presented (equation 2.13) is:

$$R_A = \nu_{A,1} r_1 + \nu_{A,2} r_2 + \nu_{A,3} r_3 \qquad\qquad (2.15)$$

This term is negative due to the consumption of A during the reaction course.

For a reaction taking place in a homogeneous phase without any change in volume and temperature, the concentration can be written as:

$$C_i = \frac{N_i}{V_r} \qquad\qquad (2.16)$$

As soon as there are temperature and volume changes, this expression becomes difficult to evaluate accurately. Therefore, the current concentration C_i is, from now on, expressed per unit of mass as:

$$C_i = \frac{N_i}{m_r} \qquad\qquad (2.17)$$

2.2.1.3   Experimental methods

Where there is a desire to explore reaction kinetics, there is a requirement of data following the reaction rates [40, 50]. The experimental methods to answer this demand are very diverse; the ones measuring the composition along the time on-line (Spectroscopy) or off-line (e.g. GC, HPLC, RMN ,...) or others by measuring a resulting change (e.g. Calorimetry).

Independently of the kind of method used, the experiments should not be performed randomly as mentioned by Coker: *"Reaction rate data obtained from laboratory studies without a proper account of the physical effects can produce erroneous rate expressions"* [51]. In addition, any kinetic analysis quality will be very sensitive to the experimental data quality. The absence of analytical data of the mixture composition, namely the concentration will also lead to considerable difficulties in the investigation of the reaction kinetics due to the analyte concentrations dependency (reactants and/or products) [52].

Despite the large amount of available and well described tools and methods to study the reaction kinetics, as showed by Magde [53], most of them are often based on spectroscopy, which does not allow to measure the thermodynamic of the reaction or at least not directly. Nevertheless, even if this last point is not fulfilled, this kind of tool is component specific which allows to follow the concentration along the time. In addition, very fast reactions can be followed, a point difficult to fulfill with calorimetric tools due to higher time response [54].
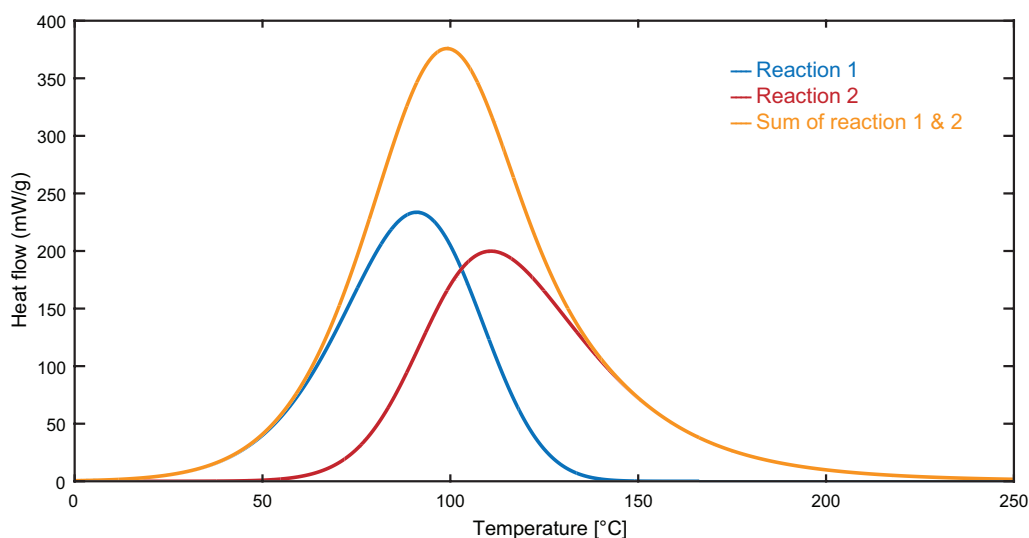
Figure 2.4 – Example of typical heat flow signal (orange) obtained from calorimetric measurement containing two underlying reactions (blue and red).

On the one hand, the latter advices lead to think that calorimetry is a good choice to consider physical effects (temperature and pressure). On the other hand, by using such method, the heat flow signals obtained can have complex shapes resulting from the sum of heat released or consumed by the different events occurring in the reaction mixture (Figure 2.4).

These events can involve physical (melting, mixing,...) as well as chemical (synthesis, decomposition,...) changes [55, 56]. Consequently, is it possible to determine the reaction kinetics from solely calorimetric measurements? This question will be approached along the further developments (Chapter 4).

2.2.1.4   Kinetic analysis

Many different methods are available to determine the value of the required parameters to describe the reaction system behaviour based on the GLMA (2.11) [53]. Graphical constructions can be used and are mainly based on linearization of the integrated rate [57]. Although such methods are widely used, they still are restricted to simple reactions. The fact that the assessment is very subjective can lead to erroneous estimations. Another method, described by Van't Hoff [58], is the differential rate linearization using logarithmic transformation. The order is obtained from the slope of the graphical construction as presented in Figure 2.5.
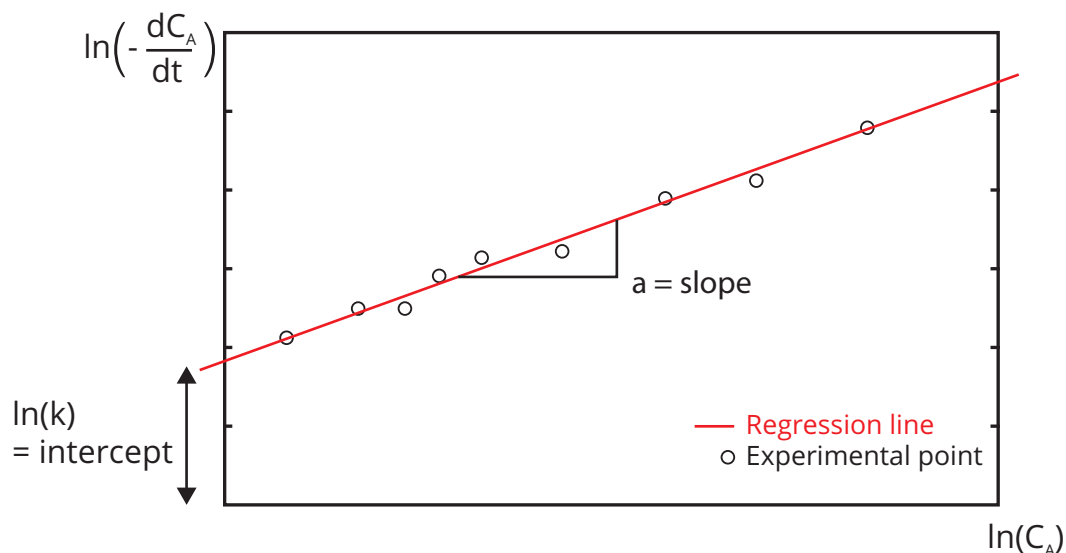
Figure 2.5 – Linearization of the transformation rate (2.19) and its experimental points. The order corresponds to the slope.

$$A \xrightarrow{k} B \tag{2.18}$$

$$R_A = -\frac{dC_A}{dt} = k \cdot C_A^a$$
$$\ln\left(-\frac{dC_A}{dt}\right) = \ln(k) + a \cdot \ln(C_A) \tag{2.19}$$

In the scenario of a bi-molecular reaction, the linearization is still solvable using Multiple Linear Regression methods. More complex reaction scheme scenarios were extensively treated by Capellos et al. [59]. These both last methods, however, are also limited; Miller has made references to both these methods as "trial and error" for the integral one and stated the differential one as being "a systematic exploration" [60, 61].

The effects of temperature can be considered through the pre-exponential factor k_0 and the activation energy E_a. They can be evaluated through the determination of the rate constant k at different temperatures. It is then possible to perform a so-called *"Arrhenius plot"* illustrated in Figure 2.6 and using the linearized expression of the Arrhenius equation (2.12):

$$ln(k) = ln(k_0) + \frac{-E_a}{R} \cdot \frac{1}{T} \tag{2.20}$$

such as

$$ln(k) = f\left(\frac{1}{T}\right) \tag{2.21}$$

Willson et al. mentioned the fact that the reactant orders can be a function of time and developed a method for deriving the non-integral reaction orders of a complex reaction ($A + B \rightarrow C$) using the ratio between pair of reaction progress rate (at two different time from the same data) [40]. This concept was implemented for the case of isothermal experiments avoiding the determination of the pre-exponential factor and activation energy as shown in equations 2.22 and 2.23.

$$\dot{X}_p = \frac{dX_p}{dt} = kC_{A,0}^{a+b-1}(1 - X_p)^a(M - X_p)^b \tag{2.22}$$

23
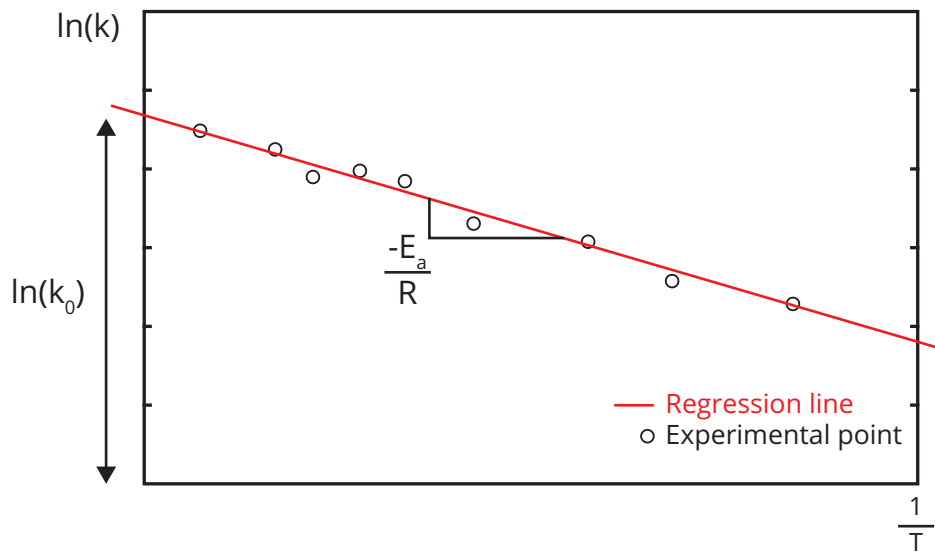
Figure 2.6 – Arrhenius plot to determine the pre-exponential factor k_0 and activation energy E_a.

$$\frac{\dot{X}_1}{\dot{X}_2} = \frac{(1 - X_1)^a (M - X_1)^b}{(1 - X_2)^a (M - X_2)^b} \tag{2.23}$$

$$M = \frac{C_{B0}}{C_{A0}} \qquad with \quad C_{B0} > C_{A0} \tag{2.24}$$

Where $(\dot{X})$ is the reaction progress rate at the time p and M the ratio between the initial concentrations of A and B, B being in excess compared to A.

Another way to differentiate the orders in case of multi-molecular reactions is to perform experiments with concentration excess, often called the isolation method [53, 59, 62]. Hence, reaction kinetic study purposes that to virtually assume a zero order of a reactant (no effect on the reaction rate), its concentration should be taken at least ten-fold excess compared to the other reactant [63]. It was shown by Blackmond that this excess does not need to be such a large number but only a known one [64].

This last section allowed to design the model structure representing the reaction mixture behaviour. However, to control the reaction course, another model structure has to be established: the reactor.

2.2.2 Reactors

Chemical reactors are at the heart of a chemical process. They serve the purpose to contain and control the reaction mixture by means of temperature, mixing and pressure. Constituted of a vessel that may vary in size from a few cm^3 to m^3, they can operate under various modes, namely batch, fed-batch or continuous (Section 2.2.2.1).

A reactor is generally equipped of a heating/cooling system to control the temperature, a stirrer to increase the homogeneity, few inlets and/or outlets and measurement probes (temperature, pH,...) to follow the process course.

The management of the reaction system implies many processes occurring at a macroscopic level, namely the reactions themselves, the mass, heat and momentum transfer phenomena. Thus, the modelling of the dynamic aspects of a reactor is performed by means of differential equations describing these governing phenomena balances [65].

The following section will then present the different modes of operation generally performed with a chemical reactor. A complete description of the mass, material and heat balances is provided for the case of a Continuous Stirred Tank Reactor, where momentum aspects were omitted by considering an homogeneous mixture.

2.2.2.1 Stirred tank reactors

In chemical reaction engineering, stirred tank reactors can be considered as ideal reactors belonging to one of the following classes [30, 31, 66, 67]:

1. **Batch reactors** (BR) are defined as closed reactors with respect to the mass balance, meaning there is no input or output after the initial charging and while the reaction proceeds (Figure 2.7). The vessel content is then removed after reaching the right specifications. Often used for small-scale operation due to quick production changeover and well-defined operating time, they allow to investigate new processes (e.g. pilot) and can be used at large-scale (e.g. polystyrene production). Their relatively high operating cost due to long downtimes is one of their drawbacks. In many cases, batch operations are not possible due to safety or selectivity issues. Nevertheless, the following class may prove to be useful in such situation [68, 69].

2. **Fed-batch reactors** (FBR) are defined as half-open reactors (Figure 2.8), where at least one of the reactant is added as the reaction proceeds or when a part of the mixture is removed along the process course. As consequences, the heat and mass balances are directly affected by a progressive addition or removal.
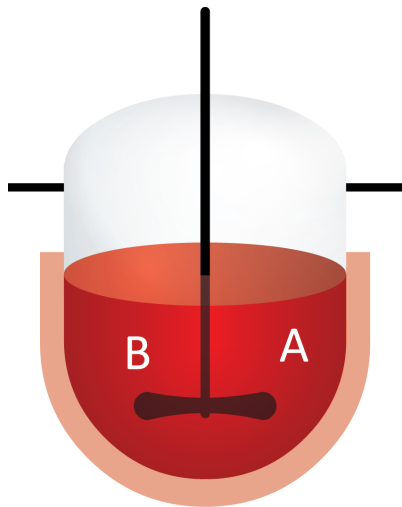
Figure 2.7 – Batch Reactor scheme (BR).
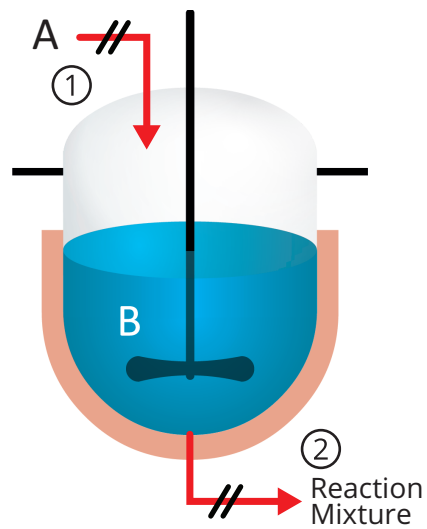
Figure 2.8 – Fed-batch Reactor scheme (FBR): 1) discontinuous input(s) only; 2) discontinuous output(s) only.
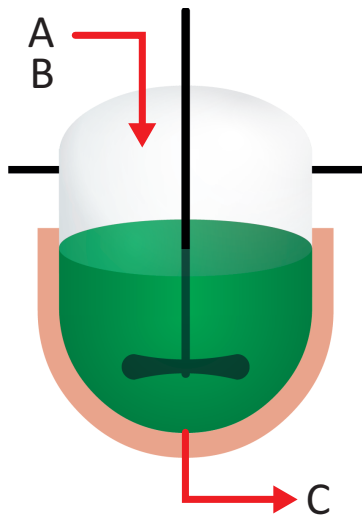
Figure 2.9 – Continuous Stirred Tank Reactor scheme (CSTR).
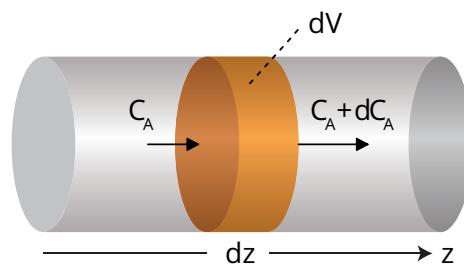
Figure 2.10 – Plug Flow Reactor scheme (PFR).

This type of process is often preferred to batch process as it offers two essential advantages in case of:

- *Exothermal reactions*: the heat production rate may be controlled by the addition in order to adjust the latter to the cooling system capacity.

- *Multiple reactions*: the reactions can be handled in a way of minimizing unwanted side reactions. Indeed, maintaining one of the reactant at a low concentration allows reducing the rate of a side reaction, favouring (the rate of formation of) the desired product as well as limiting the accumulation of unconverted material.

3. **Continuous Stirred Tank Reactor** (CSTR), oppositely to BR and FBR, this class of reactor is operated continuously, the reactants being fed while the products are withdrawn at a constant flow rate during steady state operation (Figure 2.9). Used most likely for large-scale operation due to their low operating costs, continuous reactors provide high rate of production and constant product quality due to constant conditions [67].

4. **Tubular reactors**, generally referred as Plug Flow Reactor (PFR), are also operated continuously. One or more fluid are pumped through cylindrical pipe constituting the reactor (Figure 2.10) and where reactions occur along the tube. Such configuration is characterized by the formation of a concentration gradient along the flow path. Consequently, instead of operating on a time basis as in BR configuration, this type of reactor operates on a length basis. Thus, the time to cross the reactor length (passage time) corresponds to the operating time [31, 66].

Such reactor can be modelled and approximated by assuming an infinite number of CSTR connected in series. It will however not participate in the future developments as the focus is oriented toward vessel characteristics.

2.2.2.2 Reactor model

Certain restrictions imposed by the nature must be respected when designing a new process or analyzing an existing one. Lavoisier stated: *"Rien ne se perd, rien ne se crée, tout se transforme"* [70], the principle behind this quote is the *law of conservation* which can be applied to different quantity such as mass, material or heat [69].

The dynamic behaviour of a reactor can be described using such principle coupled to differential equations representing the instantaneous state of the system. A general balance representing the different events occurring in the system and along the process

course can be established as:

$$Accumulation \quad = \quad Inputs \quad + \quad Generation \quad - \quad Outputs \quad - \quad Consumption$$

| Rate of *element* accumulation within the system | Rate of *element* input due to flow | Rate of *element* generated within the system | Rate of *element* output due to flow | Rate of *element* consumption within the system |

Where *element* can be mass ($kg \cdot s^{-1}$), material ($mol \cdot s^{-1}$) or heat (W).

In order to develop a mathematical model representing the overall reactor behaviour under different operating conditions and mode (BR, FBR, CSTR), the mass, material and heat balances have to be established. Consequently, for clarity reasons, all the balances will be applied to a CSTR, the reactors BR and FBR being simplified cases of the latter considering an evolution of the mixture mass [30, 31, 66].

2.2.2.2.1 Mass balance

As the mass cannot be generated or consumed and considering inputs/outputs available in case of CSTR, the general balance is simplified and written:

$$
\begin{array}{ccccc}
Accumulation & = & Inputs & - & Outputs \\[2mm]
\dfrac{dm_r}{dt} & = & \displaystyle\sum_{i=1}^{I} \dot{m}_{in,i} & - & \displaystyle\sum_{j=1}^{J} \dot{m}_{out,j}
\end{array}
\qquad (2.25)
$$

2.2.2.2.2 Material balance

The direct consequence of a reactive system is that the molar quantities change with the reaction progress meaning that any component may be consumed or generated due to chemical reactions or physical transformations. In addition, any component may be fed or removed from the reactor. Consequently, the material balance is written for each component individually and depends on the different events occurring in the reactor:

$$Accumulation \quad = \quad Inputs \quad - \quad Outputs \quad + \quad Generation - Consumption$$

$$(2.26)$$

$$\frac{dN_i}{dt} = \sum_{in=1}^{IN} \dot{N}_{in,i} - \sum_{out=1}^{OUT} \dot{N}_{out,i} + m_r \sum_{j=1}^{J} \nu_{ij} r_j \qquad (2.27)$$

This balance is included in the reaction kinetics (2.11). By adding a component during the process course, its respective concentration changes, causing a direct impact on the reaction rate and the heat production. The last term represents as well generation (positive) as consumption (negative).

2.2.2.2.3 Heat balance

The energy can have different forms (kinetic, potential or internal). However, considering a closed system, the energy can be transferred between itself and its surrounding under the form of heat or work. For the reactor model structure, the energy transfer phenomena will be considered exclusively existing as heat.

The heat balance becomes essential whenever temperature changes are important or in order to describe thermal behaviour of a process. Indeed, any change in temperature implies an effect on the reaction rate(s) and the cooling system.

For a better understanding, the terms of a general heat balance considering a reactive system and its reactor are highlighted in Figure 2.11.

The general heat balance can be written as:

$$q_{acc} = q_{rxtot} + q_{ex} + q_{loss} + q_{in} + q_{mix} + q_{st} \qquad (2.28)$$

The different heat flow terms involved in the heat balance are described in the further sections.

Heat accumulation

Written q_{acc}, it describes the accumulation of heat in the reaction mixture meaning the variation of the content and equipment energy due to temperature changes and is formulated:

$$q_{acc} = (m_r \cdot c_{p,r} + C_w) \cdot \frac{dT_r}{dt} \qquad (2.29)$$
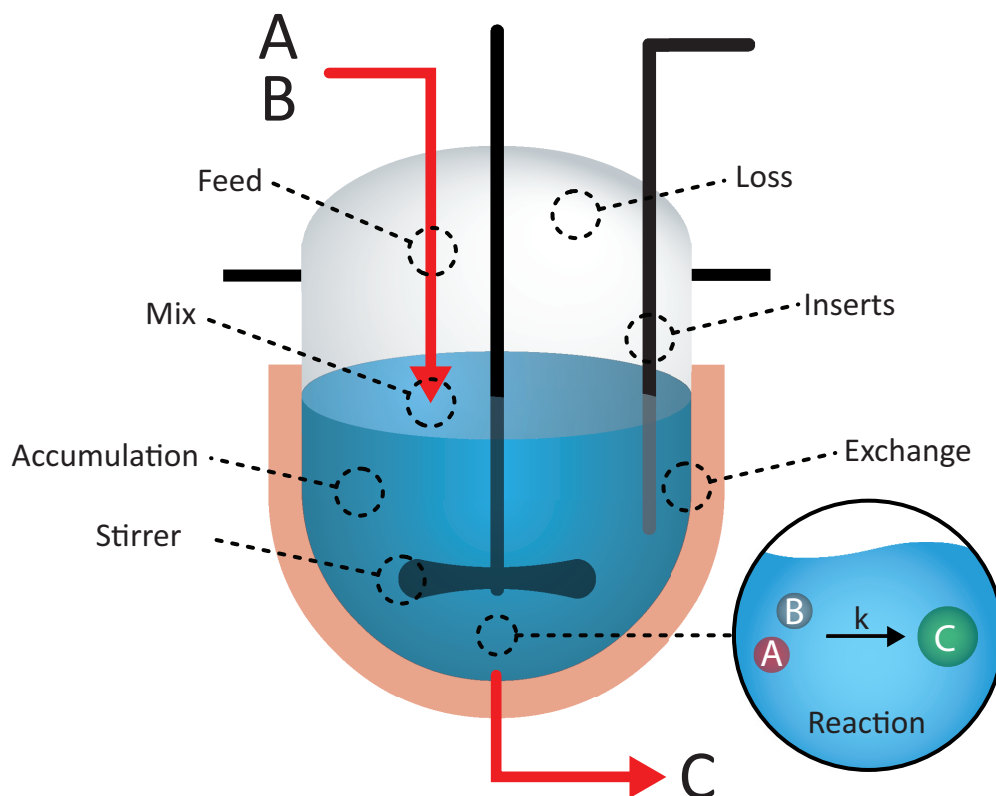
Figure 2.11 – Scheme of the different heat exchanges happening within the reactor and with its surrounding. Different types of heat transfer are noticeable: the "*loss*" with surrounding, the "*exchange*" between the reaction mixture and the cooling system, the "*feed*" effect due to a temperature difference between the feed(s) and the reaction mixture, the "*mix*" effect due to the dissolution of the feed components, the dissipated heat caused by the "*stirrer*", the "*accumulation*" of heat by the reaction mixture, the "*inserts*" and the reactor itself and finally the heat generated by the "*reaction*".

Where $c_{p,r}$ is the specific heat capacity of the reaction mixture, C_W is the sum of heat capacities considering every system components in contact with the reacting system namely the reactor wall and inserts.

This term is the consequence of the reaction heat production rate and the exchange with the heat removal system and environment losses. The heat accumulated will directly be used by the reaction mixture by a change of its temperature.

The heat capacity of the reaction mixture may change along the reaction course as the composition changes due to reactant disappearance and product appearance having different physical properties. As a consequence, the heat capacity needs to be known and is described by the relation between the composition and the corresponding

reaction mixture heat capacities as:

$$c_{p,r}(T) = \sum_{i=1}^{I} x_i c_{p,i}(T) \tag{2.30}$$

Where x_i is the mass fraction of the component i in the reaction mixture.

Heat production

The heat production corresponds to the heat released or consumed rate by a reaction that may be exothermic or endothermic. The corresponding heat flow is proportional to the respective enthalpy and is described by the reactions kinetics through the reaction rate. For a reaction j, this term is written $q_{rx,j}$ and formulated as:

$$q_{rx,j} = m_r \left(r_j \cdot (-\Delta_r H_j) \cdot \sum_{i=1}^{I} \nu_{ij} M_i \right) \tag{2.31}$$

Where $(-\Delta_r H_j)$ is the enthalpy of reaction j and M_i the molar mass of i.

In case of a reaction system involving J reactions, the apparent heat flow is the sum of every individual reaction heat flow produced within the reaction mixture:

$$q_{rxtot} = \sum_{j=1}^{J} q_{rx,j} \tag{2.32}$$

Heat removal

Written q_{ex} represents the heat exchange between the jacket and the reaction mixture across the reactor walls and is expressed as:

$$q_{ex} = U \cdot A \cdot (T_j - T_r) \tag{2.33}$$

Where U is the overall heat transfer describing the heat transfer across the wall and A the area of exchange between the reaction mixture(r) and the jacket(j).

Often, the parameters U and A are estimated together as UA which avoids any need of an accurate evaluation of the exchange area. Unfortunately, if there is presence of inputs or outputs as it is the case for FBR, the area of exchange evolves during

the process course. In general, for low viscous reaction mixture, this evolution can be considered as linear with the change of volume.

Heat losses

The terms q_{loss} describes the heat losses between the reaction mixture and the surrounding essentially through the reactor cover. Highly dependent of the insulation, these losses may more become important at higher temperature than at ambient. As the calculations can be tedious due to different heat dissipation effect (radiation, natural convection,...), a simplified expression is generally used:

$$q_{loss} = \alpha \cdot (T_{amb} - T_r) \tag{2.34}$$

Where α represents a global overall heat transfer coefficient and amb defines the surrounding.

Sensible heat due to feed

Written q_{in}, it represents the heat provided or required by the feed stream to reach the reaction mixture temperature. This heat flow is caused by the temperature difference between the feed (T_{in}) and the reaction mixture:

$$q_{in,i} = \dot{m}_{in,i} \cdot c_{p,i} \cdot (T_{in,i} - T_r) \tag{2.35}$$

If several feed streams are present simultaneously, the effects will be cumulated:

$$q_{in} = \sum_i^I q_{in,i} = \sum_i^I \dot{m}_{in,i} \cdot c_{p,i} \cdot (T_{in,i} - T_r) \tag{2.36}$$

Mixing effect

Written q_{mix}, it represents the heat linked to the mixing of streams with different composition. This thermal effect only appears for non ideal solutions. This heat can be represented as the amount of heat necessary to bring the feed component I_1 to a state $I_1{}^*$ where it will finally be able to react with I_2, a reactant initially present in the reactor. This effect can be accounted using the following reaction scheme and equation:

$$I_1 \rightarrow I_1{}^* \qquad\qquad\qquad \Delta_{mix}H_{I_1 \rightarrow I_1{}^*} \qquad\qquad (2.37)$$

$$I_1{}^* + I_2 \rightarrow P \qquad\qquad\qquad \Delta_r H \qquad\qquad (2.38)$$

$$q_{mix,i} = \dot{m}_{in,i} \cdot (-\Delta_{mix}H_{i \rightarrow i*}) \qquad\qquad (2.39)$$

Some insights on the behaviour of such process are presented by Piekarski [71] where he explains that a linear relation can be expected only if the mixed molecules have similar physical properties. In many case, this effect is hidden under the reaction heatflow which makes its determination difficult. This effect can be measured in specific conditions where the reaction mixture is at a temperature where the heat produced by the reaction system can be neglected compared to the effect of mixing as mentionned by Ubrich [72].

It can be noted that, in general, the enthalpy of mixing has a small value (exception can be made for different acid and solid dissolutions) compared to the major event normally happening namely the reaction.

Stirring

The stirrers are generally installed centrally inside the reactor vessel surrounded with baffles in order to prevent the rotation of the reaction mixture. Different types of stirrer exist and each one of them is adapted for specific type of reaction mixture (viscous (low, medium and highly), suspension, heterogeneous...).

The mechanical energy required to keep turning the stirrer is converted into kinetic energy and frictional losses through the contact between the stirrer deflectors (propeller, blade, turbine...) and the reaction mixture. Therefore, part of this heat is eventually dissipated in the reaction mixture and must be included in the heat balance as the term q_{st} [17, 65]. The heat flow generated by the stirring is proportional to two adimensional numbers, the Reynolds (Re) and Newton (Ne), also called Power number, such as [17, 73–75]:

$$Ne = f(Re) \qquad\qquad (2.40)$$

where :

$$Re = \frac{d_{st}^2 \, n \, \rho}{\mu} \qquad\qquad = \frac{\text{Inertial forces}}{\text{Viscous forces}} \qquad\qquad (2.41)$$

$$Ne = \frac{q_{st}}{d_{st}^5 \, n^3 \, \rho} \qquad\qquad = \frac{\text{Frictional forces}}{\text{Momentum forces}} \qquad\qquad (2.42)$$

This relationship is graphically demonstrated in a log-log plot of the Newton number as a function of the Reynolds number for several stirrer types considering a fully baffled reactor vessel [76]. The regime at which the stirring is performed has a great importance:

1. *Laminar*: for value of the Reynolds number of $1 \leq Re \leq 10$, the Newton number decrease linearly such as:

$$Ne = C_{lam}^{ste} Re^{-1} \qquad\qquad (2.43)$$

2. *Transitional*: for value of the Reynolds number of $10 \leq Re \leq 10000$, the Newton number decreases more gradually such as:

$$Ne = C_{trans}^{ste} Re^{-\frac{1}{3}} \qquad\qquad (2.44)$$

3. *Turbulent*: for value of the Reynolds number of $Re \geq 10000$, the Newton number exhibits constant value such as:

$$Ne = C_{tur}^{ste} \qquad\qquad (2.45)$$

Depending on the stirring regime (reg), the Newton number is obtained directly from the value of the Reynolds number for the considered agitator type (Table 2.1) and allows to evaluate the heat flow generated by the stirring:

$$q_{st} = Ne_{reg} \, \rho \, n^3 \, d_{st}^5 \qquad\qquad (2.46)$$

where reg is the regime of stirring, ρ the reaction mixture density, n the stirred speed

rate and d, the diameter of the stirrer st.

Table 2.1 – Examples of Newton for commonly used stirrers under laminar and turbulent regime [15, 30, 76, 77]. These values may change for different dimension ratios.

Type of stirrer	Ne_{lam}	Ne_{tur}
a) Propeller	40	0.35
b) Impeller	85	0.2
c) Anchor	420	0.35
d) Turbine (6 blades)	70	4.6 - 5.75

Some values of the Newton number for different type of stirrer are depicted in Table 2.1 for the laminar and turbulent regions.

2.2.2.3   Temperature control

The temperature of the reaction mixture (T_r) is an important parameter as it will directly influence the reaction kinetics and dictate the value of the rate constant. As presented in the previous section, this parameter is related to the heat balance through different aspects (cooling, loss, reaction,...). As a matter of fact, under different operating conditions, the reaction mixture temperature will not behave the same.

In terms of simulation, the reaction mixture temperature can be controlled following different modes:

1. T_r-*controlled*:   the reaction mixture temperature is a constant or follows a designed profile such as in:

   (a) Isothermal, the reaction mixture temperature is:

   $$T_r = C^{ste} \tag{2.47}$$

   With a heat balance written:

   $$q_{acc} = 0 \Leftrightarrow \frac{dT_r}{dt} = 0 \tag{2.48}$$

   (b) Non-isothermal

   $$T_r = f(t) \tag{2.49}$$

   With a heat balance written:

   $$q_{acc} = \frac{df(t)}{dt} \Leftrightarrow \frac{dT_r}{dt} = \frac{df(t)}{dt} \tag{2.50}$$

The advantage of such simulation is that the deviations due to temperature changes are eliminated; the reaction mixture follows exactly the designed temperature profile allowing the simulation of "perfect" DSC or Isothermal experiments.

2. T_j-*controlled (Isoperibolic)*: The jacket temperature (T_j) is a constant or follows a designed profile such as in:

   (a) Isothermal:

$$T_j = C^{ste} \tag{2.51}$$

   (b) Non-isothermal:

$$T_j = f(t) \tag{2.52}$$

The reaction mixture temperature is dependent on the reaction system (rx) and jacket temperature such as:

$$T_r = f(t, q_{rx}, T_j) \tag{2.53}$$

Where the heat balance is written:

$$q_{acc} = q_{rx} + q_{ex} + q_{loss} \Leftrightarrow \frac{dT_r}{dt} = \frac{1}{m_r c_{p,r} + C_w} \left(q_{rx} + q_{ex} + q_{loss}\right) \tag{2.54}$$

Such approach allows to eliminate the effect of the jacket, namely the thermal inertia of the heating/cooling system.

3. *Adiabatic*: The reaction mixture temperature is solely the result of the reaction system thermal activity, namely that all the heat released by the reaction system is used to heat the reaction mixture itself. Therefore, the reaction mixture temperature is:

$$T_r = f(t, q_{rx}) \tag{2.55}$$

Where the heat balance is written:

$$q_{acc} = q_{rx} \tag{2.56}$$

This mode is helpful to determine safety related parameters and simulate a cooling failure scenario (section 6.1).

4. *Cascade-controlled*: In order to achieve an accurate control of the reactor temperature, a cascade controller can be used. In this mode the temperature control is managed by two controllers arranged in cascade, that is, in two nested loops. The external loop, called the master, controls the temperature of the reaction mixture by delivering a set value to the inner loop (slave), which controls the cooling system temperature (T_j). The cooling system temperature set point is calculated proportionally to the deviation of the reactor temperature from its set point:

$$T_{j,set} =$$
$$T_{r,set} + K \cdot \left[(T_{r,set} - T_r) + \frac{1}{I} \int_0^t (T_{r,set} - T_r) \cdot dt + D\frac{d\,(T_{r,set} - T_r)}{dt} \right] \tag{2.57}$$

Where the constant K is the proportional gain, the constant I is the integral gain and D (not always used), the derivative gain of the cascade. These parameters are important for tuning the dynamics of the temperature control system and result in a fast answer to temperature changes.

This model is explained in further detail in Chapter 5.

These different modes of temperature control are describing the different thermal regimes a reaction mixture may encounter along the process course (Figure 2.12). It allows to simulate the reaction mixture behaviour under a wide range of operating conditions that may correspond to a calorimetric tool (see Chapter 3).
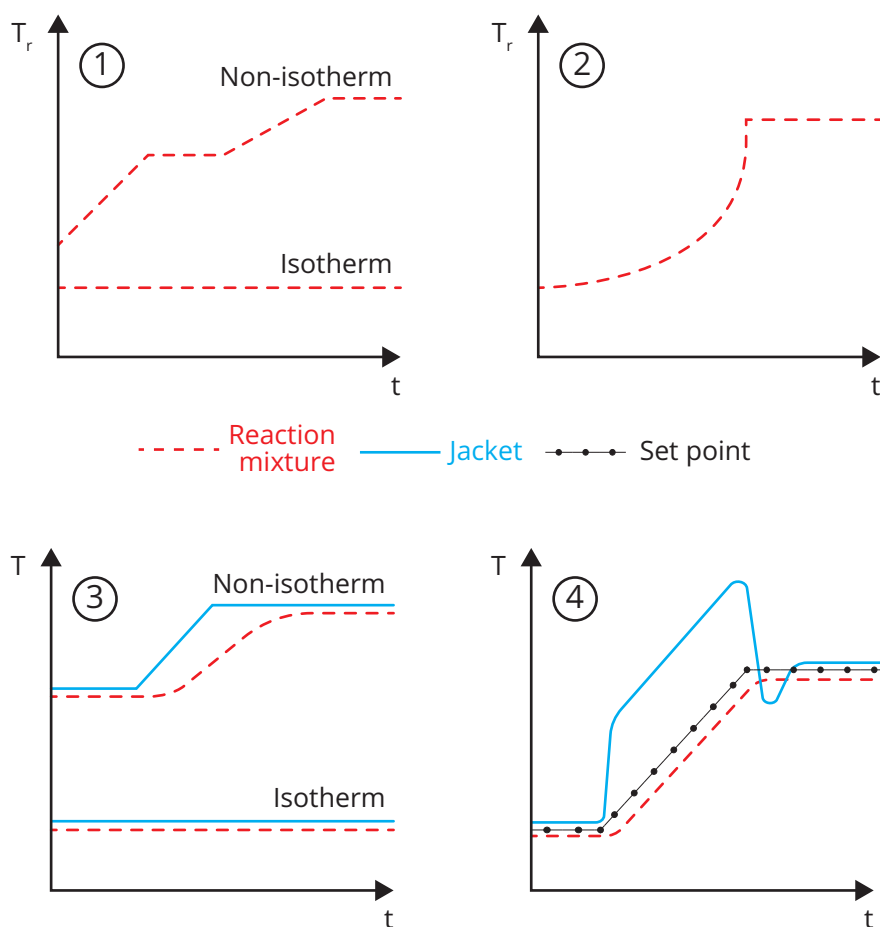
Figure 2.12 – Temperature course of the reaction mixture (dashed line), the jacket (filled line) and the set point (dot line) as a function of time for the different temperature controls: (1) T_r-controlled, (2) adiabatic, (3) T_j-controlled, (4) cascade-control.

2.3   Design of Experiment

A large number of experiments is generally performed in research, development and optimisation to characterise the behaviour of a considered system. In the field of chemistry or chemical engineering, this research can be done in labs, pilot plants, and full-scale plants [78, 79]. These experimentation may be time-consuming, costly or even infeasible due to safety reasons or amount of material available. Therefore, to explore such system in an optimal way and reduce the number of experiments, the real dynamic of the system is often reproduced by parametric models (section 2.2), whose parameters are estimated on the basis of experimental data (discussion and application in the further chapters) [80–82]. Nevertheless, even with this kind of approach, such models may still need a large amount of data to be characterised. Consequently, the set of experiment must be optimised to provide a maximum of information to describe the relationship between the inputs and the responses.

Many different Design of Experiment (DoE) methods can be used. They are generally characterised by their resulting distribution (ordered, random, cluster. . .) as shown in Figure 2.13 [80, 82, 83]. When this relationship is not explicit, however, the use of design that uniformly spread the points all over the experimental space are preferred. These design are called Space-Filling Designs (SFD) [80, 84].
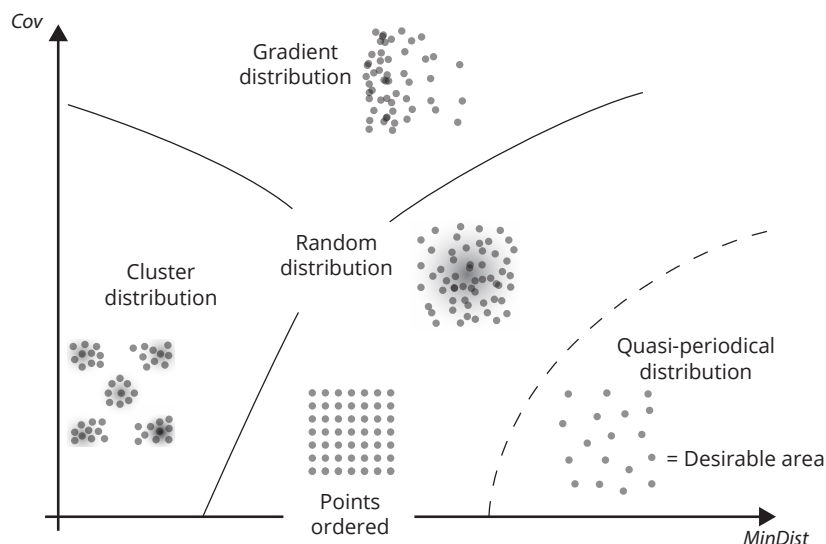
Figure 2.13 – Point distribution of different Space-Filling Designs using $MinDist$ and CoM criteria. A desirable designs should have a high value of $MinDist$, corresponding to sufficiently distant points, and a low value of CoM, corresponding to a regular distribution. Reproduced from [82].

In the last decade, uniform designs based on Space Filling Design (SFD) have been more and more used in the field of computer science due to the increasing demand to solve numerical problems involving a large number of parameters [82]. In the field of chemical engineering, the explored systems can be complex and depending on a large number of parameters as concentrations, temperature, number of reactants, feed and many others. Consequently, such method seems adapted to explore chemical system.

The method used for the further development is a Space-Filling method, the so-called WSP designs based on the Wootton, Sergent, Phan-Tan-Luu's algorithm [82]. It was mentioned by Santiago et al. that when the experimental domain depends on more than two paramaters, the space filling cannot be visually checked, therefore it is necessary to use mathematical criteria to ensure the quality of the distribution. Among several criteria available, it was chosen to consider the minimal Euclidian distance and the Coverage measure to characterise the design used for this research [80, 82–85]:

1. **Definition:** Let $X = \{x_1, x_2, ..., x_n\} \subset [0, 1]^d$, a set of n candidates (experiments) on d-dimensional space. The Euclidean distance matrix $Dist$ is an $n \times n$ matrix representing the spacing between the n candidates composing the Euclidean space and defined by

$$Dist = (d_{ij})$$
$$d_{ij} = \|x_i - x_j\|_2^2 \qquad (2.58)$$

Where $\|.\|_2$ denotes the 2-norm on $\mathbb{R}^d$.

The minimal Euclidean distance is written $MinDist$:

$$MinDist = \min_{\substack{x_i \in X \\ }} \min_{\substack{x_j \in X \\ j \neq i}} Dist \qquad (2.59)$$

This criterion shows the scattering of design candidates. A high value means that the design candidates are never too close to each other.

2. **Definition:** Let $X = \{x_1, x_2, ..., x_n\} \subset [0,1]^d$, a set of n candidates (experiments) on d-dimensional space. The Coverage Measure CoM is defined by

$$CoM = \frac{1}{\bar{\gamma}} \left(\frac{1}{n} \sum_{i=1}^{n} (\gamma_i - \bar{\gamma})^2 \right)^{\frac{1}{2}} \qquad (2.60)$$

with $\gamma_i = \min_{k \neq i} dist\left(x^i, x^k\right)$, the minimal distance between a point and his nearest neighbour and $\bar{\gamma} = \frac{1}{n} \sum_{i-1}^{n} \gamma_i$, the mean distance of γ_i.

The criterion CoM characterises the degree of distribution; a low value indicates a mesh distribution close to a regular grid which means that the points fill up well the working space.

This method is based on a space of parameters well distributed to cover the entire space in a uniform way and does not require to know any model [82, 86].

The general procedure to construct a space-filling design consists of six steps:

1. Generate a set of n candidate points
2. Calculate the distances matrix ($Dist$) of the n points
3. Choose an initial point O and a distance d_{min}
4. Eliminate the points I such as : $D_{O>I} < d_{min}$
5. The point O is replaced by the nearest candidate among the remaining ones
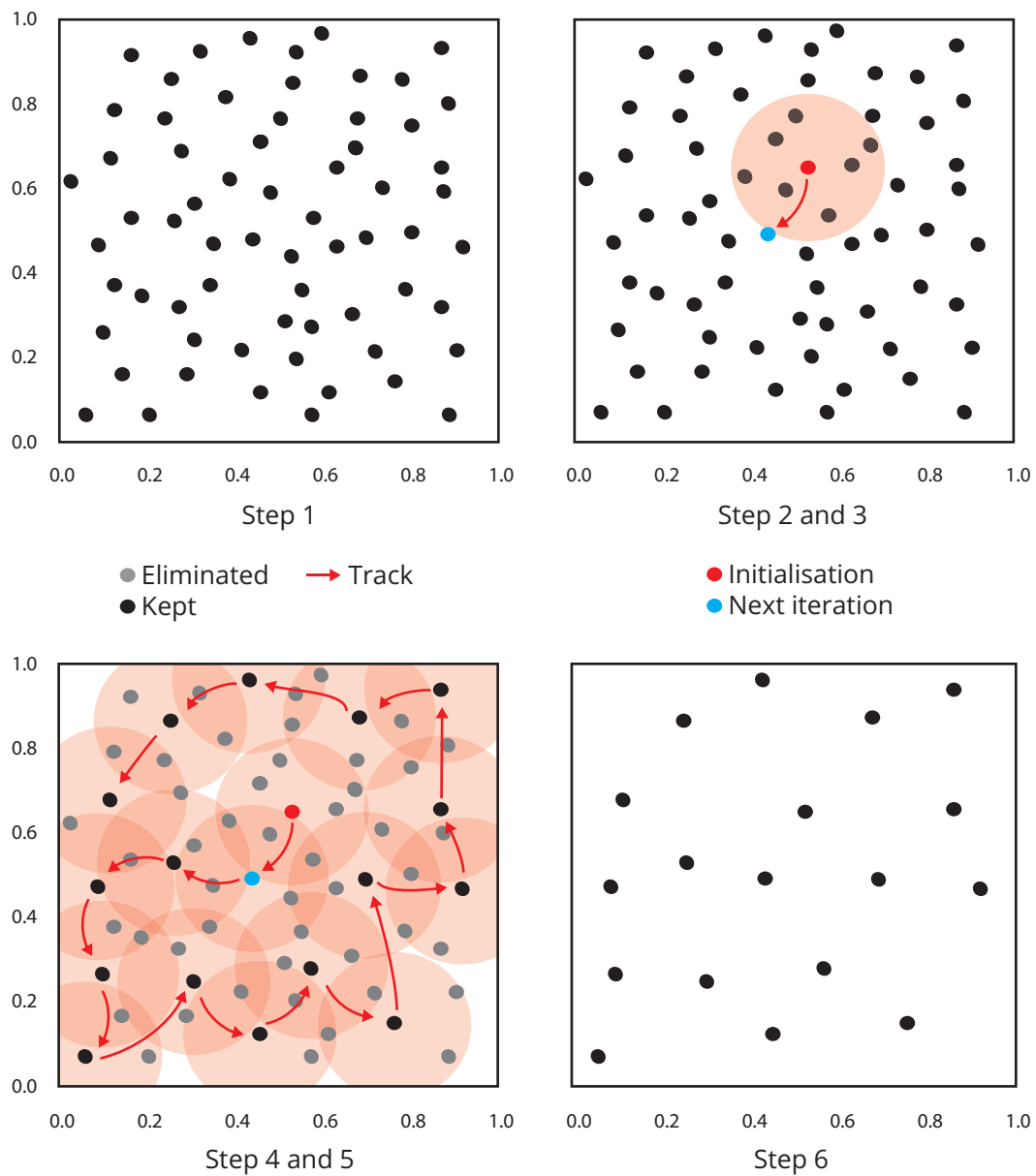
Figure 2.14 – Illustration of the different steps to perfom a Space Filling Design [82].

6. Repeat the steps 4 and 5 until the number of candidates for the final subset is reached.

Different configurations are then obtained depending on the starting candidate. For a design based on 3 variables, namely a cube, the following possibilities are available:

- Random point
- Center of the set
- Face Center of the set
- Vertex of the set

The best design is chosen in order to cover the entire space in an optimal way, meaning that is the one having a largest $MinDist$ with the smallest CoM as shown in Figure 2.13.

2.4 Parameter estimation

Once the experiments are performed, the focus can be directed toward the identification of the dynamic parameters of a reaction system including the reactor itself. The general approach to such problems can be addressed in three phases:

1. *Modelling:* development of a mathematical model whose equations describe the considered process or physical phenomena (developed in Section 2.2.1.2 and 2.2.2).
2. *Regression:* estimation of the model parameters using experimental data.
3. *Validation:* determine the related errors and deviations of the model toward the experimental data and selection for the most suited model.

The modelling part was already discussed in section 2.2 to build the general model structure (reaction kinetics and reactor). The next section will present how a mathematical model should be expressed to allow a parameter estimation.

2.4.1 The mathematical model

Let assume $f(\cdot, \cdot) : [t_0, t_f] \times \Phi \to \mathbb{R}^m$ being a general mathematical model, continuous in time $t \in \mathbb{R}^+$, from the starting time t_0 to the final time $t_m = t_f$ and where $\theta \in \Phi \subset \mathbb{R}^n$ is a vector of n parameters belonging to the parameter space Φ.

This general model is written:

$$y = f\left(t, \theta\right) \tag{2.61}$$

In the following, it is assumed that the experimental data set $\{(t_1, y_1), (t_2, y_2)..., (t_m, y_m)\}$ is considered as

$$y_i = f\left(t_i, \theta\right) + \epsilon_i \tag{2.62}$$
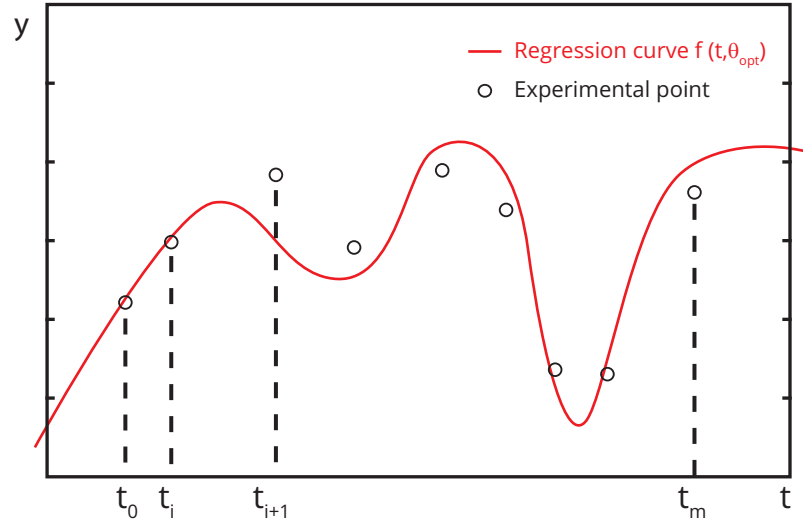
Figure 2.15 – Illustration of the parameter estimation approach by opposing the experimental points and the prediction based on retrieved parameters.

where ϵ_i, the induced error by the measurement follows a normal distribution with 0 mean and a standard deviations σ_i, namely

$$\epsilon_i \sim N(0, \sigma_i^2), \qquad i = 1, ..., m \tag{2.63}$$

It is further assumed that σ_i is the same for all measurements, such as

$$\sigma_1 = \sigma_2 = ... = \sigma_m = \sigma \tag{2.64}$$

This assumption is correct by considering that the experiments are performed using the same instrumentation.

2.4.2 The regression: a least-square approach

The strategies existing to estimate and validate unknown model parameters are various and widely available. Nevertheless, the choice in strategy will depend on the following three questions:

- Is there a large number of data available?
- Is the model analytically differentiable?
- Is the error distribution known?

Despite the large number of methods available, two categories of methods can be highlighted: Least-square methods (Gradient Descent, Gauss-Newton, Levenberg-Marquardt) or Statistical based methods (Maximum Likelihood, Unbiased Estimation, Method of Moments) [87, 88].

The objective of such methods is to determine the optimal parameter value that makes the mathematical model (2.62) "fit" as close as possible the experimental data. The ability to converge toward a solution is directly related to the complexity of the model and to the answers of the previously mentioned questions.

The decision about which method should be used is determined by the degree of knowledge about the error distribution. This question was assessed by many authors and showed that in many case where an unknown error distribution is considered, it was preferable to use least-square estimation methods [89–92]. Likewise, if the error distribution is known, statistical based methods are of great help to converge toward a solution.

Another aspect to consider is the amount of data available but also the conditions under which they were determined. This information will directly affect the quality of the parameter estimates. As the number of data grow larger and the conditions are as diverse as possible, the insight given into the parameter estimates becomes more and more reliable and accurate. The advantage of least-square method is that the error distribution can be estimated using experimental data through parameter estimation [92].

It should be kept in mind, that these parameters are random variables. Consequently, experiments taken at different times and conditions will greatly help to evaluate them and their respective error-distribution. This last point shows how problems with relatively large amount of data can be treated effectively by least-square methods. However, for problems where only a limited amount of data is available, this kind of method becomes less efficient and even, in the worst case, not applicable. This problematic has been discussed by Childers [92].

The objective of a least-square regression is to determine an optimal vector θ_{opt} which minimizes the deviations (errors) between the model predictions and the experimental data (Figure 2.15), namely the Sum of the Squares of Errors (SSE) of m experimental points:

$$SSE = \sum_{i=1}^{m} (y_i - f(t_i, \theta))^2 \tag{2.65}$$

where $m \geq N$.

This vector can be written as the solution of the previously mentioned least square problem (2.65):

$$\theta_{opt} = arg \left\{ \min_{\theta \in \Phi} \sum_{i=1}^{m} (y_i - f(t_i, \theta))^2 \right\} \tag{2.66}$$

The obtained model is now designed to describe some measurable output(s) of the considered process and can predict its behaviour under a wide range of conditions using the parameter estimates θ_{opt}.

Such problems can be very hard to solve, especially when the system presents non-linearity and non-convexity leading to the possibility of several optimum in the experimental space. In addition, the problem may not be analytically differentiable which can greatly increase the difficulties to find a solution as mentioned in the previously presented questions.

In this study, the secant version of Levenberg-Marquardt method as a gradient-based fitting method will be used to determine the optimal solution describing the experimental data, namely the parameter estimates θ_{opt}. This kind of method requires the calculation of the Jacobian (2.67) which can become difficult when the model is not differentiable. This method has been chosen for its characteristic to evaluate the Jacobian $J \in \mathbb{R}^{m \times n}$ numerically:

$$J = \begin{pmatrix} \frac{\partial f}{\partial \theta_1}(t_1, \theta) & \frac{\partial f}{\partial \theta_2}(t_1, \theta) & \cdots & \frac{\partial f}{\partial \theta_n}(t_1, \theta) \\ \frac{\partial f}{\partial \theta_1}(t_2, \theta) & \frac{\partial f}{\partial \theta_2}(t_2, \theta) & \cdots & \frac{\partial f}{\partial \theta_n}(t_2, \theta) \\ \vdots & \vdots & \ddots & \vdots \\ \frac{\partial f}{\partial \theta_1}(t_m, \theta) & \frac{\partial f}{\partial \theta_2}(t_m, \theta) & \cdots & \frac{\partial f}{\partial \theta_n}(t_m, \theta) \end{pmatrix} \tag{2.67}$$

2.4.2.1 Error of fitting

In least-squares regression analysis, the Sum of Square Errors (2.65) is used as objective function for the minimization problem. As a results, the optimal value of SSE would be 0. Since there is error associated with collecting data, it is very unlikely that any model will exactly fit experimental data. Therefore, a brief overview about error calculation is necessary to judge the quality of the fit and the parameter estimates in terms of regression.

A quantitative analysis of the error can be used to determine the quality of the parameter estimates coming from the regression. To achieve this goal, it is necessary to determine the variance of the errors:

$$\sigma_r^2 = \frac{SSE}{m - n} \tag{2.68}$$

The Jacobian J (2.67) obtained from the regression is used to calculate the Hessian $H \in \mathbb{R}^{n \times n}$:

$$H = J^T J, \tag{2.69}$$

Joining the equations 2.68 and 2.69, the matrix of covariance Cov can be determined:

$$Cov = H^{-1} \cdot \sigma_r^2 \tag{2.70}$$

The variance of the parameters $\sigma_\theta \in \mathbb{R}^N$ is then obtained from the covariance (2.70):

$$\sigma_\theta^2 = diag(Cov) \tag{2.71}$$

The parameter standard error of fitting is finally calculated as:

$$\sigma_{\theta_i} = \sqrt{\sigma_\theta^2(i)} \tag{2.72}$$

2.4.2.2   Correlation matrix

The correlation matrix is an essential tool to determine the strength and direction of the linear relationship that exists between pair of parameters. Its calculation is based on the parameter covariance (2.70) previously obtained:

$$\Psi = (\rho_{ij})$$
$$\rho_{i,j} = \frac{Cov(\theta_i, \theta_j)}{\left(\sigma_{\theta_i} \cdot \sigma_{\theta_j}\right)^{\frac{1}{2}}} \tag{2.73}$$

with $i = 1, ..., n, j = 1, ..., n$.

A positive value of the correlation coefficient $(\rho_{i,j} > 0)$ occurs when the parameters are increasing or decreasing at the same time and in the same direction, whereas a negative correlation coefficient is the opposite as the parameters increase or decrease in opposite direction $(\rho_{i,j} < 0)$. A value of $(\rho_{i,j} = 0)$ means that there is no relation between the parameters.

2.4.2.3 Coefficient of determination

The determination coefficient, referred as $R-square$ or R^2, is a criterion used to qualify the "goodness-of-fit", namely how well a model fits the observations.

The $R-square$ is computed as

$$R^2 = 1 - \frac{SSE}{SST} = \frac{SSR}{SST} \tag{2.74}$$

where SSE is the sum of squared errors between y_i, the observation and the model prediction $f(t_i, \theta)$, described as the unexplained variation (2.65).

The SSR is the sum of squares of regression, namely the explained variation:

$$SSR = \sum_{i=1}^{m} (f(t_i, \theta) - \overline{y})^2 \tag{2.75}$$

Where $\overline{y}$ is the average value of y_i.

Finally, the SST is the sum of squared deviations in y_i, explained as the total variation and described as

$$SST = SSE + SSR = \sum_{i=1}^{m} (y_i - \overline{y})^2 \tag{2.76}$$

Unfortunately, this criterion cannot be used as a stand-alone one to characterise the fit. For different set of data, Anscombe demonstrated that a same model could obtain a good $R-square$ without necessarily fit the data. This problem arised due to the statistical properties of the outliners. Consequently other criteria should be investigated and used to characterise the good behaviour of the model toward the observations [93].

2.4.2.4 Lack-of-regression

The introduction of a standard error of regression σ_r or commonly called $RMSE$ (Root-Mean-Square-Error) can greatly help to overcome the previously mentioned problem:

$$RMSE = \sqrt{\frac{SSE}{m}} = \sigma_r \tag{2.77}$$

A large value will indicate a large dispersion of the model predictions around the observations, while a low value, approaching zero, will indicates a good fit.

To illustrate this problem, two set of data were compared and are depicted in Figure 2.16 and Table 2.2: 1) a model that does not fit the observations; 2) a model that fits quiet well the observations. This example demonstrates that even for good $R-squared$, two different quality of fit can be obtained visually. Therefore, with the help of the $RMSE$, it is possible to have a better overview of the regression quality.
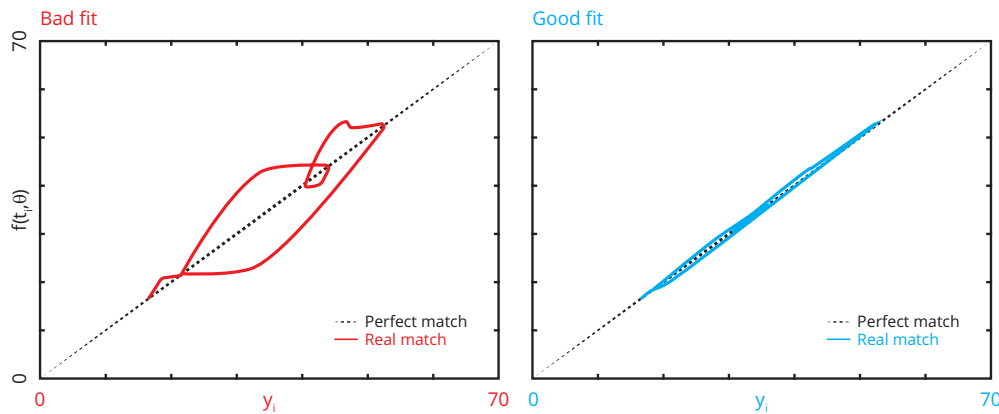
Figure 2.16 – Illustration of a bad and good regression, statistic metrics depicted in Table 2.2.

Table 2.2 – Comparison of statistic metrics between a bad and good regression.

Regression quality	R^2	σ_r
Bad	0.961	2.45
Good	0.998	0.13

2.4.3 Generalization

Chemical processes are generally described by systems depending on many variables (e.g., temperatures, concentrations). These variables are measured several times (depending of the step of measurement) along an experiment and through several runs. Therefore, the total number of points available for the parameter estimation is not coming from only one experiment but from several. This number can be calculated as $m \times p$, where p is the total amount of experiments [94]. The Total Sum of Squares Errors becomes

$$SSE_{tot} = \sum_{j=1}^{p} \sum_{i=1}^{m} (y_{i,j} - f(t_{i,j}, \theta))^2 \tag{2.78}$$

2.5 Model evaluation

Often the model evaluation focuses on the comparison of the regression quality compared to other different models. During this work, however, such comparison is not performed as the models are based on already well defined and used first principle models (section 2.2). Therefore, only the regression quality, the parameter errors and their confidence interval are analysed.

This last section presents some inputs and guidelines to perform such analysis and will finalize the model creation.

2.5.1 Validation

The problem of validation arises because during the creation process of a predictive model, some assumptions and approximations are made to bound and restrict the model to its purpose. Some typical approximations are the consideration of a sample observation that goes to infinity (although the sample observation is finite) or that the error distribution is normal (may be different than the reality) [95, 96]. These short-cuts may be interesting and sometimes useful, however, in practice these assumptions may

lead to wrong estimates, severely biased and incorrect standard error. By definition: *"Essentially, all the models are wrong, but some are useful"*, as mentioned by Box and Draper [97]. This famous quote can be separated into two main points:

1. Due to approximations and simplification, some models may be near the truth and only a little wrong. This case can be especially applied to "hard" science (e.g. physics, chemical engineering...). As an example, neglecting the heat dissipation by frictions of a rotating stirrer in a non-viscous solution may be only a little wrong. In social studies, considering a sample of 10 people about their taste in food representing the overall population of a country (e.g. Switzerland, 8 millions people) may be completely wrong.

2. The simplifications and approximations made in the models may be quite useful for a better understanding, predictions and/or optimisations of various aspects of the reality. As an example, maps are a type of model; they are wrong. But good maps are very useful [98].

In addition, a problem in the model structure can also be a large cause of error. Therefore, comparison of the model outputs (prediction) with actual observations and/or theoretical prediction is an essential step toward an accurate and valid predictive model [29]. According to Velleman: *"A model for data, no matter how elegant or correctly derived, must be discarded or revised if it does not fit the data or when new or better data are found and it fails to fit them"* [99]. These words make totally sense in the context of this work.

Resampling methods may be useful in such situation to obtain consistent estimator of bias and standard error to validate a predictive model. One can find a large number of resampling approach throughout the literature [100–103]. Among them, the Leave-One-Out (LOOCV) and Leave-p-out (LPOCV) Cross-Validation were preferred to assess the performances of the different predictive model and their estimates used along this work.

2.5.2 Cross-Validation

A general approach of the LOOCV is illustrated in Figure 2.17 and can be proceeded as follow:

1. Let $D = \{s_1, s_2, ..., s_p\}$ be a data set containing p experiments of size m, from which two subsets are formed: the training set $D_T = \{s_i, ..., s_{j-1}, s_{j+1}, ..., s_p\}$ of size $p-1$ and the validation set $D_V = \{s_j\}$ of size 1 where s_j is an experiment not comprise in D_T.

2. The training set D_T is used to evaluate the parameter estimate $\theta_{opt,j}$ of size n

while the validation set D_V is compared to its prediction P_V using the model and the parameter estimate $\theta_{opt,j}$.

3. The Sum of Squares Errors (SSE_j) between the Prediction P_V and the observation D_V is assessed and collected:

$$SSE_j = \sum_{i=1}^{m} \left(y_i - f(t_i, \theta_{opt,j})\right)^2 \tag{2.79}$$

4. The steps 1 to 3 are repeated until all observations have been considered one time as a validation set.

5. The parameter estimate values collected are averaged (individually for each parameter) and used to evaluate their respective confidence intervals.

The average value of each parameter i can be assessed as

$$\overline{\theta}_i = \frac{\sum\limits_{j=1}^{p} \theta_{i,j}}{p} \tag{2.80}$$

The standard deviation of θ_i can be determined as

$$\sigma_{\theta_i} = \sqrt{\frac{\sum_{j=1}^{p} \left(\theta_{i,j} - \overline{\theta}_i\right)^2}{p}} \tag{2.81}$$
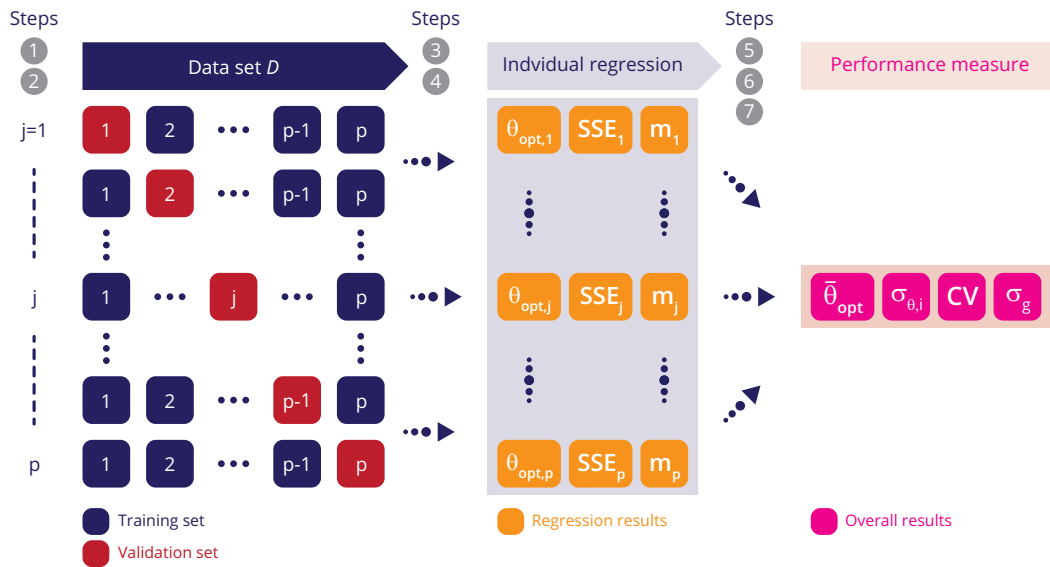
Figure 2.17 – Illustration of a the Leave-One-Out cross-validation with the corresponding steps to perform it.

Based on the given data, the confidence interval can be stated as

$$\left(\overline{\theta}_i - z^* \frac{\sigma_{\theta_i}}{\sqrt{p}} \quad ; \quad \overline{\theta}_i + z^* \frac{\sigma_{\theta_i}}{\sqrt{p}} \right) \tag{2.82}$$

where z^* is used as the confidence criteria based on the probability (99% $\rightarrow$ $z^* = 2.576$; 95% $\rightarrow z^* = 1.96$).

6. The collected SSE_j are then used to calculated the Cross-Validation criterion as follows:

$$CV = \frac{1}{p} \sum_{j=1}^{p} SSE_j \tag{2.83}$$

This criterion assesses the goodness of the estimated model based on the observed data. A valid model should show a good predictive accuracy namely a low CV. Generally used to discriminate a good model among several ones, it can be of great use to determine the necessity of new measurement as it will be shown in the further development.

7. The global standard error of prediction can be calculated as

$$\sigma_g = \sqrt{\frac{\sum_{j=1}^{p} SSE_j}{\sum_{j=1}^{p} m_j}} \tag{2.84}$$

Finally, a good predictive model will present a low CV, a low global standard deviation σ_g and a good $R - square$ at the end of the LOOCV.

The same approach can be used for LPOCV; in place of considering only one out, several are selected and taken out of the regression process.

Along with this chapter, we have presented the methods that will help the further developments. It remains, however, that without analytical data, any description of these models and also use of validation methods are impossible. Therefore, the next chapter will focus on the instruments and their operating principle that will provide accurate and useful experimental data.

3

Thermal Analysis & Calorimetry

If you give people tools, and they use their natural abilities and their curiosity, they will develop things in ways that will surprise you very much beyond what you might have expected.

Bill Gates, 1955-

Thermal Analysis (TA) and Calorimetry are respectively broadly used methods and tools which can be used for the determination of thermodynamic properties of chemical compounds or materials and also for the characterisation of reaction thermodynamics and kinetics [104]. The roots of TA and Calorimetry can be traced back to Lavoisier and Laplace in the 1780's with their controversial isothermal ice calorimeter used with the purpose to establish the thermodynamic properties of guinea pig respiration [105, 106]. In 1910, Hugh Longbourne Callendar framed the definition of calorimetry for the 11th Britannica Encyclopaedia as following: *"Calorimetry: the scientific name for the measurement of quantities of heat (Lat. calor), to be distinguished from thermometry, which signifies the measurement of temperature. A calorimeter is any piece of apparatus in which heat is measured. This distinction of meaning is purely a matter of convention, but it is very rigidly observed. Quantities of heat may be measured indirectly in a variety of ways in terms of the different effects of heat on material substances. The most important of these effects are (a) rise of temperature, (b) change of state, (c) transformation of energy"* [107].

Even if the calorimetry was known since long before, this definition was certainly the first brick of all the further development the last century was able to observe. In addition, there have been a large variety of development in this area since the mid-1970s and especially in the last two decades [108] due to the fast growing computer development. Different chemistry fields benefit of these technologies such as:

- Pharmaceutics, where thermal analysis and calorimetric instrumentation play an important role in preformulation characterisation and drug product development [109].

- Polymers, where TA and calorimetry are used to explore the thermal aging and thermodynamic properties of polymer materials (melting, crystallization, glass transition...) [110].

- Safety and process development, where calorimetry allows to assess potential secondary reactions (e.g. decompositions), which may lead to catastrophic results, or to explore the reaction system and evaluate its controllability [30, 111].

This list is non-exhaustive, but shows the versatility of calorimetry and thermal analysis that is used in very different branches of science, since thermal effects can be found practically in almost all physical phenomena.

Nowadays, a wide range of TA methods are available (Table 3.1). Among them, the focus is directed toward Differential Temperature Analysis (DTA) and Heat Flow (HF). These methods are used for several kind of calorimeters operating at different scales, such as Differential Scanning, Tian-Calvet and Reaction Calorimeters with the aim to assess reaction kinetics, and provide data for process optimisation and process safety.

Table 3.1 – List of the mostly used methods in Thermal Analysis and calorimetry

Analysed variable	Methods	Abbreviation
Mass	Thermogravimetry	TG
Temperature difference	Differential thermal analysis	DTA
Heat Flow rate	Differential scanning calorimetry	DSC
Heat Flow rate	Reaction calorimetry	RC
Evolved gas	Evolved gas analysis	EGA
and many others...		

Some of these calorimeters are presented in further details and ranked by their respective sample size, namely milligram-, gram- and kilogram-scale in the following section.

3.1 Principles of Thermal Analysis and Differential Scanning Calorimetry

Differential Thermal analysis (DTA) and Differential Scanning Calorimetry (DSC) are the most widely used thermal analysis methods [112, 113]. The concept underlying such analysis is based on a temperature (DTA) or heat flow (DSC) difference measurement between the sample and a reference, where both of them are identically subjected to an increasing or decreasing or even constant temperature profile [114].

An illustration of a classical DTA and heat-flux DSC instruments are represented in Figure 3.1: the sample and a reference are installed in a chamber (furnace) where a flow of inert gas is applied. The furnace temperature is controlled in order to follow a temperature setpoint profile while the temperature or/and heat flow difference between the two containers is recorded [113, 114]. Between these two types of technics, based on the same principle, only the location of measurement is different. In classical DTA, the sensors are generally immersed in the sample and reference. In heat-flux DSC or in the DSC after Boersma, however the sensors responsible of the temperature and/or heat flow measurement are placed under the containers and may be composed of one to several thermocouples [115].

The relation between the sample and the reference can be expressed as:

$$\Delta T = T_s - T_{ref} \tag{3.1}$$

where T is the temperature of the sample s and a reference ref.
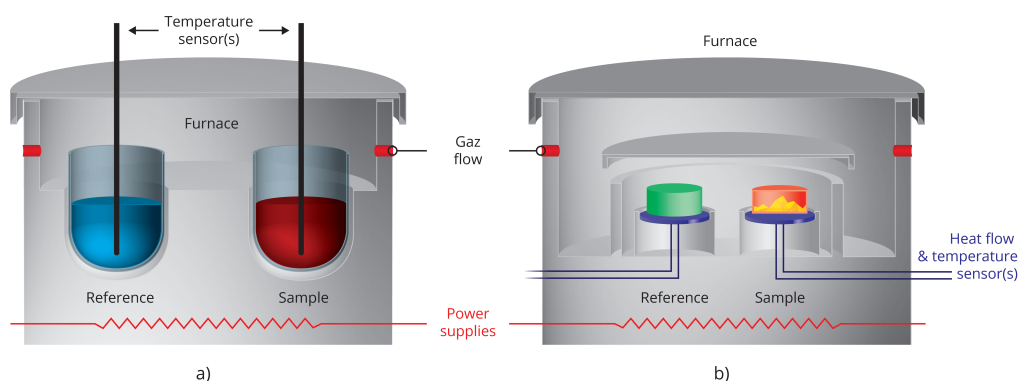
Figure 3.1 – Illustration of a) a classical DTA instrument and b) a classical DSC.

In non-isothermal experiment, no deviations in the temperatures will be observed if no physical or chemical event occurs, the temperature of the sample and the reference will simply adapt to the furnace one following temperature set profile (small deviations due to different heat capacity can be observed). In case of an endothermic event in the sample, the sample temperature falls below the reference temperature and is represented by a negative peak, whereas an exothermic event makes the sample temperature rise above the reference temperature and results in a positive peak as illustrated in Figure 3.2. In the case where the temperature difference is written in the opposite direction $(T_r - T_s)$, the same statements with an opposite direction will be applied.
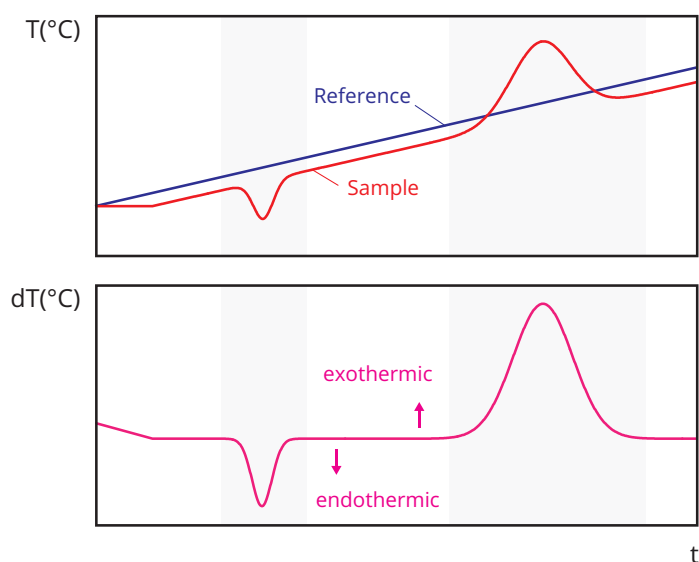
Figure 3.2 – Typical DTA Curve for a sample undergoing an endothermic melting followed by an exothermic decomposition under a linear heating ramp.

The peak area is directly related to both the thermal change ΔQ (in the case of a constant pressure) and the sample size m_s according to:

$$\Delta Q = K(T) \int\limits_{t_0}^{t_{end}} \Delta T \cdot dt = \Delta_x H \cdot m_s \qquad (3.2)$$

Where ΔH is the enthalpy of the transformation x (f: melting; r: reaction ...) in $(J \cdot g^{-1})$. The enthalpy is the first thermodynamic and safety information that can be obtained from such an analysis [116]. K is a proportionality constant that is temperature-dependent and influenced by the thermal properties of the sample and container. This relationship can be expressed as:

$$K = f(T) \qquad (3.3)$$

Once these characteristics have been defined for the considered type of container (e.g. Aluminium, Gold...) through calibrations (e.g. Indium, Tin...), the ΔT signal can be processed to give an output signal in heat flow rate units (W), an information that can be interpreted as proportional to the reaction rate, described as a differential entity, in opposition to concentration experiments, which are integral entities. This confers the heat flow a higher sensitivity to changes.

Such investigation can also help for the thermal screening of the reaction mixture and lead to the discovery of secondary reactions.

Although sensitive and convenient, DTA and DSC method contains two factors militating against their accuracy:

1. the assumption of a constant value of the sample heat capacity and,

2. the assumption of a uniform temperature and composition throughout the sample and reference along the experiment.

The second problem may be solved or at least lowered by using sufficiently small sample masses to ensure micro-mixing.

3.1.1   Application: Differential Scanning Calorimeter

Two types of Differential Scanning Calorimetry are available, differing in their respective design and measuring principle [117]:

Furnace

Reference

Sample

Gaz outlet

Individual chamber

Crucible

Gaz inlet

Temperature sensor(s)

Power supplies
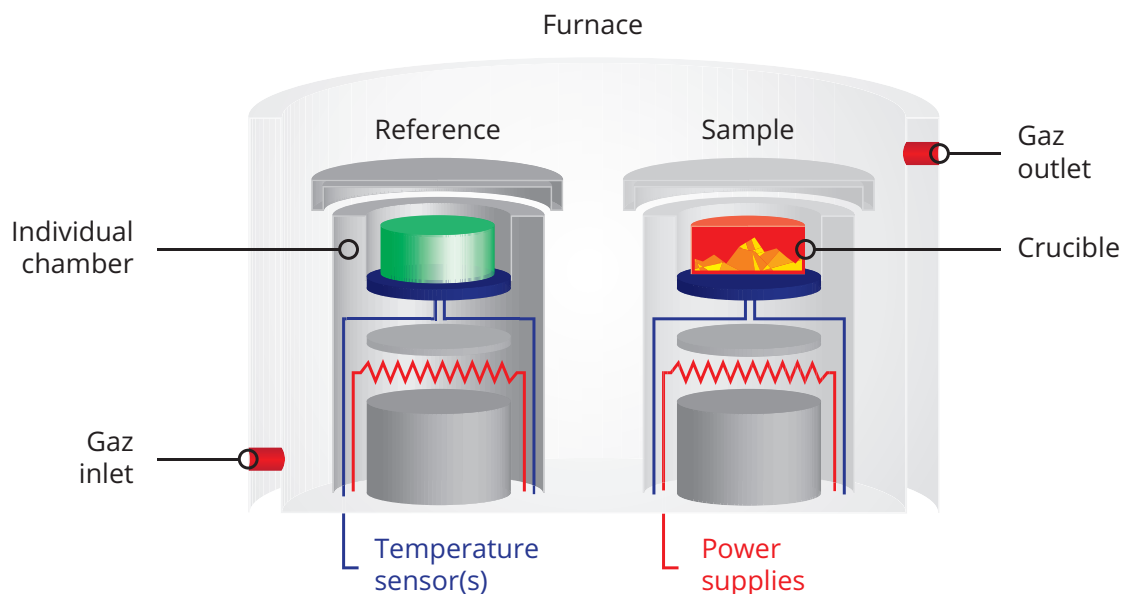
Figure 3.3 – Illustration of a power compensated Differential Scanning calorimeter.

1. *Power-compensation*: the aim of such instrument is to maintain a constant temperature difference between the sample and reference throughout the temperature setpoint profile by using power suppliers to compensate any change. The configuration is illustrated in Figure 3.3 and consists of an individual measurement element composed of a temperature sensor and a heating resistance. The heating resistance is then controlled to compensate the sample heat consumption or production in the reference and vice versa, thus, the temperature difference is kept constant despite the transformations. The signal is given by the power difference of both heating resistances (sample, reference).

2. *Heat-flux*: the configuration is slightly different (Figure 3.1b) as the containers are hold side by side in the same furnace and subjected to the same heating source. In general, each container, which possesses its own temperature sensors, is placed on its respective position on the measurement support (metallic or ceramic). The signal is given as the temperature difference (sample-reference) which is calibrated to provide the power.

A characteristic that both types of DSC have in common is that the signal is proportional to the heat flow rate and not only the heat of the event. This aspect allows to describe the time dependence of a transformation which can be really convenient for reaction kinetic study (Chapter 4) or safety assessment (Chapter 6).

In both cases, the heat flow sensors are placed under the containers making them a two-dimensional measurement system. As a result, the sample may exchange heat directly with the surrounding furnace and not be measured by the heat flow sensors

up to more than 50% [118]. Nevertheless, by assuming that the same heat losses are observed for the sample and reference, such inaccuracies can be lowered using efficient calibration methods (e.g. Tzero technology) or by using other type of sensors as presented in the next subsection.

3.1.2   Application: Tian-Calvet Calorimetry

The concept behind Tian-Calvet calorimeter remains the same as for DSC, a comparison under the same operating conditions between the sample and a reference is required. In terms of construction, however, such instrument can operate at larger sample size (up to several grams) and compared to a two-dimensional measurement system (DSC), the measurement sensor is based on a three-dimensional Tian-Calvet type (Figure 3.4b).

The heat flow sensor is formed by several rings composed of a large number of thermocouples connected in series and called "thermopile". Two thermopiles, characterised by a high thermal conductivity, are surrounding individually the sample and reference. The radial configuration of the calorimeter guarantees an almost complete collection of the heat. It was shown in different studies that Tian-Calvet can measure up to 94% of the heat exchanged with the container and leading to an accuracy of about 1% for heat capacity and latent heat determination [118].

In addition, the pressure inside the container can be followed along the experiment and thus, helpful to determine the total pressure generated during the studied events. This last aspect may be used for the correct sizing of emergency pressure relief.

3.2   Principles of heat flow calorimetry

A large number of chemical processes are accompanied by temperature changes related to heat consumption or release due to occurrence of reaction(s). As such kind of experiment is reproducible and definite, the direct evaluation of different reaction characteristics can be made and used for reaction kinetic investigation, safety assessment and/or scale-up.

In reaction calorimetry, the sample of kilogram size is not compared to a reference, oppositely to DTA or DSC. The underlying concept is based on heat and mass balances around the reactor as demonstrated along the reactor model development in Section 2.2.2. Under this denomination, two main methods can be highlighted depending on the type of quantity measured:
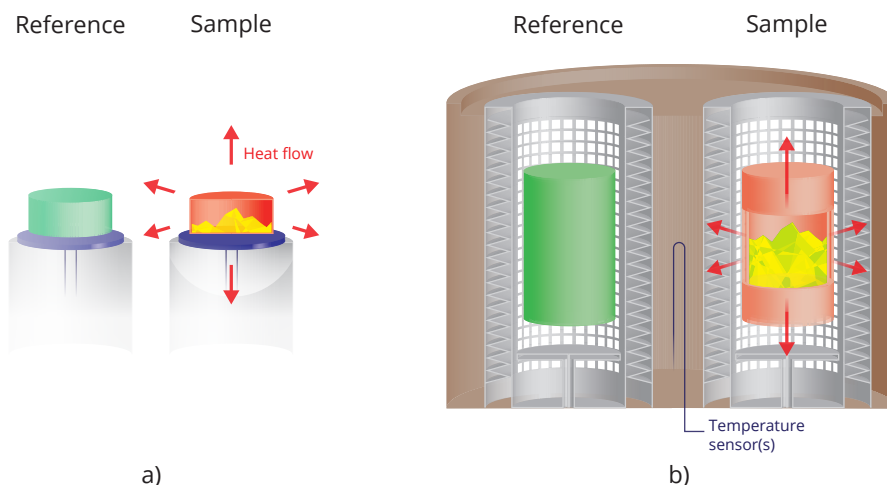
Figure 3.4 – Illustration of different sensor configurations in Differential Scanning and Calvet calorimeters.

1. *Heat flow calorimetry*: measurement of the current value of the jacket and reactor temperature.

2. *Heat balance calorimetry*: measurement of the heat carrier mass flow rate, the inlet and outlet jacket temperatures.

All of these methods have the same aim, namely characterising the heat exchanged between the heat carrier and the reaction mixture during a considered event (e.g. reaction(s), phase transition,...) under operating conditions approaching large-scale ones. Thus, the heat of the observed transformation is deduced from the basis of calibrations (heat flow) or heat balances. Other aspects of the experiment can be investigated such as the specific heat capacity, the influence of the process temperature, the feed and its temperature and many others. The following part will explain these two methods more specifically. For more information regarding the different types of Reaction Calorimeters, a recent and extensive study was performed by Zogg and al. [119] while the principles of reaction calorimetry were deeply explained by Karlsen and Villadsen [120].

3.2.1 Heat Flow Calorimetry

The principle behind the heat flow calorimetry is based on calibrations before and after the experiment in order to characterise the heat transfer through the wall (Figure 5.2) and the heat accumulation by the reaction mixture (section 2.2.2.2.3). These calibrations allows to define two parameters required to establish the differential
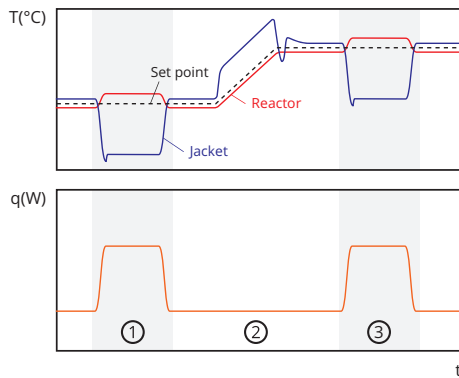
Figure 3.5 – The standard calibration is separated in three zones: 1) and 3) present the determination of the overall heat transfer coefficient UA with a Joule effect probe at the temperature T_{set} while the jacket temperature is controlled to keep the reaction mixture under isothermal conditions, 2) represent the determination of the specific heat capacity through a temperature increase using the jacket.
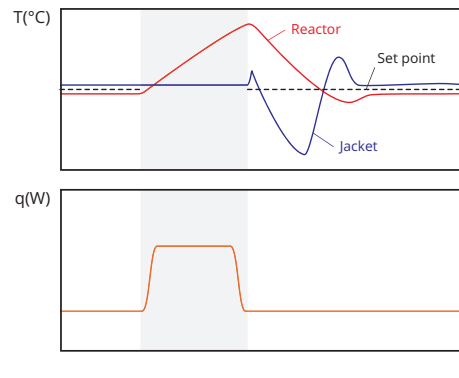
Figure 3.6 – The QuickCal is used for a rapid determination of the overall heat transfer coefficient UA and the specific heat capacity, $c_{p,r}$ through computational processing of an experiment comprising a joule effect temperature increase followed by a T_r-cascade control.

heat balance (2.28):

1. The global heat transfer coefficient UA and,

2. The heat capacity of the sample $c_{p,r}$.

Once these parameters are evaluated, an interpolation is made in order to describe their changes along the experiment course. Different types of interpolation can be used (in function of the mass, the virtual volume...).

The calibrations can be performed in two different ways:

1. *The standard calibration*: using a Joule effect to provide a defined heat quantity resulting in an answer of the jacket to keep the vessel content under isothermal conditions. Then, an increase of the sample temperature at a constant rate is applied using the controlled jacket as illustrated in Figure 3.5 and described by the relations in equation 3.4:

$$UA = \frac{\int q_c \ dt}{\int (T_r - T_a) \ dt} \qquad \longrightarrow \qquad c_{p,r} = \frac{\int UA \ (T_r - T_a) \ dt}{(T_{r,2} - T_{r,1})} \qquad (3.4)$$

q_c is the heat flow provided by a Joule effect probe, $T_{r,1}$ and $T_{r,2}$ are the bounds of the temperature ramp. Such investigation can be relatively time consuming

as it requires the system to be completely controlled and stabilized in terms of temperatures [121].

2. *The Quick Calibration*: developed by Mettler-Toledo, in this case, the temperature controller governs the jacket temperature (isoperibolic mode) and the calibration consists in a mixture of the previous method and based on a simultaneous non-linear regression. Such type of calibration consists in different phases [121]:

    (a) The reaction mixture temperature rises through a Joule effect probe releasing a constant heat flow. This increase stops after a minimum difference of $1.5°C$ while the jacket is kept constant (isoperibolic operating conditions).

    (b) the jacket is triggered and adjusted to make the reaction mixture reach a temperature set point (generally the starting temperature) while the Joule effect probe is stopped.

    (c) After the two events, a non-linear regression is performed simultaneously on both zones of the signal in order to evaluate the parameters UA and $c_{p,r}$.

Once these parameters are known, the reaction heat flow can be deduced from the general differential heat balance (2.28) assuming a non-viscous reaction mixture and no mixing effects such as:

$$q_{rxtot} = q_{acc} - (q_{ex} + q_{loss} + q_{in}) \qquad (3.5)$$

Such method confers several advantages: (i) high sensitivity due to the temperature difference between the heat carrier and reaction mixture, (ii) high accuracy and fast response and (iii) independent of the heat carrier flow rate. A major problem, however, is the determination of the exact overall heat transfer coefficient UA along the process course. The latter may change due to composition, density and viscosity or stirring rate changes having a direct impact on the heat transfer, namely the inner wall heat transfer resistance.

Different calibration procedures were developed to overcome the above-mentioned problem as *Continuous Calibration* or *Absolute Heat Flux Calibration* but will not be investigated along this research work [122–124].

3.2.2 Principles of heat balance calorimetry

Although heat flow calorimetry seems to be suitable for many points in terms of processing, it may not be always applicable (at least at large-scale) [125].

While the overall heat transfer is largely modified along the reaction course (e.g. polymerization), heat balance provides results that are independent of the changes in heat transfer properties during the reaction [110].

The method is generally performed when the physical properties of the jacket are well established and monitored along the reaction course. These properties are the mass flow, the inlet and outlet jacket temperatures and finally, the heat capacity of the heat carrier. As a result, by performing a total heat balance around the cooling system, the quantity of heat brought or removed by the jacket can be evaluated and compared to the event actually occurring in the reaction mixture. As an example, the cooling system is set to operate under isothermal conditions while an autocatalytic exothermic reaction is releasing a certain amount of heat; such event will result in a decrease of the jacket temperature. The inlet temperature will enter colder than the outlet one as the heat carrier is actually removing the heat by absorbing the heat released from the reaction mixture. This phenomena is the direct action of the cooling system operating to remove the heat generated by the reaction as illustrated in Figure 3.7 and equation 3.6.

$$Q_{event} = \dot{m}_j \; c_{p,j} \; \int_{t_0}^{t_f} \left(T_{j,out} - T_{j,in} \right) \; dt = -\Delta_r H \; m_r \tag{3.6}$$

Where in an out are the inlet and outlet measurement locations of the jacket, respectively.

A disadvantage is that the heat balance calorimetry is relatively slow and less sensitive than heat flow calorimetry due to the low flow rate used in order to get a measurable temperature difference between the jacket inlet and outlet. Such method, however, may be more suitable regarding large-scale calorimetry.

3.2.3 Application: Reaction Calorimeter RC1

The typical example to describe a heat flow calorimeter is the Mettler-Toledo RC1. This type of reactor is usually used for scale-up and safety oriented studies, it allows to perform a large number of tasks where a very fast and efficient control of the temperature is required. Such temperature control is provided by a well-build and oversized cooling system allowing fast actions as illustrated in Figure 3.8.

The special configuration of the jacket is described as follow:

  (a) A coolant tank is kept at a low temperature using a cryostat coolant circulation.
  (b) A controlled valve allows a fast addition of the cold heat carrier, while the warm one is released in the coolant tank. As a result, the heat carrier temperature is
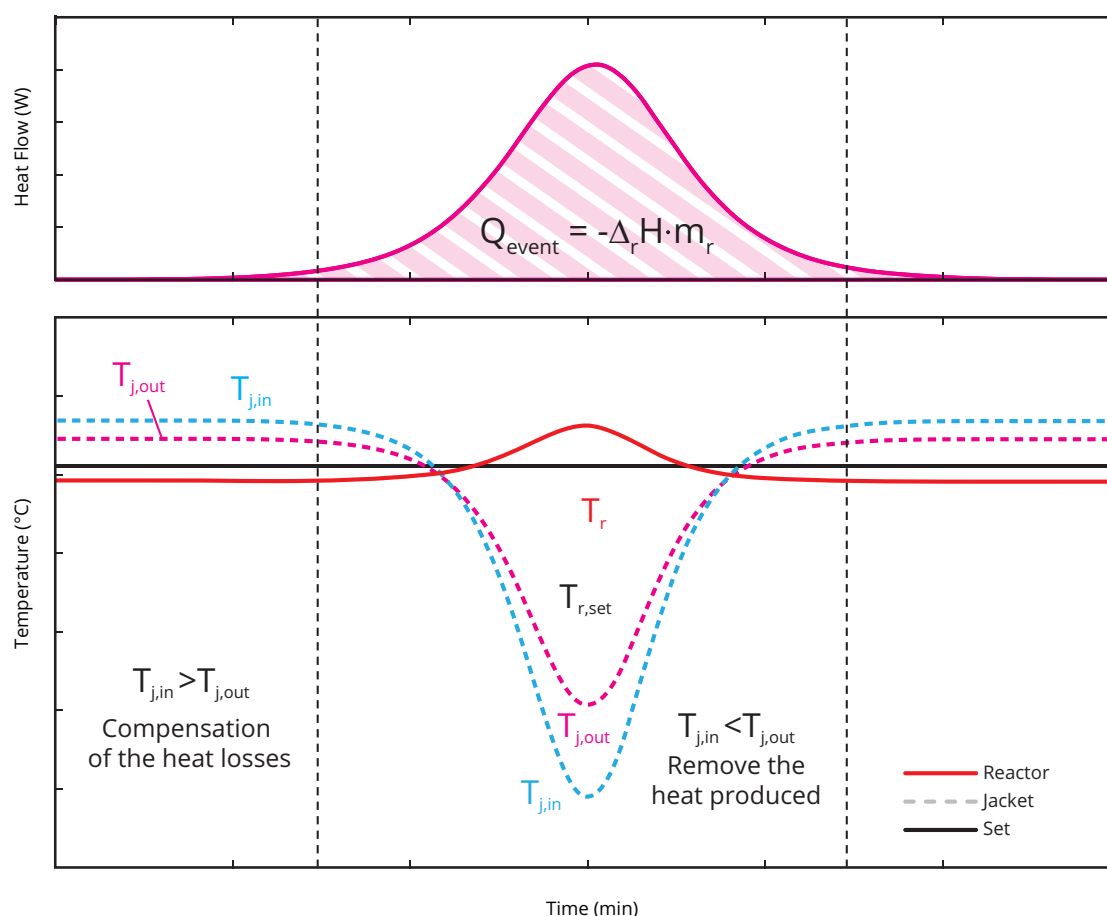
Figure 3.7 – Illustration of typical temperature profiles in the case of a Reaction Calorimeter operating in heat balance.

increased due to the addition of warm heat carrier coming from the cooling system as illustrated in Figure 3.9.

(c) The heating is performed through an electrical heater placed on the heat carrier circuit. This heater operates only in on/off control, a system quite reactive to changes.

Due to this fast heat carrier circulation, the jacket temperature is estimated as identical in inlet and outlet of the jacket. The heat flow is not calculated using directly the jacket temperature, but rather by an estimated wall temperature, accounting for the resistance of the reactor wall.

In case of emergency (e.g. safety limits triggered), the jacket operates under a full cooling state, namely the content of coolant tank replaces entirely the current warm heat carrier. As a consequence, the heat released from the reaction system is removed quickly and allowing an efficient cooling of the reaction mixture.
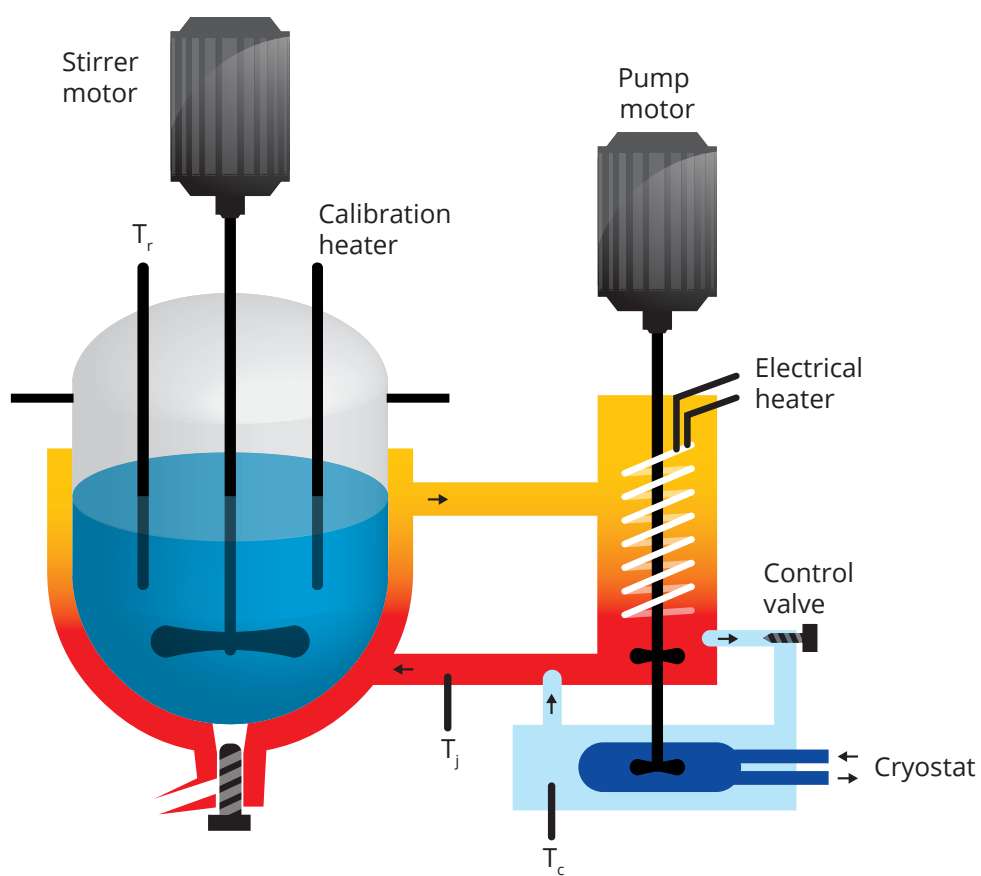
Figure 3.8 – Typical configuration of a Mettler-Toledo RC1.
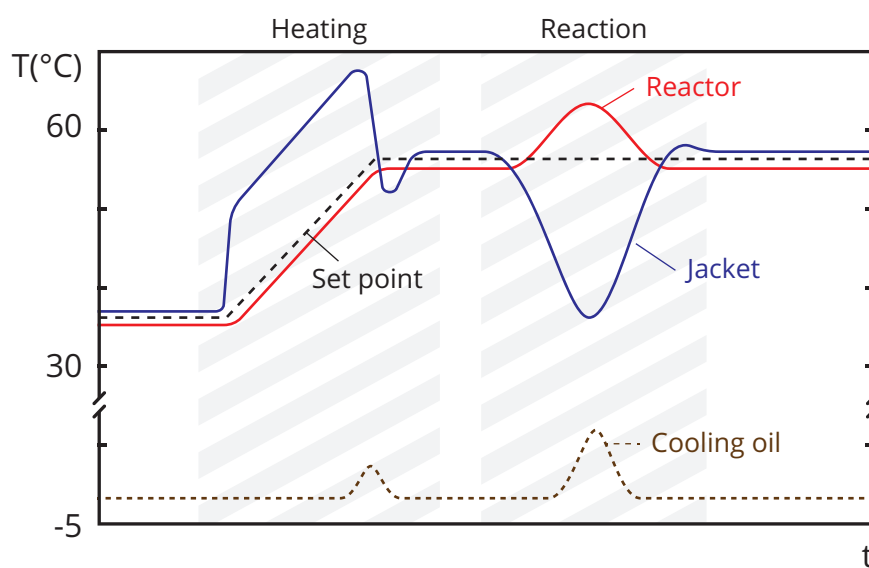
Figure 3.9 – Behaviour of the different actors of the cooling system, namely the reactor, jacket and cooling oil temperatures.

4

Reaction Kinetic Investigation

A behaviour is determined by its consequences.

Burrhus F. Skinner, 1904-1990

Nowadays, in the fine chemical industry, relatively fast and exothermic reactions are usually performed under fed-batch operating conditions, by adding one or several reactants at a sufficiently low rate to control the accumulation of unconverted reactants [126]. This accumulation is one of the major safety issue generally encountered when the rate of the reaction is slower than the rate of addition [30, 72, 127]. As soon as a sufficiently low accumulation of the added reactants is achieved, the safe operating conditions can be considered fulfilled even under equipment malfunction (e.g. adiabatic conditions) since the heat released by the reaction system will conduct to a safe reactor state [128].

Understanding and controlling this aspect is one of the most important and challenging process safety tasks [30]. One of the solutions which can help to prevent this unwanted scenario, namely the loss of control of the reaction course due to accumulation of unconverted reactant, is to develop an appropriate feeding strategy using a trial and error approach [30, 31]. This approach, however, is disadvantageous in terms of reaction time and costs. As a consequence, to solve this problem in an optimal way, the reaction kinetics has to be known [129].

In order to assess, predict and control the accumulation of unconverted reactants efficiently, save resources and effort, the overall dynamic behaviour of the reaction system can be represented by two mathematical models (Figure 2.2):

1. *The reaction kinetic model* (Section 2.2.1.2), based on an hypothesis of the reaction scheme considering the different reactions occurring during the process course and,

2. *The reactor model* (Section2.2.2.2), based on the tool dynamics and its respective experimental conditions.

Over the past years, many papers have reviewed approaches to the development of reaction kinetics models and described the insight gained from them in various domains [33]. An interesting alternative to study kinetic phenomena is using numerical simulations. This kind of investigation can be very long due to the increasingly complex models, involving a large number of parameters and demanding a huge amount of experiments and time. Therefore, a new approach to solve these problems, focusing on an exploration at different scales (minimizing the amount used), saving the number of needed experiments and simultaneously optimising their use has to be developed.

The proposed approach can be summarized in two points:

1. Plan the required experiments in a systematic way to optimally cover the experimental space (section 2.3) based on a multi-scale approach and a minimum of experiments.

2. Estimate the kinetic parameters based on models of the acquired experiments.

This two last points are extensively investigated throughout this chapter under four main parts: the first part presents a procedure and shows how concepts and mathematical expressions can describe calorimetric experiments and such at different scales. The second part is focused on the data handling followed by a third part exclusively dedicated to the regression problem of the reaction kinetics. Finally, the last part illustrates a number of simulated and real examples to demonstrate the applicability of the Reaction Kinetic Investigation.

4.1 The procedure

A reaction system is generally composed of one to several reaction pathways which may occurring simultaneously and differently according to current the operating conditions. An overview of such system behaviour may require a large number of experiments in order to widely cover the experimental space of operating conditions the reaction system may encounter. Thus, such system can be studied in an optimal way if the experiments are well distributed along the different laboratory scales (from mg to kg) and operating conditions (mode (BR, FBR), temperature-control and reactant ratios) [4]. In this manner, even critical reactions as decomposition reactions can be monitored and considered in the reaction kinetic model.

The identification of the reaction kinetic model requires some assumptions and considerations to simplify the regression problem and procedure. On the one hand, the assumption that the reaction system takes place in a homogeneous solution (perfectly mixed), allows to consider the reaction kinetics as scale-independent [130, 131]. On the other hand, each scale is characterised by its own way to control the heat transfer (oven, jacket,...), a multiscale approach allows to explore the influence of the temperature and reactant ratio under very different operating conditions [64, 132]. In addition, the evaluation of the kinetic parameters (activation energy, pre-exponential factor and reactant orders) is bounded to constant parameters along the reaction course and between the different experiments (see section 4.3).

The Reaction Kinetics Investigation is a procedure where different methods and heat flow experiments (Differencial Scanning (DSC), Calvet and Reaction Calorimetry (RC)) are used in an optimal way to get kinetic models, focusing on a multi-scales and -conditions approach. This procedure is divided into four major steps designed on the basis of the model creation (section 2.1) which are illustrated in (Figure 4.1) and are represented as follows:
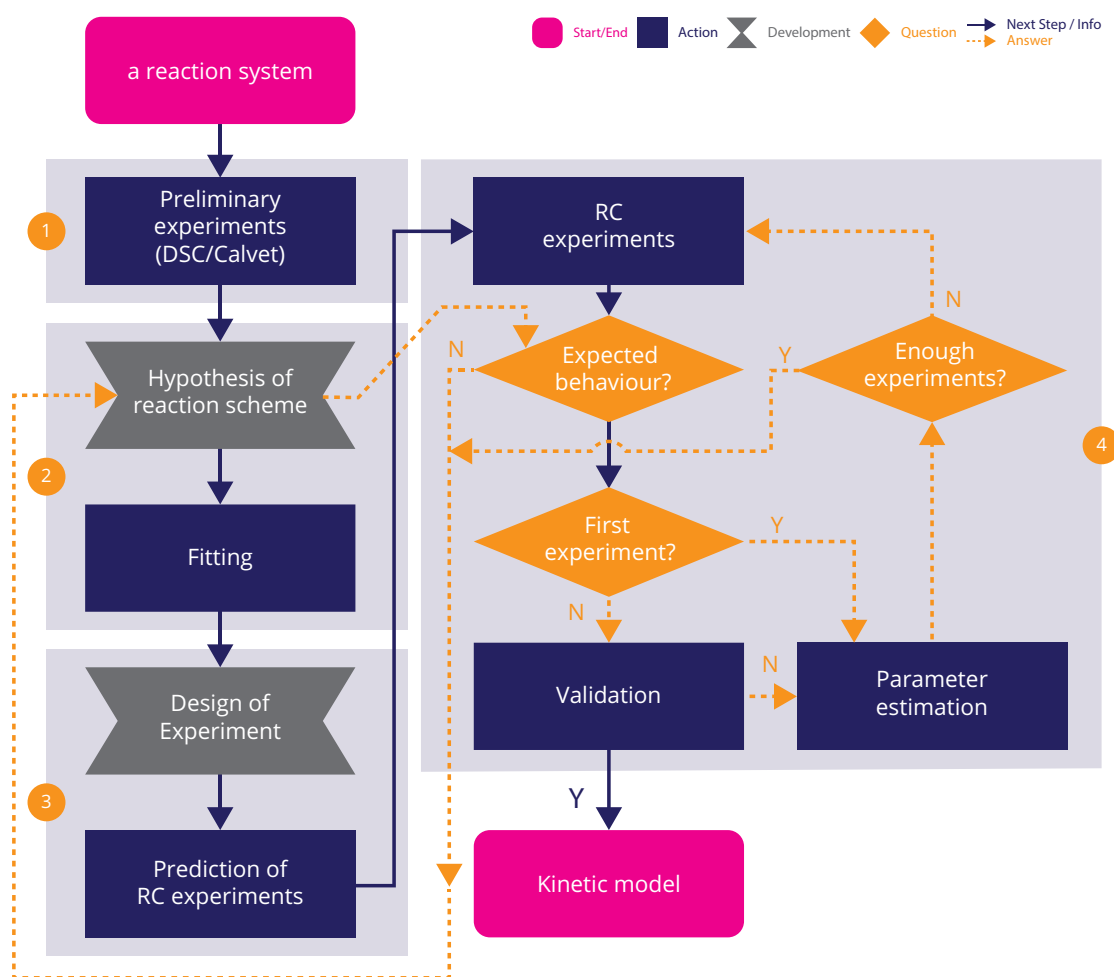
Figure 4.1 – Illustration of the Reaction Kinetic Investigation divided in four main steps: 1) Preliminary experiments, 2) Model structure creation, 3) Planning of the Reaction Calorimetry experiments and 4) Improvement of the reaction kinetic model.

Step 1: **Preliminary experiments**

The preliminary experiments will serve as screening experiment to explore the overall thermal behaviour of the considered reaction system under batch conditions (DSC (milligrams), Calvet (grams),...). This kind of experiment is mainly used for its low material consumption, a large range of temperature screening (-90 to 500 $°C$) and short experimental time. In addition, highly exothermal secondary reactions may be triggered allowing to avoid them during reaction calorimetry experiments rending those safer. Therefore, to optimally cover the temperature and concentration effects, a reaction composed of n reactants should be investigated by at least $n+1$ experiments with different reactant ratios and temperature scan rates as presented in the following example:

$$A + B + C \xrightarrow{k} D$$
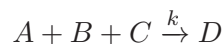
$$Where \quad n = 3$$

$$Experiment \quad 1 : 1A : 1B : 1C \qquad 2K/min$$

$$Experiment \quad 2 : 1A : 1B : 2C \qquad 1K/min$$

$$Experiment \quad 3 : 1A : 2B : 1C \qquad 1.5K/min$$

$$Experiment \quad 4 : 2A : 1B : 1C \qquad 4K/min$$

The temperature scan rate can be selected randomly or based on a Design of Experiments. The obtained heat flow information $q_{rxtot,p}^{exp}$ represents the small-scale (DSC, Calvet) parameter estimation data set.

Step 2: **Hypothesis of the reaction scheme and model approximation**

A hypothesis of the reaction scheme (summary of the overall mechanism) has to be postulated to create the framework of the reaction kinetic model. The central idea brought by this hypothesis is to define the rate expressions describing the apparent concentration of the reacting species, oppositely to elementary reactions describing the basic steps of a reaction mechanism. The chemical information, the preliminary experiments and the known or expected reactant interactions will help to postulate it.

The previously formed data set (DSC and Calvet experiments) is used to roughly estimate the different kinetic parameters (reactant orders, pre-exponential factors and activation energies). With this purpose, the reaction scheme hypothesis and the law of mass action (Section 2.2.1.2) are used together to define the structure of the reaction kinetic model. The model is then used to predict the heat flow considering the experimental conditions of the experiment (temperature profile and initial component concentrations).

The regression is then performed globally; meaning that all heat flow experiments are simultaneously regressed using the same reaction kinetic parameters and model structure.

Step 3: **Design of Experiment and RC predictions**

Using the obtained preliminary information, larger scale experiments (hg, kg), closer to industrial practice can be designed. A Design of Experiment (DoE) is established considering fed-batch operating conditions in order to screen the influence of: 1) the reaction mixture temperature ($T_{r,set}$); 2) the number

71
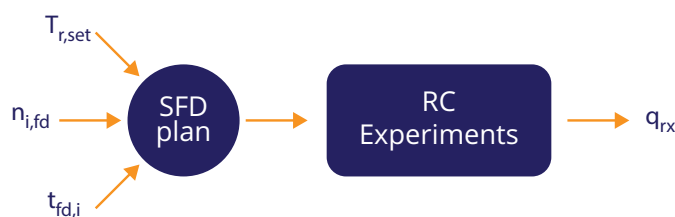
Figure 4.2 – Illustration of the Design of Experiment applied for RC experiments.

of moles added through the feed ($n_{i,fd}$) and 3) the time to feed them ($t_{fd,i}$) as illustrated in Figure 4.2.

Based on Space Filling Design methods (section 2.3), the number of different experiments can be chosen and uniformly distributed to the experimental space. A point worth mentioning when solely low reactant quantities are available.

The experimental space is defined using the preliminary information: the process temperature range is chosen such as secondary or unwanted reactions are avoided (on the basis of the preliminary DSC curves); the time to feed is evaluated by simulation using the developed preliminary model and the different thermodynamic information collected through DSC curves and literacy; finally, the number of moles added should allow to reach different ratio between the reactant, namely sub- and overstoechiometric state. It is not mandatory to have large ratio but only known ones [64].

Predictions using the roughly evaluated kinetic parameters in *Step 2* are performed to assess the potential risk scenarios of the RC experiments (e.g trigger secondary reactions).

Step 4: **RC experiments, improvement of the reaction kinetic model and validation**

For the RC experiments, the model development takes place as an iterative process, the reaction kinetic model is updated at each new experiment cycle. Thus, the model structure and parameters are adapted to describe as good as possible the real reaction system [133]. Moreover, the RC experiments are performed according to the previously obtained DoE and preliminary risk assessment (Step 3) and analysed according to the following points:

(a) Firstly, a visual check is performed; the experiment is qualitatively compared to its prediction to answer if the general behaviour is logically represented (heat flow comparison). In the case of large deviations (autocatalytic effect, unexpected peak...), the reaction scheme hypothesis may be wrong and should be redefined or corrected.

On the contrary, if the results are acceptable, a validation can be attempted (except for the 1st RC experiment, see point (d)).

(b) The validation is assessed quantitatively and depends greatly on the required model quality. The deviations between an experiment which was not comprised in the regression set and its respective prediction are estimated and analysed. A model is considered as satisfactory if its standard error of deviations is sufficiently small to be acceptable. If the validation is not satisfactory, the current experiment is added to the regression set and new parameters are evaluated.

(c) In case of non-significant change, meaning that the standard error of deviation between the data set and their respective predictions is not decreasing, the hypothesis of the reaction scheme may be erroneous and should be re-evaluated.

(d) Special attention should be given to the first RC experiment; this experiment cannot undergo validation as the effects brought by the latter are not yet considered in the regression set (feed, mass and volume change,...). As a consequence, the validation can only start after the second RC experiment.

The iteration restarts by doing a different experiment where experimental conditions derived from the DoE (*Step 3*). A prediction of the thermal behaviour of the reactive system can be performed using the new fitted kinetic parameters and avoid potentially dangerous conditions. The iteration will stop as soon as the validation is satisfactory according to the termination conditions defined by the purpose and need of the reaction kinetic model.

4.2 Data handling

Every calorimetric experiment can be considered as an experiment that has been performed in a reactor of a specific size (mg, g, kg), operating conditions (temperature scanning, isotherm, isoperibolic, adiabatic) and mode (batch, fed-batch or continuous) as explain in Chapter 3. These conditions can greatly differ from instrument to instrument making the obtained data different and full of information regarding the thermal behaviour of the reaction system considered.

These data differ in their way to describe the experiment. As a consequence, they have to be handled differently:

1. *Heat flow data*:

This type of data generally contain the temperature of the reaction mixture T_r (may be written T_s, for sample temperature) and its corresponding heat flow q_{rxtot}^{exp} as a function of time t (Table 4.1).

Most of the calorimeters require the initial mass of the sample analyzed. In case of reaction kinetic study, it is essential to record the initial composition as well.

Table 4.1 – Illustration of typical data obtained from heat flow data (mainly DSC and Calvet data).

index	$Time\ (s)$	$T_r\ (°C)$	$q_{rxtot}^{exp}\ (W)$
0	0	$T_{r,0}$	0
⋮	⋮	⋮	⋮

2. *Temperature and calibration data*:

Oppositely to *heat flow data*, in such experiment, the heat flow q_{rxtot}^{exp} is calculated from a full heat balance (as presented in paragraph 2.2.2.2.3 and 3.2). The reaction mixture and jacket temperatures, respectively T_r and T_j and the mass profile m_r are recorded along the experiment course.

Calibrations of the normalised heat transfer coefficient UA and the reaction mixture heat capacity $c_{p,r}$ (before and after the experiment) are necessary to consider the composition and volume changes (only for fed-batch mode) as presented in Table 4.2. The initial composition has to be recorded for the reaction kinetic study.

Table 4.2 – Illustration of typical data obtained from temperature and calibration data (mainly RC data).

| index | $Time$ | m_r | T_r | T_j | UA | $c_{p,r}$ | q_{rxtot}^{exp} |
Units	(s)	(g)	$(°C)$	$(°C)$	$(W \cdot K^{-1})$	$(J \cdot g^{-1} \cdot K^{-1})$	(W)
0	0	$m_{r,0}$	$T_{r,0}$	$T_{j,0}$	UA_0	$c_{p,r0}$	0
⋮	⋮	⋮	⋮	⋮	⋮	⋮	⋮

The information gained from such experiments allows to build up the data linking the heat flow with the operating conditions. The kinetic parameters of the reaction resulting in the heat evolution were processed with AKTS-Reaction Calorimetry Software after the optimisation of the baseline as presented in the next section and illustrated in Figure 4.3 [134].
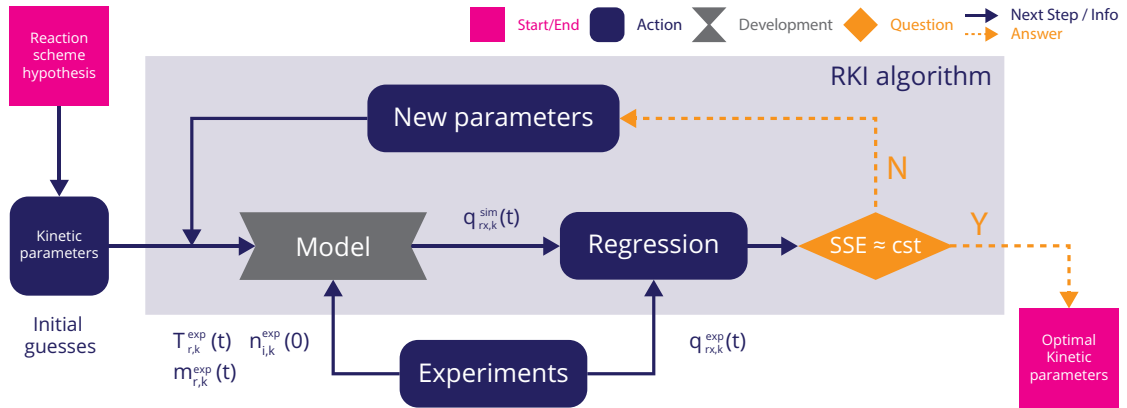
Figure 4.3 – Workflow of the regression problem to evaluate the reaction kinetic parameters (RKI algorithm) on the basis of experimental data at different scales.

4.3 The regression problem

The elaboration of the reaction kinetic model consists of a regression problem whose parameters are identified considering a non-linear least-squares fitting method (section 2.4). The modelled heat flow $q^{sim}_{rxtot,k}$ is compared to its respective experimental one $q^{exp}_{rxtot,k}$ as illustrated in Figure 4.3.

This problem can be expressed by the following minimization problem:

$$\min_{x} \sum_{k=1}^{p} \sum_{i=1}^{m} \left(q^{sim}_{rxtot,k}\left(t_i, x\right) - q^{exp}_{rxtot,k}\left(t_i\right) \right)^2 \tag{4.1}$$

where x is a vector of kinetic parameters considering all reactions j postulated in the reaction scheme hypothesis. This vector is described as:

$$x = \begin{cases} E_{a,1...j} & \in [0,\infty[\\ k_{0,1...j} & \in [0,\infty[\\ a_{1...i,1...j} & \in [0,\infty[\\ \Delta_r H_{1...j} & \in]-\infty,\infty[\end{cases} \tag{4.2}$$

$t \in [t_0, t_f]$ represents the time, whereas t_0 is the starting time and t_f the ending time of the experiment k containing m data points. The model describes the overall heat flow $q^{sim}_{rxtot,k}$ produced by the reaction system considering the reaction scheme hypothesis

and which is the solution of the following first-order differential equation:

$$q_{rxtot,k}^{sim} = m_{r,k} \sum_{j}^{J} \left(r_j \left(-\Delta_r H_j \right) \sum_{i=1}^{I} \nu_{i,j} M_i \right) \tag{4.3}$$

subject to the following conditions:

$$q_{rxtot,k}^{sim} \left(t_0 \right) = q_{rxtot,k}^{exp} \left(t_0 \right) \tag{4.4}$$

$$T_{r,k}^{sim} \left(t \right) = T_{r,k}^{exp} \left(t \right) \tag{4.5}$$

$$m_{r,k}^{sim} \left(t \right) = m_{r,k}^{exp} \left(t \right) \tag{4.6}$$

The continuous conditions may be constant (batch mode) or continuous (fed-batch mode) when the change are occurring over time.

The heat flow is directly proportional to the reaction rate, described by the reaction kinetics and dependent of the temperature. Therefore, by imposing the reaction mixture temperature profile provided by the experimental data, the simulated heat flow should be identical to the experimental one as long as the kinetic parameters are well-defined. With this assumption, it is possible to evaluate the optimal parameters describing as good as possible the experimental data.

As last assumption for the regression problem, the kinetic parameters are considered as independent over the experiment k and temperature, the temperature effect being described by Arrhenius law 2.12.

The parameter vector x can be expressed as:

$$x \perp T \tag{4.7}$$

$$x_1 = x_2 = ... = x_p = cst$$

4.4   Applied examples

4.4.1   Simulation of a complex reaction scheme

Simulated data of a complex reaction scheme were created using the model postulated in Section 2.2.1.   The data processing was performed using commercial software packages, namely AKTS-Reaction Calorimetry Software and MATLAB [134, 135].

In such an investigation, the reaction scheme and kinetic parameters are known unequivocally. As a result, the applicability range and limits of the developed procedure can be tested.

4.4.1.1 Reaction system

Suppose a complex reaction scheme occurring in a homogeneous solution, according to the following scheme:

$$A + B \xrightarrow{k_1} C$$
$$B + C \xrightarrow{k_2} D$$

(4.8)

The reaction kinetic parameters used to describe this system are presented in Table 4.3 and which the rates of reaction are:

$$r_1 = k_1 C_A^{a1} C_B^{b1}$$
$$r_2 = k_2 C_B^{b2} C_C^{c2}$$

(4.9)

and the transformation rates:

$$R_A = -r_1$$
$$R_B = -r_1 - r_2$$
$$R_C = r_1 - r_2$$
$$R_D = r_2$$

(4.10)

4.4.1.2 Preliminary experiments

The reaction kinetics depends on the parameter values characterizing specifically a considered reaction system. This preliminary investigation allows to discover and understand how the different species interact with each other and giving access to the stoichiometric coefficient interpretation. In addition, the data are used to define the rate equations, which give also access to roughly estimated kinetic parameters.

Table 4.3 – Reaction kinetic parameters used for the demonstration of the procedure presented in section 4.1 and for the reaction scheme presented in equation 4.8.

Reaction 1				
	k_0	E_a	$\Delta_r H$	*Orders*
Units	$(g^{0.5}s^{-1}mol^{-0.5})$	$(J \cdot mol^{-1})$	$(kJ \cdot mol^{-1})$	$(-)$
Value	$1 \cdot 10^8$	65000	-50	$a1 = 1$ $b1 = 0.5$
Reaction 2				
Units	$(g^{1.2}s^{-1}mol^{-1.2})$	$(J \cdot mol^{-1})$	$(kJ \cdot mol^{-1})$	$(-)$
Value	$1 \cdot 10^9$	75000	-54	$b2 = 1.2$ $c2 = 1$

The reaction system considered here is constituted of 4 species (A, B, C and D) as described in equation 4.8. The physical properties, namely the molar mass and specific heat capacity, necessary for the simulations are presented in Table 4.4 while the different simulated experiments with their specific conditions (rate and composition) are depicted in Table 4.5.

A first non-isothermal DSC experiment is simulated between the two main reactants, namely a reaction mixture of A and B with a ratio of 1A:2B (Figure 4.4A). This experiment highlights the effect of the concentration of B on the reaction rate. A second experiment performed with a molar ratio A/B of 1.2/1 demonstrates the effects of the concentration A (Figure 4.4B).

These last two DSC curves demonstrate the presence of at least two reactions: a first one occurring between 0 and 150 $°C$ followed by a second one in the range between 90 and 350 $°C$ (not visible in Figure 4.4B). In addition, the ratio of 1A:2B leads to assume a first reaction between A and B (which is confirmed by the Figure 4.4B) followed by another reaction which can be a consecutive or a decomposition reaction (Figure 4.4A). As this investigation is applied on simulated data, it is assumed that individual DSC experiments for each species were performed and did not demonstrate any secondary reaction. Therefore, it can be assumed that an interaction between the combination product of A and B and the remaining quantity of B exists. This fact is demonstrated by using a small quantity of the species C with B as illustrated in the Figure 4.4C.

Regarding the different comments previously established from the preliminary experiments, the following points can be underlined:

- There are at least two reactions: two peaks on the Figure 4.4A.
- The first peak (Figure 4.4B) represents the reaction of reactant A with reactant B.
- The reactants B and C react together if the ratio of B over A is bigger than 1 (Figure 4.4A and Figure 4.4C).

Table 4.4 – Physical properties of the different species considered in the reaction scheme 4.8.

Species	Molar mass $(g \cdot mol^{-1})$	Heat capacity $(J \cdot g^{-1} \cdot K^{-1})$
A	100	4.18
B	100	4.18
C	200	4.18
D	300	4.18

Table 4.5 – Summary of the simulated preliminary experiments for the reaction scheme 4.8.

Experiment	Heating rate $(K \cdot min^{-1})$	A	B	C	D	Mass mg
		$(mmol) \cdot 10^{-1}$				
A	4	1	2	0	0	30
B	2	1.2	1	0	0	22
C	4	0	1	1	0	30
D	1	1	1	0.5	0	30

Table 4.6 – Predictive accuracy for the retrieved parameters.

R^2 $(-)$	σ_r $(mW \cdot g^{-1})$	Δ_{max} $(mW \cdot g^{-1})$
1	$2.8 \cdot 10^{-2}$	$5.2 \cdot 10^{-2}$

- No decomposition reactions are considered as it was mentioned.

Obviously, to ensure the robustness of the procedure, the real reaction scheme presented in equation 4.8 will be used for the next assessment of this example. However, this first investigation gives a good insight into how to use and extract information efficiently from DSC and Calvet experiment.

4.4.1.3   Fitting of the preliminary experiments

Using the reaction scheme hypothesis and the simulations performed in the previous section, the retrieved parameter values are the original parameters used as inputs. This point was successfully fulfilled even with different sets of initial guess and trials. The respective determination coefficient and standard error of deviations are depicted in Table 4.6 based on data that were not used for the regression.

The parameter deviations and correlation are represented in appendix A.1 and A.2. These deviations are mainly due to the fitting and integration parameters used during the regression resolution, but remains totally acceptable.
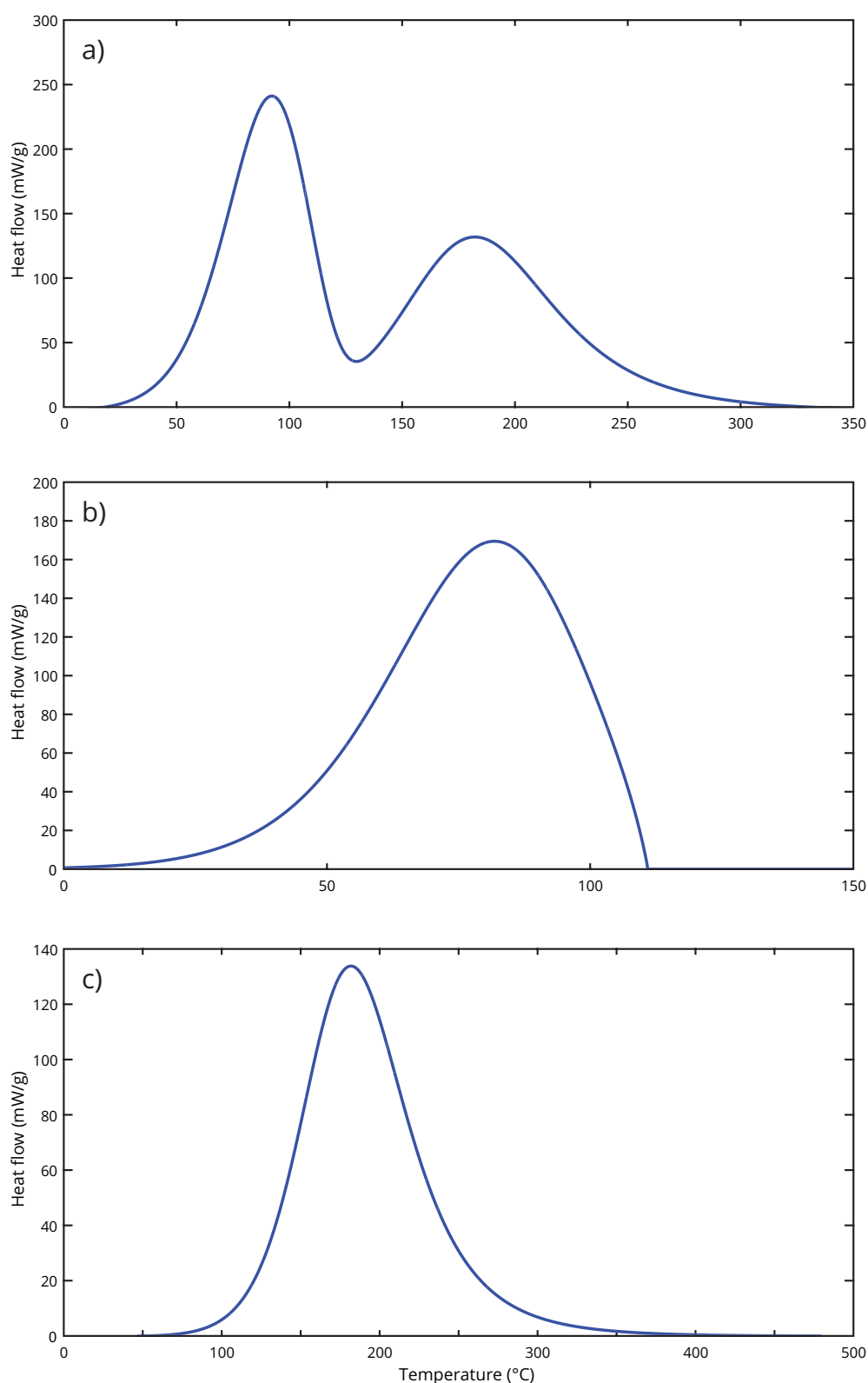
Figure 4.4 – Non-isothermal DSC experiments simulated with AKTS-Reaction Calorimetry Software for different ratios and heating rates: A) 1A:2B under $4K \cdot min^{-1}$; B) 1.2A:1B under $2K \cdot min^{-1}$; C) 1B:1C under $4K \cdot min^{-1}$ [134].

Table 4.7 – Variable ranges for the Design of Experiment of the simulated example (reaction 4.8).

	Temperature	Time to feed	Number of added moles
Units	$T_{r,set}$ $(°C)$	$t_{fd,B}$ (min)	$n_{fd,B}$ (mol)
Min	50	60	1
Max	80	120	2.5

4.4.1.4   Design of Experiment and RC predictions

From the preliminary experiments, two reactions were identified. Assuming the first reaction (first peak on Figure 4.4A) as the one to be preferred and the second as the one that should not be triggered for safety or quality reasons, the range of application for the time to feed, the amount of added reactant and the process temperature can be determined. The first reaction occurs between 50 and 150 $°C$, operating at higher temperature will lead the reaction mixture to reach a temperature range where the second reaction is triggered. Consequently, the operating temperature range should be estimated between 50 and 80 $°C$.

In terms of number of moles of B added to the reaction mixture, a ratio between 0.5 and 1.5 should be expected. Considering the reactor as initially charged with 2 moles of A, the amount chosen for the feed should be between 1 and 3 moles. Due to the size of the reactor (0.5L), the maximum amount that can be added is 2.5 moles of B.

The time to feed will have a direct influence on the amount of accumulation and thus, the experiment safety. A too fast addition will result in a large accumulation (approaching batch conditions) and oppositely, a too slow one will lead to a long experiment time. Therefore, this parameter should be carefully considered as it may result to critical outcomes. In addition, different feed rates will lead to different thermal behaviours due to a constant evolution of the species ratios, a point that will help in the differentiation of the reactant orders. The selected time to feed should be in the range of 60 to 120 min.

Following the different points formulated previously to design the experimental space (Table 4.7), predictions of the resulting SFD plan (Table 4.8) were performed to evaluate the risk potential each experiment may encounter. The maximum amount of accumulation has been also determined individually and is depicted in Table 4.8.

Table 4.8 – Space Filling Design performed for the simulated example (Reaction 4.8) for Reaction Calorimetry experiments ($CoM = 0.17$ and $MinDist = 0.78$ for a plan normalised to 1). The maximum amount of accumulation was also evaluated for each experiment.

Exp. Units	$T_{r,set}$ ($°C$)	$n_{fd,b}$ (mol)	$t_{fd,B}$ (min)	$Accumulation$ ($\%$)
1	79.21	1.97	118.34	12
2	53.42	2.27	118.71	43
3	67.49	1.04	101.90	6
4	51.26	1.11	68.54	39
5	56.40	2.25	71.59	49
6	77.77	1.78	70.73	14

4.4.1.5   Validation of the algorithm

The purpose of this example is to evaluate the efficiency of the Reaction Kinetic Investigation (procedure and regression algorithm). In addition, the simulated data are "perfect", namely that no erroneous baseline or noise are accounted for them.

Different sets of data may be composed depending on the type of experiments and combination. Therefore, to cover the range of applicability of the approach, 3 different sets of data were investigated:

- *DSC and Calvet data set*: the retrieved parameters represent accurately the original parameters used to simulate the data (Appendix A.1); It was possible to assess good parameters as sufficiently large and disparate reactant ratios were considered. The resulting correlation matrix (Appendix A.2), however, demonstrates a high number of correlated parameters, meaning that other experiments may be required to confirm the validity of the model.
- *RC data set*: As the simulated experiments were performed in such manner to only highlight the first reaction, a comparison with a simulated DSC experiment demonstrated that the obtained parameters are in good accordance with the first reaction but poor in prediction for the second one (Figure 4.5).
  By selecting only RC experiments, a lack of information regarding the second reaction is clearly observable, leading to a poor prediction of the overall reaction system.
  For this configuration, the correlation matrix showed a decreasing number of correlated parameters for the first reaction; the opposite behaviour, however, is logically observed for the second reaction as the experiments does not contain it (Appendix A.3).
- *Combination of DSC, Calvet and RC data*: the obtained parameters reflect, for the first reaction, the one used as inputs for the simulation. Regarding the second
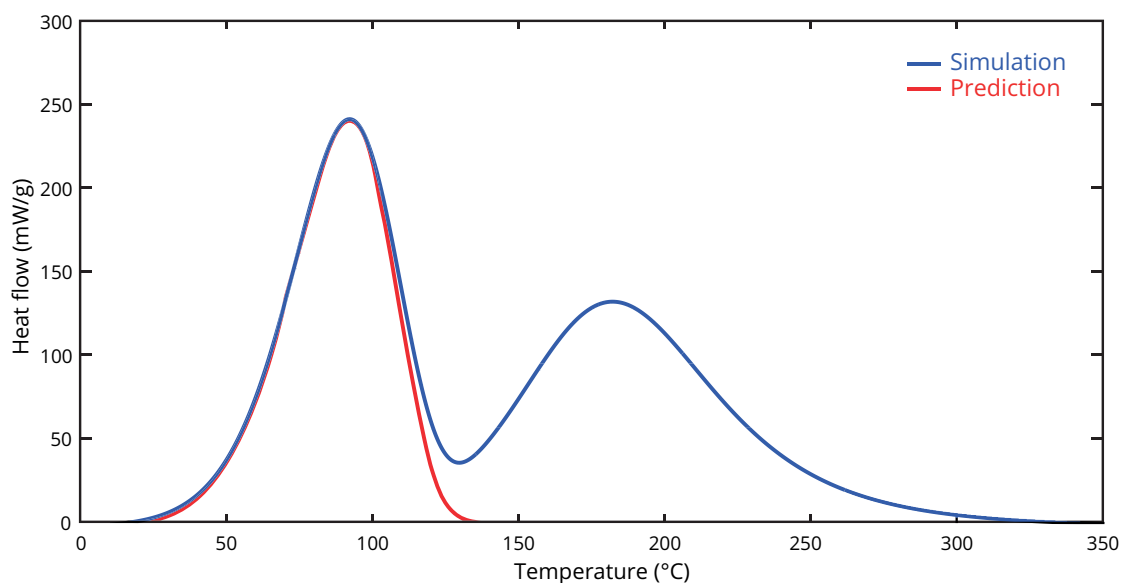
Figure 4.5 – Simulation of the DSC experiment 1 from the preliminary investigation (Table 4.5) using kinetic parameters retrieved from solely RC experiments.

reaction, this configuration seems to be failing. This result is mainly caused by the effect of a large number of RC experiments compared to DSC and Calvet(6 vs 3). In terms of regression, their weight and thus influence of each experiment is proportional to the number of points, on the regression and therefore, the final parameter estimates.

In summary, on the one hand, the algorithm can work quite well with solely DSC and Calvet experiments. These data require only to be performed under different reactant ratios in order to underline the effects of each reactant toward the reaction kinetics. On the other hand, RC experiments may be used alone but will only give a partial view of the reaction kinetics, some aspects like thermal safety of undesired reactions happening out of the experimental domain (higher temperatures) will logically not be handled correctly due to a lack of information.

This example operates on the basis of simulated data, therefore different effects such as heat exchange properties, heat losses, or mixing occurring in real RC experiments were not totally accounted in the model. However, it can be concluded that the procedure and algorithm operates in a correct and efficient way to retrieve the kinetic parameters. Special care should be taken to the construction of the reaction scheme as it may lead to different results depending on the correctness of the latter. A model is never right but, in the optimal case, it may be useful and only partially wrong [97].

4.4.2   Esterification

In opposition with simulated data previously presented, the system considered for the next example is an experimental study of the exothermic esterification of acetic anhydride and methanol (Figure 4.6) with the aim to prepare a scale-up of this reaction system. This reaction system is widely used as a test for safety-oriented studies and as such, is adequate to test the Reaction Kinetic Investigation under real conditions [136–139].

acetic anhydride   methanol   acetic acid   methyl acetate
        (A)   (B)   (C)   (D)
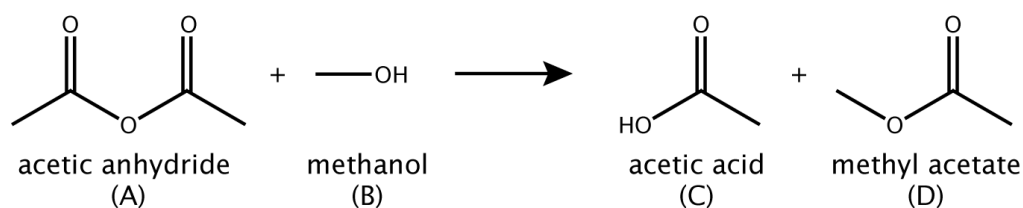
Figure 4.6 – Methanol / Acetic anhydride esterification.

4.4.2.1   Preliminary experiments

Two non-isothermal DSC and Calvet experiments at different heating rates and between 25 and 300 $^{\circ}C$ have been carried out. One of them is represented in Figure 4.7. The experimental conditions are depicted in Table 4.9.

The number of DSC and Calvet experiments was voluntary kept low to test the procedure to its limits. It would have been good to have more information here to determine the veracity of the reaction scheme (see next section).

Table 4.9 – Experimental conditions and compositions of the preliminary experiments for the reaction scheme illustrated in Figure 4.6 performed using DSC and Calvet calorimetry.

Type of instrument	Rate	Mole ($mmol$)					Mass	Scale
	$K \cdot min^{-1}$	A	B	C	D	Total		
Mettler-Toledo® DSC 821e	4	0.0741	0.0740	0	0	9.93		mg
Setaram® C80	0.1	15	14.8	0	0	1.99		g
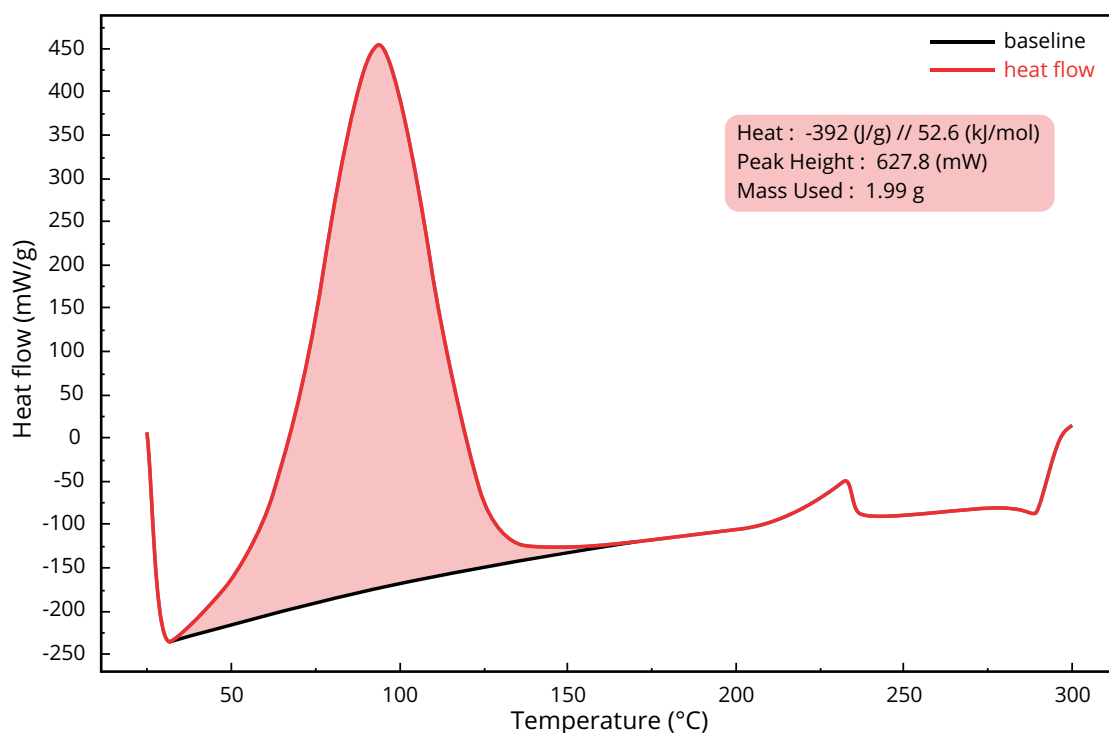
Figure 4.7 – Calvet experiment performed for a mixture of Acetic Anhydride and Methanol (1A:1B) under a $0.1 K \cdot min^{-1}$ ramp.

4.4.2.2 Hypothesis of the reaction scheme

A two-step reaction scheme was proposed by Bohm et al. considering the autocatalytic behaviour due to acetic acid formation [140]. This scheme is written as:

$$A + B \rightarrow C + D$$
$$A + B + C \rightarrow 2C + D$$

$$(4.11)$$
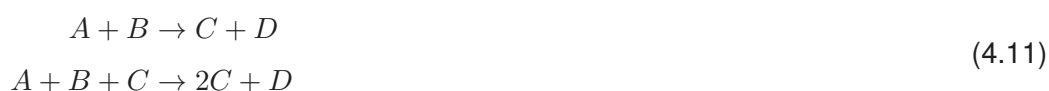
The proposal of such an autocatalytic behaviour was confirmed by the extensive work of Widell on the esterification of acetic anhydride by methanol but also by 2-butanol [137]. Therefore, this reaction scheme is used as a hypothesis to define the different rate expressions and parameters of the reaction model such as:

$$r_1 = k_1 C_A^{a1} C_B^{b1}$$
$$r_2 = k_2 C_A^{a2} C_B^{b2} C_C^{c2}$$

$$(4.12)$$

and the transformation rates are:

$$R_A = \qquad\qquad\qquad -r_1 - r_2 \qquad\qquad\qquad (4.13)$$

$$R_B = \qquad\qquad\qquad -r_1 - r_2 \qquad\qquad\qquad (4.14)$$

$$R_C = \qquad\qquad r_1 - r_2 + 2r_2 = r_1 + r_2 \qquad\qquad (4.15)$$

$$R_D = \qquad\qquad\qquad r_1 + r_2 \qquad\qquad\qquad (4.16)$$

4.4.2.3 Regression problem

The study of the parameters obtained from the regression over the preliminary experiments, showed to be unsatisfactory due to very disparate parameter values and low predictive accuracy toward the RC experiments as illustrated in Figure 4.8. The preliminary study is mainly performed to screen the experimental domain and the possibility of secondary reactions. Therefore, even with a good fit ($R - squared$ and σ_g relatively good along the regressed data), the model was not able to demonstrate a good predictive accuracy while confronted to RC experiments. This result was demonstrated by a cross-validation performed on the preliminary experiments by selecting different sets of initial guess and led, in each case, to different parameter values. Mathematically, this problem arises when the surface response covered by the experiments is not sufficient or well defined, namely that different set of parameters may be able to describe correctly the experimental data but may result in a poor predictive power. Among these sets of parameters, it exists one set that is optimally better than the others and generally called the "global optimum". Therefore, if the reaction system is covered by sufficiently different experimental conditions, the algorithm will be able to converge toward an optimum which may be the global one.

Another aspect worth mentioning is the construction of the baseline. In fact, an erroneous baseline leads to a wrong integral (enthalpy) and delivers a wrong normalised heat flow signal, which will directly impact the reaction kinetics.

4.4.2.4 Design of Experiments

Considering the esterification reaction system, the operating temperature range should be below the boiling point of the reaction mixture (estimated at $65°$), but nevertheless sufficiently large and adapted to have an appropriate experiment duration as well as inherently safe RC experiments. Moreover, no significant secondary reactions were detected in the temperature range of the investigation or above (Figure 4.7).

Based on the preliminary model and using the physical properties of the participating
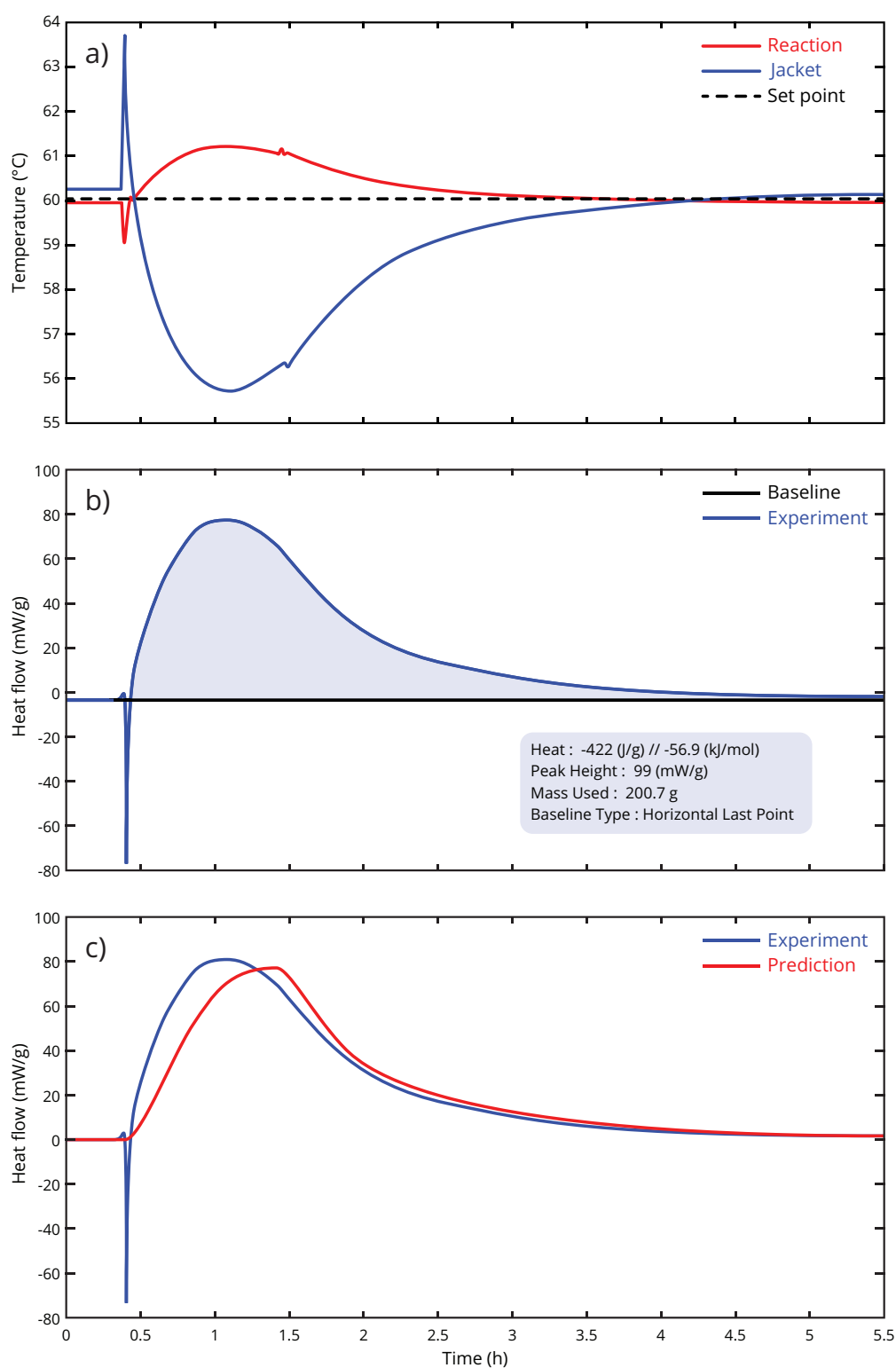
Figure 4.8 – Reaction model behaviour toward the RC experiment 5: a) Temperature profiles along the process course, b) Baseline and heat flow information regarding the reaction, c) Erroneous prediction using the preliminary estimated parameters, a lack of information is clearly noticeable.

Table 4.10 – Variable ranges for the Design of Experiment for a Reaction Calorimeter filled with 1.5 moles of Acetic Anhydride (A) and where the methanol (B) is fed.

	Temperature	**Time to feed**	**Number of added moles**
	$T_{r,set}$	$t_{fd,B}$	$n_{fd,B}$
Units	[$°C$]	[min]	[mol]
Min	40	60	0.7
Max	60.3	120	1.5

Table 4.11 – Design of Experiment resulting based on Space Filling method applied on a candidate set of 10000 randomly generated points resulting in a $minDist$ = 0.8500 and CoM = 0.0020 [82]. Results: average heat capacity ($c_{p,average}$), obtained heat (Q_r) and reaction enthalpy ($\Delta_r H$) for the RC experiments with an initial load of 1.5 moles of acetic anhydride (A).

	Design of Experiment				**Results**	
Exp.	$T_{r,set}$	$n_{fd,B}$	$t_{fd,B}$	$c_{p,average}$	Q_r	$\Delta_r H$
Units	($°C$)	(mol)	(min)	($JK^{-1}g^{-1}$)	(kJ)	($kJmol^{-1}$)
1	50.1	1.09	91	2.1	-61.3	-56.2
2	60.3	0.69	64	2.1	-36.3	-52.7
3	41.4	0.69	121	2.1	-43.6	-63.6
4	40	1.49	117	2.1	-76.4	-51.1
5	60.1	1.48	63	2.1	-84.1	-56.7
6	60	0.69	120	2.1	-40.8	-58.7
Average				**2.08**		**-56.5 ± 4.7**

species (boiling points, heat capacities,...), it was possible to roughly predict the process behaviour under diverse operating conditions (Table 4.10).

An experimental design, based on Space Filling method was used to define six sets of experimental conditions, as shown in Table 4.11. Each of the three variables depicted in Table 4.10 appears at a minimum of three levels; a criterion which was needed to extract the value of the activation energy [130, 141].

The determined mean reaction enthalpy corresponds to -56.5 ± 4.7 ($kJ \cdot mol^{-1}$), a lower value than the one found in literature, 67.3 ± 3.0 ($kJ \cdot mol^{-1}$) [136] as well as 65.99 ($kJ \cdot mol^{-1}$) based on on-line tabulated standard enthalpies of formation [142]. This deviation is explained by a too high operating temperature, causing heat losses by evaporation considering a boiling point of 56 $°C$ and 64 $°C$ for methyl acetate and methanol respectively. Nevertheless, these data are a good input to create the data basis for the regression and to create a reaction model.
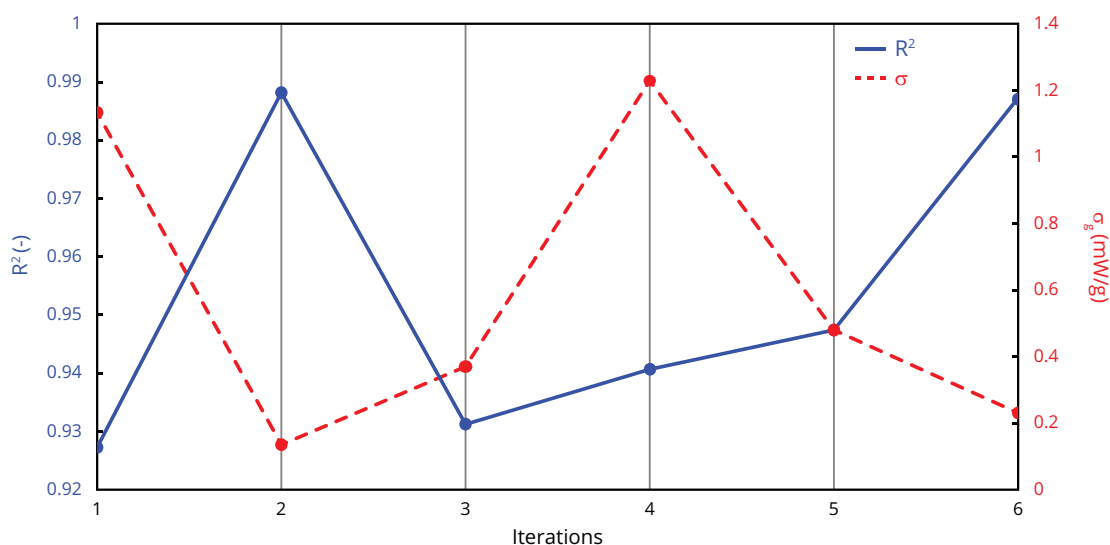
Figure 4.9 – (left): Determination coefficient as function of the iterations; (right): Standard deviations σ_g toward the next experiment based on a cross-validation approach.

4.4.2.5 The reaction kinetic model

Using the RKI procedure on the obtained data (DSC, Calvet and RC experiments) and the previously proposed reaction scheme, the kinetic parameter values were determined as depicted in Table 4.12. As initial guesses for the kinetic parameters, the ones that led to the best regression model during the preliminary investigation were selected.

At each iteration of the procedure (Step 2 to 4 in Figure 4.1), a new RC experiment was added and the resulting error (R^2 and σ_r) between the model prediction and the next experiment not included in the regression data set was computed (Figure 4.9).

After the second iteration (Preliminary and one RC experiment), the obtained parameters were unsatisfactory. The model was able to describe the next experiment only during the feeding part but unable to predict accurately the ending part of the heat flow signal. At this stage of the procedure, it is still convenient to continue the procedure.

An analysis of the correlation matrix along the procedure demonstrated a tangible decrease of correlated parameters to finally get a convenient model able to describe the studied experimental domain. The resulting model parameters are depicted in Table 4.12, and allows to predict the behaviour of the esterification reaction system in a broad range of operating conditions.

Table 4.12 – Kinetic parameters of the esterification of acetic anhydride by methanol calculated with the assumption of an autocatalytic effect of the acetic acid (product) applying AKTS-Reaction Calorimetry Software [134].

Reaction 1			
	k_0	E_a	$\Delta_r H$	*Orders*
Units	$(g^{0.28}s^{-1}mol^{-0.28})$	$(Jmol^{-1})$	$(kJmol^{-1})$	$(-)$
Value	$1.28 \cdot 10^7$	65663	-54.7	$m_A = 0.65$ $m_B = 0.63$
Reaction 2			
Units	$(g^{1.28}s^{-1}mol^{-1.28})$	$(Jmol^{-1})$	$(kJmol^{-1})$	$(-)$
Value	$8.63 \cdot 10^7$	54942	-50.5	$m_A = 1.06$ $m_B = 0.69$ $m_C = 0.53$

4.4.2.6   Validation of the approach

In order to validate the model, a Leave-One-Out Cross-Validation was performed with the complete set of data (DSC, Calvet and RC experiments). The resulting model (Table 4.12) is compared to two different experiments, namely a DSC and a RC experiments that were not used to solve the regression problem, as illustrated in Figure 4.10.

The reaction model describes the RC experiment quite better than the DSC one in terms of standard deviations (Table 4.13) and visually. As explained during the simulated example (Section 4.4.1), the deviations noticeable in the DSC experiment may be due to a large number of RC experiments in the regression data set and focused on a narrow temperature range. In other words, the DSC experiments are less represented in the regression problem. The effects of the events occurring at temperatures higher (DSC) than those explored by the RC experiments are lowered during the regression process. Therefore, the regression is more focused on the RC experiments leading to an optimum displaced toward the RC scale.

Other facts such as micro-mixing or difficulties in the baseline definition may have

Table 4.13 – Errors and determination coefficient depicted by the model predictions regarding the experiments presented in Figure 4.10.

	$\sigma_{q_{rx}}$	R^2
Units	$(mW \cdot g^{-1})$	$(-)$
DSC	7.75	0.9905
RC	4.81	0.9792
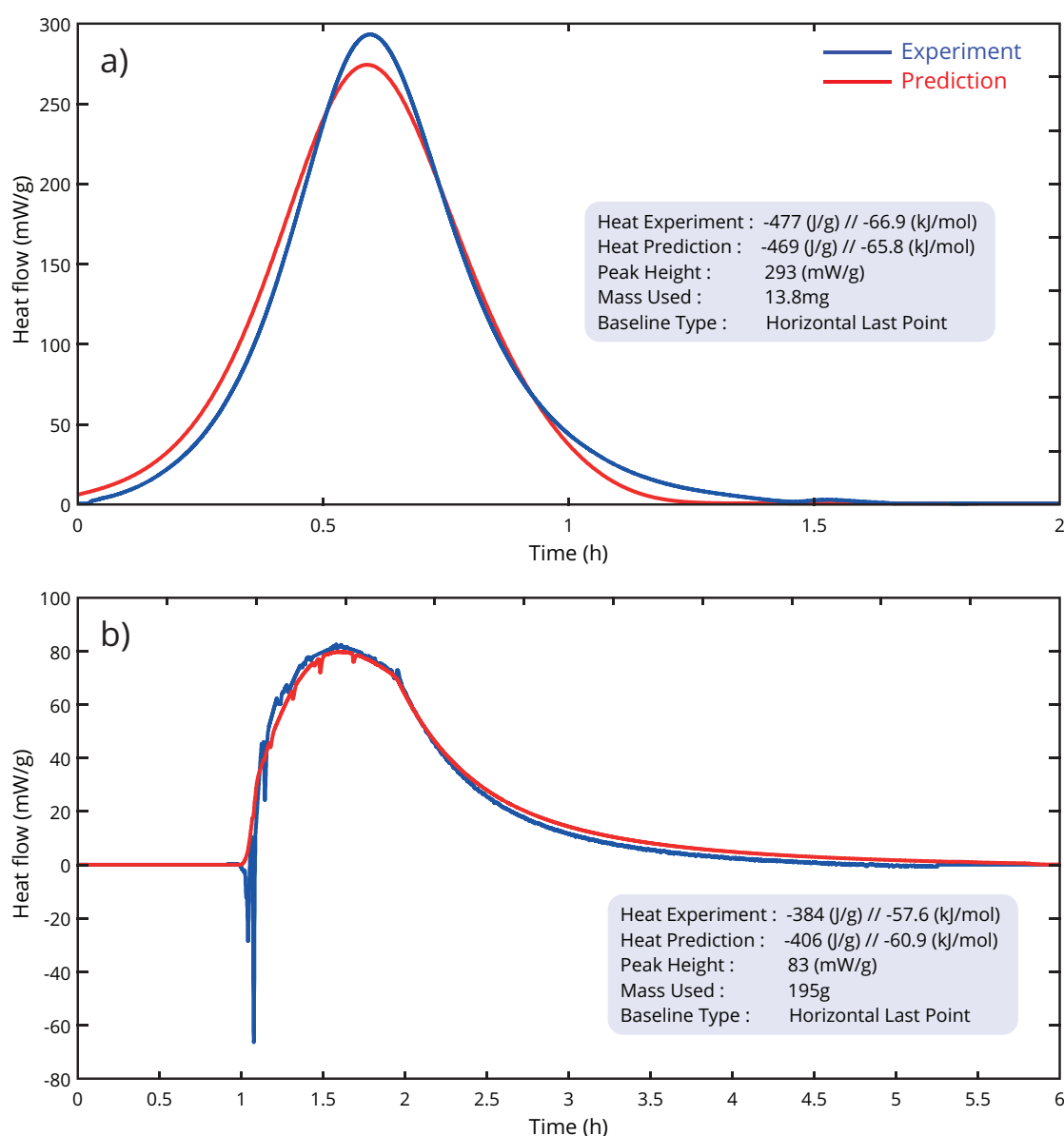
Figure 4.10 – Validation: comparison of the experiments with their respective prediction using the optimised reaction kinetic model: a) DSC at 1.5 $K \cdot min^{-1}$ and b) RC1 at $62°C$.

caused this slight misfit observed in the DSC experiments (no mechanical mixing). However, the reaction enthalpy depicted by the DSC experiment and prediction seems to be in good accordance with the literature. As a result, the developed reaction model is able to describe RC experiment as well as DSC ones with a good accuracy. Therefore, this model can be used for further development as scale-up of safety assessment in the range where it was defined and validated.

4.5   Conclusion

The Reaction Kinetic Investigation demonstrated that an approach based on a multi-scale, -conditions and -ratios is an effective way to characterize a reactive system. In addition, the use of calorimetry as a non-invasive method (DSC, Calvet and RC) in combination with the Law of Mass Action allowed, to model and predict accurately the events occurring in the reaction mixture under a wide range of conditions. The resulting model led to a better understanding toward the link existing between the different system variables (temperature, initial concentrations and type of experiment) and the kinetic parameters.

By knowing the reaction kinetics, one can predict the thermal behaviour, but also the concentration profiles, information primordial to evaluate the accumulation of non-converted reactants. Therefore, the Reaction Kinetic Investigation is an important step toward an efficient control of the thermal potential that may lead to disastrous consequences if equipment malfunction or cooling failure may occur.

The main drawbacks of this procedure, however, are the choice of the initial guesses for the kinetic parameters and the reaction scheme hypothesis; the procedure was only tested on relatively well-known systems but showed to be already efficient, despite the fact that no analytical data regarding the reaction course were provided. To overcome the issues concerning the definition and structure of the model, three solutions may be suggested:

1. To test different reactions scheme hypothesis and develop a method of selection (e.g. statistical error analysis) [132, 143],

2. To identify the initial guesses by the mean of other methods and models (e.g. isoconversional for the activation energy),

3. To add some information on the mixture composition profile to the data set, namely concentrations along the process course (e.g. in-situ IR) or the state of conversion (e.g. RMN along the experiment).

Another issue occurred during the construction of the baseline, which is well known to be a problem of the calorimetric methods. As a matter of fact, the type of baseline, its beginning and end are generally set manually. A difficult task that may lead to erroneous evaluation. Therefore, special care should be taken here or at least a consistency check based on the energies should be performed.

As outlook for this chapter, only linear feed profiles were explored during the different RC experiments; it would be interesting to investigate different kinds of feed and non-isothermal temperatures profiles to separate in a more efficient way the different

reactant orders, Arrhenius parameters and reactions.

Regarding a scale-up study, the dynamic behaviour of the reacting system was characterized in terms of temperature and concentration profiles and allowed to describe these profiles under a wide range of operating conditions based on DSC and RC experiments (isothermal, non-isothermal...). This aspect alone, however, will not be sufficient for a correct scale-up. Beside the reaction kinetic aspects, other aspects of the reaction control are essential for a successful scale-up, namely mastering the behaviour of the whole system including the reaction mixture and the heating/cooling system with its temperature control. This also requires the knowledge of the heat transfer parameters. This essential topic will be assessed along the next chapter.

5

Reactor Dynamics Investigation

We must reason in natural philosophy not from what we hope, or even expect, but from what we perceive.

Humphry Davy, 1778-1829

Chapter 5: Reactor Dynamics Investigation

The fine chemical industry needs increasingly faster time-to-market as well as economically efficient and safe processes. In addition, the growing product variety requires more versatile production plants able to produce from small amounts up to several hundred tons per year [144].

As a result, the time devoted to development is limited and the production often takes place in multipurpose plants. A given process can then run in different reactors where the behaviour of the reaction system may change from one equipment to another, causing difficulties to perform a correct scale-up of a process at industrial scale [5, 7, 145].

The key point of such scale-up is to understand the behaviour of a chemical reaction performed at laboratory scale in order to anticipate its behaviour at industrial scale (considering economic, safety and ecological aspects) [146]. Thus, any industrial-scale chemical process is the result of a successful scale-up scenario carried out by a series of successive tests at different stages, from small experimentation to full scale production [5]. In many cases, however, the experience showed that the road leading to a successful process is not straightforward, being rather a succession of many trials and errors followed by the eventual elaboration of clever decisions [2]. Consequently, a general procedure that leads from laboratory to industrial scale, does not exist.

In terms of safety, one of the problems generally encountered is the lack of controllability due to the accumulation of unconverted reactants. This accumulation can remain undiscovered under nominal operating conditions. In case of failure, however, it can suddenly be revealed, as it leads to an uncontrollable reactor state [128]. Understanding and controlling this aspect necessarily becomes a matter of great importance.

One solution would be, to avoid batch reactor, to move towards fed-batch reactor or even to Continuous Stirred Tank Reactor. Their ability to control the reaction by adapting the feed rate and avoiding a rapid heat accumulation makes them a better choice for a safe operation. On the contrary, as one of the reactants is fed, the SBR is operated at a lower concentration which may be disadvantageous considering reaction time, productivity and costs. This problem can be solved or at least mitigated by using an optimal feed strategy, taking the reaction kinetics and reactor dynamics into account [129].

Generally, the solution of such a scale-up problem is the result of a perfect match between two dynamics: the reaction dynamics (governed by the kinetics) presented previously in Chapter 4 and the dynamics of the reactor temperature control (heat transfer and control). For this specific case, a novel approach has been developed to determine the reactor thermal dynamics with a minimum and well-planned experiments. This approach focuses on answering the following questions:

1. What are the relevant heat transfer phenomena occurring in a chemical reactor?
2. How to model the thermal behaviour of such equipment?
3. What kind of information are necessary to describe the thermal behaviour of a chemical reactor?

This chapter is divided in three main parts: the first part gives an overview of reactor dynamic modelling with a special focus on the different aspects of thermodynamics and temperature control. The second part is exclusively dedicated to the Reactor Dynamic Investigation (RDI) procedure. Finally, the third part illustrates a number of simulated and applied examples for the application of the RDI.

5.1 Reactor dynamics modelling

Modelling and simulation methods are commonly used to design and optimise processes, to predict flow as well as heat and mass transfers. In the present work, we only consider the heat transfer aspects, which means that the method applies essentially on homogeneous reaction mixtures, where the mass transfer is fast compared to the reaction rate. The complexity and variety of these phenomena in reality require a simplification of the models to be handled more easily without losing in accuracy.

The simplified reactor model comprises 3 parts as illustrated in Figure 5.1: 1) the reactor heat transfers (Section 2.2.2); 2) the coolant temperature PID controller and finally 3) the jacket temperature behaviour. The following sections describe in detail the development of such model.

5.1.1 The reactor heat transfers

One of the fundamental principles of physics and modelling is the conservation of mass and energy [31]. To understand and describe a dynamic system accurately, these different balances have to be defined and evaluated (section 5.1).

Considering batch operating conditions, the mass balance around the reactor can be approximated to zero (no evaporation, no input or output). On the contrary, the heat balance is more complicated as demonstrated in paragraph 2.2.2.2.3. A simplified heat balance for a non-viscous and non-reactive system can be written with only heat
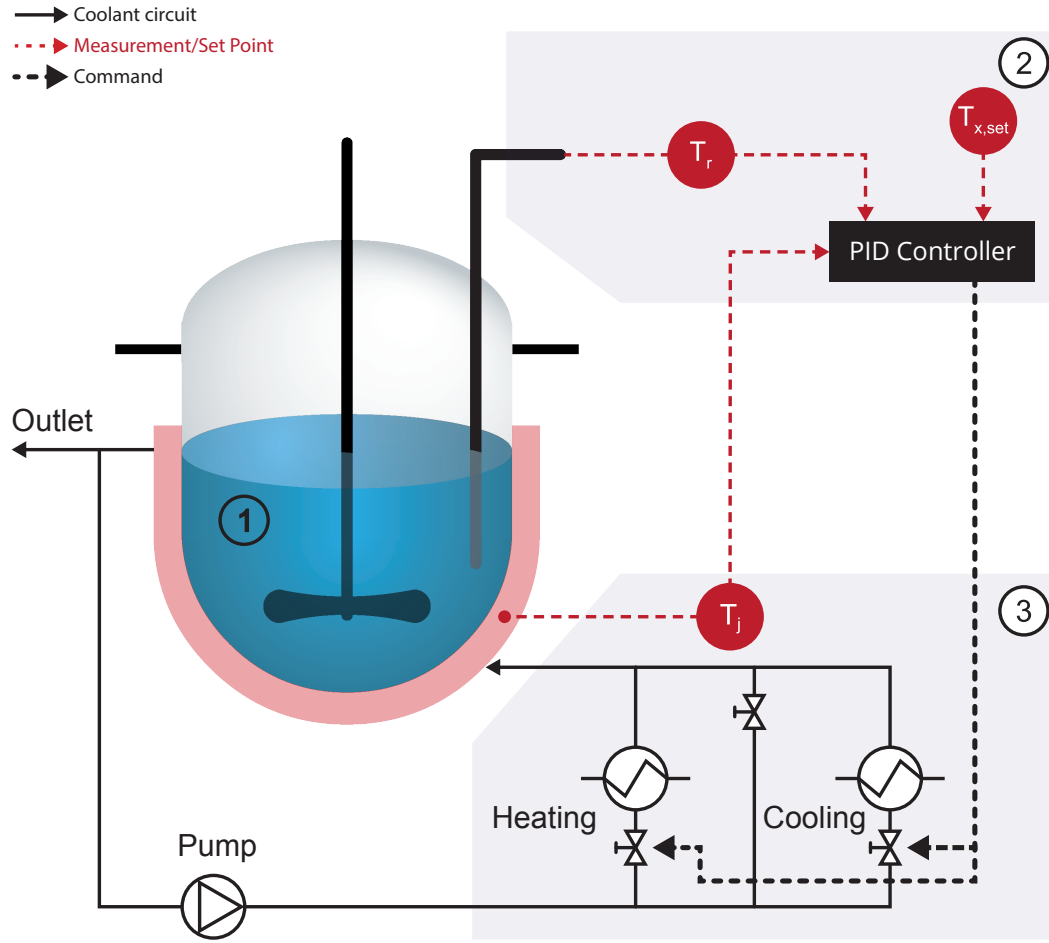
Figure 5.1 – Temperature control with a heat carrier circulation loop and its different connections with the reactor model: 1) heat balances 2) PID controller model 3) Thermal behaviour of the jacket.

accumulation, exchanges and losses as:

$$(m_r c_{p,r} + C_w) \frac{dT_r}{dt} = U A (T_j - T_r) + \alpha (T_{amb} - T_r) \tag{5.1}$$

Where the thermal dynamic characteristics are described by the overall heat transfer coefficient U, the heat exchange area A, the heat loss coefficient α and the heat capacity of the equipments C_w.

In terms of reactor thermal dynamics, one has mainly the desire to investigate the heat removal capacity: how will the heating/cooling system manage the heat released or consumed? Is it sufficient?

Under normal operating conditions, the heat transfer occurring between the jacket
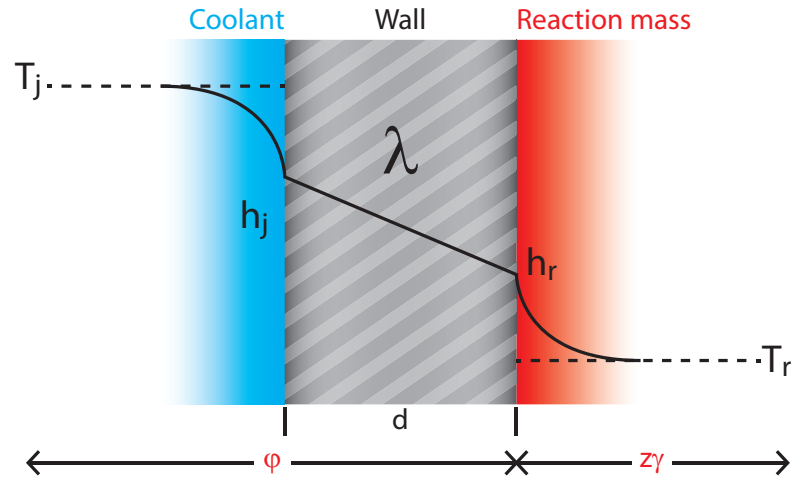
Figure 5.2 – Illustration of the overall heat transfer coefficient U.

coolant and the reaction mixture is generally described by the overall heat transfer coefficient U which can be illustrated as a series of resistances, a model commonly called the two film theory [30, 147]. As an example, the heat transferred from the reaction mixture to the jacket coolant during a cooling phase involves three different phenomena as presented in Figure 5.2:

1. Forced convection in the inner film (reaction mixture side).
2. Conduction through the wall.
3. Forced convection in the outer film (coolant side).

The term "forced" is used to describe the convection due to the fluid in motion caused by an external force such as a stirrer, pump or fan.

As a result, the overall heat transfer coefficient U can be expressed as follows:

$$\frac{1}{U} = \underbrace{\underbrace{\frac{1}{h_r}}_{\text{reaction mixture dependent}}}_{\frac{1}{z\gamma}} + \underbrace{\underbrace{\frac{d}{\lambda} + \frac{1}{h_j}}_{\text{reactor dependent}}}_{\frac{1}{\varphi}} \qquad (5.2)$$

$$\qquad (5.3)$$

where h_r and h_j are respectively, the inner and outer film heat transfer coefficient $(Wm^{-2}K^{-1})$, λ is the thermal conductivity of the reactor wall $(Wm^{-1}K^{-1})$ and d its thickness (m).

The equation 5.3 describes two distinct zones of the heat transfer between the reaction mixture and the jacket coolant:

1. The internal film heat transfer coefficient h_r which is derived from the Nusselt's correlation such as:

$$Nu = C^{ste} \cdot Re^{\frac{2}{3}} \cdot Pr^{\frac{1}{3}} \cdot \left(\frac{\mu}{\mu_w}\right)^{0.14} \tag{5.4}$$

Where:

$$Nu = \frac{h_r \cdot d_r}{\lambda} \qquad Re = \frac{n \cdot d_s^2 \cdot \rho}{\mu} \qquad Pr = \frac{\mu \cdot c_{p,r}}{\lambda} \tag{5.5}$$

After rearragement, this coefficient becomes the result of two distinct effects, namely the internal geometric characteristics of the reactor and stirrer (z) and the physical properties of the contents (γ):

$$h_r = \underbrace{\frac{n^{\frac{2}{3}} d_{st}^{\frac{4}{3}}}{d_r g^{\frac{1}{3}}}}_{z} \qquad \underbrace{\sqrt[3]{\frac{\rho^2 \lambda^2 c_{p,r} g}{\mu}}}_{\gamma} \tag{5.6}$$

where n is the stirrer speed rate, g the gravitational constant, d the diameter of respectively s, the stirrer and r, the reactor.

2. The external film and wall depending on the jacket characteristics contained in φ.

The evaluation of these parameters is difficult as they change from vessel to vessel and for each new combination of vessel-reaction mixture. It may become even more complicated for a reactive system as the heat transfer of the inner wall may change along the process course due to a change of composition (e.g. reactions). This last fact explains why a correct scale-up of the overall heat transfer coefficient can be long, complicated and requires a special attention.

Over the past three decades, various methods were developed to characterize the overall heat transfer coefficient U such as theoretical estimation from empirical relations, calibrations (essentially at small-scale), heat balance or by means of graphical construction [148, 149]..

One of them is the *Wilson plot* which is a mixture of theoretical relations and graphical construction, it offers a quite straightforward route to the vessel and reaction mixture heat transfer coefficients [148–150]. It needs to be performed at different temperatures and stirring regime in order to have a clear picture of the overall heat transfer. From the equation 5.3, the following relationship can be graphically build in order to estimate φ

and $z\gamma$ for a considered temperature T_r:

$$\frac{1}{U} = f\left(n^{-\frac{2}{3}}\right) = \frac{1}{\varphi} + \frac{1}{z\gamma} \tag{5.7}$$

The overall heat transfer coefficient U has to be evaluated by means of cooling curves at industrial scale, a particularly time consuming step [30]. In addition, to be consistent in the application of the two film theory, the vessel heat transfer coefficient φ should be considered dependent of the jacket temperature T_j while the reaction mixture heat transfer should be considered dependent of the reaction mixture temperature T_r such as:

$$\frac{1}{U\left(T_r, T_j\right)} = \frac{1}{\varphi\left(T_j\right)} + \frac{1}{z\gamma\left(T_r\right)} \tag{5.8}$$

5.1.2 The temperature controller

The main goal of a temperature control system for a chemical reactor is to make the system follow an imposed temperature-time profile for the jacket or the reaction mixture [151, 152]. Consequently, two temperature control strategies can generally be applied for an industrial reactor: T_r-mode (direct temperature control) or T_j-mode (indirect temperature control).

In case of T_r-mode, the temperature control of the reactor is based on two nested loops or a cascade controller (Figure 5.3): the external loop, the master controller (Tr-controller) compares a given temperature set point ($T_{r,set}$) with the actual reactor temperature (T_r) and computes the set point ($T_{j,set}$) for the internal loop also called
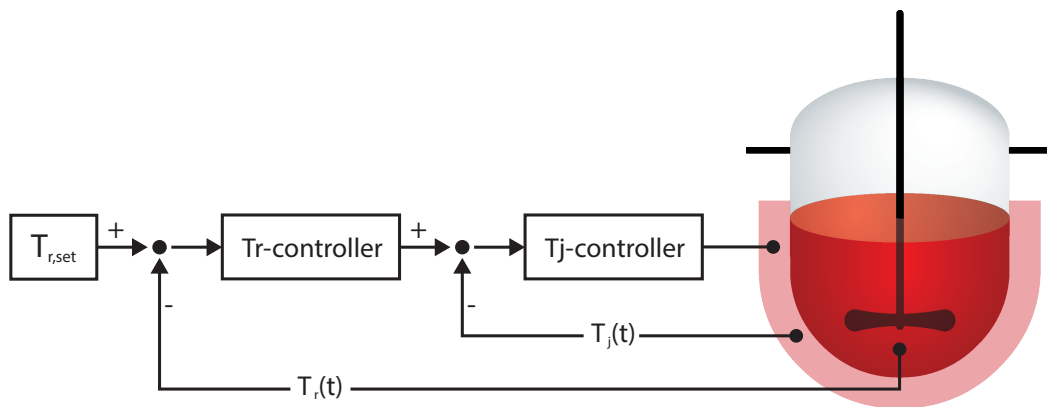
Figure 5.3 – Illustration of T_r-mode control in an industrial reactor.
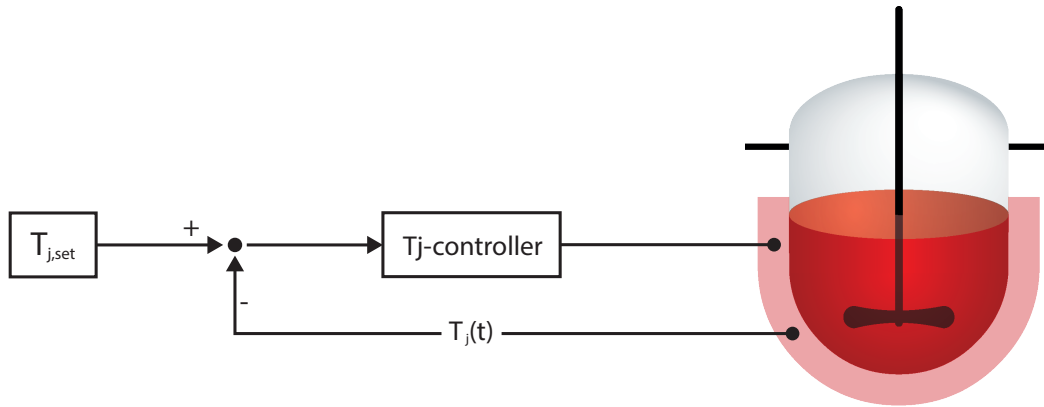
Figure 5.4 – Illustration of T_j-mode control in an industrial reactor.

slave controller, controlling the jacket temperature in order to make the reactor temperature track its set point [30, 153].

In the case of T_j-mode, there is only one controller for the jacket temperature (Figure 5.4). In such situation, the reaction mixture temperature changes according to the heat balance.

At industrial scale, the reactor heating/cooling system consists of a heat carrier circulation loop where the temperature controller intervene directly on the heating and cooling valves by using a conventional PID approach (Figure 5.1). Nevertheless, modelling such system can be a challenging task due to high complexity as the control of each utility is independent.

The set point of the jacket temperature ($T_{ctrl,set}$) that is imposed to the heating/cooling unit is obtained from a conventional PID equation [154]:

$$T_{ctrl,set} =$$
$$T_{x,set} + K \cdot \left[(T_{x,set} - T_x) + \frac{1}{I} \int_0^t (T_{x,set} - T_x) \cdot dt + D \frac{d(T_{x,set} - T_x)}{dt} \right] \quad (5.9)$$

where the subscript x is related to the type of control strategy chosen ($x = r$ for T_r-mode; $x = j$ for T_j-mode). The PID controller parameters are K the proportional gain $(-)$, I the reset time (s^{-1}) and D the derivative time (s). If the heating and cooling control systems exhibit different behaviours, two different sets of PID parameters may be considered, namely an individual set of PID parameters in heating and cooling conditions, respectively.
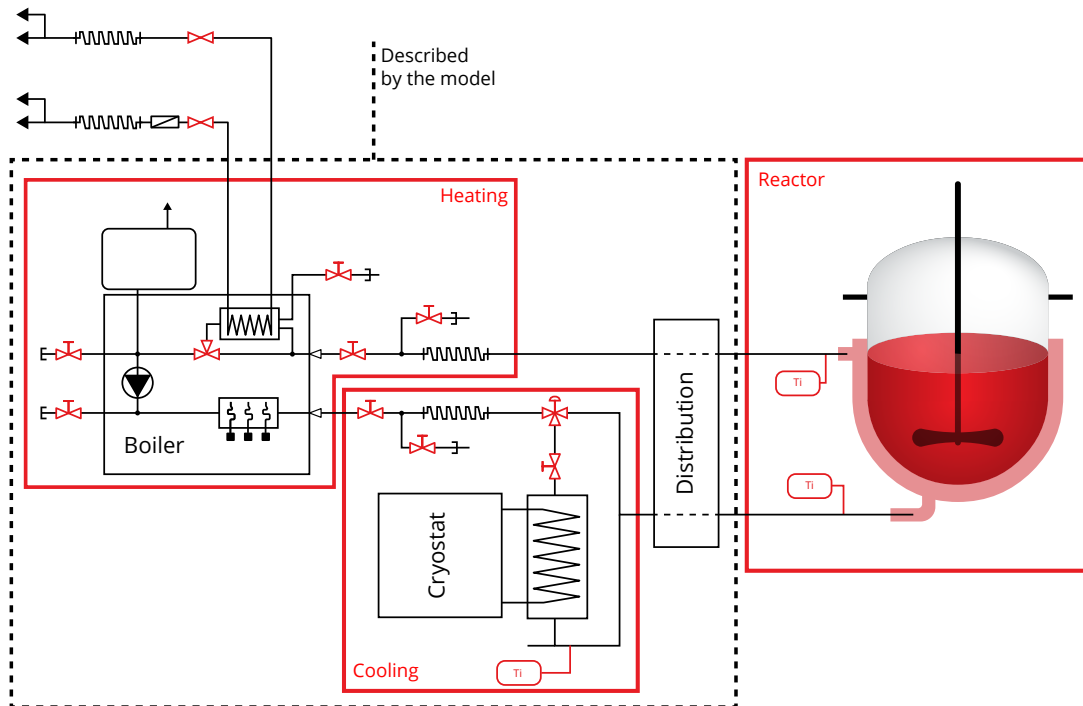
Figure 5.5 – Illustration of a typical Piping and Instrumentation Diagram of a process comprising a reactor with its separated heating and cooling system (simplified for the explanation). Such representation can explain the choice of a single or two utilities to describe the dynamic behaviour of the reactor.

In general, the full PID expression (equation 5.9) is applied for systems having fast responses such as electronic systems. In the case of reactor temperature control, however, the system responses are relatively slow. Therefore, a simplified version of the equation 5.9 containing only the proportional and integral parts will be considered.

A clear distinction should be made between this model and the reality. As a matter of fact, the control strategy is normally applied at several levels, for example, on a pump to increase the flow rate or on the opening of a valve still using a PID equation. The model presented here, however, evaluate the temperature the heating/cooling system should reach in order to make the jacket temperature follow the defined set point ($T_{x,set}$). This model describes an hypothetical controller of the heating/cooling unit and is by definition, a simplification of the combination of controllers placed in the real system (reactor, heating and cooling units, pumps and valves...) as illustrated in Figure 5.5. This approach allows to predict the controller's behaviour of the heating/cooling system. Another aspect to be considered is the inertia of the heating/cooling system, a part presented in the next subsection.

5.1.3 The jacket behaviour

The profile of the jacket temperature depends on the parameters of the temperature control algorithm, the dynamics inherent to the heat carrier flow and on the temperature of the utilities used for heating and cooling.

The minimal and maximal temperatures of the jacket are considered as follows:

$$if\ T_{ctrl,set} < T_{j,min}\ then$$

$$T_{ctrl,set} = T_{j,min}$$

$$else\ if\ T_{ctrl,set} > T_{j,max}\ then \tag{5.10}$$

$$T_{ctrl,set} = T_{j,max}$$

$$end$$

The dynamic behaviour is described using first-order differential equations considering the thermal inertia of the heating/cooling system given by their respective time constants [30, 155, 156]:

- In cooling case ($T_{ctrl,set} < T_j$):

$$\frac{dT_j}{dt} = \frac{T_{ctrl,set} - T_j}{\tau_c} \tag{5.11}$$

- In heating case ($T_{ctrl,set} > T_j$):

$$\frac{dT_j}{dt} = \frac{T_{ctrl,set} - T_j}{\tau_h} \tag{5.12}$$

- No change needed ($T_{ctrl,set} = T_j$)

$$\frac{dT_j}{dt} = 0 \tag{5.13}$$

where τ_h and τ_c are the time constants for heating and cooling, respectively. The parameters of equations 5.9 through 5.13 must be identified for each reactor to be used in scale-up. A systematic procedure was developed with this purpose.

5.2 Procedure

The following procedure was designed to assess the thermal dynamics of an industrial scale reactor and create a model representing its overall thermal behaviour under normal and reactive operating conditions.

After the reactor model has been created, it now needs to be fed correctly in order to match efficiently to the studied system. The evaluation of the dynamic parameters describing the heating/cooling behaviour requires a disturbance of the latter obtained from temperature changes. As a result, the procedure is performed with different reactor amounts of an inert solvent with known physical properties and consists of three isothermal steps, separated by temperature ramps at a constant temperature heating/cooling rate. The overall workflow of the procedure is illustrated in Figure 5.6 and divided in six steps:

Step 1: Three heating/cooling experiments at different degrees of filling, separated by isothermal stages, are performed resulting in three temperature profiles, respectively the reaction mixture (T_r), the jacket (T_j) and the set-point ($T_{x,set}$), for each experiment.

Step 2: The reactor and jacket temperature profiles obtained, allow to evaluate the parameters of the dynamic model: the overall heat transfer coefficient (U), the heat loss coefficient (α) and the heat capacity of the equipment (C_W).

The obtained temperature profiles were designed such as during the isothermal stage (Figure 5.7a), the derivative of the reactor temperature can be approximated to zero:

$$-q_{ex} \cong q_{loss} \tag{5.14}$$

Oppositely, during heating/cooling ramps (Figure 5.7b), the heat balance is dominated by the heat exchange between the reaction mixture and the jacket. Therefore, the heat loss term can be neglected resulting in the following
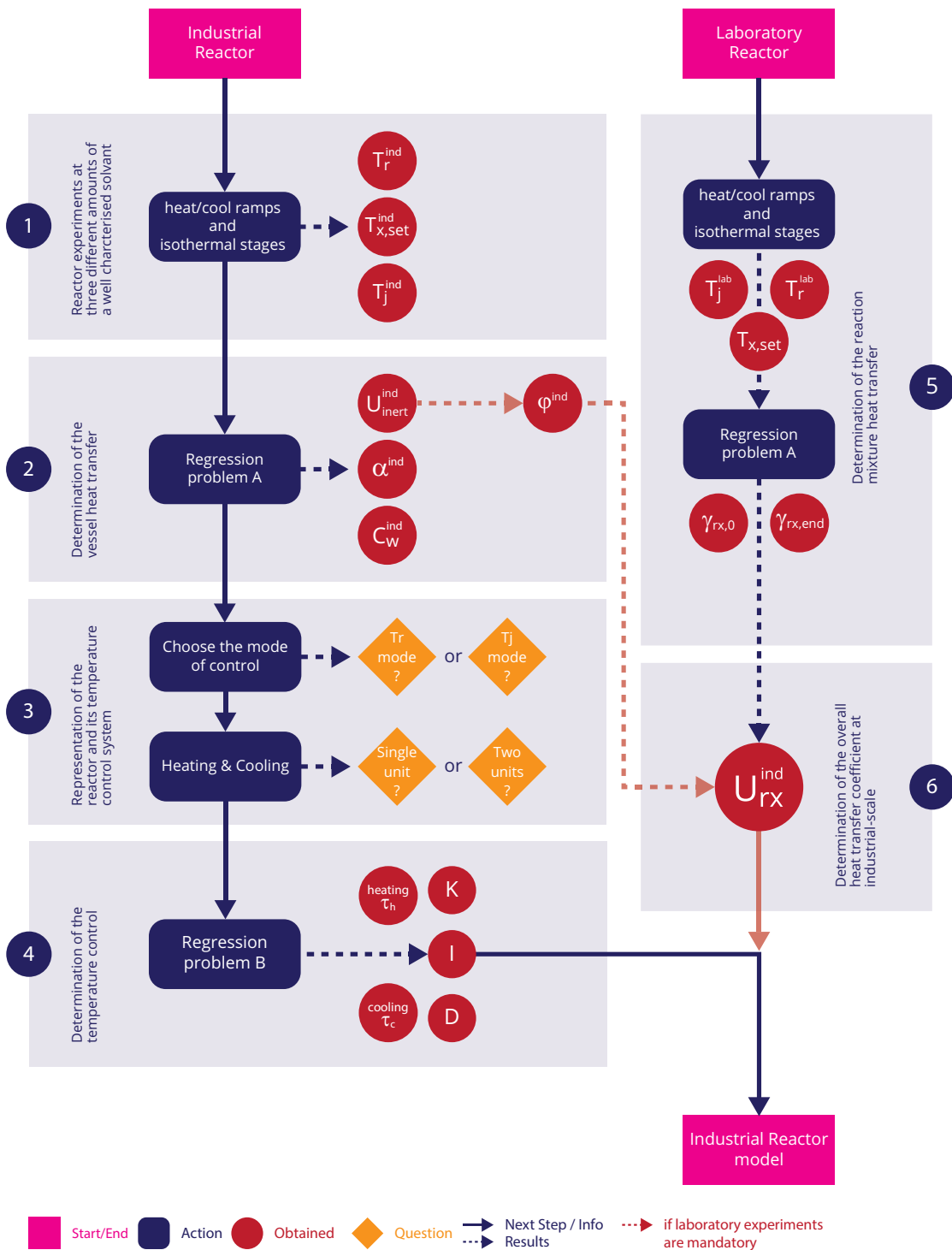
Figure 5.6 – Reactor Dynamics Investigation comprised of six main steps: 1) Experiments carried out at three different amount of an inert and well characterised solvent at industrial scale; 2) Characterization of the heat transfer characteristics of the industrial reactor; 3) Representation of the reactor temperature control; 4) Characterization of the temperature control and jacket behaviour, 5) Determination of the reaction mixture heat transfer at laboratory scale and 6) Evaluation of the overall heat transfer coefficient at industrial scale.
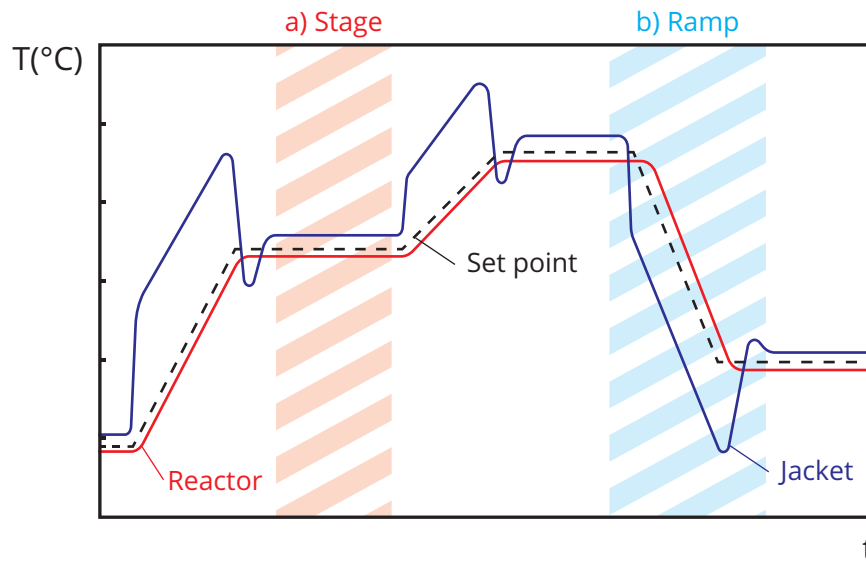
Figure 5.7 – Illustration of a typical temperature profiles composed of a) stages and b) ramps.

dependence:

$$q_{acc} \cong q_{ex} \tag{5.15}$$

Step 3: The model structure has to be defined according to the nature of the equipment itself. The reactor can operate under different conditions, namely T_r or T_j-modes. In addition, the temperature control can have different set of parameters depending on the mode of operation (heating or cooling). The physical system can either be represented as a:

(a) *Single unit*, meaning that only one set of parameters is necessary to describe the heating and cooling system; or,

(b) *Two units*, when two sets of parameters are required to describe heating and cooling system, respectively.

Step 4: The next step is to evaluate the parameters of the temperature controller itself using a non-linear regression approach (section 2.4).

Step 5: Under reactive conditions, the reaction mixture undergoes multiple changes in terms of composition and physical properties. As a result, the overall heat transfer coefficient U, more precisely the reaction mixture heat transfer γ_r may evolve during the process course. Thus, as a first approximation, this coefficient may be considered as a function of the time or the mass loaded (fed-batch operating conditions) between two instants in time: at t_0, the beginning of the process, and at t_{end}, its end. Based on this assumption,

this coefficient needs to be evaluated in at least these two points.

Considering the industrial scale, such investigation may be complicated or even impossible to perform for safety or economic reasons. Therefore, another approach has to be adopted.

The RDI steps 1 and 2 are coupled together with the two film theory in order to evaluate the reaction mixture heat transfer at industrial scale using calorimetry at laboratory scale. This approach is described by the following substeps at laboratory scale:

(a) Perform the RDI steps 1 and 2 to evaluate the vessel heat transfer coefficient φ_{lab} of the laboratory scale reactor with an inert solvent.

(b) Deduce the reaction mixture heat transfer coefficient γ_{rx} before and after the reaction(s) using the step 2 of the RDI (Section 5.3.1.2):
- at the beginning: $\gamma_{rx,0}$
- at the end: $\gamma_{rx,end}$

Step 6: In order to finalize the industrial reactor model, the overall heat transfer coefficient for any time t, between t_0 and t_{end} and considering the industrial mixing conditions z_{ind} is evaluated:

$$\frac{1}{U_{ind,t}} = \frac{1}{\varphi_{ind}} + \frac{1}{z_{ind}\gamma_{rx,t}} \tag{5.16}$$

If only the overall heat transfer is required, namely that the RDI can be performed directly at industrial scale with the reactive mixture (under safe operating conditions), the latter can be evaluated directly from industrial scale experiments as illustrated in Figure 5.6.

5.3 Regression problems

The identification of the reactor model parameters consists of two regression problems: 1) The heat transfers and 2) the temperature control. Such problems are solved using non-linear regression methods as presented in Section 2.4.1.
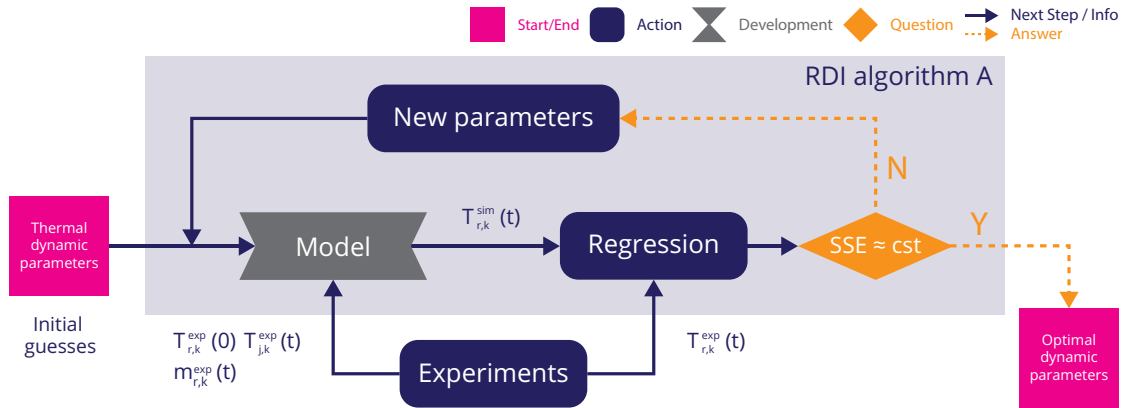
Figure 5.8 – Workflow of the regression problem applied for the overall heat transfer coefficient U.

5.3.1 Heat transfers

5.3.1.1 The overall heat transfer (A)

The goal of such regression problem is to characterize the different heat transfer events occuring inside and around the reactor, namely the heat transfer between the coolant and the reaction mixture (U), the heat losses (α) and the accumulation of heat in the equipment (C_w). The developed procedure is presented in Figure 5.8. The steps 2 and 5 of the procedure depict the regression of the quantity expressed as:

$$\min_{x} \sum_{k=1}^{p} \sum_{i=1}^{m} \left(T_{r,k}^{sim}\left(x, t_i\right) - T_{r,k}^{exp}\left(t_i\right) \right)^2 \tag{5.17}$$

where $x = U, \alpha, C_W \in [0, \infty[$, $t \in [t_0, t_f]$. t represents the time, whereas t_0 is the starting point, t_f the ending point of the experiment k comprising m experimental points. The model is given by the reactor temperature which is the solution of the first-order differential equation:

$$\frac{dT_{r,k}^{sim}\left(x, t_i\right)}{dt} = \frac{U \cdot A_p \left(T_{j,k}^{exp}\left(t_i\right) - T_{r,k}^{sim}\left(x, t_i\right) \right) + \alpha \left(T_{amb,k}^{exp}\left(t_i\right) - T_{r,k}^{sim}\left(x, t_i\right) \right)}{m_{r,k}^{exp} c_{p,r} + C_w} \tag{5.18}$$

109

subject to the following initial conditions:

$$T_{r,k}^{sim}\left(t_0\right) = T_{r,k}^{exp}\left(t_0\right) \tag{5.19}$$

To avoid any complication in the regression problem, the overall heat transfer coefficient U and the heat loss coefficient α are considered as temperature-, volume- and mass-independent. Although the reactor heat capacity C_w should be volume-dependent, it will be considered as a constant in the overall approach, such as the parameters are:

$$
\begin{aligned}
U &= U_1 = ... = U_p \\
\alpha &= \alpha_1 = ... = \alpha_p \\
C_w &= C_{w,1} = ... = C_{w,p}
\end{aligned}
\tag{5.20}
$$

This assumption will be discussed in more details along an example depicted in Section 5.4.1.2.

5.3.1.2 Evaluation of the vessel and reaction mixture heat transfer coefficients

As mentioned in Section 5.1.1, the heat transfer problem can be separated into two distinct zones according to their influence: 1) the jacket and wall (vessel) and 2) the reaction mixture.

As a matter of fact, this problem has to be solved globally. The overall heat transfer coefficient has to be evaluated as presented in Section 5.3.1.1 and used to evaluate the vessel and reaction mixture heat transfer coefficients. Some requirements have to be fulfilled for each individual coefficient:

1. *Vessel heat transfer coefficient* φ: its determination requires an experiment performed with an inert solvent which the physical properties are well defined and is convenient for the range of temperature reached by the process (RDI step 2). The average value of this parameter is deduced from the two film theory

(equation 5.6) such as:

$$\frac{1}{\varphi_{mean}} = \frac{\sum_{p=1}^{P} \sum_{i=1}^{m} \left(\frac{1}{U_{mean,inert}} - \frac{1}{z\gamma_p(t_i)} \right)}{P \cdot m} \tag{5.21}$$

This parameter requires to be defined only one time per reactor as long as the coolant stays unchanged.

2. *Reaction mixture heat transfer coefficient* γ: its determination requires an experiment performed with the reactive mixture in the same vessel used in the previous determination. This parameter is then deduced:

$$\frac{1}{\gamma_{rx,mean}} = \left(\frac{1}{\overline{U}_{rx}} - \frac{1}{\varphi_{mean}} \right) \cdot z \tag{5.22}$$

This parameter is solely dependent of the physical properties of the reaction mixture, meaning that it can be considered scale-independent as demonstrated in equation 5.6. As a result, the overall heat transfer coefficient under reactive conditions can be evaluated at industrial scale using laboratory scale experiments.

5.3.2 Temperature control and jacket behaviour (B)

Once the thermal dynamic behaviour has been evaluated and defined, a characterization of the temperature control and jacket behaviour can be conducted. An algorithm has been developed in order to solve the following regression problem (Figure 5.9):

$$\min_{y} \sum_{k=1}^{p} \sum_{i=1}^{m} \left(\left(T_{r,k}^{sim}(y,t_i) - T_{r,k}^{exp}(t_i) \right)^2 + \left(T_{j,k}^{sim}(y,t_i) - T_{j,k}^{exp}(t_i) \right)^2 \right) \tag{5.23}$$

where $y = K, I, D, \tau_c, \tau_h \in [0, \infty[$, $t \in [t_0, t_f]$. t represents the time, whereas t_0 is the starting point and t_f the ending point of the experiment k and m the experiment point. The model is given by the reactor temperature $T_{r,k}^{sim}$ and jacket one $T_{j,k}^{sim}$ which result
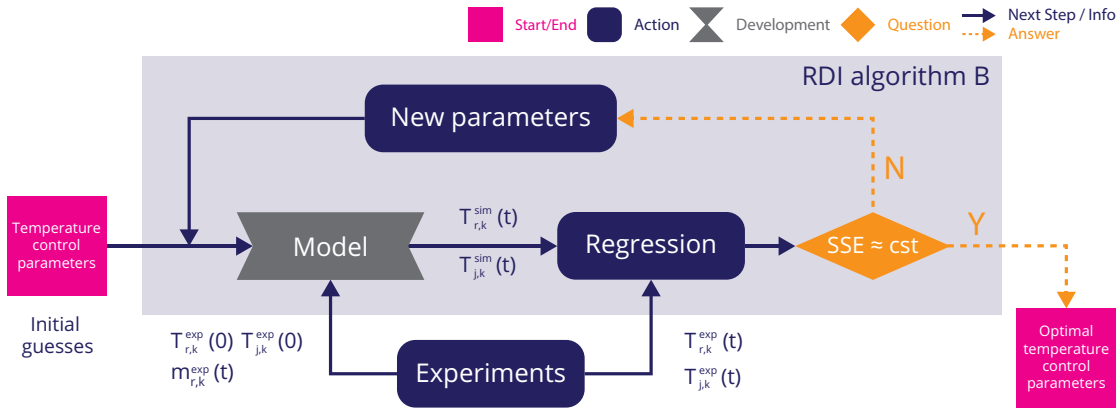
Figure 5.9 – Workflow of the temperature control regression problem.

from the solutions of the first-order differential equations:

$$\frac{dT_{r,k}^{sim}\left(y,t_i\right)}{dt} = \frac{U_{opt}A_p\left(T_{j,k}^{sim}\left(y,t_i\right) - T_{r,k}^{sim}\left(y,t_i\right)\right) + \alpha_{opt}\left(T_{amb,k}^{exp}\left(t_i\right) - T_{r,k}^{sim}\left(y,t_i\right)\right)}{m_{r,k}^{exp}c_{p,r} + C_{W,opt}}$$

(5.24)

$$\frac{dT_{j,k}^{sim}\left(y,t_i\right)}{dt} = \begin{cases} \frac{T_{ctrl,set,k}^{sim}(y,t_i) - T_{j,k}^{sim}(y,t_i)}{\tau_c} & if \quad T_{ctrl,set,k}^{sim}\left(y,t_i\right) < T_{j,k}^{sim}\left(y,t_i\right) \\ \frac{T_{ctrl,set,k}^{sim}(y,t_i) - T_{j,k}^{sim}(y,t_i)}{\tau_h} & if \quad T_{ctrl,set,k}^{sim}\left(y,t_i\right) > T_{j,k}^{sim}\left(y,t_i\right) \\ 0 & if \quad T_{ctrl,set,k}^{sim}\left(y,t_i\right) = T_{j,k}^{sim}\left(y,t_i\right) \end{cases}$$

(5.25)

subject to the following initial conditions:

$$T_{r,k}^{sim}\left(t_0\right) = T_{r,k}^{exp}\left(t_0\right)$$

(5.26)

$$T_{j,k}^{sim}\left(t_0\right) = T_{j,k}^{exp}\left(t_0\right)$$

(5.27)

Oppositely to the first regression problem, to obtain the temperature control behaviour of the reactor, the jacket temperature of the simulation is, this time, calculated based on the model presented in the equations 5.9 to 5.13. All the control parameters are independent of the reactor temperature and reaction mixture entered.

5.4 Applications

5.4.1 Simulated reactor

The use of simulated data can greatly help to test the developed procedure and its algorithm. On the one hand, the parameters are unequivocally known. On the other hand, it serves the purpose to evaluate the procedure ability to nourish properly the algorithm.

In this first application, thermal behaviour simulations of a reactor were performed based on the reactor model presented above (section 5.1) and considering the overall heat transfer as a function of the temperature of the jacket and the reaction mixture such as:

$$\frac{1}{U\left(T_r, T_j\right)} = \frac{1}{\varphi\left(T_j\right)} + \frac{1}{z\gamma\left(T_r\right)} \tag{5.28}$$

The reaction mixture is characterized by the physical properties of water while the jacket and wall heat transfer follows a linear behaviour in function of the jacket temperature:

$$\varphi\left(T_j\right) = a_\varphi T_j + b_\varphi \tag{5.29}$$

The thermal dynamic behaviour of the reactor is described by a model comprising heat transfer and geometric parameter as well as temperature control parameters depicted in Table 5.2 and 5.3, respectively.

The data were generated following the RDI procedure requirements, namely three experiments composed of temperature stages and ramps for different degrees of filling. The temperature set profiles were planned using Space Filling Design (section 2.3), based on the ranges presented in Table 5.1. For each experiment, the starting temperature and set point are at $25°C$.

Table 5.1 – Range of operating conditions for the Space Filling Design used in the experiment plan simulations. The obtained plans are depicted in Table A.5.

	Temperature	Ramp
Units	$(°C)$	$(°C/min)$
min	10	0.2
max	80	1.2

Table 5.2 – Reactor thermal dynamic parameters used for the reactor model. The heat transfer of the mixture γ is calculated in function of the temperature T_r based on the water physical properties available in [157].

Parameters	φ	z	γ	R_{AV}	α	T_{amb}
Units	$(W \cdot m^{-2} \cdot K^{-1})$	(-)	$(W \cdot m^{-2} \cdot K^{-1})$	(m^{-1})	$(W \cdot K^{-1})$	$(°C)$
Value	$a = 0.01$ $b = 500$	0.1003	see [157]	4.2	9	20
Equation	(5.29)	(5.6)	(5.6)			

Table 5.3 – Temperature control and jacket behaviour parameters used for the reactor model.

Parameters	K	I	D	$\tau_{heating}$	$\tau_{cooling}$	T_{min}	T_{max}
Units	$(-)$	(s^{-1})	(s)	(s)	(s)	$(°C)$	$(°C)$
Value	4	10000	0	450	320	5	180

5.4.1.1 Heat transfer problem

The regression problem A (Section 5.3.1.1) was addressed to the simulated data. The obtained results are depicted in Table 5.4 and validated through a Leave-p-Out Cross-validation. As the purpose of such study is to evaluate the procedure and its algorithms, only the errors between the real and the retrieved parameter values are shown.

Table 5.4 – Retrieved thermal dynamic parameters and their respective deviations obtained from a leave-p-out cross-validation.

	U	φ	α
Units	$(W \cdot m^{-2} \cdot K^{-1})$	$(W \cdot m^{-2} \cdot K^{-1})$	$(W \cdot K^{-1})$
Real averaged value	432.7	503.3	9
Retrieved value	434.5	504.6	10.7
Standard value	1.4	1.8	0.8
Confidence interval	3.5	4.8	1.9

The equipment heat capacity has been ignored for the regression problem and will be discussed in Section 5.4.1.3.

Following this investigation, it was also possible to determine the vessel heat transfer coefficient such as:

$$\varphi_{mean} = \left(\frac{1}{U_{mean}} - \frac{1}{z\gamma_{mean}} \right)^{-1} \tag{5.30}$$

The obtained value is compared to the averaged one used for the simulated data (Table 5.4) and depicts a relatively good behaviour.

5.4.1.2   Temperature control and jacket behaviour problem

The obtained parameters with their respective errors and confidence intervals are presented in Table 5.5.

These results depends greatly on the quality of the thermal dynamic parameters. Thus, if the thermal dynamic is assessed correctly, following the RDI requirements, the temperature control and jacket behaviour parameters can be evaluated with a good accuracy. This last point was successfully reached even using an averaged overall heat transfer coefficient considered independent of the temperature. Physically wrong, this assumption allows to greatly simplify the regression problem and demonstrates to be relevant to decrease the correlation between the different parameters.

Table 5.5 – Retrieved temperature control and jacket behaviour parameters from a Leave-p-Out Cross-validation.

Parameters	P	I	τ_h	τ_C
Parameters	$(-)$	(s^{-1})	(s)	(s)
Average	4.00	10116.26	450.45	320.21
Standard deviation	0.00	1.84	0.04	0.02
Confidence interval (99%)	0.00	4.70	0.10	0.05
Deviations real value (%)	0.05	1.16	0.10	0.06

5.4.1.3   Discussion

Using behavioural simulations is very helpful for the understanding of the type of experiment required to nourish the algorithm. The procedure was used on this basis and proved to be relevant. In addition, the latter demonstrated a good ability to gain enough information and at the same time, feed properly the algorithm. The overall approach also showed to be robust and efficient concerning the evaluation of the thermal dynamic, temperature control and jacket behaviour parameters.

The heat balance used to describe the thermal behaviour of the reactor is highlighted by three parameters: the overall heat transfer coefficient U, the heat loss coefficient α and the equipment heat capacity C_w. The identification of C_w value demonstrated to be particularly difficult as a strong correlation exists between the latter and the two other

parameters (U and α). This observation is the result of their interdependence existing in the model and appearing in the regression problem (A) as:

$$\frac{UA}{m_r c_{p,r} + C_w} \quad , \quad \frac{\alpha}{m_r c_{p,r} + C_w} \tag{5.31}$$

The equipment heat capacity C_w can have an infinite number of possible values answering the regression problem, as long as the value of the fractions presented in equation 5.31 are kept identical. The relationships existing between these parameters are especially appreciable at small-scale oppositely to large-scale as demonstrated at:

- Small-scale:

$$m_r c_{p,r} \geq C_w \tag{5.32}$$

- Large-scale:

$$m_r c_{p,r} \gg C_w \tag{5.33}$$

A study of the equipment heat capacity C_w on the maximum jacket temperature reached in heating phase was performed using the developed reactor model and is illustrated in Figure 5.10. Although neglecting this parameter at large-scale will not have a big impact on the retrieved parameters (Figure 5.10d), at small-scale, this effect will be less mitigated as depicted in Figure 5.10c.

As a consequence, the model used for the regression problem has to be simplified to finally contain only the overall heat transfer coefficient U and the heat loss one α. The equations 5.18 and 5.24 become respectively:

$$\frac{dT_{r,k}^{sim}(x,t_i)}{dt} = \frac{UA_p \left(T_{j,k}^{exp}(t_i) - T_{r,k}^{sim}(x,t_i) \right) + \alpha \left(T_{amb,k}^{exp}(t_i) - T_{r,k}^{sim}(x,t_i) \right)}{m_{r,k}^{exp} c_{p,r}} \tag{5.34}$$

and

$$\frac{dT_{r,k}^{sim}(y,t_i)}{dt} = \frac{U_{opt}A_p \left(T_{j,k}^{sim}(y,t_i) - T_{r,k}^{sim}(y,t_i) \right) + \alpha_{opt} \left(T_{amb,k}^{exp}(t_i) - T_{r,k}^{sim}(y,t_i) \right)}{m_{r,k}^{exp} c_{p,r}}$$

$$\tag{5.35}$$
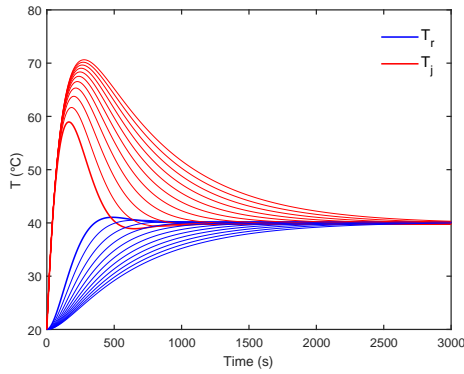
(a) 0.5L reactor filled with water for $U = 180W \cdot m^{-2} \cdot K^{-1}$ and $A = 0.032m^2$.
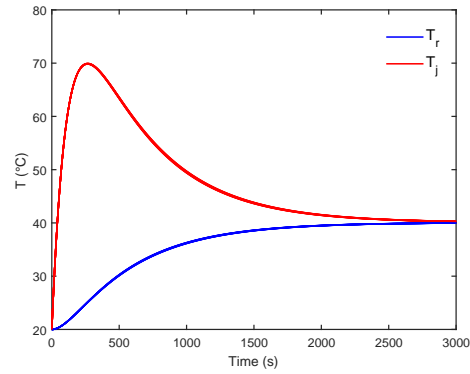
(b) $1m^3$ reactor model filled with water for $U = 800W \cdot m^{-2} \cdot K^{-1}$ and $A = 2.9m^2$.
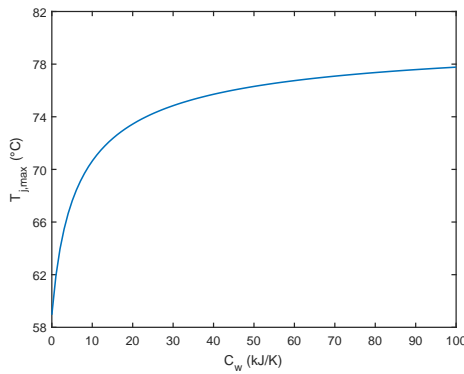
(c)
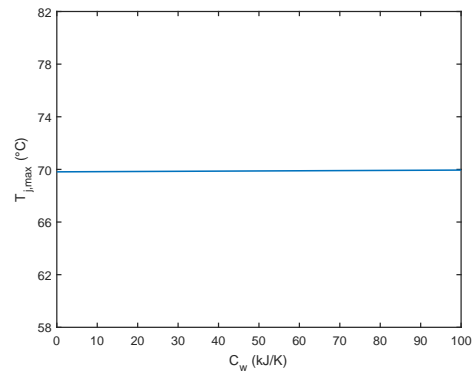
(d)

Figure 5.10 – Effect of the reactor heat capacity C_w on the overall behaviour with a) and b): temperature profiles in heating phase for different C_w in, respectively, small and large scales. c) and d): maximum jacket temperature reached in function of C_w in heating phase in, respectively, small and large scale.

On the one hand, this value can still be relevant if a noticeable effects of the equipment are known. On the other hand, this effect will be "diluted" in the overall heat transfer and in the heat loss coefficient. As a secondary solution, if one knows the mass of the equipment in direct contact with the reaction mixture and their specific heat capacity (reactor and inserts), the C_w can be estimated as:

$$C_w = \sum_{i=1}^{I} m_i c_{p,i} \tag{5.36}$$

Where i represents the equipments.

In terms of temperature control, the main issue that may be encountered, arises when a process command (often called "actuator") has a nonlinear behaviour (e.g. $T_{ctrl,set}$).

This fact will lead to some discrepancy in the PID control, making the regression difficult.

This type of discrepancy is highlighted when an actuator is working in the saturation region, meaning that the command will have no effect on the actuator output. In case of the PID equation (5.9), the $T_{ctrl,set}$ will stay locked on the defined bound (T_{min} or T_{max}). This problem often happens when the integral part of the PID equation (5.9) is not reinitialized and keeps the error accumulated during the experiment. This phenomena is called "the wind-up effect" and can be managed by anti wind-up methods as presented by Johnson and Moradi but is not assessed during this work [158].

5.4.2 Non-reactive system

Considering the different points discussed above, real reactors of two different scales were investigated:

1. Laboratory scale: a 0.5L Mettler-Toledo® RC1e Calorimeter.

2. Pilot scale: a 100L industrial reactor.

All the developments and data processing of the next sections were performed using commercial software packages (AKTS-Reaction Calorimetry Software [134] and MathWorks MATLAB [135]).

5.4.2.1 Laboratory scale

The behaviour of a 0.5L Mettler-Toledo RC1e® calorimeter has been studied, using the Reactor Dynamic Investigation presented previously. Three experiments with different amounts of water were performed, based on a Space Filling Design (section 2.3) and using the range developed in the simulation example (Table 5.1).

The RC1e calorimeter was operating in T_r-mode using a very fast heat carrier circulation in the jacket and an impeller rotating at 500 rpm without baffles, but with inserts as the temperature and calibration probes. An homogeneous reactor content is assumed in terms of temperature and material.

Heat transfer problem

Following the same approach as in the simulation example, the best estimated parameters were obtained and are listed in Table 5.6.

A study considering the equipment heat capacity C_w was performed. The correlation matrix obtained through the different iterations of the leave-p-out cross-validation

demonstrated a large dependency of this parameter with the others, a relationship already discussed and illustrated during the simulated data investigation (Section5.4.1). In addition, equalling C_w to zero, in this case, would be a good approximation, as the reactor is build in glass, a material having a low specific heat capacity ($0.67\ J \cdot K^{-1} \cdot g^{-1}$) and leading to small influences compared to the others phenomena (heat exchange with the jacket and losses).

The approach was tested with different sets of initial guess not containing C_w and resulting, in every case, to the same set of parameters (with very small deviations). Thus, the initial guess have, in this case, no influence on the parameter estimates.

Table 5.6 – Comparison between different methods to define the overall heat transfer coefficient U and the resulting standard error of predictions when applied to the model. The RDI method was processed with AKTS-Reaction Calorimetry Software [134] while the Standard and Quickcal methods were computed in Mettler-Toledo iRCcontrol Software [121].

	U	α	σ_{T_r}	Max_{T_r}	$R^2_{T_r}$
Units	$(W \cdot m^{-2} \cdot K^{-1})$	$(W \cdot K^{-1})$	$(°C)$	$(°C)$	$(-)$
RDI with T_j	161.2	0.05	0.16	1.5	0.9962
RDI with T_a	181.5	0.05	0.17	1.1	0.9995
Standard method	182.6	0.1*	0.64	1.4	0.9866
Quickcal	184.2	0.1*	0.53	0.63	0.9870

The overall heat transfer coefficients obtained were compared with the ones evaluated by calibration (Standard and QuickCal methods) and demonstrated small variations but remaining in the same ranges (Table 5.6). Depending on the method used, it may require the specific heat capacity which can have a direct influence on the final value of the overall heat transfer coefficient. Oppositely, in the RDI, the specific heat capacity
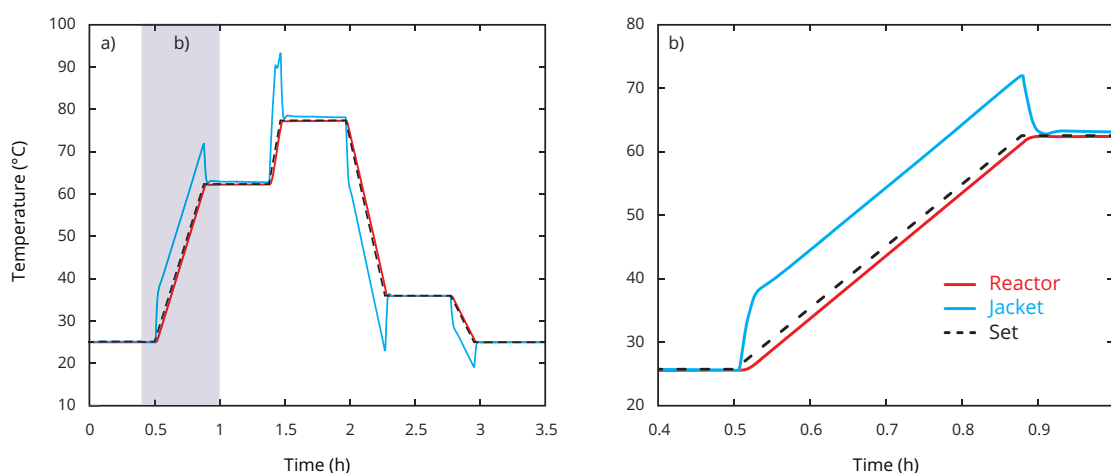
Figure 5.11 – Temperatures monitored in a 0.5L Mettler-Toledo® RC1e (324g of water) under Tr-mode: a) the full experiment b) zoom showing the grey part of experiment.

$c_{p,r}$ is considered known (water: estimated at 4.18 $J \cdot K^{-1} \cdot g^{-1}$).

Another aspect investigated during this analysis was the consideration of the jacket temperature T_j and the corrected jacket temperature T_a. In terms of location, T_j is measured at the inlet of the RC1e jacket while T_a is estimated at the surface of the reactor wall on the jacket side as illustrated in Figure 5.12. Significant deviations in the obtained parameters are appreciable between these two locations as shown in Table 5.6.

Is the algorithm not able to retrieve the correct overall heat transfer? As a matter of fact, the retrieved values, in both cases, are correct as long as they are used to compare the model predictions to the measurement in their respective location. In T_j-case, the distance between the two temperature measurement points is larger than in T_a-case. This has the effect to virtually increase the resistance on the jacket side while T_r still changes in a similar manner for both cases as illustrated in Figure 5.12 and by the following relation considering no losses:

$$
\begin{aligned}
m_r c_{p,r} \frac{dT_r}{dt} &= U_j A \left(T_j - T_r \right) \\
&= U_a A \left(T_a - T_r \right)
\end{aligned}
\tag{5.37}
$$

leading to:

$$
\begin{aligned}
\left(T_j - T_r \right) &> \left(T_a - T_r \right) \\
U_j &< U_a
\end{aligned}
\tag{5.38}
$$

As a conclusion, the location of the jacket temperature measurement may play an essential role regarding the definition of the real thermal dynamics of a reactor. The overall heat transfer obtained through the RDI, however, will still describe the correct behaviour in the measurement location.

Concerning the heat loss coefficient, the obtained value is approaching zero which is also the result of the reactor construction; the reactor is equipped of a double jacket and disposes of an excellent insulation. Regarding the parameter quality, the correlations demonstrated the requirement of a minimum of two experiments. By using an unique experiment, the heat loss coefficient showed to be highly correlated to the overall heat transfer coefficient (>0.8). In addition, in the case of the RC1e, the obtained value cannot be evaluated using a heat balance approach as only the inlet jacket temperature is measured. This attempt would also demonstrate that the inlet and outlet jacket
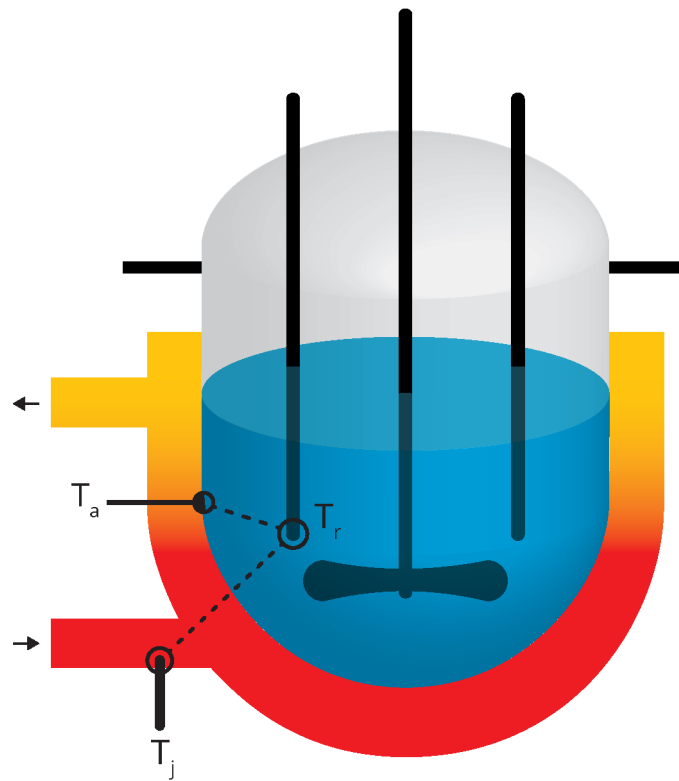
Figure 5.12 – Locations of the different Temperature measurements: T_r, T_j, T_a in the 0.5 Mettler-Toledo® RC1e calorimeter.

temperatures are extremely close and would result in a poor heat balance. Therefore, the value obtained from the RDI cannot be compared nor confirmed. However, this value remains logical, credible and remarkably useful for the establishment of the reactor dynamic model.

Temperature control and jacket behaviour

Besides the flow dynamics of the heat carrier, another important aspect is the device dynamics resulting from the application of a temperature controller. In case of the RC1e calorimeter, a PI controller is considered. The heating and cooling are assumed to have different behaviours, a hypothesis supported by the construction of the RC1e calorimeter itself (Section 3.2.3).

The obtained parameters are depicted in Table 5.7 under the consideration of the jacket temperature and the corrected one.

The retrieved P value is close to the value actually used in the real controller in both cases, T_j or T_a [121]. The reset time I obtained during the regression exhibited, for each iteration, a large value meaning that the integral part of the PID equation (5.9) may be neglected. Therefore, as a simplification, the reset time I was bounded to

Table 5.7 – Retrieved temperature control and jacket behaviour parameters based on the jacket temperature T_j, the corrected jacket temperature T_a, using the RDI for a 0.5L Mettler-Toledo® RC1e containing three different amounts of water using AKTS-Reaction Calorimetry Software [134].

	P	I	τ_h	τ_c
Units	$(-)$	(s^{-1})	(s)	(s)
RDI with T_j	7.5	99999	30.1	25.9
Real values with T_j	7	99999	31.7	25.7
RDI with T_a	6.2	99999	48.6	24.5
Real values with T_a	7	99999	45.1	43.2

Table 5.8 – Errors depicted by the model predictions regarding the experiments.

σ_{T_r}	$\Delta T_{r,max}$	σ_{T_j}	$\Delta T_{j,max}$	$R^2_{T_r}$	$R^2_{T_j}$
	$(°C)$			$(-)$	
0.1	0.3	0.4	4	1	0.99

99999.

Regarding the time constants, some experiments with step changes under T_j-mode were performed in heating and cooling phases. The study was focused solely on the jacket behaviour which parameters were estimated graphically and over the RDI algorithm. The reactor was considered having no controller ($P = 0$) to ensure the algorithm to estimate only the time constants. The retrieved time constants are depicted in Table 5.7 and demonstrated in both cases (T_j and T_a) to be similar. An exception can be observed for the cooling time constant estimated graphically from T_a. This deviation may be explained by the fact that this signal is calculated and may be have an incorrect behaviour under extreme heating and cooling operating conditions.

Discussion

The RC1e calorimeter is well known for its fast response to changes, which is directly confirmed by the obtained thermal dynamic and temperature control parameters (Table 5.6 and 5.7). The consideration of the two temperature measurement locations demonstrated different behaviours. However, in both cases, the model exhibits a fast response to changes and remains valid. As a result, the standard temperature deviation between the model and the experiments were studied and demonstrates significantly good results. These differences are amounted to 0.1 and 0.4°C respectively, for the reaction mixture and the jacket (Table 5.8).

Some large deviations ($\sim$4°C) are mainly observed when the temperature controller of the RC1e exhibits an unusual behaviour as presented in Figure 5.14. The most

likely cause is a presumed anti wind-up action. Others deviations are observable when a sudden change is applied (set-point or quickcal events). As a result, small delays appear, however, the model catches up quickly and restores the correct behaviour (Figure 5.13).

An analysis of the obtained correlation matrix after each cross-validation iteration, showed that none of the parameters were correlated. This result demonstrates two points:

1. the procedure supplies correctly the algorithm and allows to separate efficiently the parameters,

2. the model structure is sufficiently accurate to describe almost perfectly the dynamic behaviour of the considered reactor.

In summary, it was possible to quite accurately describe the behaviour of a lab-scale reactor (Table 5.8), the 0.5L Mettler-Toledo® RC1e calorimeter using only temperature experiments. The model-based approach coupled to the RDI procedure demonstrates once again its robustness and efficiency.
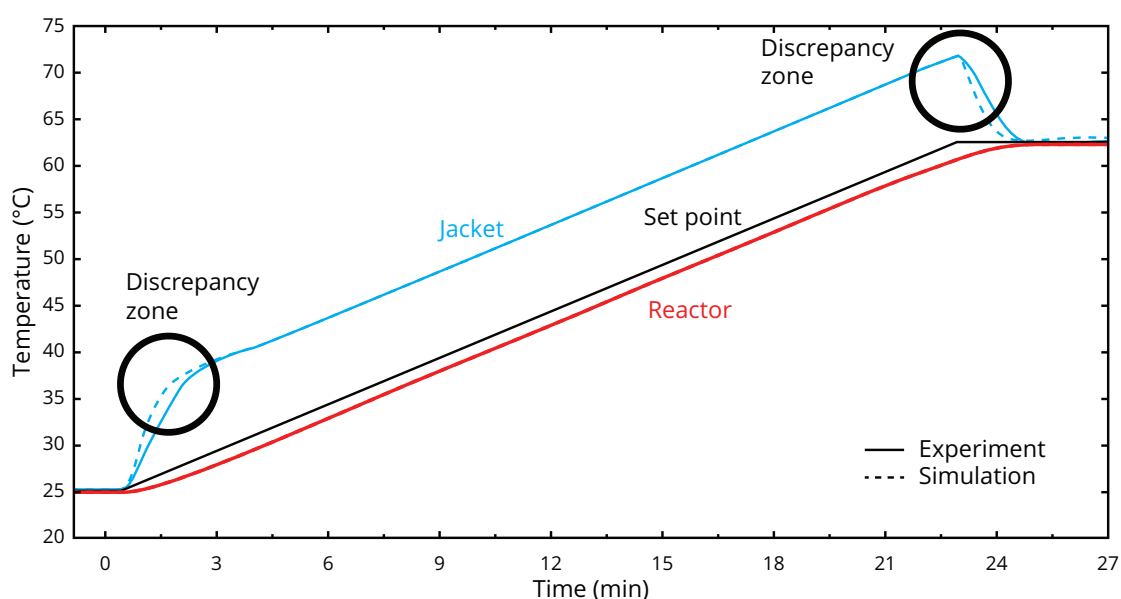
Figure 5.13 – Observed deviations when a change in the temperature set point occurs in the 0.5 Mettler-Toledo® RC1e calorimeter.

5.4.2.2 Pilot reactor

The RDI was, this time, used for a 100L pilot-scale reactor operating under T_r- and T_j-mode. As a first step, the pilot reactor was operating under T_j-mode using a simple
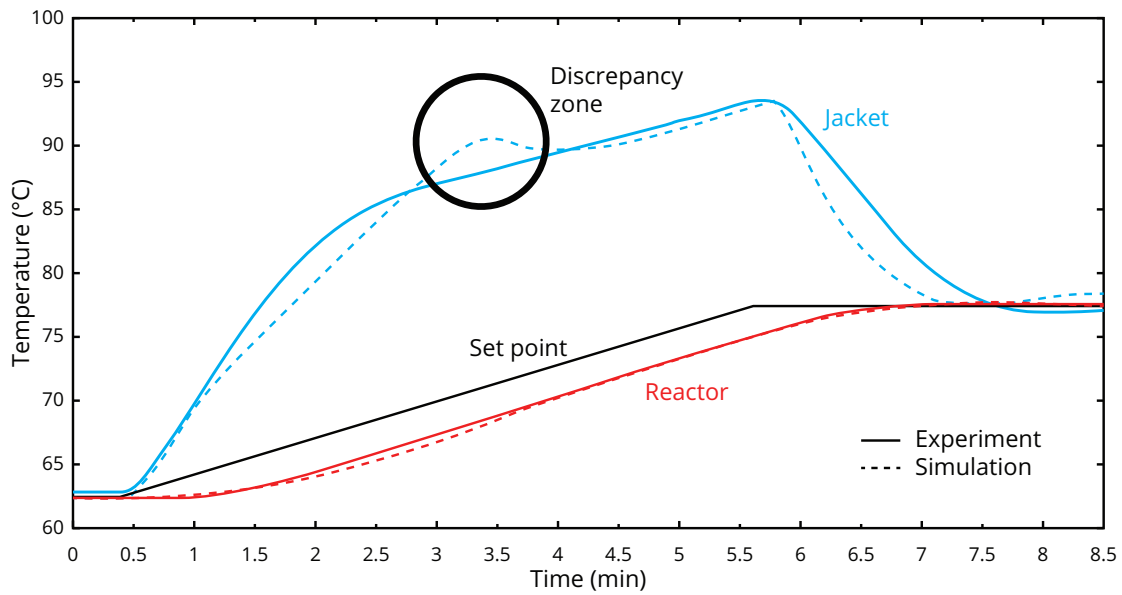
Figure 5.14 – Example of discrepancy demonstrated in the 0.5 Mettler-Toledo® RC1e calorimeter.

external jacket, equipped of a pitched-blade stirrer running at 50 rpm without baffles. As for the laboratory-scale reactor, the reaction mixture is assumed homogeneous. The same statement can be made for the T_r-mode.

Heat transfer problem

The jacket temperature was estimated as the arithmetic mean between the input and the output jacket temperatures for a constant flow rate. The arithmetic mean replaced the usually applied logarithmic one, as there were no noticeable difference between
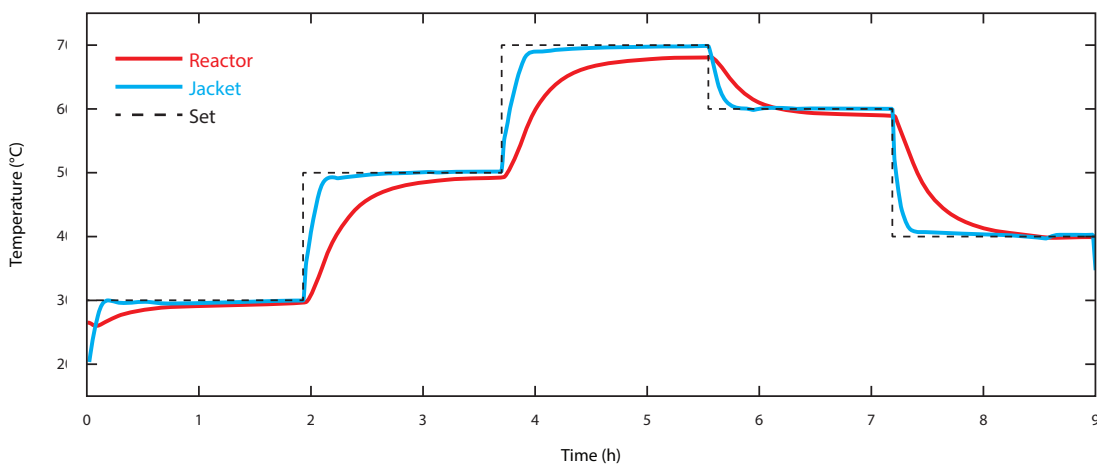
Figure 5.15 – Temperatures monitored in a pilot-scale reactor (70kg of water) under T_j-mode.

Table 5.9 – Thermal dynamic parameters calculated with AKTS-Reaction Calorimetry Software for T_j-, T_r- and coupled modes [134].

	T_j-mode	T_r-mode	Coupled
		U	
Units		$(W \cdot m^{-2} \cdot K^{-1})$	
Value	428.83	425.00	424.39
Standard deviation	28.56	7.54	10.44
Confidence interval (99%)	73.57	19.42	26.90
		α	
Units		$(W \cdot K^{-1})$	
Value	9.73	8.24	8.93
Standard deviation	1.52	0.27	0.75
Confidence interval (99%)	3.91	0.70	1.94

them for such experiments.

The mode of temperature control has no meaning in the assessment of the heat transfer dynamics, solely the temperature differences between the jacket and the reaction mixture during the heating/cooling ramps and the stages are relevant. The obtained thermal dynamic parameters are represented in Table 5.9 for the different modes and also when all the experiments are coupled. The obtained overall heat transfer coefficient U, in all cases, demonstrates to be higher than the laboratory scale. This fact is due to a better heat transfer material constituting the wall. Steel material ($\lambda \approx$ 15-30 $W \cdot m^{-2} \cdot K^{-1}$) replaces the glass material ($\lambda \approx 1\ W \cdot m^{-2} \cdot K^{-1}$) used at laboratory scale and allows a better thermal conductivity through the wall [159]. The heat losses are also larger as the reactor insulation is weaker than the one at laboratory scale.

The respective deviations are also analysed and show a prediction of the reaction mixture temperature relatively good with a standard error of $0.35°C$ and a maximum deviation of $1.35°C$ (Table 5.10). This investigation was performed only for water, however, these results demonstrates that the procedure is entirely applicable as well as at laboratory as at larger scales.

Table 5.10 – Errors and confidence intervals on the reaction mixture temperature between the experiments and their respective predictions under different modes and couplings.

	T_j-mode	T_r-mode	Coupled
Units		$(°C)$	
σ_{T_r}	0.34	0.36	0.35
$\Delta T_{r,max}$	1.29	1.27	1.35

Temperature control and jacket behaviour

Such reactor size implies much more inertia than at laboratory scale; therefore, the heating/cooling system response to or for a change demonstrates higher time constants, in both case, T_r and T_j-mode.

The differentiation in the temperature control mode is appreciable in terms of P parameter values as shown in Table 5.11. On the one hand, in T_j-mode, the proportional part exhibits a value approaching zero resulting in a non-existence of control. On the other hand, the T_r-mode exhibits a value having an effect on the temperature controller behaviour. This can be explained that in T_j-mode, the heating/cooling system is not controlled by the events occurring in the reaction mixture, the temperature of the coolant is set and totally managed by the heating/cooling internal controller. This aspect cannot be described by using the presented model but shows how the reactor may interact with the heating/cooling system depending on the mode of control.

Table 5.11 – Temperature control parameters with their respective errors and confidence intervals under T_r- and T_j-modes calculated by AKTS-Reaction Calorimeter Software [134]. * If the algorithm evaluates a value for the reset time I greater than 99999, itss value is bounded at this maximum.

Mode	Units	P $(-)$	I (s^{-1})	τ_h (s)	τ_c (s)
	Value	0.76	99999*	601	402
T_j	Standard deviation	0.25	–	100	70
	Confidence interval	0.63	–	258	179
	Value	2.43	99999*	1093	534
T_r	Standard deviation	0.09	–	104	34
	Confidence interval	0.24	–	268	88

Discussion

Once again, the RDI proved to be robust and efficient for the identification of the thermal dynamic regardless of the temperature-mode of control. Although the interval of confidences are quite wide for the time constant, an efficient smoothing of the data should decrease significantly their values (especially for the jacket temperature signal).

The different modes of temperature control are characterized by their way to influence the system temperatures (reaction mixture and jacket). A behaviour logically described by the obtained parameters under T_r- as well as T_j-mode.

The heating/cooling system possesses generally its own temperature controller, therefore operating in T_j-mode will demonstrate the inertia of the heating/cooling system in a relatively good way through the definition of the time constants.
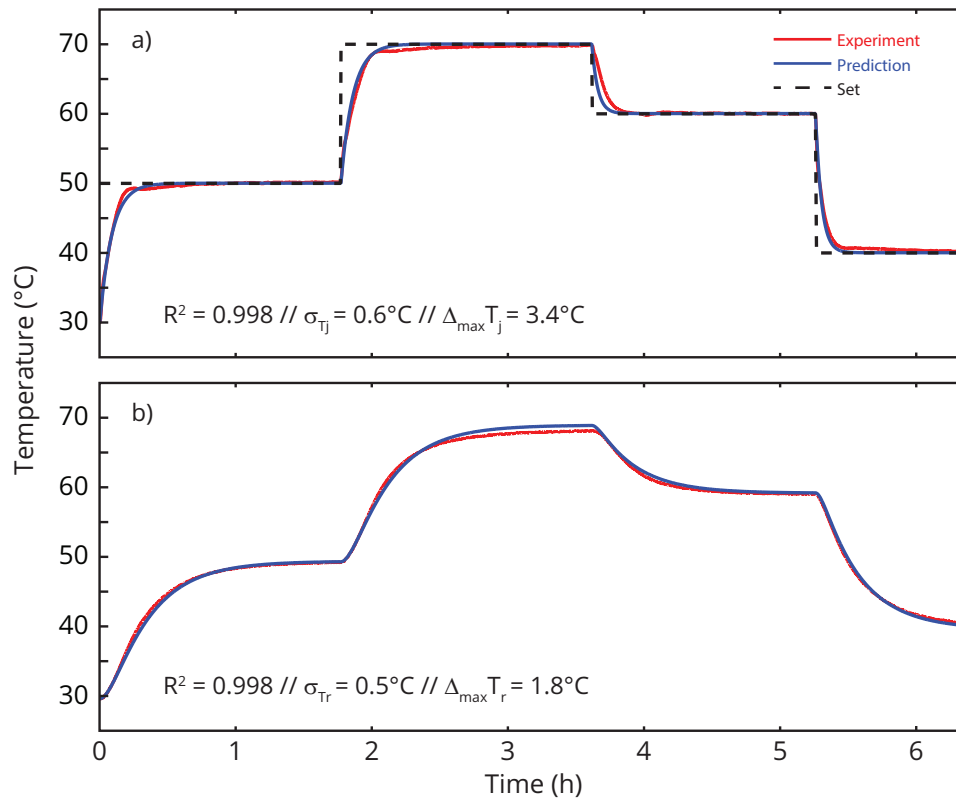
Figure 5.16 – Temperature profiles measured: a)T_j and b) T_r versus their respective prediction in a pilot-scale reactor filled with $95kg$ of water and operating in T_j-mode (error analysis depicted in Table 5.12).

The type of experiment at pilot-scale were limited to step changes, as a consequence, the overall behaviour of the temperature control may not be well distinguished from the time constant. The obtained PID parameters (Table 5.11), however, may not be as good as they could be but remain able to describe in a relatively good way the overall behaviour as depicted in Table 5.12 and illustrated in Figure 5.16.

Another aspect has to be considered, greater deviations were observed at higher temperatures. This issue is mainly due to the higher vapour pressure of water leading to evaporation. Nevertheless, the quality of the fit can be considered as satisfactory since the model had a standard temperature deviation smaller than $1°C$ in all the cases.

Table 5.12 – Resulting deviations and determination coefficient for both mode of control, namely T_r- and T_j-mode.

	T_r			T_j		
	σ_{T_r}	Max_{T_r}	$R^2_{T_r}$	σ_{T_j}	Max_{T_j}	$R^2_{T_j}$
T_r-mode	1.5	6.4	0.987	3.0	12.4	0.960
T_j-mode	0.5	1.8	0.998	0.6	3.4	0.998

Table 5.13 – Kinetic parameters of the reaction scheme depicted in (5.39).

	Reaction 1			
	k_0	E_a	$\Delta_r H$	Orders
Units	$\left(g \cdot s^{-1} \cdot mol^{-1}\right)$	$\left(J \cdot mol^{-1}\right)$	$\left(J \cdot g^{-1}\right)$	$(-)$
Value	10^{10}	60000	-55	$o_A = 1$ $o_B = 1$

5.4.3 Reactive system

The next section will especially investigate two different types of disturbance along the process course:

1. Physical properties unchanged: Simulated reaction system.

2. Physical properties changed: Esterification of acetic anhydride with methanol.

5.4.3.1 Simulation of a hazardous reaction system

In order to prove the robustness of the described procedure, a hypothetic hazardous reaction with a high accumulation heat potential was explored at laboratory scale under batch operating conditions. A highly exothermic autocatalytic reaction (equation 5.39) simulated by AKTS-Reaction Calorimetry Software was chosen as a challenging task to test the temperature control model [134].

In this kind of reaction, the auto-accelerating rate period is followed by a decelerating one. Such a scenario of heat evolution leads to a fast and visible jacket response. The application of highly exothermic autocatalytic reaction allows to identify whether the Reactor Dynamic Investigation is suited to describe the heating/cooling phases as well as reactive conditions.

$$A + B \rightarrow 2B \tag{5.39}$$

The kinetic parameters describing this system are listed in Table 5.13.

In order to recreate the heat flow profile in different operating conditions, an electrical heating element was developed. The heat flow profile was computed using the known reaction kinetics information, taking into account the actual reactor mass and temperature, and supplying the corresponding heat by Joule effect into the sample.
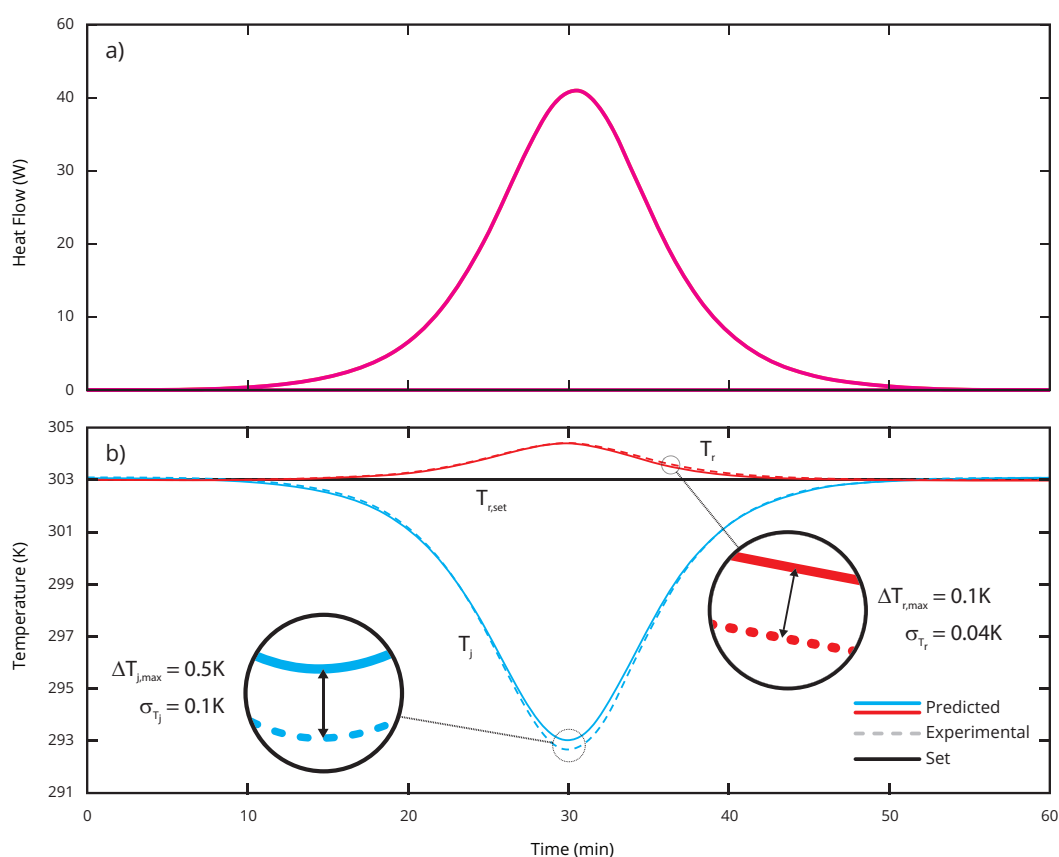
Figure 5.17 – Simulation of a reaction through a joule-effect: a) Produced heat flow and b) Profiles of the predicted versus experimental temperatures of the reactor (T_r) and jacket (T_j) during the reaction course in a 0.5L Mettler-Toledo® RC1e (350g of water). The maximal differences between the reactor and jacket temperatures (ΔT_i) during the reaction course amounted to 0.1 and 0.5K with a standard deviation (σ_i) of 0.04 and $0.1K$, respectively. The heat flow as a function of time is displayed in the top part of the plot.

This precisely controlled heating element allows to mimic experimentally the thermal effect of a reaction without the risk of loss of control.

The Reactor Dynamics Investigation was performed for the RC1e with a stirrer rotating at 500 rpm. The obtained parameters were used to predict an experiment course carried out in T_r-mode (Figure 5.17) in a 350g reaction mixture assuming the reaction parameters according to those depicted in Table 5.13. The predicted and measured temperature profiles are in good accordance. Small deviations are mainly exhibited around heating/cooling transition but they remain in an acceptable range.

The robustness was tested by imposing an external heat profile based on an autocatalytic reaction system. It was proven that even with perturbations, the obtained parameters were still able to describe correctly the reactor behaviour. The results have shown that the proper elaboration of the isothermal and temperature-ramp stages could allow to fully characterise the thermal dynamics of the reactor.

5.4.3.2 Esterification

As a last example for the RDI procedure, a real reactive system is investigated at laboratory scale: the esterification of acetic anhydride with methanol (Section 4.4.2) in a Mettler-Toledo® RC1e of 0.5L operating under T_r-mode.

An experiment comprising the following phases was performed:

1. Heating/cooling ramps followed by isothermal stages are performed on the initial reaction mixture constituted of only acetic anhydride ($295g$).

2. The reaction is performed in T_r-mode ($55°C$) under fed-batch operating conditions ($1h$ feed, $64g$ of methanol) following by a waiting time of $8.5h$ to let the reaction proceed to completion.

3. Heating/cooling ramps followed by isothermal stages are performed on the final reaction mixture, constituted of the remaining acetic anhydride, acetic acid and methyl acetate (considering the methanol completely converted).

The obtained thermal dynamic and temperature control parameters are depicted in Table 5.14 and 5.15, respectively. A comparison between the experimental temperatures and the predicted ones is illustrated in Figure 5.18 and the resulting errors are depicted in Table 5.16.

Table 5.14 – Thermal dynamic parameters for the esterification of acetic anhydride and methanol before and after reaction.

	φ	γ_0	γ_{end}
Units	$(W \cdot m^{-2} \cdot K^{-1})$		
Value	181.7	9233	5009
z	0.19		
	U_0	U_{end}	
Units	$(W \cdot m^{-2} \cdot K^{-1})$		
Value	164.6	152.6	

Table 5.15 – Temperature control parameters for the esterification of acetic anhydride and methanol.

	P	I	τ_h	τ_c
Units	$(-)$	s^{-1}	(s)	(s)
Value	3.4	99999*	33	27
Standard deviation	0.3	-	3	3
Confidence interval	0.65	-	7	8
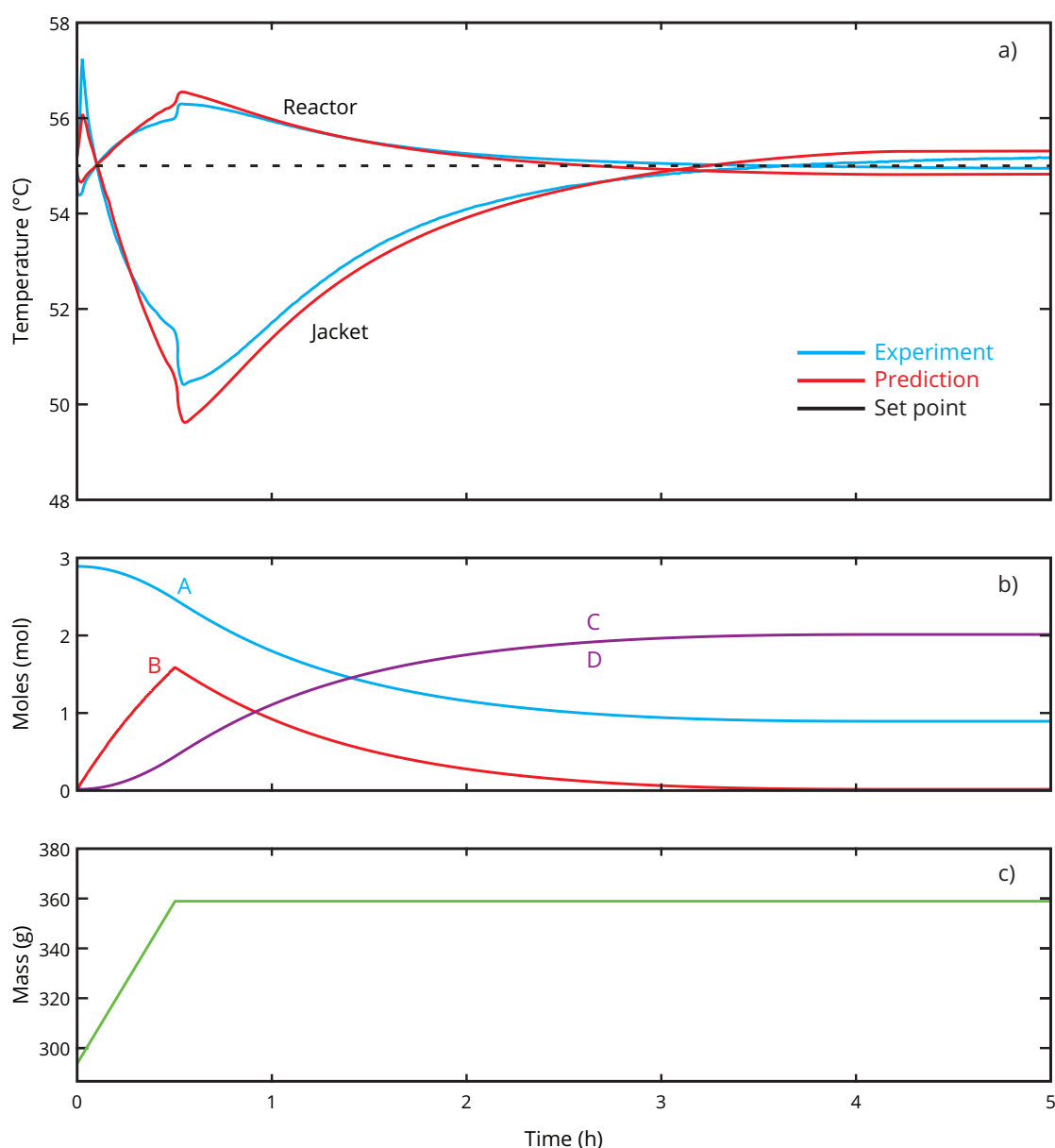
Figure 5.18 – Comparison between predictions and experimental data for the esterification of acetic anhydride with methanol obtained in a 0.5 Mettler-Toledo® RC1e calorimeter: a) Temperature predictions versus the experimental ones; b) Mole profile of the different species present in the reaction mixture and c) Mass profile along the process course. The resulting errors are depicted in Table 5.16.

Discussion

The primary goal of such a model is to predict the reaction mixture and reactor thermal behaviour at any time, a point answered by this example under reactive conditions. Although some deviations are noticeable, the overall behaviour is covered by the model.

The predicted jacket temperatures reach lower values than the ones exhibited by the experiment. These deviations can be explained by phenomena such as evaporation

Table 5.16 – Standard and maximum deviations for the reaction mixture and jacket temperatures along the reactive process for a T_r-mode.

	T_r	T_j
units	$°C$	$°C$
σ_i	0.1	0.4
$\Delta T_{i,max}$	0.2	2.4

along the process course and not accounted in the model. These aspects may have helped to consume the heat generated by the reaction system, requiring less effort from the cooling system in the real case.

The effects of evaporation (endothermic) could have been added to the model to obtain a behaviour approaching the reality. Nevertheless, to simplify and decrease the requirement of thermodynamic data, it was better to keep the model as simple as possible.

The reactor model remains valid as it allows to determine the jacket temperature required in the case where these phenomena were not present with a sufficient accuracy (Table 5.16). This last point has to be carefully handled at larger scale as these events may not help the jacket as efficiently as at laboratory scale.

5.5 Conclusion

A simple and general procedure has been developed to determine the overall reactor thermal behaviour considering three dominating aspects of the heat transfer system: 1) heat balance, 2) PID temperature control and 3) jacket behaviour.

With this purpose, temperature heating/cooling ramps as well as isothermal stages were investigated under a wide range of operating conditions and reactor sizes. The obtained results demonstrate, that using such a strategy is experimentally easy to perform, allows a good understanding of heating/cooling system and shows to be in good accordance with the experiments for non-reactive as well as reactive operating conditions.

The consistency and robustness of the procedure and the algorithm were assessed under various conditions and control types. The predictions performed, using the reactor model with the retrieved dynamic parameters, seem to be robust to small disturbances (external heating source and reaction). In addition, it is well known that small systems are more sensitive to changes. Despite this fact, it was possible to obtain an accurate model and predictions at small as well as large-scale.

The industrial system was explored using temperature step-changes which allowed describing the temperature controller behaviour under drastic change of set point. The procedure may be more efficient using data based on temperature ramps as they allow to have the system under soft and progressive changes leading to a better overview of the temperature controller work. Oppositely, step changes may bring the system in extreme state resulting in a different behaviour than normal operating conditions and will not allow an accurate description of the temperature controller behaviour.

The described model-based procedure may be of great help for an efficient and safe scale-up, allowing to describe the behaviour through predictions before any real experiment. Nevertheless, having a good knowledge of the reactor thermal dynamics and its temperature control behaviours is not sufficient to guarantee the safety of a chemical process.

Once the reaction kinetics and reactor dynamics are developed, an overview of the process dynamic behaviour can be established to form an overall model comprising the thermal aspects of the process. As a result, the thermal potential of the considered system can be evaluated during the process course.

This thermal potential is often poorly estimated and may lead to critical reactor state. The use of the overall model, composed by the reaction kinetic and the reactor thermal dynamic models (Chapters 4 and 5), is of first importance to determine the optimal operating conditions for an inherently safe process. Therefore, to guarantee an economically and inherently safe process, different requirements have to be fulfilled. The next chapter will use the developed models together in order to build an overall model, which can be used to evaluate the thermal potential during the process course. This knowledge will help to determine the best operating conditions with a safety perspective.

6

Risk Assessment and Process Optimisation

Once we know our weaknesses they cease to do us any harm.

Georg C. Lichtenberg, 1742-1799

Avoiding incidents related to chemical production is a significant concern in fine chemical industries. On the one hand, chemical risks may be due to reactivity and toxicity of the involved chemicals. On the contrary, controlling chemical reactions (especially exothermic reactions) and associated hazards are present as soon as a production is initiated. Therefore, without an adequate control, a chemical reaction may turn into a runaway and lead to severe consequences. Over the last twenty years, such unfortunate examples have been witnessed: AZF in France (2001), Synthron (2006) or T2 incident in the US (2007), to only cite a few [160–162].

As root causes of these runaways, one can mention a large range of issues such as poor operating conditions, failure of control or equipment, inappropriate materials, and many others. The potential risk of failure or incident cannot be completely erased. However, adequate measures may decrease the incidents to minor issues [9, 10, 72].

The traditional approach would be to control such hazardous situations by setting safety barriers to protect the surrounding people, environment, and property. This approach has demonstrated to be highly effective in decreasing the casualties (rupture disk, quenching, . . .). However, it cannot prevent them.

Another concept, namely *"inherent safety"*, was introduced by Kletz in the late 70's as a different objective in process development. The term *"inherent"* identifies a permanent and essential element, quality or attribute that something or someone possesses [163, 164]. Therefore, the term *"inherently safe"* characterizes a chemical process which the design eliminates or at least reduces the potential hazards associated with the operations or material used [164]. Furthermore, Kletz quoted: *"What you don't have can't leak"* [165]: since chemical incidents always result from a loss of containment, such a statement represents a robust solution to safety problems. The concept postulated behind this quote is that the best way to reduce risk is to avoid the hazard rather than control it, in opposition to the traditional approach consisting of adding safety barriers only once the process has been designed [166].

6.1 Cooling failure scenario

Regardless the kind of failure that may happen and whether the process is conducted in batch- or fed-batch mode, the reaction mixture will possess, in most cases of the fine chemistry, a thermal potential (exothermic system). This thermal potential is essentially due to the amount of unconverted reactant accumulated along the process that has not yet reacted (from feed or production of unstable materials). If the cooling system suffers a breakdown or is not active, the heat released by the reaction mixture will not be removed, and the reactor will operate under conditions approaching an adiabatic

situation. At first, the accumulated heat will cause a gradual rise in the reaction mixture temperature. The reaction rate and consequently the heat production will increase exponentially (equation 2.12) and finally result in an uncontrollable reactor state. This increase of temperature may trigger other events such as secondary decomposition reactions often accompanied by gas release. The gas produced may result in a pressure increase and, ultimately, lead to the explosion of the reactor if no measures are taken before the point of no return [145].

The *"cooling failure scenario"*, first developed by Gygax and then improved by Stoessel, well describes such incident sequence [30, 167]. This scenario illustrates four successive steps (Figure 6.1):

1. The process is brought to the process temperature (T_p) and operates under normal conditions.
2. At the worst time t^*, a cooling failure arises.
3. The heat released by the synthesis reaction due to the amount of remaining (batch) or accumulated (fed-batch) reactant results in an increase of temperature. The reached temperature is called the Maximum Temperature of the Synthesis Reaction (MTSR).
4. At this temperature, secondary reactions may be triggered and cause an exponential temperature rise towards a final temperature (T_{end}).

The relevant safety parameters that describe such cooling failure scenario are illustrated in Figure 6.1. This includes: the process temperature (T_p), the Time to Maximum Rate under adiabatic conditions (TMR_{ad}) of the synthesis reaction (rx) and the decomposition (dec), the different adiabatic rise (ΔT_{ad}) and ending in a final temperature (T_{end}).

In a batch process, the accumulation of unconverted reactant is maximum already from the start of the reaction and will decrease proportionally to the reaction progress until the reaction has proceeded to completion. When a reaction is highly exothermic or when the amount of accumulated reactant during the process is important, operating in fed-batch conditions offers several advantages [168]:

1. The progress of the reaction can be controlled by a progressive feed of reactant to improve selectivity, productivity, and safety.

2. The feed rate can be designed to have different behaviour (linear, sigmoidal, exponential...).

However, in the case of cooling failure, an inappropriate feed profile may result in a too large accumulation and lead to unexpected situations with more or less severe consequences [72, 127].
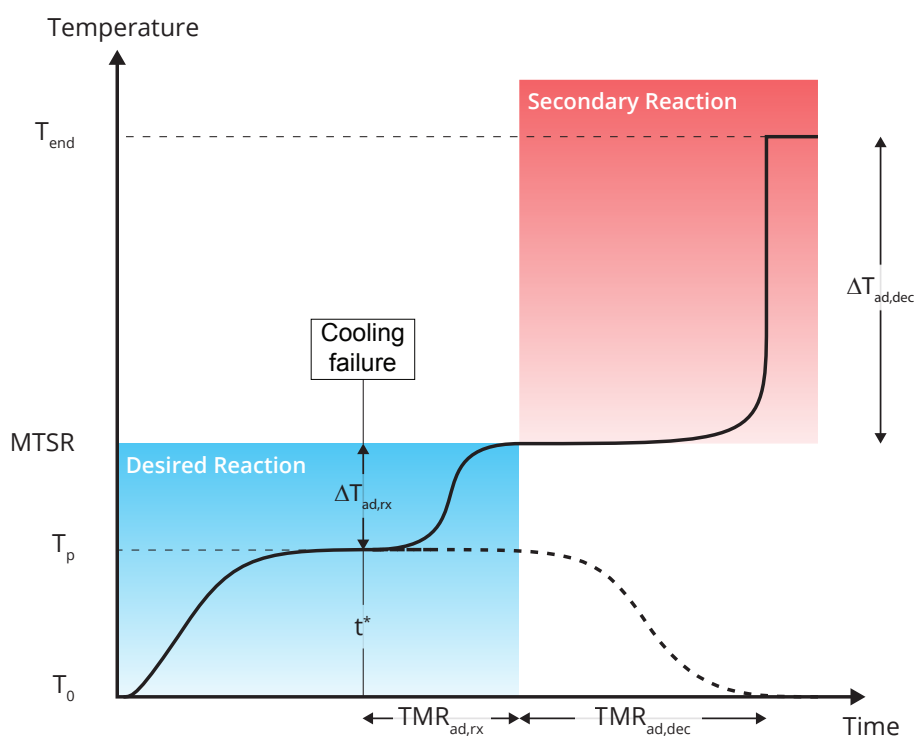
Figure 6.1 – Cooling Failure Scenario: After a cooling failure at t^*, the temperature rises from process temperature (T_p) to the Maximum Temperature of Synthesis Reaction ($MTSR$). The time to reach this temperature is characterised as the Time to Maximum Rate under adiabatic conditions of the desired reaction ($TMR_{ad,rx}$). At this temperature, a secondary decomposition reaction may be triggered. The blue part (left-hand) of the scheme is devoted to the desired reactions with the temperature increase to the MTSR in case of cooling failure. In the red zone (right-hand), the temperature increase due to the secondary reactions is shown, accompanied by its characteristic time to maximum rate under adiabatic conditions ($TMR_{ad,dec}$) [30].

Serra et al. have demonstrated several scenarios where a batch process may not always be the most hazardous, oppositely to fed-batch accumulation or start-up of continuous reactors [169]. A fed-batch process may conduct to even more critical situations when the feed is not immediately stopped after the cooling failure. However, when a well-chosen feed function is applied, the safety constraints can be respected without any decrease in productivity [72].

All things considered, an important objective in the fine chemical industry is to find the operating conditions that maximize profit while ensuring safe operations. For a fed-batch process, a correct design of the feed profile and operating conditions respecting simultaneously safety, selectivity and productivity will undoubtedly lead to an inherently safer and effective process.

Over the past decade, different approaches have been developed to determine parameters that lead to such a process. Ubrich et al. showed how a feed profile for a

second order reaction could be improved considering production and safety constraints [168, 170]. Westerterp and co-workers demonstrated how to determine safe operating conditions with the help of a safety diagram, and to ensure an inherent safe process [171, 172]. Copelli et al. developed an optimisation of the operating conditions based on topological criteria for arbitrary reaction scheme and detection of the QFS region ("Quick start", "Fair conversion" and "Smooth temperature profile") [32, 173]. Maestri and Rota build a general criterion comparing the apparent reaction kinetics during the feed operation to the heat-removal contribution [174, 175].

Among these developments, the determination and consideration of the reaction kinetics (feed profile effect, side or decomposition reactions) is frequently approximated for a single reaction or left out to avoid cost and time consumption; the dynamics of the reactor temperature control is not taken into account: the reactor temperature is assumed to be equal to the set point. The innovation of the present thesis is to combine both dynamic aspects, the reaction kinetics and the reactor dynamics by performing well-planned experiments to identify the required parameters as presented in Chapters 4 and 5, respectively.

This novel approach considering simultaneously the reaction kinetics and the reactor dynamics has been developed with the goal to answer the following questions and lead to a successful scale-up:

1. Is the industrial reactor able to control the temperature of the reaction mixture?
2. What are the safety relevant parameters to govern the reaction system in a given industrial reactor?
3. How can the reactor be brought into a safe state in case of malfunction?

This chapter shows how the kinetic models developed in Chapter 2, based on calorimetric experiments (Chapter 4) are combined with the reactor dynamics (Chapter 5) to design a safe process, namely first defining the optimal operating parameters minimizing the thermal potential while remaining productive and inherently safe. The first section mainly highlights the different ways to evaluate the thermal potential for simple and complex reaction schemes. In a second part, a strategy to determine an optimal feed profile leading to an inherently safer process is presented. And finally, a third section is exclusively dedicated to examples of applications.

6.2 Evaluate, track and control the thermal potential

During the design of the operation sequence for a fed-batch reactor, one has generally the desire to find the optimal set of operating conditions that leads to an inherently safe and economically viable process. This set is significantly dependent on the amount of

accumulated reactant controllable by the process and directly affects the selectivity as well as the safety.

The concept of unconverted reactant accumulation represents a latent thermal potential that will remain undiscovered as long as the system is well controlled, especially as long as the cooling system is active and efficient. In the case of cooling failure or equipment malfunction, however, this potential will be unleashed resulting in an inevitable increase of the temperature directly proportional to the amount accumulated. This temperature increase may trigger secondary reactions if not correctly managed. Henceforth, it becomes essential to evaluate and control the thermal potential along the process course.

With this perspective, two distinct families of reaction schemes may have to be considered:

1. *Simple reaction scheme:* mainly single bimolecular and consecutive reactions (well separated on the temperature domain).

2. *Complex reaction scheme:* composition of consecutive and parallel reactions.

Depending on the kind of reaction system studied, the determination of the thermal potential will not always be feasible through solely experiments as presented in the next sections.

6.2.1 Simple reaction scheme

Assume an irreversible and one-step reaction occurring in a homogeneous reaction mixture under fed-batch conditions:

$$A + B \rightarrow C \tag{6.1}$$

and where A is the fed reactant.

From this point, two situations regarding the reaction rate may be encountered:

(a) *High reaction rate*: characterizing fast reactions, a high reaction rate results in an added reactant immediately consumed, and no significant accumulation of unconverted reactant is then observed as well as a heat production rate directly proportional to the feed rate. In this situation, the reaction rate is not kinetically but feed rate controlled.

(b) *Low reaction rate*: oppositely to high reaction rates, if the feed rate is greater than the reaction rate, the fed reactant will not be immediately consumed resulting in an accumulation [30, 32]. The reaction rates being a function of the reactant concentrations (except for zero-order reaction), the fed reactant A has first to reach a certain level before the reaction rate can be appreciable. This phenomenon is noticeable by a rapid increase of the concentration of the fed-reactant at the beginning of the operation (Figure 6.2).

Considering slow reaction, the temperature that may be reached in case of cooling failure is greatly dependent on the amount of accumulated reactant X_{acc}. This temperature can be evaluated using the following equation:

$$T_{cf} = T_r + X_{acc}\Delta T_{ad,rx}\frac{m_{r,f}}{m_r(t)} \tag{6.2}$$

where $m_{r,f}$ represents the mass of the reaction mixture at the end of the feed and $m_r(t)$ the current reaction mixture mass. $\Delta T_{ad,rx}$ symbolizes the adiabatic temperature rise obtained from the reaction enthalpy $(-\Delta_r H)$ and specific heat capacity of the reaction mixture $(c_{p,r})$:

$$\Delta T_{ad,rx} = \frac{(-\Delta_r H_{rx}) \cdot C_0}{\rho \cdot c_{p,r}} \tag{6.3}$$

Where C_0 is the maximum concentration of the limiting reactant and ρ, the density of the reaction mixture.

In batch mode, the accumulation is maximum at the start of the process ($X_{acc,0} = 1$. Later, as the reaction proceeds, this amount is equivalent to the remaining amount of limiting reactant such as:

$$X_{acc} = 1 - X_r \tag{6.4}$$

Since the lowest concentration dictates the accumulation, different factors will influence its behaviour under fed-batch operation:

1. *Before the stoichiometric point*: the fed reactant A limits the production of C, namely that the amount of C cannot be greater than the molar amount of A already fed ($X_r \leq X_{fd}$). The accumulation is then obtained as follows:
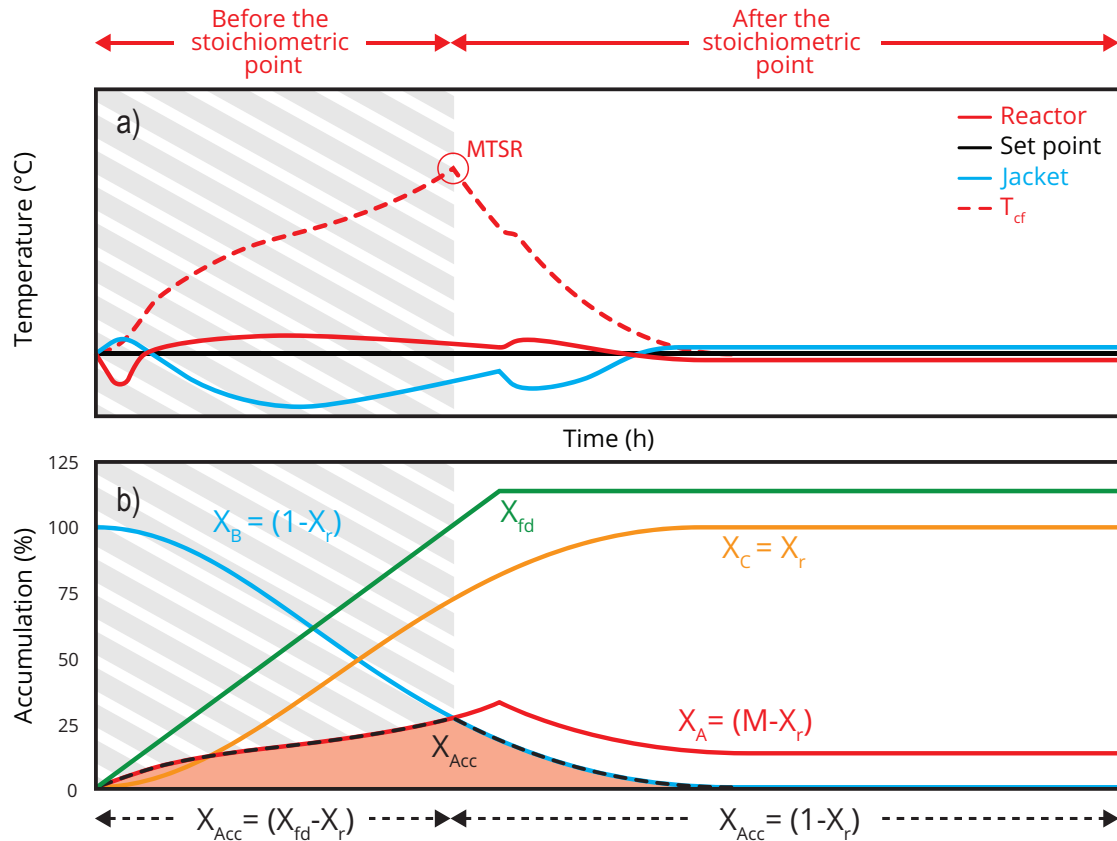
Figure 6.2 – Cooling Failure Scenario for a simple reaction scheme: a) temperature profiles (reactor, jacket and setpoint) before and after a cooling failure, b) thermal potential contribution of each species in the reaction system with a 10% molar excess of A ($M = 1.1$ see equation 6.5).

$$X_{acc} = X_{fd} - X_r = \frac{M \cdot t}{t_{fd}} - X_r = \frac{N_{A,fed}(t)}{N_{B,0}} - X_r \qquad (6.5)$$

$$with \quad M = \frac{N_{A,tot}}{N_{B,0}}$$

where X_{fd} represents the progress of the feed operation as a function of the molar ratio M, time t and the time to feed t_{fd}. $N_{A,tot}$ indicates the molar amount of A at the end of the feed operation. Once the feed has reached the stoichiometric point, namely that the amount of A fed is equivalent to the total amount of B initially charged ($N_{A,fed} = N_{B,0}$), then X_{fd} evolves until reaching M.

2. *After the stoichiometric point*: the situation becomes identical to a batch-mode and X_{fd} is replaced by 1. From this point, any extra addition of reactant A has no effect on the accumulation and only serves the purpose to keep a convenient reaction rate. Therefore, the generation of C will not exceed the maximum molar
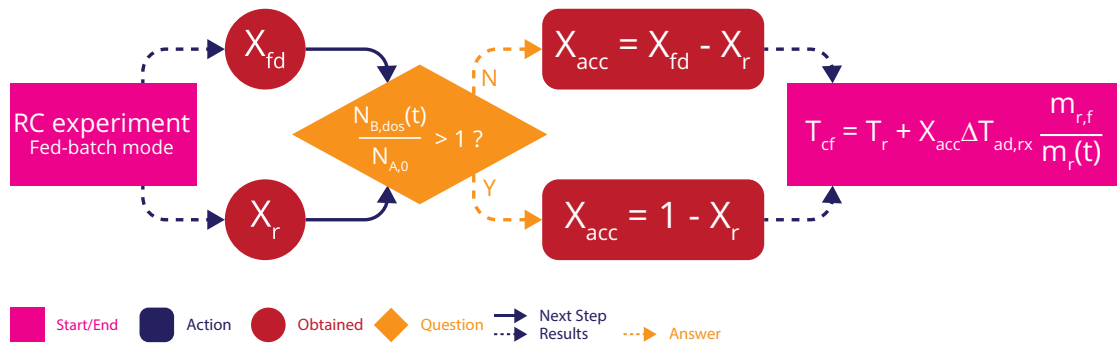
Figure 6.3 – Pathway to calculate the accumulation of unconverted reactant and evaluate the temperature reached after a cooling failure scenario for a simple reaction scheme.

amount of the limiting reactant and thus, will be independent of the feed such as:

$$X_{acc} = 1 - X_r \tag{6.6}$$

This chain of events is illustrated in Figure 6.2 and demonstrates clearly the two situations. The resulting accumulation is also depicted in the figure and shows the relationships that exist between the feed (X_{fd}), the conversion (X_r) and the molar ratio (M).

The overall pathway to evaluate the accumulation of unconverted reactant and estimate the temperature in the case of cooling failure is depicted in Figure 6.3.

The determination of the accumulation requires the knowledge of the molar conversion. As a matter of fact, for a single reaction, the thermal conversion can be considered equivalent to the molar conversion such as:

$$X_r = X_{th} = \frac{\int_0^t q_{rx}dt}{\int_0^\infty q_{rx}dt} \tag{6.7}$$

Where q_{rx} is the experimental heat flow, for example, obtained in a Reaction Calorimeter under fed-batch operating conditions. Notice that the RC experiment may be replaced by other techniques such as chemical analysis, delivering the information about the reaction progress X_r.

The Maximum Temperature of the Synthesis Reaction ($MTSR$) reached after a cooling

failure can be deduced as:

$$MTSR = T_r + X_{acc,max} \Delta T_{ad,rx} \frac{m_{r,f}}{m_{r,max}} \tag{6.8}$$

Where $m_{r,max}$ depicts the reaction mixture mass at the instant of maximum accumulation.

At this temperature, secondary reactions, such as decomposition of the product C may be triggered, generating additional heat and consequently, causing a further increase of temperature.

The problem encountered, however, with such an approach appears once it is applied to several reactions. The determination of the accumulation will require a perfect knowledge of the stoichiometry of the different events occurring and their individual reaction enthalpies. This information is difficult to obtain as they may be interconnected and often lead to erroneous interpretation of the accumulation. Consequently, the need of the reaction kinetics may be a good alternative.

6.2.2 Complex reaction scheme

A complex reaction scheme is considered when more than one stoichiometric equation is required to describe the reaction system. In such case, the accumulation of one reactant will not define the thermal potential of the reaction mixture anymore, as it was the case for simple reaction systems [30, 176]. Different contributions such as parallel or consecutive reactions may enter the scenario leading to an increase of this thermal potential and making its determination algebraically difficult.

As a simple example of this kind of issue, a secondary reaction is added to the reaction system 6.1, the product C decomposes in D such as:

$$A + B \rightarrow C$$
$$C \rightarrow D \tag{6.9}$$

The thermal potential generated by such reaction system is not solely due to reactant accumulation from the first reaction, but also due to the amount of C produced. This production will increase significantly the thermal potential to such an extent that in case of a cooling failure, the secondary reaction may be initiated, exceeding the
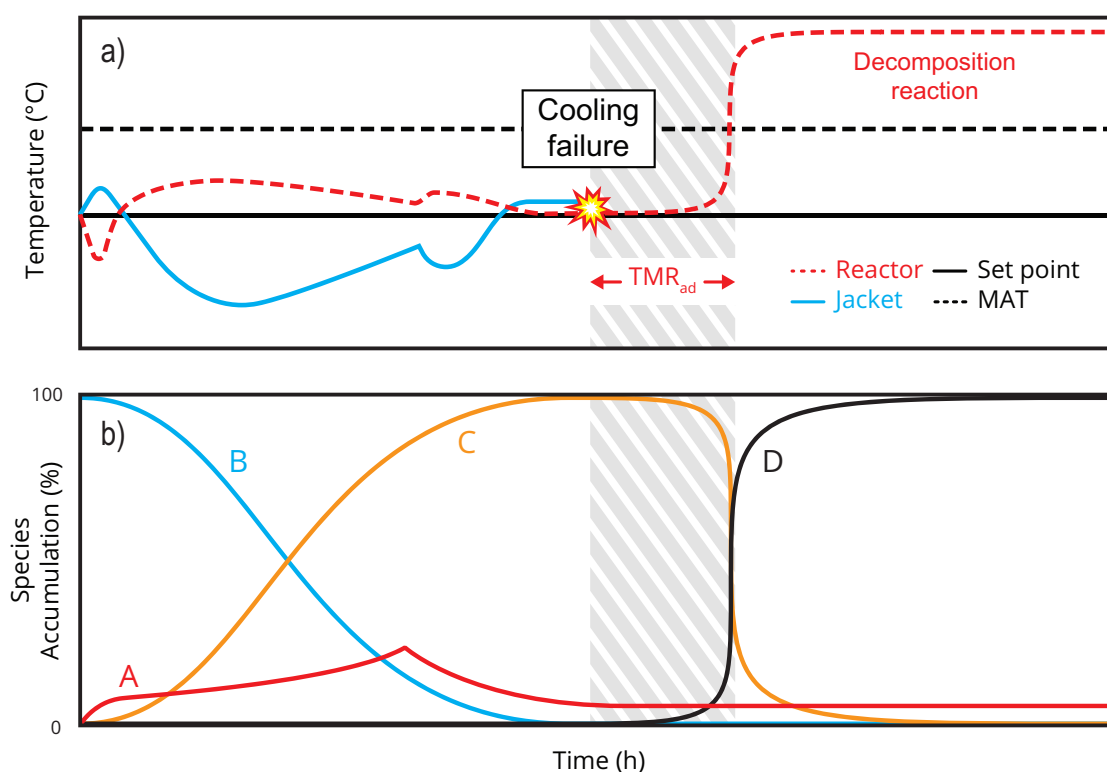
Figure 6.4 – Cooling Failure Scenario for a complex reaction scheme (equation 6.9): a) temperature profiles (reactor, jacket, setpoint and maximum allowable temperature MAT) before and after a cooling failure, b) accumulation of each species in the reaction system along the cooling failure scenario.

maximum allowable temperature (MAT) and lead to an uncontrollable state, even if the accumulation of the first reaction is controlled. The Figure 6.4 demonstrates that the only barrier that exists to prevent such situation is an adequate choice of operating conditions and feed strategy. Indeed, in case of system breakdown, an appropriate feed profile will conduct to a sufficiently long TMR_{ad}, allowing to bring the reactor to a safe state and avoiding a runaway.

The knowledge of the reaction kinetics brings out the possibility to evaluate the outcomes and state of a reactive system throughout the type of temperature control (Section 2.2.2.3). Thus, it becomes interesting to consider different temperature controls to represent real conditions. This approach can be integrated in the evaluation of the thermal potential by associating normal and abnormal operating conditions namely, real thermal dynamics and temperature cascade-control (Chapter 5), followed by adiabatic conditions.

The temperature reached after a cooling failure or system breakdown can be written as $T_{cf}(t, t_{pred})$, where t is the time when the breakdown occurs and t_{pred}, the prediction horizon under adiabatic conditions. Graphically, t_{pred} represents the allowable TMR_{ad}

of the considered system as illustrated in Figure 6.4. As a result, a sufficiently long TMR_{ad} ensures to let enough time for suitable safety measures.

Considering this last parameter, in combination with the current operating temperature T_r and the adiabatic temperature rise under batch operating conditions ($\Delta T_{ad,batch}$), one can evaluate the instantaneous thermal potential Th as:

$$Th(t) = \frac{T_{cf}(t, t_{pred}) - T_r(t)}{\Delta T_{ad,batch}} = \frac{\Delta T_{ad,sys}(t)}{\Delta T_{ad,batch}} \tag{6.10}$$

where $\Delta T_{ad,sys}$ is the adiabatic temperature rise for the current system (composition, reactor and jacket temperatures) as well as for a prediction horizon t_{pred}. $\Delta T_{ad,batch}$ represents the adiabatic rise of a batch reactor initially charged with the total amount of reactants.

Under normal operation, regardless the typology of the problem considered (safety or productivity), the constraint that generally requires to be fulfilled is the Maximum Allowed Temperature (MAT). Therefore, the thermal potential should be kept under a critical limit to ensure safe operation such as:

$$Th_{crit} = \frac{MAT - T_r(t)}{\Delta T_{ad,batch}} = \frac{\Delta T_{ad,crit}}{\Delta T_{ad,batch}} \tag{6.11}$$

Inherently safe operating conditions are characterized by a thermal potential which can variate between 0 and the critical thermal potential such as $Th \leq Th_{crit}$. Therefore, by coupling the instantaneous and critical thermal potential together (equations 6.10 and 6.11), it is possible to define a new dimensionless parameter, the normalised thermal potential:

$$\theta_{Gu} = \frac{Th}{Th_{crit}} = \frac{\Delta T_{ad,sys}(t)}{\Delta T_{ad,crit}(t)} \tag{6.12}$$

with a parameter respecting the following condition:

$$0 \leq \theta_{Gu} \leq 1 \tag{6.13}$$

Therefore, such operating conditions are achieved as long as θ_{Gu} is between 0 and
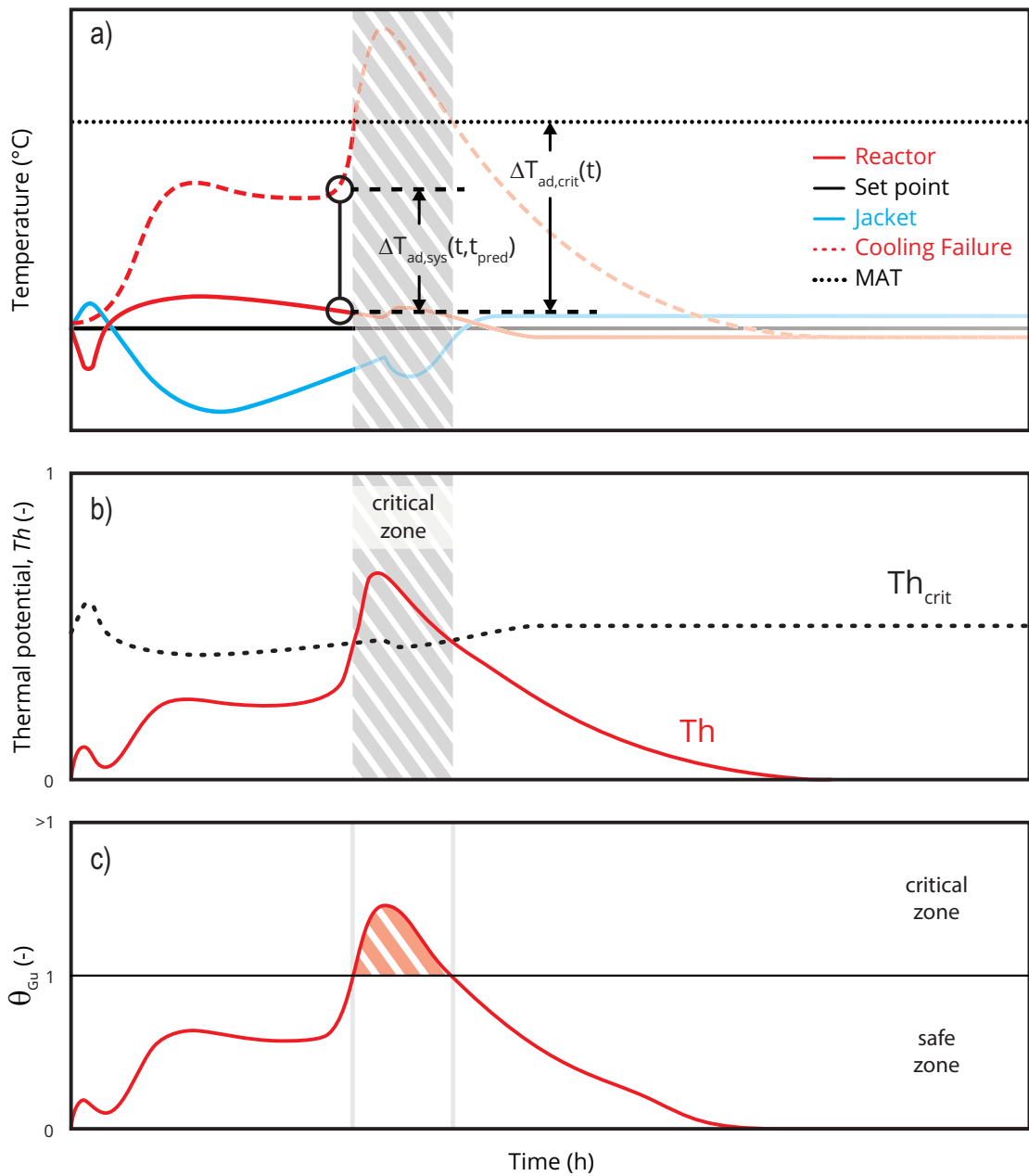
Figure 6.5 – Interpretation of the thermal potential for a complex reaction scheme with safe and critical zone of operation: a) normal operation with the corresponding temperature in case of cooling failure (T_{cf}), the Maximum Allowable Temperature (MAT) and the resulting adiabatic rises $\Delta T_{ad,sys}$ and $\Delta T_{ad,crit}$; b) the resulting thermal potential curves: Th and Th_{crit} presented in equations 6.10 and 6.11, respectively; c) Discrimination of safe ($0 \leq \theta_{Gu} \leq 1$) and critical ($\theta_{Gu} \geq 1$) region.

1. A value of θ_{Gu} greater than 1 corresponds to the critical region, meaning that if a breakdown occurs, the process may not be safe anymore.

The Figure 6.5 illustrates the evaluation of the thermal potential along a process under normal operating conditions. The temperature in case of cooling failure is calculated on

the basis of the reaction kinetics and the current reactor state (dependent of the thermal dynamics) as illustrated in Figure 6.5a. The thermal potential is then compared to the critical thermal potential to shape the θ_{Gu} (Figure 6.5b). The overall concept is then normalized to efficiently discriminate safe from critical operating zones as depicted in Figure 6.5c.

Such criterion, compared to the ones currently available throughout the literature [32, 171–174], offers a direct overview of the system state toward an inherently safer process. As a matter of fact, it considers reaction kinetics and reactor dynamics through the establishment of the T_{cf} while it allows checking the current system state visually, indicating in which region the process is actually operating (safe versus critical). Indeed, as soon as the process is operating in the safe zone, it is respecting the QFS conditions defined as a "Quick start", a "Fair conversion" and "Smooth temperature profile" [174].

Despite the fact that a process is operating within the safe zone, the operating conditions may not be optimal regarding the productivity. Indeed, any process should be designed to respect safety as well as productivity. In the case of fed-batch operation, the evaluation of optimal operating conditions have to be separated into two distinct phases:

1. *The feeding phase*: the feed rate controls the thermal potential, meaning that an appropriate feed profile strategy should result in a suitable T_{cf} while, isothermal conditions are respected (Section 6.3.1),

2. *The post feed phase*: once the total amount of reactants is fed, the process is turned into a batch-mode, meaning that the only way to control the reaction course is by adjusting the cooling system.

Considering the aforementioned phases, the operating conditions can be designed through the normalised thermal potential θ_{Gu}; in the first phase, the feed rate is adjusted to let the process remain in the safe zone while, in the second phase, an appropriate temperature set point profile $(T_{r,set}(t))$ is estimated on the basis of a desired $\theta_{Gu,set}$ defined as:

$$\theta_{Gu,set}(t) = \frac{T_{cf}(t, t_{pred}) - T_r(t)}{MAT - T_{r,set}(t)} \tag{6.14}$$

$$\Rightarrow T_{r,set} = MAT - \frac{T_{cf}(t, t_{pred}) - T_r(t)}{\theta_{Gu,set}(t)} \tag{6.15}$$

Optimal operating conditions can then be considered achieved when they lead to an acceptable thermal potential ($\theta_{Gu} \leq 1$) as well as a maximisation of the productivity all along the process course ($\theta_{Gu} = 1$). As an example, if a cooling failure occurs, a

correct definition of the operating conditions accompanied by reasonable safety limits, will result in a sufficiently long time to ensure adequate safety measure and bring the process to a safe state.

6.3 Feed strategy optimisation

In normal fed-batch operation, various operational as well as quality and safety related constraints have to be met to make the process efficient and economically relevant. Particular events, however, may happen during the process course as previously discussed and may lead to difficult situations. Dynamic process simulation can prevent and explore the results of such situations. As a matter of fact, the dynamic behaviour of a process can be accurately described through the Reaction Kinetic (Chapter 4) and Reactor Dynamic Investigations (Chapter 5). The combination of the reaction kinetics and the reactor dynamics shaped by the obtained parameters will then conduct to the creation of the *process implementation model*, a path illustrated in Figure 6.6.

The process implementation model allows the exploration of a wide range of operating conditions such as normal as well as abnormal conditions. With such an asset, the evaluation of the process performances and resulting thermal potential along the process course is possible through dynamic simulation. It also can helps to determine the optimal operating conditions that will make the process economically relevant and safe as detailed in the next section.
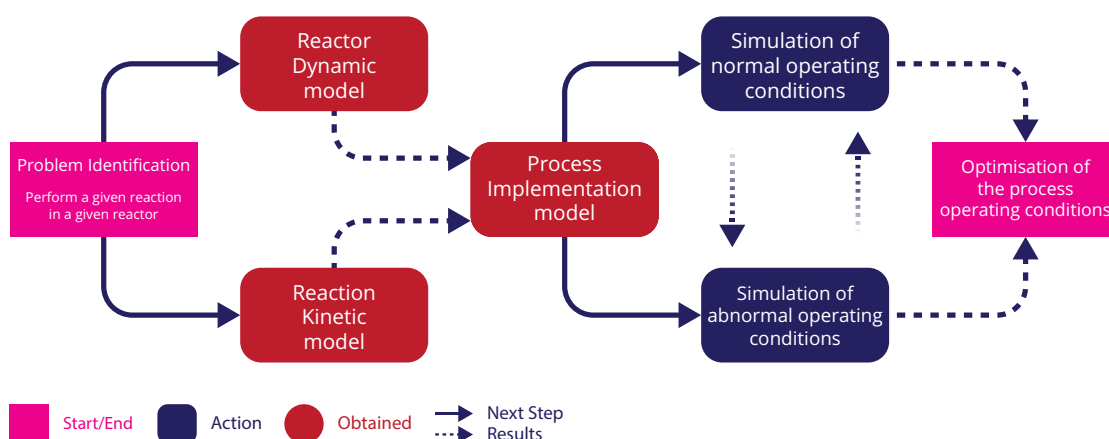
Figure 6.6 – Workflow of the different approaches and the resulting models interconnections: the reaction kinetic and reactor dynamic models are used to shape the process implementation model allowing to describe normal and abnormal operating conditions. The last model can then be used to predict and identify operating conditions ensuring an inherently safe process.
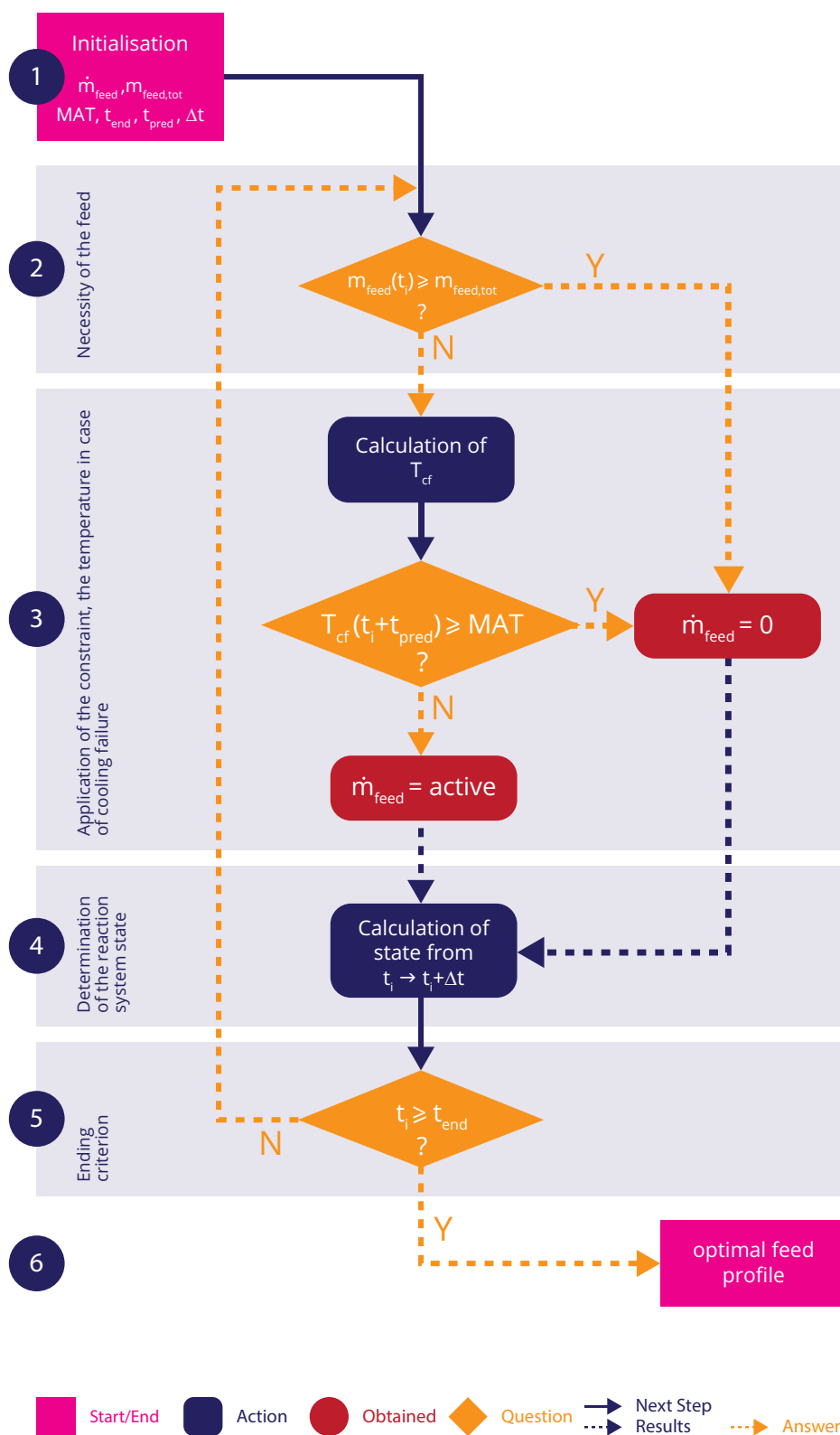
Figure 6.7 – algorithm to determine the optimal feed profile under a on/off set point.

6.3.1 The Procedure

In order to get a safe process, several points regarding the thermal safety should be addressed. These points are generally answered through the establishment of a cooling failure scenario (section 6.1). It appears that one of the main variables to consider during such assessment is the end temperature that can be reached by the reaction mixture if a cooling failure may occur (T_{cf}). Indeed, depending on the reaction mixture state (composition and temperature), the reached temperature may be sufficiently high to trigger secondary reactions (decomposition or gas production). If such state materializes, several questions arise:

1. Would the consequences be worse than just reaching this temperature?

2. After such events, what would the newly reached temperature be?

3. Is it the worst moment during the process course for a cooling failure to occur?

Dynamic simulations are an excellent way to predict and answer the overall cooling failure scenario all along the process course. On the basis of this model, the piece-wise optimisation of the feed strategy is performed through simulations of the cooling failure (all along the process course) and involving six key steps as illustrated in Figure 6.7:

Step 1: *Initialisation:* The optimisation starts with a clear definition of the initial/end conditions and the safety constraints. The initial conditions contain the different initial temperatures (reactor and jacket) and the temperature set point profile. The maximum feed rate allowable by the system as well as the amount at which the addition has to be stopped, are necessary. In terms of safety, three parameters have to be declared to set correctly the constraints:

1. The Maximum Allowable Temperature (MAT),

2. The step interval to check the future abnormal behaviour (Δt) and,

3. the prediction horizon under adiabatic conditions (t_{pred}) serving the purpose to check, if under a cooling failure situation, the MAT is exceeded. The prediction horizon can be referred to the time available to bring the reactor to a safe state in case of the cooling failure or equipment malfunction and to apply safety countermeasure (quenching, inhibitor injection, evacuation...).

An illustration of these different parameters and their implications on the dynamic simulation is depicted in Figure 6.8

Step 2: *Feed rate (active or inactive?):* The optimisation of the feed profile is only active when the total amount has not yet been reached. If it is the case,
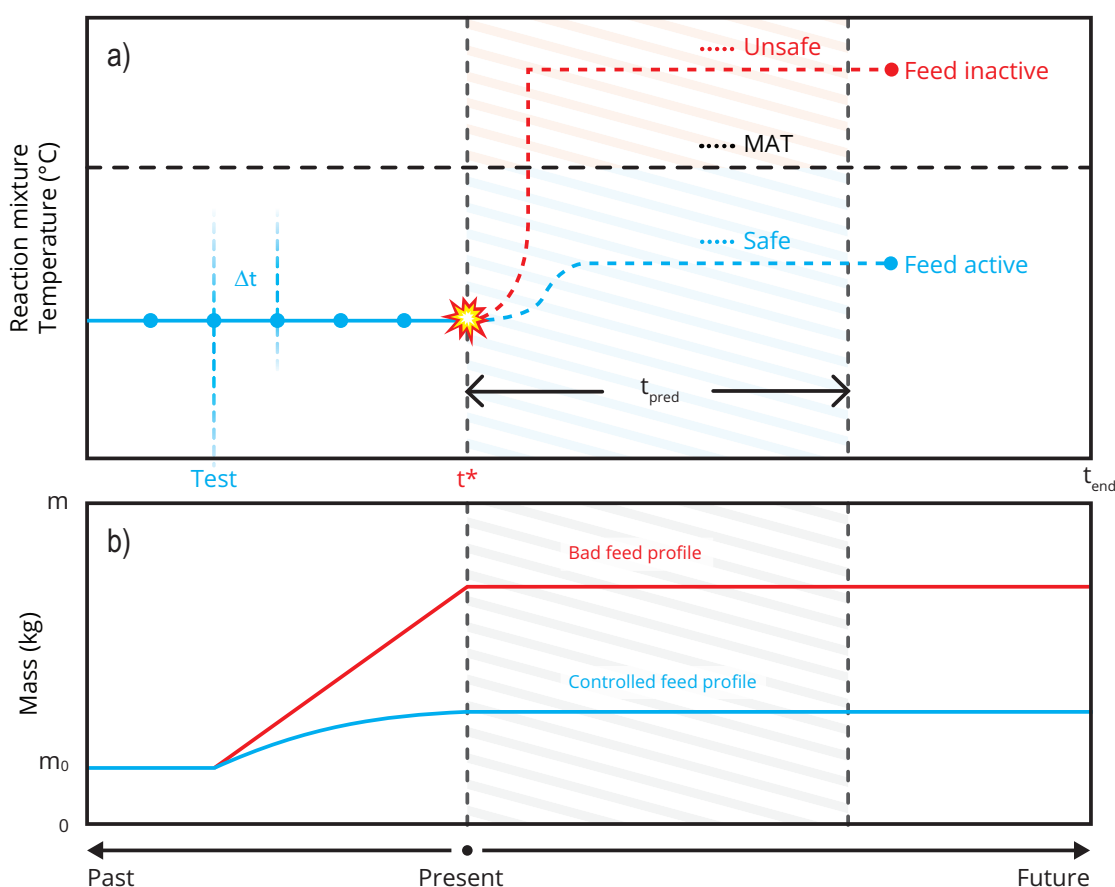
Figure 6.8 – Initialisation of the conditions for the feed profile strategy optimisation: a) check of the temperature in case of cooling failure at different time interval ΔT over a horizon prediction time t_{pred} and b) the mass profile resulting from a controlled feed profile.

the procedure can proceed to Step 3. Oppositely, when the total amount reactant(s) is reached, the optimisation becomes inactive and the feed rate is turned to zero. From this point the process is continued until the desired specification are reached (Step 5).

Step 3: *Application of the constraint*: This step is the core of the optimisation procedure. Hence, let us consider a time t when a cooling failure occurs. The process is turned to adiabatic conditions. If no measures are undertaken, the reaction system (exothermic) will release heat resulting in an increase of the reaction rate. Depending of the amount of unconverted reactants, the temperature rise will not be the same. Therefore, the reaction model is used to evaluate the temperature the reaction mixture will reach under such conditions and after a certain prediction horizon (t_{pred}). From this point, two situations appear:

    1. The final reached temperature is higher than the Maximum Allowable

Temperature (MAT), the feed is stopped.

    2. The final reached temperature is lower than the MAT, the feed remains active.

Step 4: *Determination of the reaction system state:* The state is calculated from t_i to $t_i + \Delta t$ considering the state of the feed (active or 0). After the desired sampling time Δt, the optimisation is restarted.

Step 5: *Ending criteria:* the ending time has been reached, the simulation is stopped. Other ending criteria such as conversion, selectivity or productivity can be set.

Step 6: *Optimal feed profile:* the feed profile is optimised to fulfil the chosen safety constraint(s) and the dynamic of the reactive system. This profile can be experimentally validated to confirm the correct choice of constraints. If the results are unsatisfactory, the experiment is added to the reaction data basis to improve the model, and a new optimisation of the feed can be undertaken (Chapter 4).

It should be kept in mind that a simulation never replaces an experiment. This approach allows, however, to define near optimal operating conditions respecting the model dynamics and minimizing the number of required experiments. The results of this optimisation, also, greatly depend on the quality of developed reaction kinetic and reactor dynamic models. Hence, the range of applicability will directly be function of them. Consequently, a validation of the determined operating conditions should never be avoided. In addition, even if the validation is erroneous, such experiment can bring valuable information to improve the process implementation model.

"There is never too much information on a dynamic system, but some are more useful than others. It only depends on how we use them."

6.4 Application

In fed-batch operation, many strategies can be used to improve the process safety: the temperature control strategy, the feed control strategy, and also the choice of reactant(s) initially charged or fed [30]. Although the feed can control the process course, an inappropriate feed profile may result in a too large accumulation and lead to unexpected situations with more or less severe consequences [72, 127]. Different types of feed strategy can be employed to control such situation:

    1. To operate with a constant feed rate, sufficiently slow to avoid or at least minimize the reactant accumulation [127] or,

2. To operate with a feed rate designed under constraints based on physical considerations (volume at the end of the operation, flow rate,. . .) and safety concerns (the system must remain safe under normal operating conditions,. . .) [72].

The definition of the reactor temperature remains, with the feed strategy, a difficult task for the thermal risk assessment. Therefore, the applications presented along the following investigations will serve the purpose to demonstrate different situations where the models and approaches developed in Chapters 4, 5 and 6 are of great help. The risk assessment will proceed in a logical way from batch to fed-batch operation by simulating different process behaviours and diagrams:

1. *Batch operation*

   (a) Cooling failure scenario

   (b) Constraint definition

   (c) Semenov Diagram

   (d) Operating temperature effects

2. *Fed-batch operation*

   (a) Effects of linear feed profiles

   (b) Optimised feed profile strategy under constraints

   (c) Thermal potential management

These investigations are not exhaustive but have the purpose of exposing different aspects where the developed models are useful. The overall approach was applied using commercial software packages (AKTS-Reaction Calorimetry Software and MATLAB [134, 135]).

6.4.1   Simulated example

Ideas are quite easy, however, applications may sometimes be hard. Therefore, a hypothetical reaction model based on the development in Chapter 4 is very convenient to explore the presented approach. On the one hand, the different reaction rates describing the reactive system are directly translated in mathematical expressions from a proposed reaction scheme and used to simulate the resulting heat flow. On the other hand, the dynamic of the vessel (Chapter 5) can also be integrated to the simulation in order to explore the effects of a feed profile strategy simultaneously with the heat transfer under a wide range of operating conditions.

Table 6.1 – Reaction kinetic parameters and corresponding reaction rates used for the demonstration of the procedure presented in section 4.1.

Reaction 1

	k_0	E_a	$\Delta_r H$	*Orders*
Units	$(g \cdot s^{-1} \cdot mol^{-1})$	$(kJ \cdot mol^{-1})$	$(kJ \cdot mol^{-1})$	$(-)$
Value	$1 \cdot 10^7$	58	-225	$a1 = 1 \; ; b1 = 1$
Rate	$r_1 = k_1 C_A^{a1} C_B^{b1}$			$(mol \cdot g^{-1} \cdot s^{-1})$

Reaction 2

Units	$(g^2 \cdot s^{-1} \cdot mol^{-2})$	$(kJ \cdot mol^{-1})$	$(kJ \cdot mol^{-1})$	$(-)$
Value	$5 \cdot 10^{10}$	59	-240	$a2 = 1 \; ; b2 = 1 \; ; d2 = 1$
Rate	$r_2 = k_2 C_A^{a2} C_B^{b2} C_D^{d2}$			$(mol \cdot g^{-1} \cdot s^{-1})$

Reaction 3

Units	(s^{-1})	$(kJ \cdot mol^{-1})$	$(kJ \cdot mol^{-1})$	$(-)$
Value	$1 \cdot 10^7$	100	-360	$e3 = 1$
Rate	$r_3 = k_3 C_E^{e3}$			$(mol \cdot g^{-1} \cdot s^{-1})$

6.4.1.1 Reaction system

This first application investigates a hypothetical reaction system composed of two parallel reactions followed by a secondary reaction:

$$
\begin{aligned}
2A + B &\rightarrow C \\
A + B + D &\rightarrow \boldsymbol{E} \\
E &\rightarrow F
\end{aligned}
\tag{6.16}
$$

Table 6.1 and 6.2 summarize, respectively the kinetic parameters and thermophysical properties used for this investigation.

For this reaction system, the focus is directed toward the production of **E** while competitive reactions are present.

Preliminary overview

 A DSC was simulated at 4 $K \cdot min^{-1}$ with a molar composition of 1A:1.2B:1D; it demonstrates the existence of two exothermic peaks. As a matter of fact, the two

Table 6.2 – Physical properties and transformation rates of the different species considered in the reaction scheme 6.16.

Species	Molar mass $(g \cdot mol^{-1})$	Heat capacity $(J \cdot g^{-1} \cdot K^{-1})$	Transformation rate $(mol \cdot g^{-1} \cdot s^{-1})$
A	100	4.18	$R_A = -2r_1 - r_2$
B	100	4.18	$R_B = -r_1 - r_2$
C	300	4.18	$R_C = r_1$
D	100	4.18	$R_D = -r_2$
E	300	4.18	$R_E = r_2 - r_3$
F	300	1	$R_F = r_3$

parallel reactions take place and result in two individual peaks dissimulated under the first peak as illustrated in Figure 6.9. Other molar ratios were tested and always resulted in a single first peak. Another point also highlighted by this thermogram is the operating temperature range namely, from $0°C$ to $160°C$ (grey zone on Figure 6.9).

For safety reasons and for the next developments, this hypothetical reactive system is considered as unstable if the temperature should exceed $125°C$ (e.g. evaporation
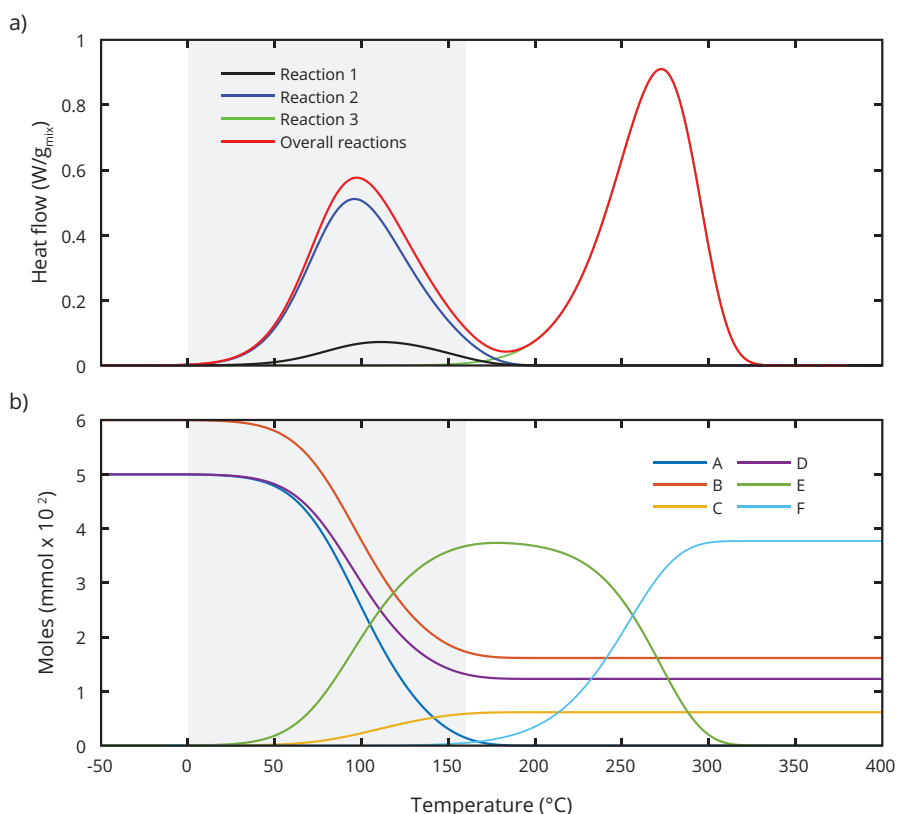
Figure 6.9 – DSC at $4K \cdot min^{-1}$ of the reactive system summarized in the reaction scheme 6.16 with a) the heat flow and b) its corresponding molar profiles. The grey zone represents the range of operating temperature where mainly the parallel reaction system is taking place.
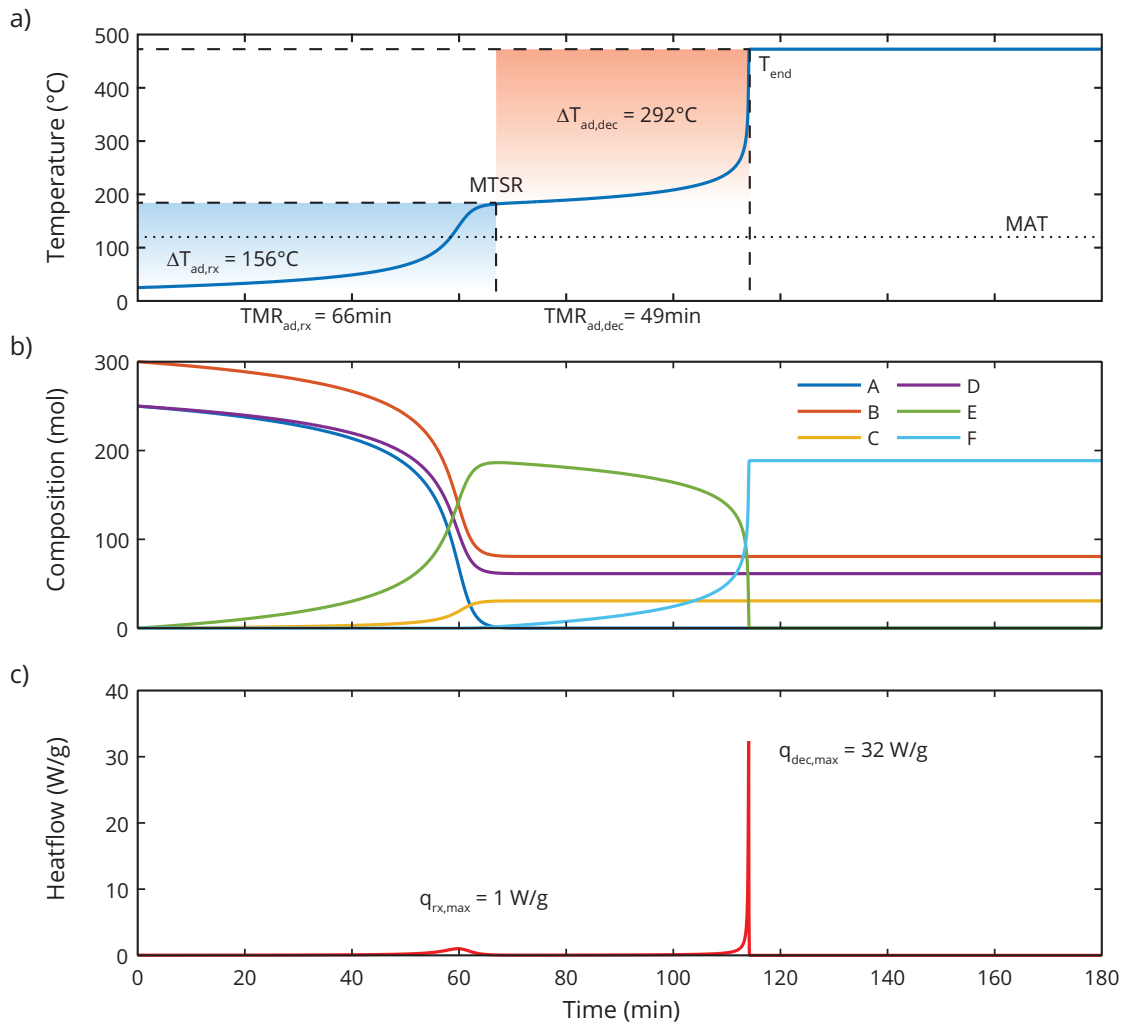
Figure 6.10 – Cooling failure scenario for the reaction system 6.16: a) Temperature under adiabatic conditions; b) molar profiles during the runaway and c) the heat flow generated during the runaway.

or decomposition) and will define the Maximum Allowable Temperature (MAT) with a safety margin of $5°C$ at $120°C$.

6.4.1.2 Batch process

Cooling failure scenario

Considering a batch reactor with a molar ratio of 1A:1.2B:1D, a cooling failure scenario starting at $25°C$ would lead to a $MTSR$ of $181°C$ ($\Delta T_{ad,rx} = 156°C$), occurring in a short time ($TMR_{ad} = 66min$).

At the $MSTR$, a secondary reaction is active and characterized by an adiabatic rise of $\Delta T_{ad} = 292°C$, occurring in less than $49min$ (Figure 6.10). Such circumstances would

lead to a loss of containment and disastrous consequences if the cooling fails.

Two other temperatures describing the reaction mixture thermal stability were evaluated using simulations; the temperatures at which the time to reach a critical state correspond to $8h$ and $24h$. Placing a Maximum Allowable Temperature (MAT) at $120°C$, these temperatures correspond to $-2°C$ and $-14°C$, for T_{D8} and T_{D24} respectively.

Under such characteristics, this reaction system describes a criticality of 5 according to the Stoessel's classification of exothermic reaction processes [30]. Either evaporating cooling or emergency pressure relief cannot serve as a safety barrier; the system is too fast. In fact, from $25°C$, the temperature reaches the safety limit of $120°C$ in less than $58min$. Therefore, as soon as a cooling failure occurs, the secondary reaction will be triggered under a short time.

The process, under batch-mode, is clearly not viable in the case of failure, it has to be handled differently to decrease and control the latent thermal potential under any circumstances.

Semenov Diagram

A Semenov diagram of the process is represented in Figure 6.11 and demonstrates a reactor able to control the heat released from $10°C$ to $70°C$ under normal operating conditions. This diagram, however, supposes a cooling system without inertia meaning a heat removal capacity instantaneously at its optimal performances, an assumption that may be misleading in reality. The real cooling system is governed by different dynamics (Chapter 5):

1. The heat exchange between the reaction mixture and the coolant,

2. The thermal inertia of the coolant described by time constants in cooling and heating phases and,

3. The temperature-controller.

In practice, even if the controller is designed to deliver a fast response, the heat carrier response will be limited due to the system thermal inertia at industrial-scale.

The process implementation model can be useful in such situation to introduce a new diagram where the dynamic aspects are taken into account; under normal operation, the cooling system will remove the heat produced by the reaction system, however, if the heat produced is significantly higher than the heat removal, a temperature increase will appear. Therefore, this new diagram considers the dynamic aspects of the overall system by comparing the maximum heat flow (along the process course) to the instantaneous heat removal. As a matter of fact, the cooling system is reactive to a change and not pro-active. Consequently, a delay in its answer appears, nevertheless
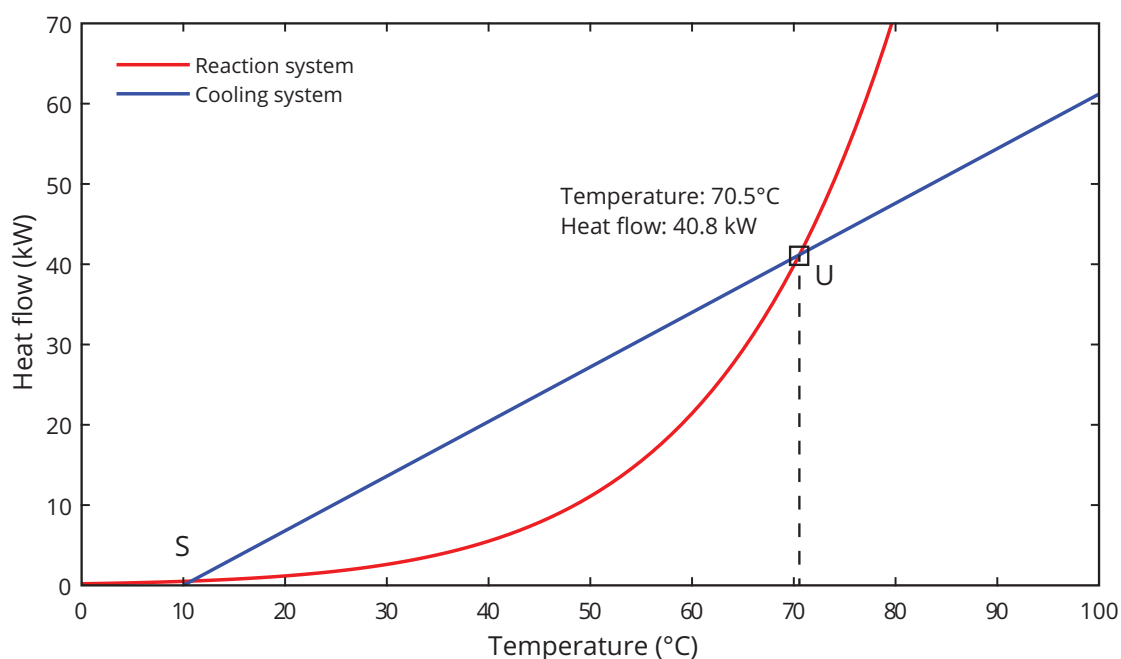
Figure 6.11 – Semenov diagram: comparison between the maximum heat released by the reaction system presented in equation 6.16 and the maximum heat removal from the cooling system, considering a standard reactor of 100L ($Area = 0.84m^2$; $T_{j,min} = 10°C$; $U = 425W \cdot K^{-1} \cdot m^{-2}$) with a mixture composed of 300 moles of B, 250 moles of A and D. S and U representing stable and unstable operating point, respectively.

the reactor will remain under control for small temperature difference between the reaction mixture and jacket. Incorrect operating conditions, however, will conduct to a cooling system unable to control the heat produced and a temperature increase will take place in the reaction mixture, accelerating exponentially the reaction rate.

Simulations considering this aspect were also investigated and mainly conducted to temperature excursion exceeding the MAT, already for initial process temperature above $50°C$ (Figure 6.12), in opposition to the classical Semenov Diagram.

These results lead to two alternatives for the operating conditions:

1. Remaining in batch-mode but drastically decrease the process temperature to be safe even under cooling failure situation, or,

2. Changing the operating mode into fed-batch and determine the best feed profile strategy considering safety constraints and a suitable process temperature.

On the one hand, the first alternative is not economically valid or even unrealistic for such a TMR_{ad} at $25°C$; it would result in a substantial increase of the operating time to achieve convenient specifications (selectivity, conversion, productivity). In this case, a set point temperature of $-2°C$ and more than $100h$ of operation are required to
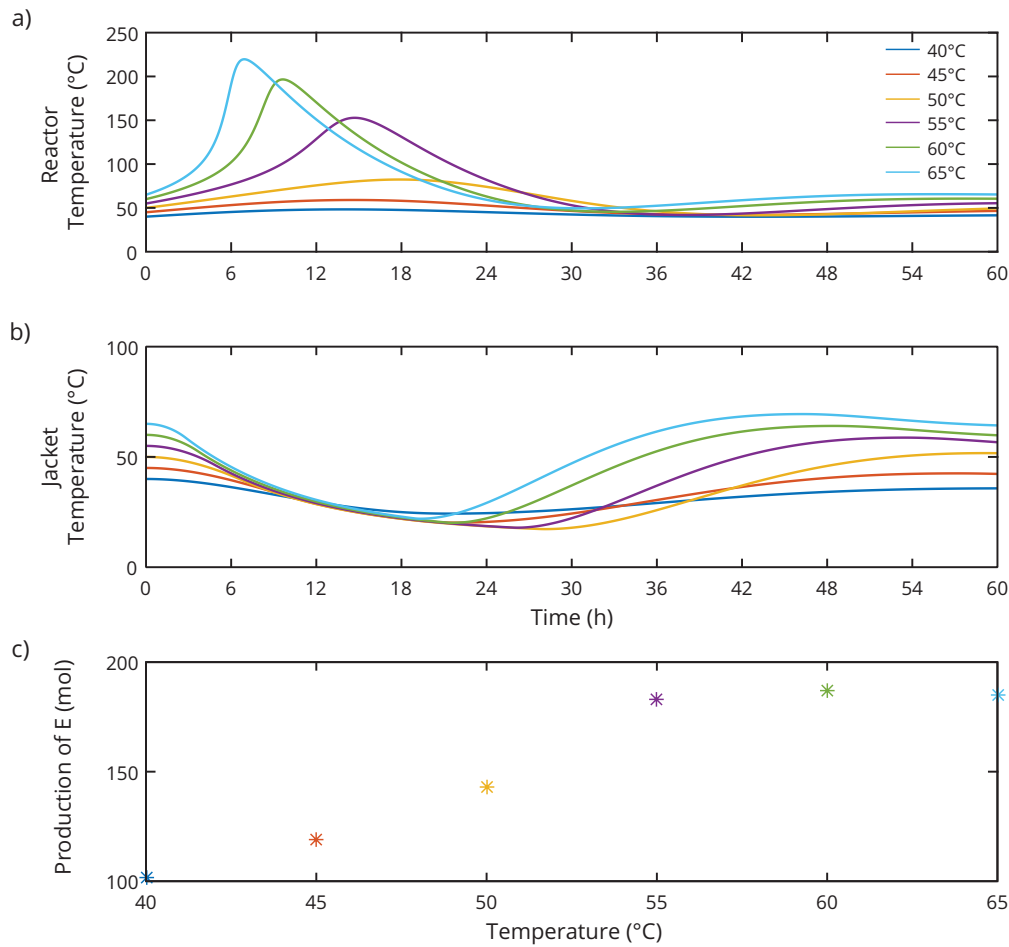
Figure 6.12 – Influence of the initial temperature and set point on the temperature profiles and selectivity for a reactor of 100L ($Area = 0.84m^2$; $U = 425W \cdot K^{-1} \cdot m^{-2}$; $P = 2.43$; $I = 99999s^{-1}$; $\tau_c = 534s$; $\tau_h = 1093s$; $T_{j,min} = 15°C$; $T_{j,max} = 130°C$) with a mixture composed of 300 moles of B, 250 moles of A and D: a) Reactor temperature; b) Jacket temperature and c) Production of the product E after $8h$.

achieve a production of 150 moles of E and not exceeding $120°C$ under cooling failure conditions (considering $8h$ for emergency measures). On the other hand, the second alternative may bring productivity by continually respecting the safety limits while the process operates at a favourable rate and temperature.

6.4.1.3   Fed-batch process

Several simulations at a process temperature of $50°C$ were performed in fed-batch mode and under different linear feeds of A. This mode shows improvements on two major aspects:

1. The process respects the safety limit if a convenient feed profile strategy and process temperature are selected, namely a feed leading to a temperature in

case of cooling failure under the MAT (Figure 6.13) and,

2. By reducing to a minimum the concentration of one of the reactants, the selectivity over the product E is clearly improved (Figure 6.14).

The feed profile strategy was applied considering a safety limit at $120°C$ and which the initial conditions are depicted in Table A.6. Under linear feed strategy, the minimum time to feed and corresponding to an emergency time of $8h$, ensuring a cooling failure temperature under the MAT is $230min$ (Figure 6.13). This time, however, can still be improved. Indeed, an optimised profile respecting, at any moment, the safety limits and is illustrated in Figure 6.14. Such approach decreases significantly the time to feed, improve the safety and the operation time. A feed profile designed on $140min$ and a total of $8h$ are required to reach a production of E as good as the results obtained under batch-mode (Figure 6.14). The obtained specifications are compared in Table 6.3 and show that a fed-batch mode is perfectly suitable for such reaction system regarding thermal safety and productivity.

Management of the thermal potential

This example perfectly illustrates the problem of thermal potential. Indeed, even with consistent modifications of the operating conditions and imposing a minimum accumulation of a primary reactant, the thermal potential due to the secondary reaction
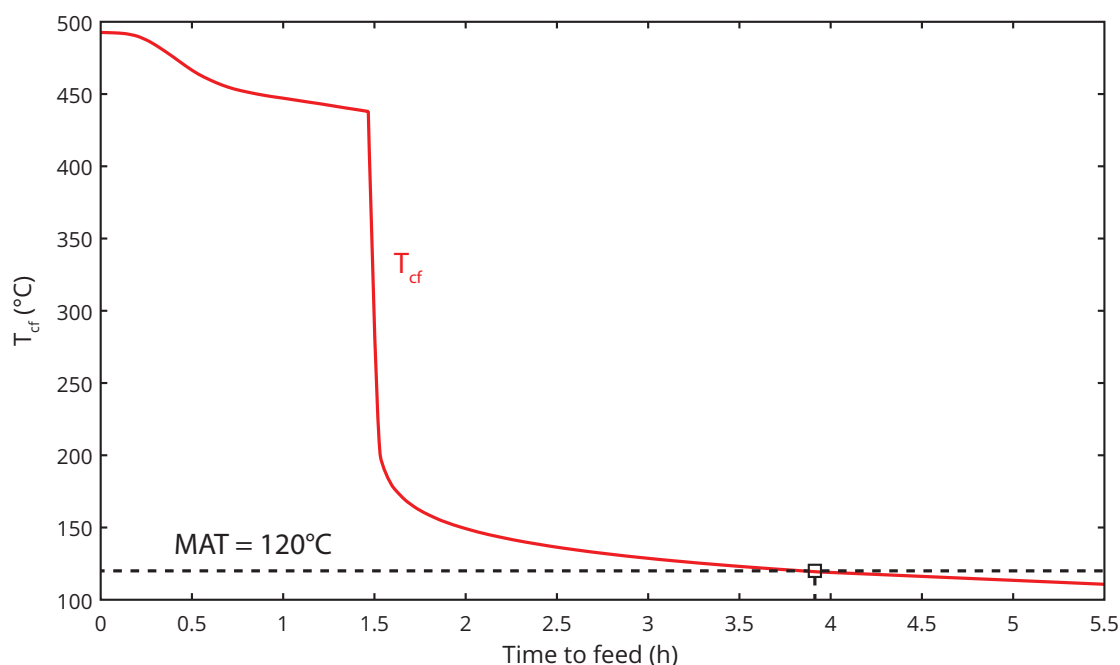
Figure 6.13 – Temperature reached in case of cooling failure (after $8h$) as a function of linear feeds of A (250 moles) for the reaction system 6.16 and an operating temperature of $50°$.
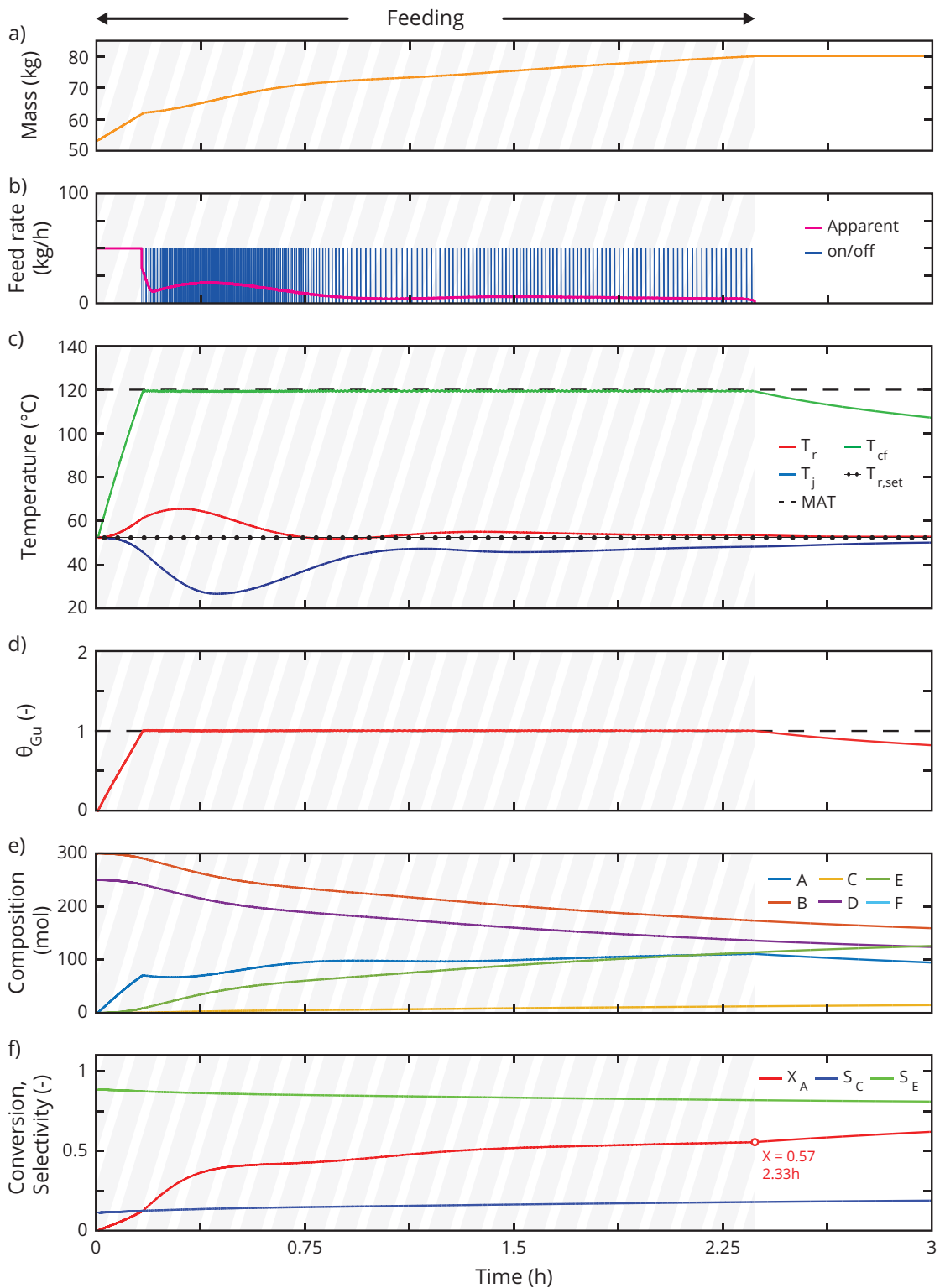
Figure 6.14 – Feed profile strategy allowing to remain inherently safe ($TMR_{ad} \leq 8h$ and check interval of $5s$) during the feed phase ($\dot{m} = 50kg \cdot h^{-1}$) for the considered reaction system (equation 6.16): a) Mass profile, b) Feed rate profile under on/off flow control or apparent flow for a fed reactant at $20°C$, c) Temperature profiles, d) Thermal potential, e) Composition along the process course and finally f) some indications about the conversion of A and selectivity of products C and E.
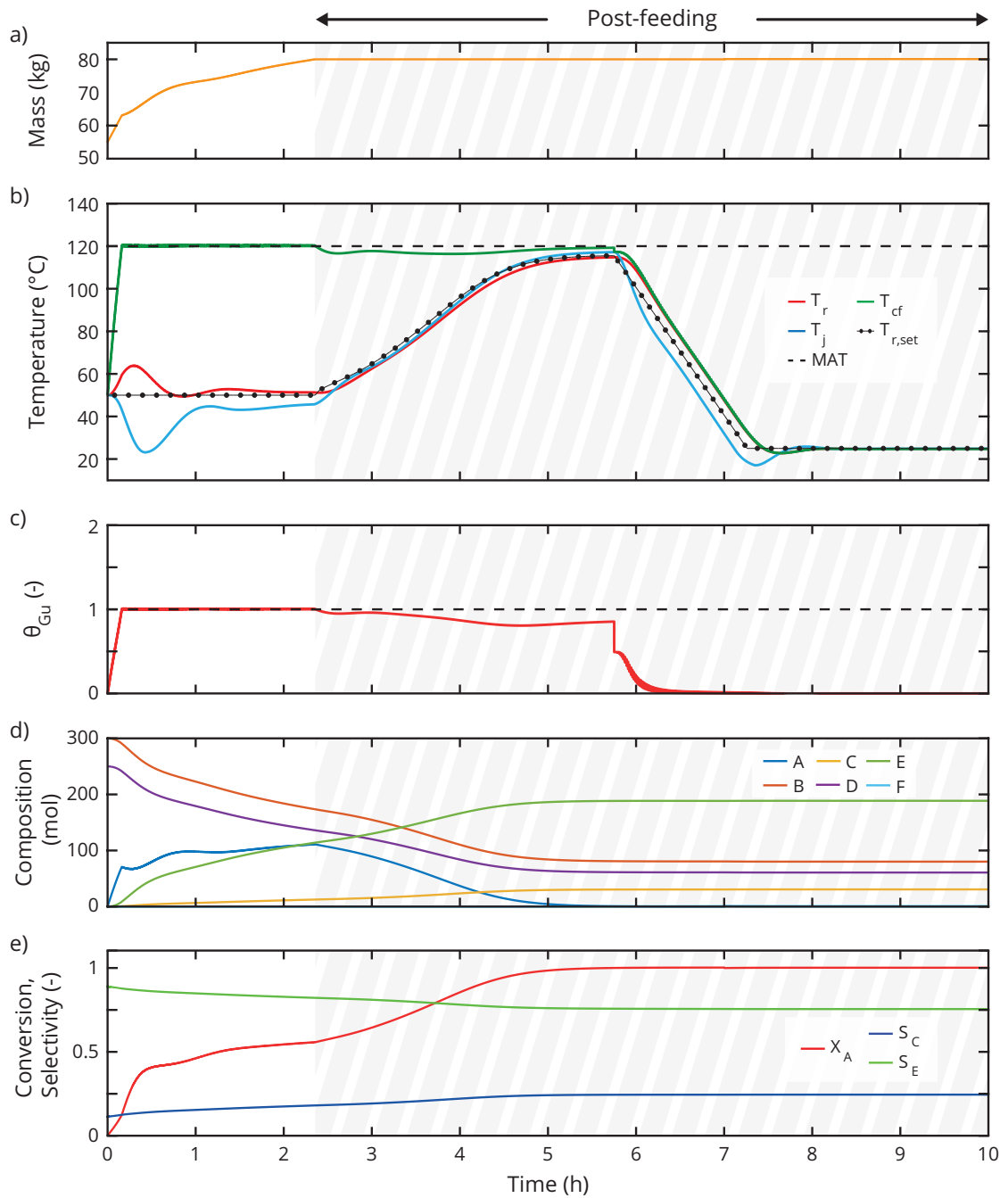
Figure 6.15 – Optimised feed and temperature profiles to remain safe ($\theta_{Gu} \leq 1$) and productive all along the process course for the considered reaction system (equation 6.16): a) Mass profile, b) Temperature profiles, c) Thermal potential, d) Composition along the process course and finally e) some indications about the conversion of A and selectivity of products C and E. The feed rate profile can be observed in Figure 6.14 as only the post feeding phase was modified in the present study.

Table 6.3 – Summary of the end specifications and operation times for the reaction system equation 6.16 for different operating modes: Batch and Fed-batch (*: optimised feed profiles; **: optimised feed and $T_{r,set}$ profiles using the θ_{Gu}.

	Operating temperature	Time to feed	Time of operation	Conversion of A	Selectivity of E	of C	Fig.
Units	$(°C)$	(min)	(h)	(-)	(-)	(-)	
Batch	50	0	8	0.86	0.77	0.23	
Fed-Batch*	50	140	8	0.83	0.78	0.22	6.14
Fed-Batch**	50-120	140	5	0.99	0.76	0.24	6.15

$(E \rightarrow F)$ is continuously present. As a matter of fact, by increasing the production of E, this potential can only grow. If the system operates, for any reasons, under adiabatic conditions, the time to exceed the safety limit will constantly be smaller than $24h$ without any way to decrease it under fed-batch operating conditions.

Few options, however, may be used to mitigate this issue:

1. Operate at a temperature where the time to maximum rate is sufficiently long (e.g. $TMR_{ad} \geq 8h$), and imposes a feed profile strategy under safety constraint or,

2. Change the process into a continuous one, removing the product E and storing it at a suitable temperature to avoid secondary reactions, or,

3. Once the production of E reaches proper specifications, cool the system at a safe temperature to decrease and avoid secondary reaction.

An investigation of the last option demonstrates that the temperature in case of cooling failure was controllable ($\theta_{Gu} \leq 1$). After the feed operation, the thermal potential decreases progressively, an aspect which offers the possibility to increase the process temperature and reach a suitable production of E in a shorter time, meaning to maximise the production and have a θ_{Gu} approaching 1. Once the specifications are reached, a progressive decrease of the temperature brings the process to a safe state. This operation reduces the thermal potential θ_{Gu} to a minimum and allows other manipulations of the product E. The Figure 6.15 illustrates the progress of such procedure.

This example essentially focused on the thermal potential management. However, regarding productivity, the selectivity is an important aspect which requires to be simultaneously considered with the thermal potential in the optimisation problem. In such situation, one has only to modify the objective function (thermal potential vs. thermal potential and selectivity) and apply the same approach as presented in this chapter, namely the consideration of different phases and their respective means of control (feed and/or temperature).

6.4.2 Esterification

6.4.2.1 The reaction system

Following the same path of investigation as the simulated example, this application is, however, based on a real reaction system: the esterification of acetic anhydride with the methanol. The reaction scheme describing this system presents an autocatalytic behaviour which is illustrated by the following pathway:

$$A + B \rightarrow C + D$$
$$A + B + C \rightarrow 2C + D \tag{6.17}$$

Where A is the acetic anhydride, B, the methanol, C, the acetic acid and D, the methyl acetate.

This reaction system was already investigated, discussed and modelled in Section 4.4.2. For the following developments, the reactor dynamics and temperature control parameters are considered equivalent to a 100L pilot reactor operating in T_r-mode (presented in Table 5.9 and 5.11).

6.4.2.2 Batch process

Cooling failure scenario

In case of cooling failure, the reaction system operates under adiabatic conditions (Figure 6.16). In the worst case, the heat released is completely converted in temperature increase without consideration for evaporation or other events. For the current reaction system, this scenario represents an adiabatic temperature rise of $205°C$ in approximately $67min$.

Such consequences would certainly lead to a loss of containment with spillage of flammable compounds and possibly result in a secondary explosion. The thermal stability of the reaction mixture goes hand-in-hand with two different temperatures, the $T_{D,24}$ and $T_{D,8}$. These temperatures are extremely low for this autocatalytic system, namely -10 and $1°C$, respectively. Therefore, any loss of control of the cooling system will result in difficult situations as the further investigation will demonstrate.

Another issue encountered in such a production is the low boiling point of the reaction mixture; the methanol ($64°C$) and the production of methyl acetate ($56°C$) dictate this temperature, approximated at $65°C$ at the end of the process (mixture of acetic acid ($118°C$) and methyl acetate). Runaway situation will exceed this temperature, resulting

165
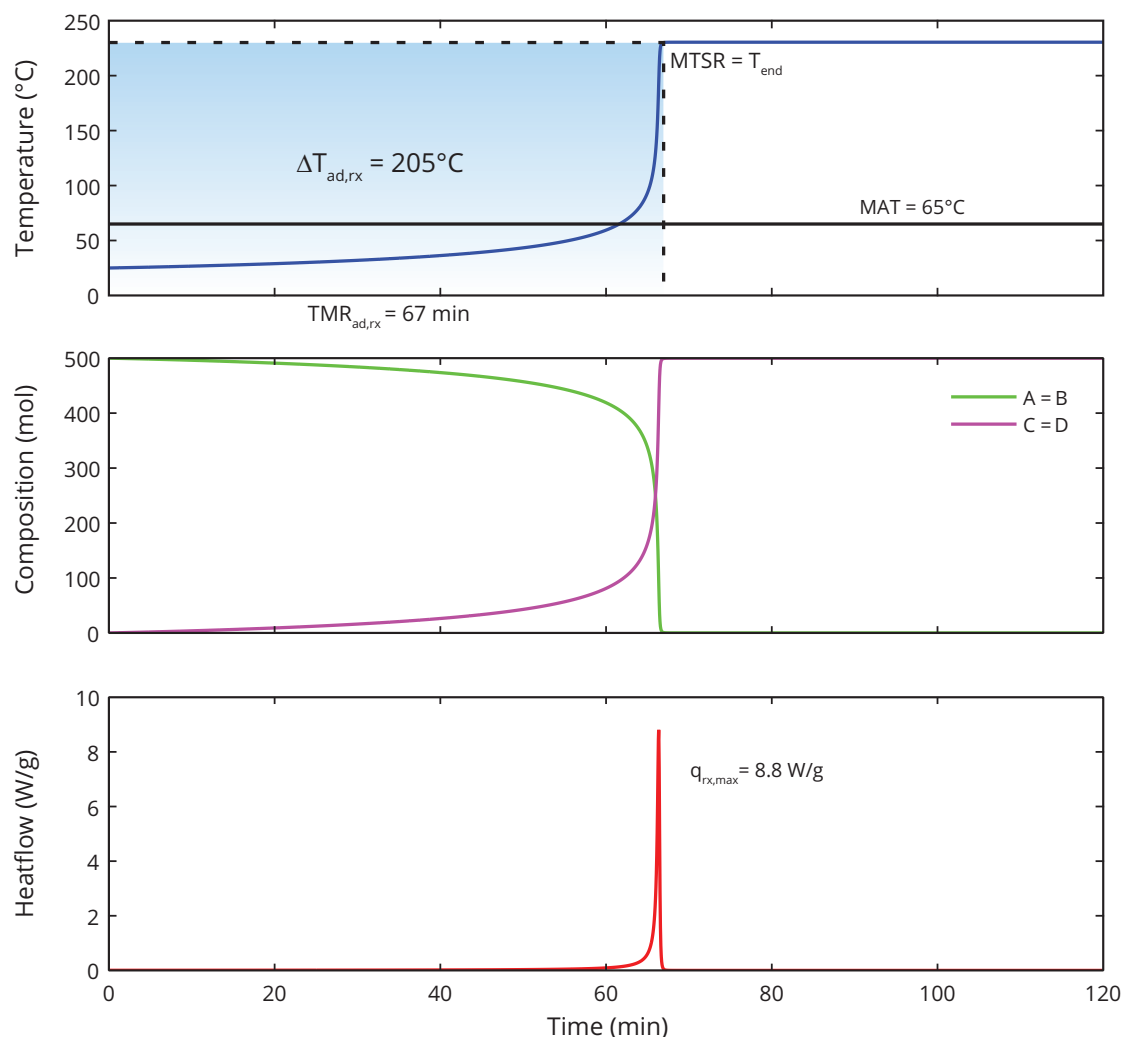
Figure 6.16 – Cooling failure scenario for batch-mode of the autocatytic esterfication presented in equation 6.17 for an equimolar composition (500 mol of A and B): (A) Reaction Temperature profile and MAT;(B) Composition in the bulk along the process and, (C) the reaction system heatflow.

in a relevant pressure increase, leading eventually to a burst of the reactor. Henceforth, this point defines the MAT with a safety margin of $5°C$ at $60°C$.

Under such characteristics, this reaction system describes a criticality of 3 as long as no secondary reactions are considered. Evaporating cooling or emergency pressure relief may serve as a safety barrier if correctly designed and operating at all time. The evaporating barrier may give enough time to react even if this reaction system is relatively fast. In fact, from $25°C$, the temperature reaches the safety limit of $65°C$ in less than $60min$. Therefore, performing this reaction under batch-mode, is not viable in the case of failure and will definitely not lead to an inherently safe process; it has to be handled differently to decrease and control the latent thermal potential under any
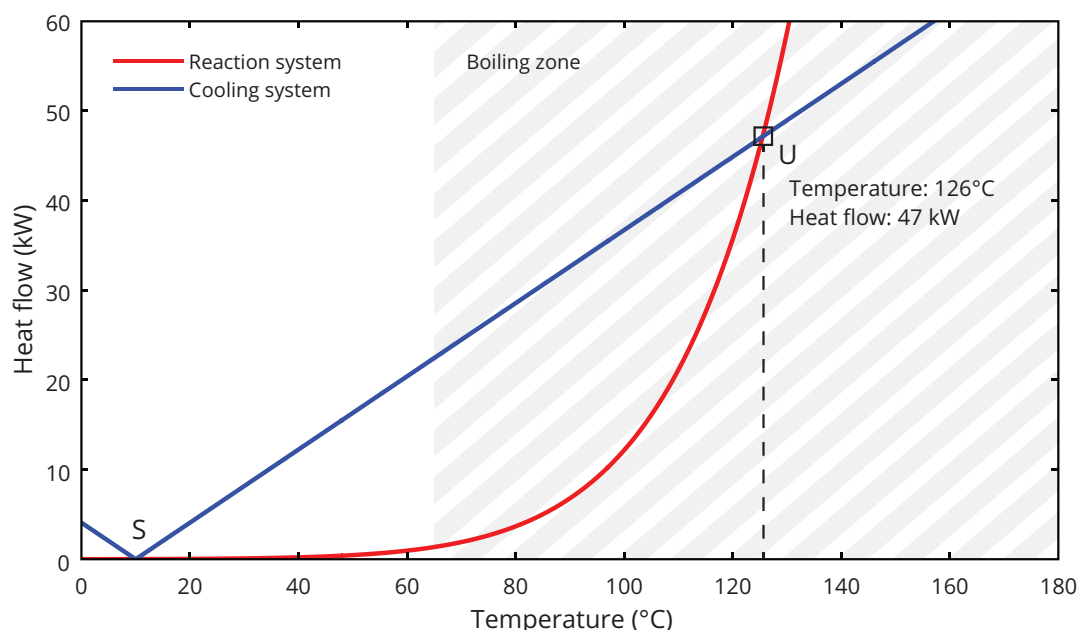
Figure 6.17 – Semenov Diagram: comparison between the maximum heat released by the reaction system presented in equation 6.17 and the maximum heat removal from the cooling system, considering a standard reactor of 100L ($Area = 0.84m^2$; $T_{j,min} = 10°C$; $U = 425W \cdot K^{-1} \cdot m^{-2}$) with an equimolar mixture composed of 500 moles of A and B. S and U representing stable and unstable operating point, respectively.

circumstances.

Semenov diagram

The Semenov diagram demonstrates a reactor able to handle this reaction system on a broad range of temperature, from 10 to $120°C$ (Figure 6.17). Therefore, under normal operating conditions, the reactor design would be suitable for the considered reaction system, regarding the operating temperature without considering, the boiling temperature.

This diagram, as demonstrated for the simulated example, that such approach to determine the safe operating region may be misleading in reality.

The Figure 6.18 describes such event for different set point temperatures. The dynamic behaviours of the reactor and jacket demonstrate how the selection of the operating temperature is a crucial step toward an inherently safe process. Thus, by comparing the classical Semenov Diagram indicating a broad range of favourable operating temperatures ($< 120°$) and the dynamic investigation, one can notice that the range is clearly limited due to the dynamic aspects of the cooling system and not any more solely by its maximum heat exchange capacity.
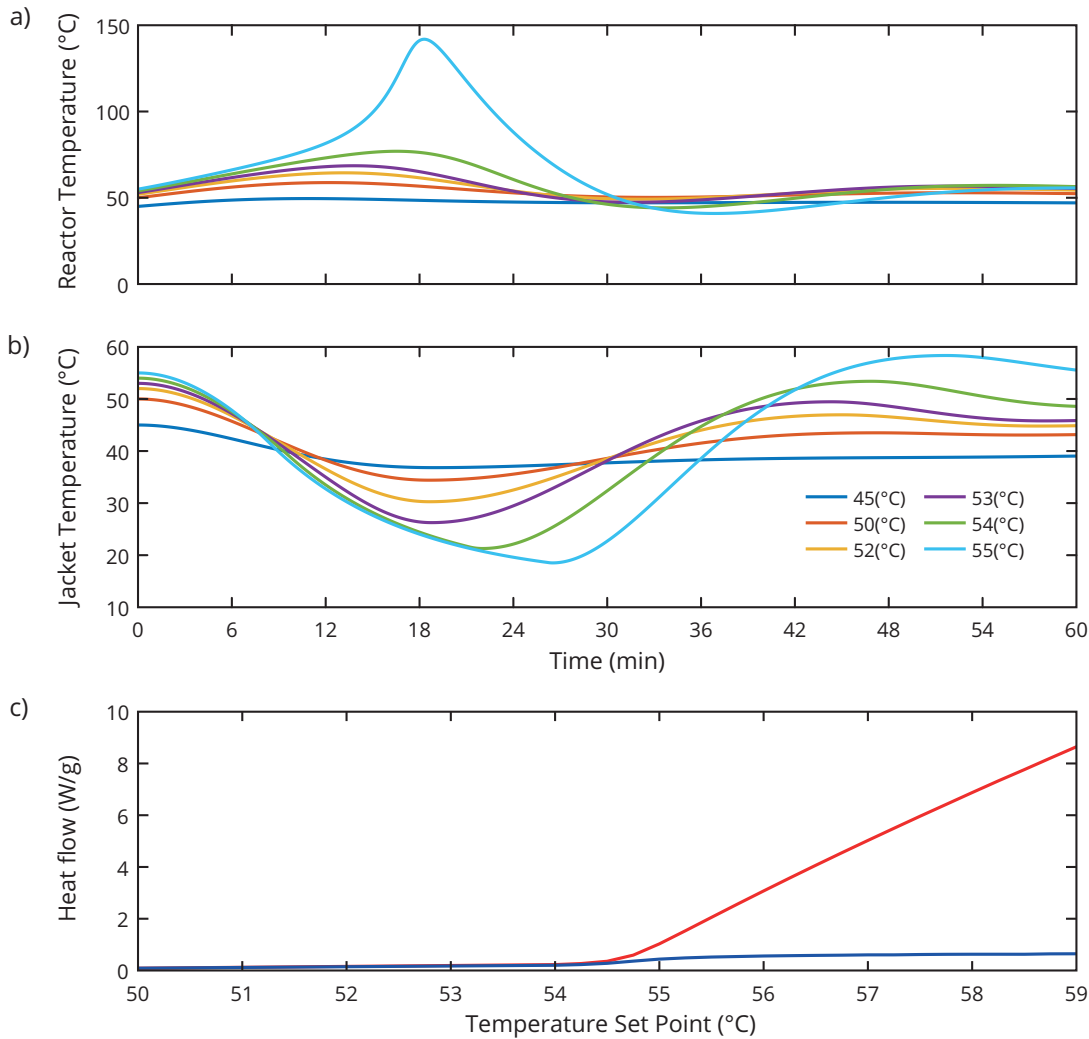
Figure 6.18 – Dynamic Semenov Diagram: influence of the temperature set point for the reaction system presented in equation 6.17, considering a standard reactor of 100L ($Area = 0.84m^2$; $U = 425W \cdot K^{-1} \cdot m^{-2}$; $P = 2.43$; $I = 99999s^{-1}$; $\tau_c = 534s$; $\tau_h = 1093s$; $T_{j,min} = 15°C$; $T_{j,max} = 130°C$)) with an equimolar mixture (15kmol of A and B): : a) Reactor temperature; b) Jacket temperature and c) Production of the product E after $8h$.

The discussed MAT of $65°C$ is also confirmed as an unstable operating temperature. Therefore, the operating temperature must be chosen appropriately to obtain an economically reasonable process time, meaning as short as possible and sufficiently low to control the heat release rate. In this case, a low temperature would be preferred to keep the process safe. Unfortunately, maintaining a low temperature is not economically viable. Moreover, if isothermal conditions are sought, the jacket temperature has to respond fast, meaning a cooling system having small time constants. Consequently, this kind of conditions may be difficult to achieve in practice.

Another path to control this reaction under batch conditions would be to carry out a
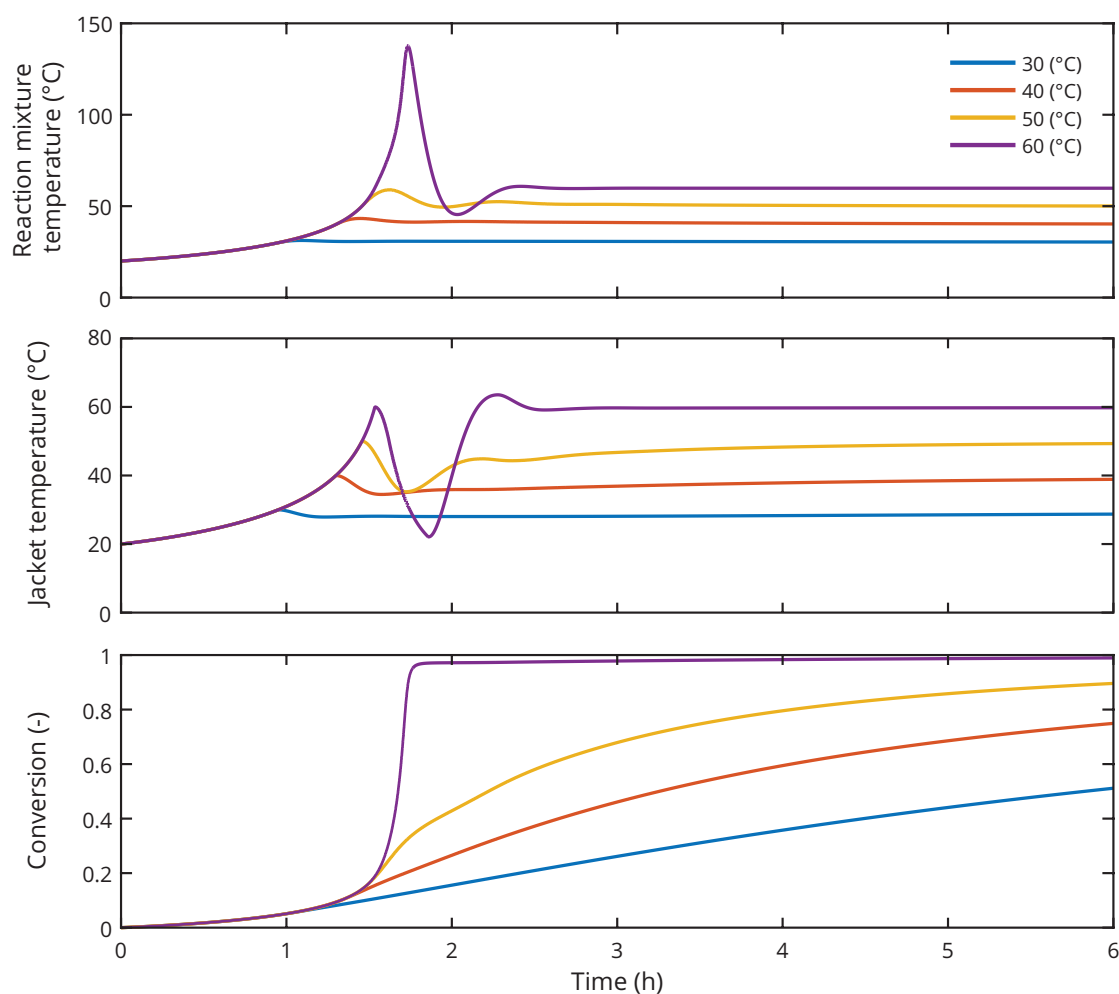
Figure 6.19 – Reactor (A) and Jacket (B) temperature profiles as a function of time and the resulting conversion (C) for different switching temperatures of the cooling system from a starting temperature of $20°C$.

step control at the beginning: start at a low temperature and then let the reaction progress adiabatically until the temperature reaches a switch value (T_s), where the cooling system is activated (Figure 6.19).

This type of control results in poor conversion for batch processes under control. Another critical point remaining is the maximum Temperature reached in case of Cooling Failure (T_{cf}). Consequently, to avoid a rise of pressure, the T_{cf} should remain under the boiling point. Unfortunately, this condition can never be achieved in batch operation mode; only the temperature can be adjusted to keep the system under control.

This assessment remains global and does not take into account additional equipment such as burst disk or condenser. Nevertheless, it shows that for this kind of reaction, batch processes are not the most suitable. Moreover, the worst moment for a cooling
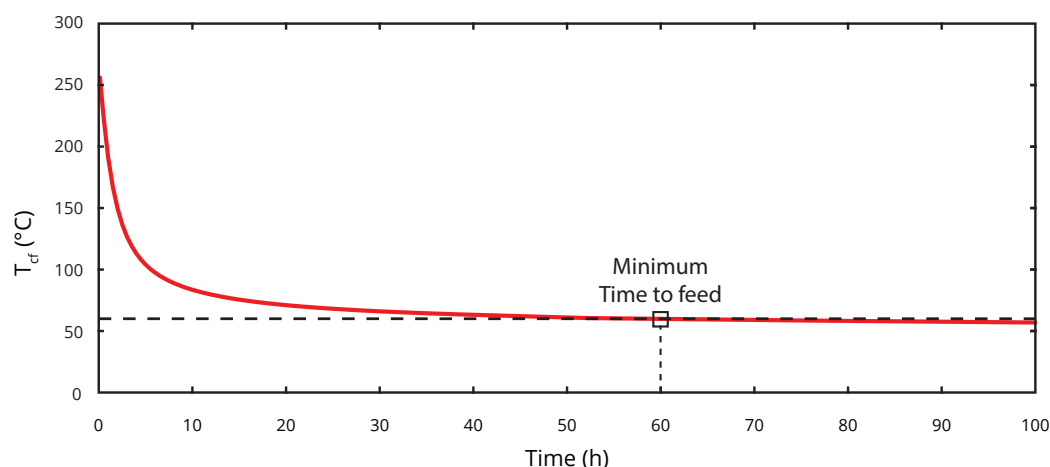
Figure 6.20 – Temperature reached in case of cooling failure as a function of a linear feed of A (500 moles) for the reaction system 6.17 and a feed temperature of $20°C$.

failure is, in this case, at the beginning. At this time, the thermal potential is maximal, making this mode not safe for such an autocatalytic reaction.

6.4.2.3 Fed-batch process

As mentioned previously in the batch process section, to maintain isothermal conditions, the cooling system should be able to remove the heat released by the reaction system at any moment. Therefore, the process can operate in fed-batch mode where the feed allows a control of the heat produced by the reaction system.

By applying a linear feed profile strategy, the resulting T_{cf} is clearly decreased. This phenomena is depicted in Figure 6.20 and demonstrates how a correct selection of the feed profile strategy is primordial to ensure an inherently safe process.

As a matter of fact, a linear feed is not always optimal regarding operation time and selectivity (depend on the reaction system). Indeed, more than $60h$ are required to remain under the MAT in the case of cooling failure. Therefore, the selection of convenient constraints ensuring an inherently safe system is primordial. The procedure developed in Section 6.3.1 has been applied with success to determine an optimal feed profile strategy and satisfy at any moment the constraint based on the cooling failure temperature.

This application demonstrates that an adequate feed (not linear anymore), in addition to a convenient operating temperature, decreases the operation time significantly as depicted in Figure 6.21. The thermal potential is minimized to an extent that remain controllable by the system even under failure ($\theta_{Gu} \leq 1$).
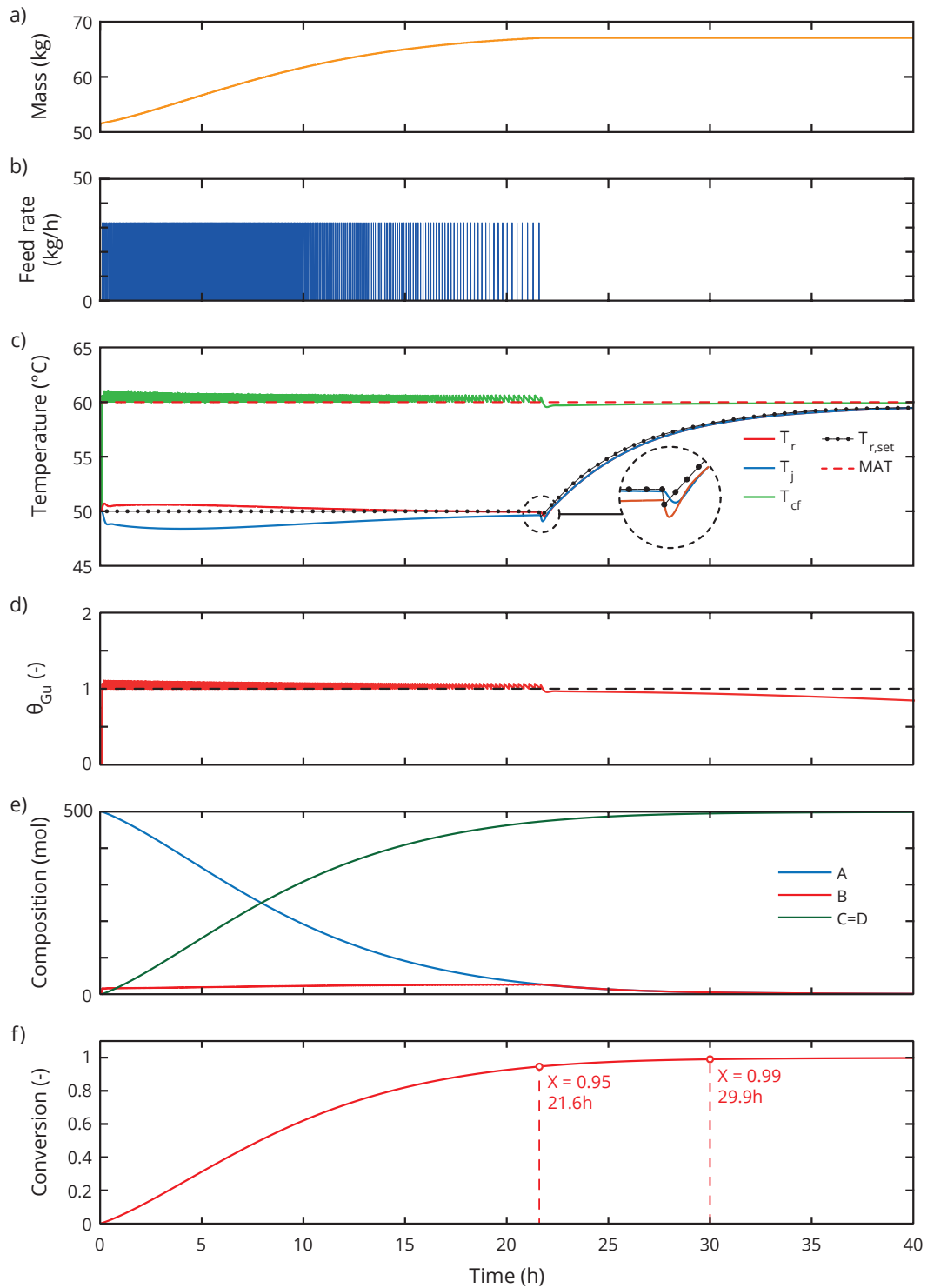
Figure 6.21 – Feed profile strategy and temperature optimization allowing to remain inherently safe ($TMR_{ad} \leq 8h$ and check interval of $5s$) during the feed phase ($\dot{m} = 32kg \cdot h^{-1}$) for the considered esterification (equation 6.17): a) Mass profile; b) Feed rate profile under on/off flow control for a fed reactant at $20°C$, c) Temperature profiles, d) Thermal potential, e)Composition along the process course and finally f) some indications about the conversion of $AcOAc$.

Practically, such feed profile strategy may be approximated by several linear curves, only requiring to change the feed rate at suitable moments. The temperature profile, on the other side, considers a reactor controlled in T_r-mode and a definition of the $T_{r,set}$ from a $\theta_{Gu,set} = 1$. This last optimisation shows how a strategic feed profile can maximise the productivity from 95% at $22h$ to 99% after $30h$. Of course, this facts are applied to a common esterification. Nevertheless, the overall approach depicts nice results toward an inherently safe process while remaining productive (increase of the product yield).

6.5 Conclusion

The latent thermal potential behind any reactive system is what makes a process dangerous. Under normal operating conditions, this potential remains inactive. However, under cooling failure or equipment malfunction, this potential may be unleashed and lead to a temperature increase that may trigger secondary reactions and gas formation. The gas production, if gas production takes place, may result in a pressure increase and, ultimately, in the reactor burst if no measures are applied before the point of no return.

In fed-batch operation, this thermal potential is profoundly related to the considered reaction system and reactor dynamics. Therefore, an approach has been developed with the aim of filling the lack of knowledge regarding the overall system, predicting its behaviour under normal and abnormal conditions, and preventing incidents from occurring. The combination of the reaction kinetic (Chapter 4) and reactor dynamic models (Chapter 5) developed in the previous chapters are essential bricks to build a model that describe the system, the Process Implementation Model (Figure 6.6).

This model demonstrated, through dynamic simulations, to bring a better understanding of the relevant parameters governing the process operation and thermal potential. As a result, a certain number of questions have to be answered for a correct design of safe and productive operating conditions, namely:

1. Is the considered industrial reactor able to control the temperature of the reaction mixture?
2. What are the safety relevant parameters to govern the reaction system in a given industrial reactor?
3. How can the reactor be brought into a safe state in case of malfunction?

A clear and direct answer to these questions is not possible, as dynamic aspects may have to be considered. Dynamic process simulation may help to fill this lack. As a matter of fact, by describing the behaviour of an industrial reactor, it is possible to

evaluate its ability to control the reaction mixture temperature and reaction system course. Besides, the dynamic behaviour greatly depends on the selected operating conditions. If the latter are well selected, the considered reactor should be able, in most cases, to control the heat released by the reaction system. Therefore, as presented in this chapter regarding the thermal potential, a systematic approach is of great value to define a Process Implementation Model and help to define how and in which equipment the process should be performed to ensure an inherently safer process.

The second question refers to the relevant parameters governing the dynamic behaviour of the system. This point was already addressed by many authors. They designed different diagnostic parameters and criteria describing the process safety by considering approximated reactor characteristics and reaction kinetics for single reaction system [111, 174]. Despite their great value for the evaluation of a safe operating zone, their determination will not need a significantly less amount of time and information as required to shape the process implementation model. Also, the process implementation model, compared to these approaches, is explicit and allows to test and explore a broad range of operating conditions, different reactors or tuning of the temperature controller through simulations. Once near optimal operating conditions respecting the system dynamics are determined, additional experiments can be undertaken to confirm them and, therefore, avoid the general approach of trial and error.

This last point is only one of the possible applications of the process implementation model. As the real system defines the model (Chapters 4 and 5), many others aspects such as selectivity or productivity optimisation can be studied. It can also jointly be used with a scale-down approach to simulate the behaviour of the industrial-scale reactor at lab-scale [155].

The development of an alternative path to evaluate the thermal potential for complex reaction systems was performed in parallel to the establishment of the normalised thermal potential θ_{Gu}, a dimensionless number which discriminates whether the process is under a safe or critical regime. The correct definition of operating conditions will result in a process that continually operates in the safe zone. Therefore, by placing suitable constraints on the feed profile strategy as well as on the temperature set point, a process may be optimised to ensure inherent safety. The different examples give a good insight in how this dimensionless number be used to identify the optimal operating conditions.

Another point to consider for this approach is its capacity to deal with synthesis, as well as secondary reactions to determine the thermal potential. In opposition to the current method that determines the accumulation where solely the energy of the synthesis reaction is considered. When dealing with potentially runaway reactions, however, gas

formation due to evaporation or decomposition may have to be considered. Therefore, the pressure issues and vent sizing would be an exciting challenge to improve the process implementation model.

7

Real Case Investigation

A man should never be ashamed to own that he has been in the wrong, which is but saying in other words that he is wiser today than he was yesterday.

Alexander Pope, 1688-1744

Within the fine chemical industry, the demands regarding the process differ from one field to another. As an example, in reaction engineering, the problems encountered deals with yield and selectivity optimisation while, in pharma, other aspects of validation have to be fulfilled. Such processes require being well-known to maintain the product specifications within the quality control bounds for allowable variations in the processing conditions [12]. It becomes apparent that modelling can significantly help to define the optimal route as soon as the kinetics and process dynamics are known.

A specific problem encountered in scale-up of fed-batch reactors is the thermal potential due to the accumulation of non-converted reactants but also by the production of hazardous materials (Chapter 6). This result may lead to an uncontrolled temperature increase in case of process control malfunction or if one of the following scenarios materializes:

1. The heat released by the reaction exceeds the heat removal capacity of the reactor or,

2. The cooling dynamics of the system is insufficiently fast to control the heat released during a transient change.

Therefore, understanding and mastering these aspects is one of the most important and challenging process safety tasks. One from possible solutions would be to adapt the feed rate to avoid rapid heat accumulation. Nevertheless, this approach is disadvantageous in terms of reaction time (Chapter 6) and costs involved. In order to quantify and manage this problem in an optimal way, the reaction kinetics and reactor dynamics must be known [30, 130, 155].

As an overall example, the discussion will be focused on a real case incident with the aim to answer the following questions:

1. How to characterize the reactive system and its process?

2. How to deal with the safety issues?

The previous chapters demonstrated that characterization of the reaction kinetics as well as reactor dynamics were primordial for a correct scale-up, but also to build the process implementation model. This model is then clearly necessary to assess correct operating conditions ensuring an inherently safe process. In addition, Caygill stated that safety incidents were very illustrative of the problem that may occur due to wrong scale-up and process development [12]. Therefore, this overall conceptual approach will be applied on a real case incident.

7.1 The case history

Between 1990 and 1998, Morton International Inc. produced a dye for the petroleum industry called Automate Yellow 96 (AY96). The thermal studies performed between 1986 and 1990 showed a slow and exothermic synthesis reaction followed by a highly exothermic decomposition of the product as illustrated in Figure 7.1. The reaction scheme of the reactive system is presented in Figure 7.2.
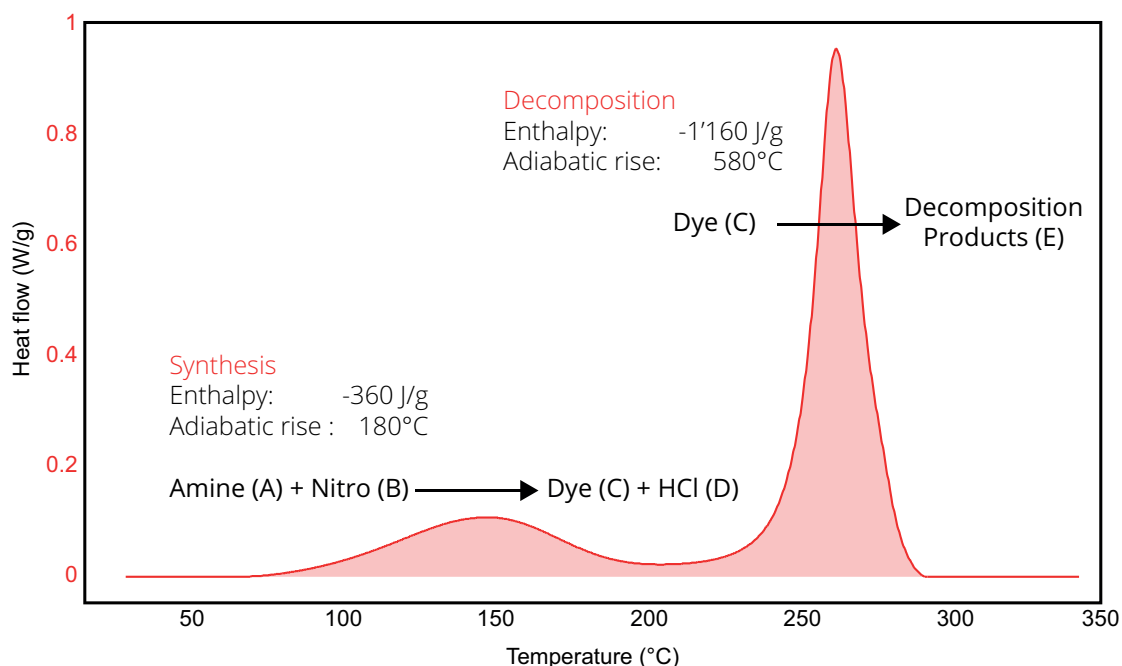
Figure 7.1 – Thermal behaviour of the synthesis and decomposition reaction scheme of the Automate Yellow 96 (AY96) assessed in a Setaram C80 at $1\,Kmin^{-1}$ (after processing).
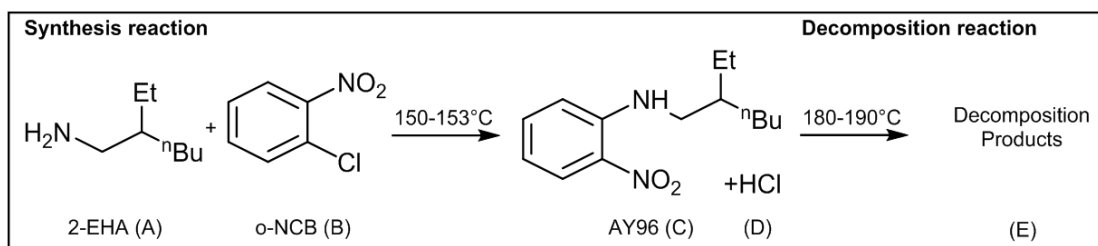
Figure 7.2 – Synthesis and decomposition reaction scheme of the Automate Yellow 96 (AY96).

The decomposition reaction was underestimated during the scale-up investigation as the company continued to increase the production scale by maintaining the same operating conditions and even moving from a fed-batch toward a batch process. Besides, temperature was controlled manually by the operators who repeatedly reported that significant temperature deviations in the 7.6 m^3 production vessel were

observed. Few of their notes are summarized in Figure 7.3.

"Cooling not controlling temp."	*"Temp override to 120°C, cooling inadequate to control temp."*	*"Cooling water of no use."*
Batch 3, 1991	**Batch 5**, November 1991	**Batch 28**, April 1997

Figure 7.3 – Operator messages regarding the deviations [6].

Despite several supervisors comments, the temperature excursions were ignored; it has been believed that high temperature rises were a quality concern and not a safety issue (Figure 7.4).

> *"DO NOT heat batch above 160°C or yield and quality will be lower."*
>
> On batch sheets of Yellow 96

Figure 7.4 – Knowledge of the supervisors toward temperature excursions of the AY96 production [6].

On the 8th April 1998, at the Paterson site (New Jersey, USA), an explosion and fire occurred due to the decomposition of AY96 causing many damages, hazardous material release and injuring nine employees, including two of them seriously [6].

7.2   Reaction Kinetic Investigation

The Reaction Kinetics Investigation of a complex reaction system can be a long and exhausting task, requiring numerous experiments and not always leading directly to a kinetic model. One can find a literature with many approaches applied to get the reaction kinetics [33, 177]; unfortunately, they are often adequate only for single-step reactions or simple reaction schemes [40]. Such issue may be avoided by using the Reaction Kinetic Investigation as presented in Chapter 4. This approach was henceforth applied here, on the Morton reaction system with only a limited number of data.

7.2.1   Reaction kinetic model

The experimental data required (Table 7.1) to estimate the kinetics parameters were collected from four reaction calorimetry experiments (Mettler-Toledo RC1e) in fed-batch mode performed in the temperature range of 110 - 130 $°C$ with reaction masses between 235 and 430 g. Additionally, two experiments were performed in a Calvet

Calorimeter (C80 Setaram) in batch mode at heating rates of 0.1 and $1\ {}^{\circ}C \cdot min^{-1}$ with sample masses of 179 mg and 716 mg, respectively.

Table 7.1 – Operating conditions for the RC experiments with a feed of 2-EHA (A), the reactor being initially charged with o-NCB (B).

Experiment	Temperature	Time to feed	2-EHA (fed)	o-NCB
Units	$({}^{\circ}C)$	(min)	(mol)	(mol)
1	110	232.5	1.4	1.17
2	120	277	1.51	1.5
3	125	65.5	0.39	1.17
4	130	242	1	1

The reaction system investigated (Figure 7.2) is described by a two-step reaction scheme considering an autocatalytic decomposition :

$$A + B \rightarrow C + D \tag{7.1}$$
$$C \rightarrow E \tag{7.2}$$
$$C + E \rightarrow 2E \tag{7.3}$$

The kinetic model is based on the generalized law of mass action (Section 2.2.1.2) and compared to the experimental data as illustrated in Figure 7.5 [130]. The best estimated values of the reaction kinetic parameters are listed in Table 7.2 and were obtained with AKTS-Reaction Calorimetry Software following the procedure developed in Chapter 4 [134].

In order to simplify the model and decrease the number of kinetic parameters, the reaction scheme (7.2) describing the production of E from the dye (C) was omitted by including virtually a small amount of decomposition products in the autocatalytic model at the beginning of each simulation.

7.3   Reactor Dynamic Investigation

In order to control the reaction course and avoid a runaway incident, it is essential to understand how the reactor heating/cooling systems behave and to assess their performance and limitations. The thermal behaviour and temperature control of a reactor can be assessed following the procedure presented in the Chapter 5.
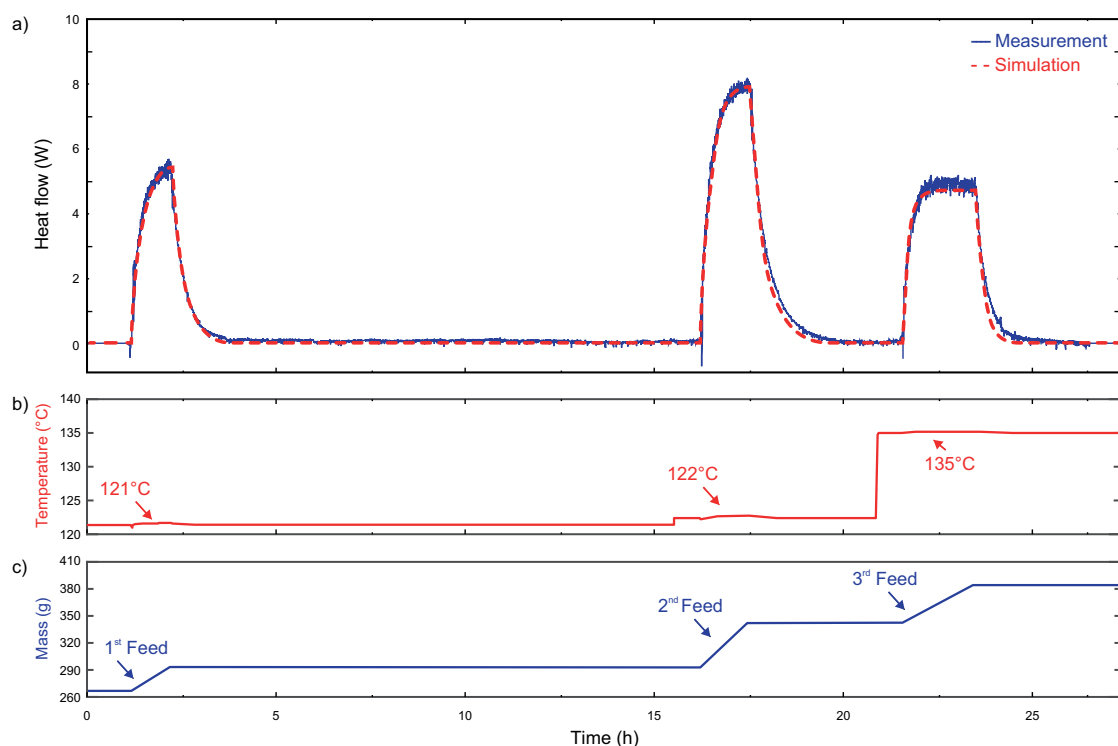
Figure 7.5 – Validation of the reaction kinetic model: a) Comparison of the simulated heatflow with an experiment not included in the data set for the fitting; b) Temperature profile composed of 3 different temperature set points and; c) and linear feed profiles.

Table 7.2 – Estimated reaction kinetic parameters for the proposed reaction scheme of the AY96 synthesis.

Reaction 1

$k_{0,1}$	$E_{a,1}$	$\Delta_r H_1$	Orders
$\left(g^{0.42}s^{-1}mol^{-0.42}\right)$	$\left(kJ \cdot mol^{-1}\right)$	$\left(kJ \cdot mol^{-1}\right)$	$(-)$
$7 \cdot 10^8$	83.4	-106	$a1 = 0.94$ $b1 = 0.48$
Rate		$r_1 = k_1 C_A^{a1} C_B^{b1}$	$\left(mol \cdot g^{-1} \cdot s^{-1}\right)$

Reaction 2

$k_{0,2}$	$E_{a,2}$	$\Delta_r H_2$	Orders
$\left(g^{0.48}s^{-1}mol^{-0.48}\right)$	$\left(kJ \cdot mol^{-1}\right)$	$\left(kJ \cdot mol^{-1}\right)$	$(-)$
$4 \cdot 10^{10}$	123.6	-168	$c2 = 0.83$ $e2 = 0.65$
Rate		$r_1 = k_1 C_C^{c2} C_E^{e2}$	$\left(mol \cdot g^{-1} \cdot s^{-1}\right)$

Table 7.3 – a) Estimated characteristics and thermal dynamics, and b) reactor inertia and PID temperature controller parameters involved in the Morton International Inc. incident.

a)	*Volume*	*o-NCB*	*2-EHA*	U	A_{max}	R_{AV}	α
Units	(m^3)	$(kmol)$	$(kmol)$	$(Wm^{-2}K^{-1})$	(m^2)	(m^{-1})	$(W \cdot K^{-1})$
Value	7.6	15.9	15.3	700	7.4	1.47	12
b)	$\tau_{heating}$	$\tau_{cooling}$	K	I	D	T_{min}	T_{max}
Units	(s)	(s)	$(-)$	(s)	(s)	$(°C)$	$(°C)$
Value	1500	1500	4	4000	10	5	180

7.3.1 Reactor model

Based on the CSB investigation report and the reactor model presented in Chapter 5, dynamic simulations of a reactor representing the one in operation during the Morton International Inc. incident were investigated [6]. The reactor characteristics were estimated based on typical reactors of the same volume: thermal dynamics and temperature control are depicted in Table 7.3.

The implication of the reactor heat capacity C_w was omitted for its insignificant effect on the thermal dynamics as explained in Section 5.4.1.3.

7.4 Thermal risk assessment

The next sections will present the different steps the Morton incident underwent regarding the thermal potential and temperatures. The different models and developments made in the previous chapters will be applied to simulate the reactor thermal behaviour during this incident, optimise the feed profile strategy to ensure an inherently safer process during the feed phase, to finally perform an improvement of the operating temperature.

7.4.1 Incident simulation

The main reason leading to the incident of Morton International Inc. is clearly the choice of operating in batch mode and the increase in reactor size (from 3.8 to $7.6m^3$). As a matter of fact, operating under batch conditions means a maximum of thermal potential from the start without any other way to control it than by the cooling system (Figure 7.6b). In addition, the operating temperature $(150°C)$ was near to the boiling point of 2-EHA $(160°C)$. As far as the system is designed for it, it is not an issue. However, it was not the case as the condensers were undersized. The decomposition
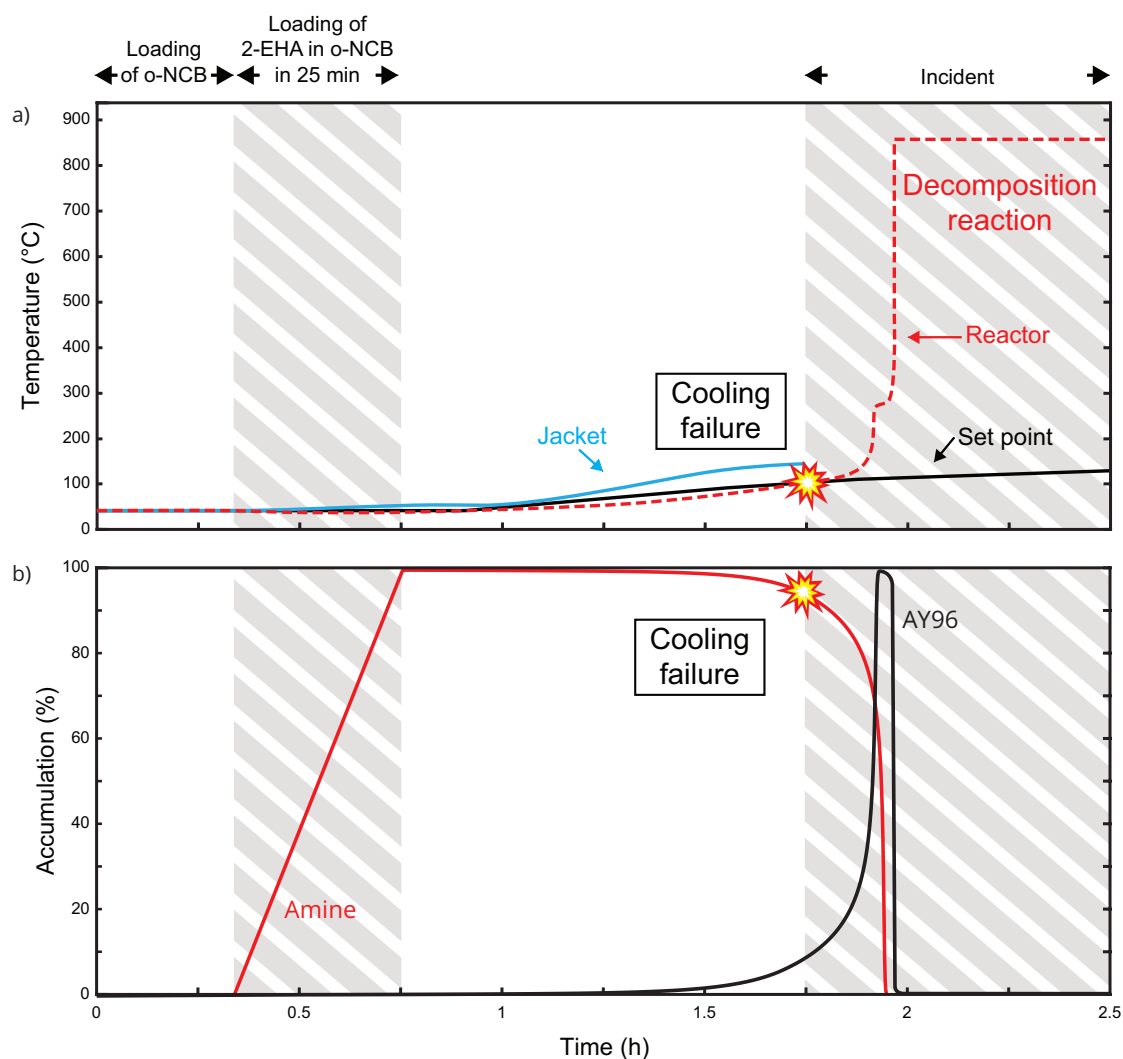
Figure 7.6 – Morton incident events: a) Influence of cooling failure and loading of 2-EHA in o-NCB on the temperature profile, when using the temperature ramp applied during the incident; b) Accumulation of non-converted reactants (feed of 2-EHA and production of $AY96$) along the process course during the incident.

temperature at $180 - 190°C$ was also a parameter that result to very short Time to Maximum Rate under adiabatic conditions for both the reaction and decomposition (< 1 min).

A simulation based on the operating temperature setpoint profile applied by Morton and the estimated dynamic parameters was performed with AKTS-Reaction Calorimetry Software, demonstrates the inadequate capacity of the system to control the heat release rate (Figure 7.6a) [134]. The high criticality of 5, according to the Stoessel's classification of exothermic reaction processes characterizes this process correctly.

7.4.2 Process optimisation

The process optimisation should not only focus on productivity or safety individually, but on coupling these two aspects together. As demonstrated and mentioned in the previous chapters, an inherently safer process is achieved if the thermal potential is controlled all along the process course. Therefore, a correct selection of operating conditions leads to a minimization of the thermal potential, but still allows a decent productivity. Thus, in case of cooling failure, the process remains in a safe state at any moment.

The overall concept consisting of building individual models and then combining them to shape a Process Implementation model (Chapter 6) has been applied to this real case incident. The resulting model allows exploring different operating conditions through dynamic simulations. The obtained results demonstrate that the optimal operating time is a function of the process temperature and the feed rate during the feeding phase, while it is only a function of the operating temperature of the post feed phase. As a matter of fact, a lower temperature than $150°C$ (Morton Inc. process temperature), coupled to a fed-batch mode leads to an inherently safer process respecting the *QFS* criteria. Nevertheless, a too low process temperature has a direct effect on the reaction rate and conducts to a greater accumulation of the fed reactant. Even if this fact is compensated by a correct feed strategy, it requests, however, a stronger effort of the cooling system during normal operating conditions and does not respect the *QFS* criteria anymore.

Using the procedure and models developed, the safety constraint can be respected in any case. As soon as the operating temperature is selected under the *MAT*, the feed is adapted to keep a safe process course, minimizing the accumulation of the fed reactant to a decent level and considering the secondary reaction that may appear along the process course. For this case, the constraint is based on the *MAT*, which is the boiling point of the 2-EHA, namely $160°C$. In order to appreciate a safety margin, the *MAT* has been decreased to $155°C$. Nonetheless, dynamic simulations demonstrate that optimal operating conditions that allows a minimization of the feed time as well as the time to reach a conversion of 99% of the fed reactant exist and respect the constraint all along the process course. These results were computed with AKTS-Reaction Calorimetry Software and are depicted in Figure 7.7 [134].

The normalised thermal potential θ_{Gu} has also been computed for the same operating conditions and demonstrated that the process respects the constraint in any situation and under a $24h$ time to react. Therefore, it is entirely feasible to remain inherently safe if a correct selection of the operating condition is performed.

These results anew highlight the lack of knowledge of the reactive system that existed
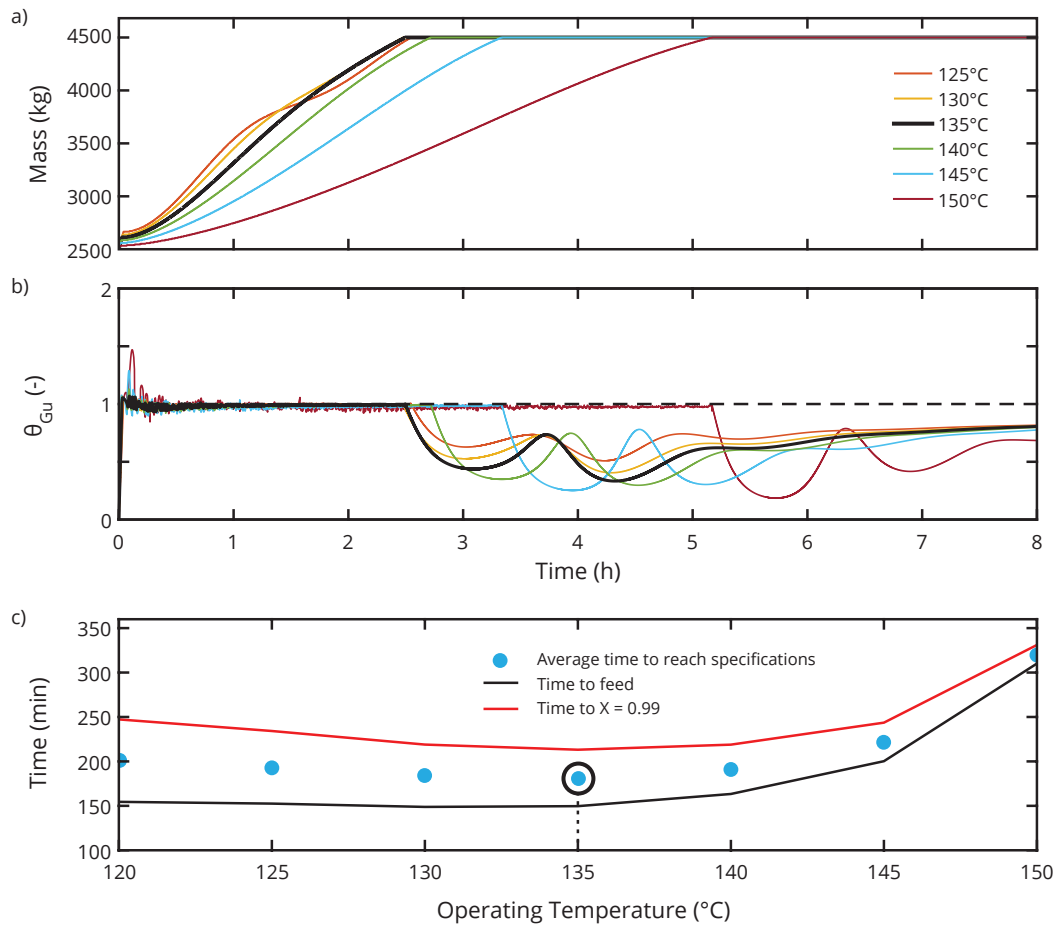
Figure 7.7 – Exploration of different operating conditions for the production of $AY96$ with a composition and dynamic parameters depicted in Table 7.1: a) Application of the feed profile strategy and the resulting mass profile; b) The normalised thermal potential θ_{Gu} along the process course; c) Definition of the optimal operating temperature leading to a minimization of the operating time between the feeding and the post feed phases.

during the process development of the AY96 production. With a better understanding, this accident may have been foreseen by just operating at a lower temperature and staying in fed-batch mode.

As a summary, the process should have been handled under fed-batch mode (as it was already stated from the start), at an operating temperature of $135°C$ (feeding phase) with an optimised feed strategy in $156min$ and reaching a conversion of 99% in less than $4h$ (oppositely to more than $6h$ at Morton Inc.). Such operating conditions ensure an inherently safer process remaining economically viable. The process course considering these conditions and an optimisation of the post feed phase is illustrated in Figure 7.8.
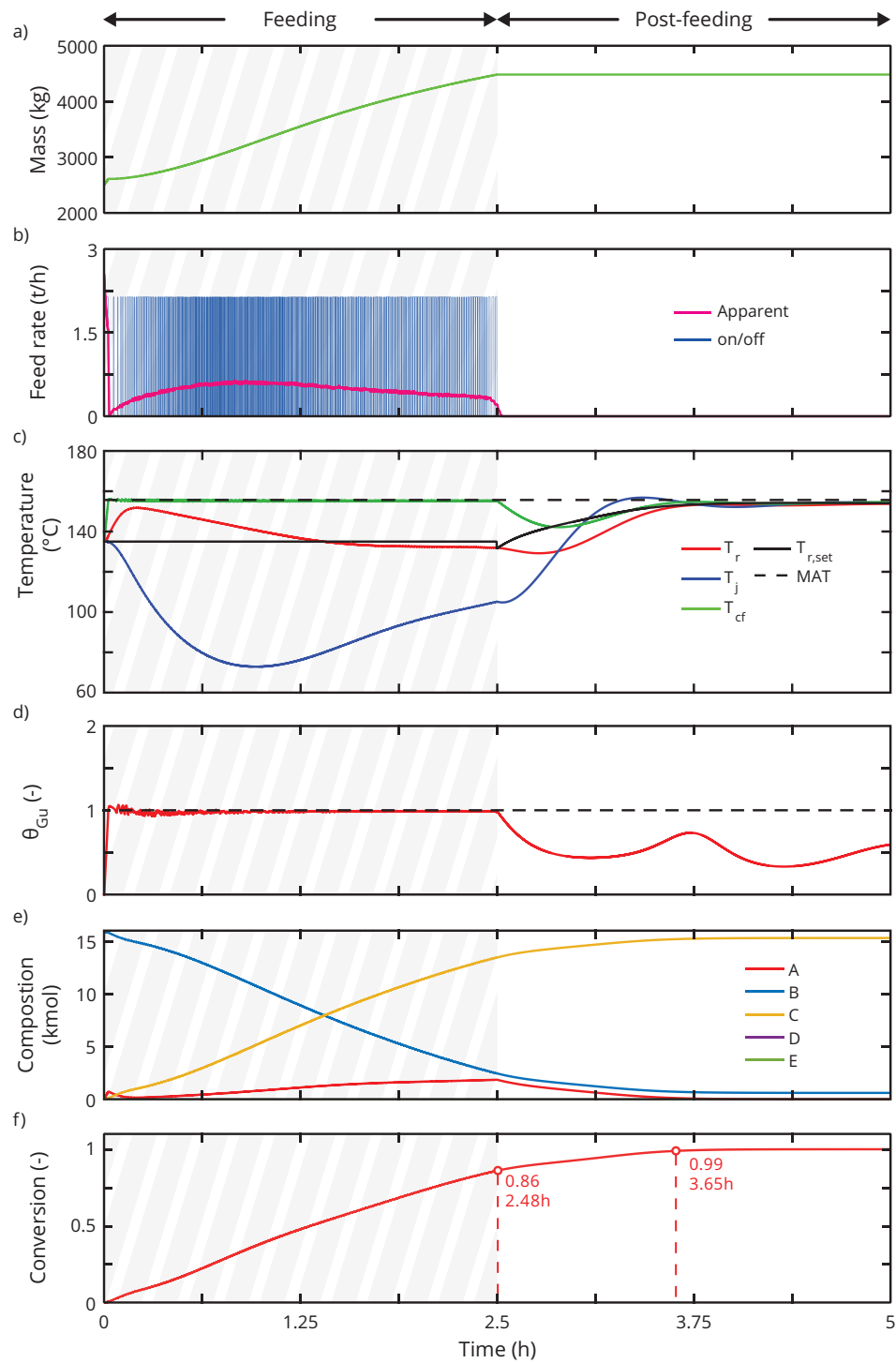
Figure 7.8 – Fed-batch process operating under safety constraint by adjusting the feed rate in order to have a temperature in case of cooling failure T_{cf} remaining below the maximum allowed temperature MAT ($155°C$). a) Mass profile and b) The corresponding feed rate respecting the constraint, c) Reactor and jacket temperature profiles under normal operating condition with its corresponding T_{cf} and constraint MAT, d) Normalised thermal potential, e) Composition and finally f) Conversion of the $2-EHA$. These results were computed using AKTS-Reaction Calorimetry Software [134].

7.5 Conclusion

This investigation highlighted the different issues encountered during the scale-up of a dye production. The thermal potential present at any moment along the process course is not only due to the accumulation of unconverted reactants but also due to the production of hazardous materials. The incident demonstrates by its consequences that the combination of thermal potential namely, the synthesis reaction followed by the autocatalytic decomposition, results in disastrous outcomes if not assessed correctly.

The novel proposed investigation procedure based on the relationship between reaction kinetics (Chapter 4) and reactor dynamics (Chapter 5) allows an optimisation of the productivity all along the process while remaining within safe limits. Compared to conventional scale-up methods based on trial and error, this approach simplifies and decreases the development time by several steps. Moreover, having kinetic and reactor dynamic models contribute significantly to a better understanding of the process controllability at industrial scale which allows the definition of safer operating conditions.

8

Conclusion & Perspectives

The intelligent man is one who has successfully fulfilled many accomplishments, and is yet willing to learn more.

Ed Parker, 1931-1990

8.1 Conclusion

In recent years, a growing effort work has been devoted to the concept of inherent safety in process development, which aims to modify the process in order to avoid or significantly decrease hazards, instead of accepting them and setting barriers to handle them. Although this principle is known since the late 70's, the uptake of this concept is slow and major accidents keep on happening. Accidents that are often caused by a lack of knowledge of the chemical reaction, poor reactor design or erroneous selection of operating conditions. In this context, a correct scale-up route could have identified and prevented such scenario if the concept of inherent safety was applied from the beginning.

The latent thermal potential is one of the main reasons accidents occur. Under normal operating conditions, this potential remains inactive. However, under cooling failure or equipment malfunction, this potential may be unleashed and lead to a temperature increase which may trigger secondary reactions and gas formation. The gas produced, may result in a pressure increase and, ultimately, in explosion if no measures are applied before the point of no return.

This problem is encountered in the scale-up and design of fed-batch reactors as a result of, firstly, an accumulation of non-converted reactants due to a feed rate higher than the reaction rates and secondly, by the production of hazardous materials. This thermal potential is profoundly related to the considered reaction system, the reactor dynamics, and the selected operating conditions. Therefore, a novel scale-up methodology has been developed, focusing on filling the lack of knowledge of the reaction system, predicting its behaviour under normal and abnormal conditions, and preventing incidents from occurring.

The core idea of this methodology is to model the system by two major aspects:

1. *The reaction kinetics* which describes the reaction and transformation rates occurring in the reaction mixture and,

2. *The reactor behaviour* which highlights how the latter controls the reaction course by adjusting the temperature of its cooling system and the adopted feed profile strategy.

Different procedures and models were developed to characterize these two aspects individually, and finally, to build a model that represents the overall process. At first, the procedure created for the Reaction Kinetic Investigation demonstrated that an approach based on multi-scales, -conditions and -ratios could be an efficient path to characterize a reactive system taking place in a homogeneous solution. Furthermore, the use of calorimetry as a non-invasive method (DSC, Calvet, and RC) in combination with the

Law of Mass Action allowed, to model and predict accurately the events arising in the reaction mixture under a wide range of operating conditions. The resulting model significantly contributes to a better understanding of the parameters influencing the reaction rates. The main benefit of such an approach is to be fast and straightforward to gain valuable information regarding the reaction kinetics. The disadvantages, however, come from the fact that the composition profiles are not obtained during the reaction course but obtained through the parameter estimation and simulation. This fact may bring out some difficulties into the establishment of the reaction scheme hypothesis, while a chemist or chemical engineer may come up with an acceptable answer if sufficient and well-planned experiments are performed.

The Reactor Dynamics Investigation approached the second aspect by using a straightforward and general model-based procedure, characterizing the overall reactor thermal behaviour by considering three attributes of the heat transfer system:

1. The reactor heat balance,

2. The PID temperature control and,

3. The jacket behaviour.

Temperature heating/cooling ramps, as well as isothermal stages performed directly in the industrial reactor, demonstrated to be an experimentally direct and efficient strategy to explore these different dynamics together. The consistency and robustness of such procedure coupled with a parameter estimation algorithm were assessed for various reactor sizes, conditions, and temperature control types. The predictions performed, using the reactor model with the retrieved dynamic parameters, exhibited a logical behaviour and were robust with respect to little changes. Small systems were also modelled accurately despite the fact that they are more sensitive to changes.

The reactor dynamic parameters were considered as temperature-independent. In reality, this assumption is physically incorrect. Therefore, a possible adjustment of the model and algorithm may be performed to ensure a determination of temperature dependency, although the opposite assumption, namely temperature-independent parameters, already shows excellent results.

Nevertheless, having a good knowledge of the reaction kinetics and the reactor thermal dynamics is not sufficient to guarantee the safety of a chemical process. As a matter of fact, the dynamic behaviour of the overall system greatly depends on the selected operating conditions. If the latter are correctly selected, the considered reactor should, in most cases, be able to control the heat released by the reaction system.

The establishment of the two previous dynamic models, namely the reaction kinetics and reactor dynamics, shows to be essential bricks to build an overall model that

describes the system, namely the Process Implementation Model. This model is underlined by its ability to predict the considered process under different combinations of temperature control and allows to evaluate how the process should be handled to ensure inherent safety.

The overall methodology, compared to conventional approaches, is explicit and allows to test and explore a broad range of process variants through dynamic simulations, avoiding a large number of experiments. Once near optimal operating conditions respecting the system dynamics and safety constraints are identified through simulations, additional experiments can be performed to confirm the selected operating conditions and avoid the general approach of trial and error.

The quality of each model will be directly defined by the purpose of the latter but also by the amount of information available on the considered system. Consequently, with this idea in mind, all the procedures were designed to enable the chemical engineer to improve the model accuracy. By simply adding new experiments to the data set, the parameter estimation algorithm can be used to evaluate more representative parameters.

These developments lead to the establishment of a new dimensionless number; the θ_{Gu}; this number demonstrates its usefulness for the determination of the current operating region namely, safe, critical or runaway. Through some modifications of the latter number, it allows the identification of optimal operating conditions after the feed phase, ensuring a process to remain in a safe state even under cooling failure scenario, but still improving the production.

This research has permitted to establish a new process scale-up methodology, regarding the assessment of the thermal potential. The obtained results demonstrated that a multi-scale approach combined with modelling and inherent safety, lead to a better understanding of the system (reactions and reactor together). This approach also notably helps to optimise the operating conditions that will make the process respect safety constraints and remain economically favorable, even under a cooling failure scenario.

8.2 Perspectives

The modern chemical and process industry is experiencing decisive changes to improve productivity and safety. The plants are being completely automated decreasing to a minimum human intervention [178]. This evolution heads toward new challenges that can be summarized by producing predictive models of high quality which can make a difference in improving scale-up, process performances and control.

190

Some issues regarding the scale-up were highlighted in the introduction. The different dynamics representing the system are often ignored, not reproduced correctly at laboratory-scale or their importance underestimated through the increase of scale namely:

1. The reaction kinetics,

2. The reactor dynamics,

3. The mixing.

8.2.1 The mixing

The procedures documented in this thesis have shown significant improvement concerning the determination of the reaction kinetics and reactor dynamics for homogeneous solutions. The mixing, however, was assumed to have no implication on the dynamic system. This assumption may be misleading for complex systems such as heterogeneous systems. As a matter of fact, a poorly designed mixing process may lead to a reduced mass- and heat-transfer that may result in the formation of hot spots due to local chemical reactions. Consequently, what are the requirements to model the mixing dynamics?

Although mixing effects have been studied for decades, and the recent remarkable advances performed in the science of computational flow dynamics (CFD), the tentatives to reproduce the desired mixing characteristics through a scale-up remain of weak efficiency. The mixing is such a complex phenomenon that it is still difficult to perform a scale-up through a systematic procedure and allowing to fill the gap between the laboratory and the industrial scale. Though some paths are available for such a scale-up, it is, however, often based on empirical correlations or approaches that try to keep constant different geometry ratio and/or conditions and/or dimensionless numbers [179]. Based on the developed methods in Chapter 2, this aspect gives the opportunity to improve the overall approach presented in this thesis, by considering the mixing effect directly in the Process Implementation model and would undoubtedly lead to a better understanding of the factors influencing the mixing.

8.2.2 A better scale-up

Our imagination and outlook have also expanded to recognize that predictions and models are not the only requirements for a productive and inherently safer process. Experimentation is also a factor that significantly influences the knowledge regarding

the considered system and therefore, the resulting model quality. Procedures and also instrument development are an absolute necessity to meet the demands of such lack.

In addition, performing an experiment at already large-scale may be challenging and also dangerous, especially if the system is not well characterized or designed for the considered purpose. Therefore, it is often preferable to perform an experiment on a laboratory scale with a reactor reproducing the large-scale behaviour.

Such approach can be made using three different ways:

1. Adapt the laboratory jacket temperature to make the reaction mixture temperature follow the same path as the industrial reactor [155],

2. Restrict the heat removal power to be proportionally similar at the laboratory than at industrial scale [180],

3. Reproduce the industrial reactor time constant at laboratory scale by adjusting the heat exchange area and jacket temperature.

These approaches always aim at reproducing the same reaction mixture temperature profile at laboratory than at industrial scale. In such a case, for a homogeneous reaction, the reaction rates can be assumed identical as well as the heat flow production per unit of mass.

Zufferey et al. developed and intensively discussed through applications the first approach [155]. Their methodology uses a model predictive control (on-line) where the reaction heat flow at laboratory scale under a defined time interval (e.g. 2s) is calculated, then multiplied by a scale-up factor S_F (equation 8.2) and finally used to describe the large-scale reaction heat flow. The future reaction mixture temperature at large scale is calculated through a dynamic model and set as a new set point of the laboratory reaction mixture temperature. Thus, the laboratory reaction mixture is operating under same conditions as at industrial scale.

This method involves many calculations and a good knowledge of the industrial reactor but offers a path that avoids characterizing the reaction kinetics. Despite this last fact, this approach does not let room for a post-optimization of the operating conditions (except through experimentation).

Davis and Viswanath investigated and discussed the second approach and demonstrated how a correct definition of the laboratory jacket temperature set point can lead to the behaviour of a considered industrial reactor [180]. A simple relationship

allows to reproduce this profile for a batch-mode experiment:

$$T_{j,lab} = \left(1 - \frac{UA_{ind}}{S_F \cdot UA_{lab}}\right) \cdot Tr + \left(\frac{UA_{ind}}{S_F \cdot UA_{lab}}\right) \cdot T_{j,ind} \tag{8.1}$$

where the overall heat transfer coefficient UA is time-dependent and S_F relates the ratio of the reaction mass in the laboratory reactor to the reaction mass in the industrial reactor such that:

$$S_F = \frac{m_r^{ind}}{m_r^{lab}} \tag{8.2}$$

The fed-batch mode is also discussed and demonstrated with explicit equations along their research [180].

This methodology has shown that the heat flow determination along the process course is not required to operate and thus can be applied in any computer-controlled jacketed reactor correctly characterized.

The last concept, resulting from the present work, can be based on the postulation of the heat loss similarity [45]. Such an assumption is applied e.g. in the UN Manual describing the procedure of the prediction of the thermal behaviour of decomposition reaction at large-scale from the results collected at laboratory-scale [181]. According to this concept the heat loss per unit of the reaction mass in the small-scale test should be similar to that one at the large-scale experiment. This condition is achieved when both systems have the same time constant (τ):

$$\tau_1 = \tau_2$$
$$\frac{m_{r,1} c_{p,r}}{U_1 A_1} = \frac{m_{r,2} c_{p,r}}{U_2 A_2} \tag{8.3}$$

with the indices 1 and 2 representing the large and laboratory reaction vessels, respectively. In the above equation, the symbols m_r, $c_{p,r}$, U and A represent the reaction mass, specific heat capacity of the reaction mass, overall heat transfer coefficient and heat exchange area, respectively. As an example illustrating this procedure, one can assume that a Dewar filled with a liquid (low viscous liquids, lumped systems) has a similar thermal behaviour as a large container filled with the same liquid as long as the heat losses are similar in both systems. This approach, applicable for comparing any reaction vessels of different sizes, can be also applied

for the determination of the thermal behaviour of large-scale reactors using results of small-scale tests performed in laboratory reactors. The requirement of an identical heat exchange with the jacket per unit of the reaction mass for both, the large-scale and the small-scale reactors, may be expressed as:

$$\frac{q_{ex,1}}{m_{r,1}} = \frac{q_{ex,2}}{m_{r,2}}$$

$$\frac{U_1 A_1}{m_{r,1}} (T_{j,1} - T_{r,1}) = \frac{U_2 A_2}{m_{r,2}} (T_{j,2} - T_{r,2}) \tag{8.4}$$

The heat production rate is dependent on the kinetics of the investigated chemical reaction. The kinetic parameters of the reaction are mass-independent. Consequently, to achieve the same reaction temperature T_r in both systems (after neglection of mixing effects) such as:

$$T_r = T_{r,2} = T_{r,1}$$

$$c_{p,r} = c_{p,r1} = c_{p,r2} \tag{8.5}$$

the following condition has to be fulfilled to achieve the same reaction rate per unit of mass in both reactors:

$$\frac{m_{r,2} c_{p,r}}{U_2 A_2} (T_{j,1} - T_r) = \frac{m_{r,1} c_{p,r}}{U_1 A_1} (T_{j,2} - T_r) \tag{8.6}$$

which can be simplified to:

$$\tau_{r,2} (T_{j,1} - T_r) = \tau_{r,1} (T_{j,2} - T_r) \tag{8.7}$$

where τ_r represents the reactor time constant in both systems. After rearrangement, we obtain:

$$T_{j,2} = \frac{\tau_{r,2}}{\tau_{r,1}} (T_{j,1} - T_r) + T_r \tag{8.8}$$

The time constant $\tau_{r,1}$ can be determined directly from the Reactor Dynamic

Investigation proposed in section 5.2 or using cooling curves [30]. The overall heat transfer coefficient U_1 or the term $U_1 A_1$ of the large-scale reactor can be estimated experimentally by at least one experiment carried out in the large-scale reaction vessel filled with an inert medium (such as water or unreactive solvent) under either heating or cooling modes with the reactor filled to at least two different fill levels. Thereafter, the overall heat transfer coefficient U_1, the term $U_1 A_1$ and the corresponding reactor time constant $\tau_{r,1}$ for all other possible reactants or reaction mixtures can be estimated by means of laboratory experiments and scaled applying the two film theory as presented in section 5.2.

As a consequence, for the same initial temperature $T_{r,0} = T_r(t = 0)$, we can have two possibilities:

(i) If $\tau_{r,1} \neq \tau_{r,2}$, the temperature of the reaction mixture T_r will be the same in both reactors during reaction if one adjusts the temperature of the jacket of the laboratory reactor $T_{j,2}$ in such a way that the condition depicted in equation 8.8 will be fulfilled.

(ii) If $\tau_r = \tau_{r,1} = \tau_{r,2}$, we have

$$T_j = T_{j,2} = T_{j,1} \tag{8.9}$$

what means that if the same jacket temperature profile T_j, is applied during all reaction course for both, the laboratory- and large-scale reactors, then the evolution of the temperature T_r, according to the concept of heat loss similarity, will be the same in both systems. The model can obviously be enhanced by considering the other terms of the heat balance such as the thermal inertia of the small reactor, etc.

However, the dynamics of the reactor temperature namely the time constants at laboratory- and large-scale are different. Their values, dependent on the ratio of the mass proportional to volume with the dimension m^3 and to the heat exchange area with the dimension m^2, vary non-linearly with the reactor scale. Therefore, it is obvious that due to the significantly larger volumes of the industrial reactors, their time constant values are larger i.e. $\tau_{r,1} > \tau_{r,2}$. The main resistance to heat exchange between the reaction mixture and the medium in the jacket is considered to occur in the immediate neighbourhood of the reactor walls. Therefore, fulfilling the condition of heat loss similarity can be obtained by adjusting the heat exchange area of the laboratory reactor in such a way that the equality $\tau_{r,1} = \tau_{r,2}$ is secured at all time. This can be achieved by:

1. A partly filled inner jacket, in contact with the reaction mixture in a triple wall

reactor as illustrated in Figure 8.1a [182]. In such a configuration, the inner jacket defines and regulates the heat exchange area whereas the external jacket operates as the heating and cooling system,

2. Immersion of a partly filled jacket of a double wall reactor in a temperature-regulated bath which consequently plays the role of the reactor jacket either during heating or cooling (Figure 8.1b).

(a) Triple wall reactor configuration.

(b) Double wall reactor configuration immersed in a temperature-regulated bath.
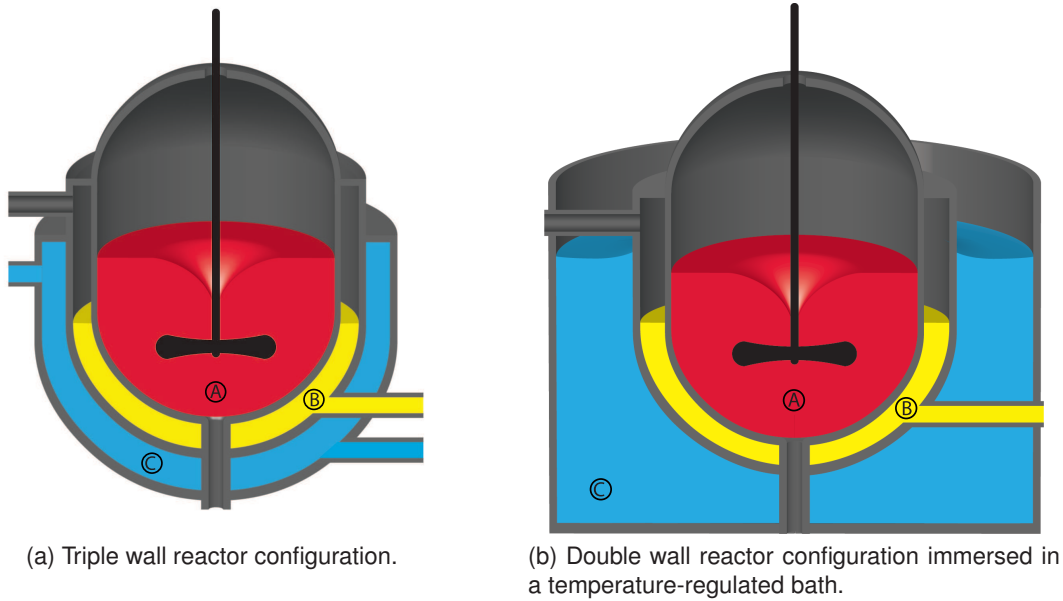
Figure 8.1 – Reactor configuration to perform a control of the heat exchange area: A) the reaction mass, B) the inner jacket and C) the external jacket or temperature regulated bath.

Such configuration has a direct effect on the overall heat transfer coefficient U:

$$\frac{1}{U} = \frac{1}{h_j} + \frac{d_{wall}}{\lambda_{wall}} + \frac{d_{j,fluid}}{\lambda_{eq,fluid}} + \frac{d_{wall}}{\lambda_{wall}} + \frac{1}{h_r} \tag{8.10}$$

where d represents the thickness and λ the thermal conductivity of each layer constituting the jacket of triple wall reactor, and h_r and h_j represent the coefficients of heat transfer by convection at the wall surface in the reaction vessel and in the external jacket, respectively (Figure 8.2). Depending on the type of medium which is used to partly fill the inner jacket which can be in liquid, gaseous or even solid state, its equivalent thermal conductivity influences the value of the overall heat transfer. For a static fluid, the equivalent thermal conductivity arises from the natural convection resulting from buoyancy forces due to density differences caused by temperature variations in the fluid with $\lambda_{eq,fluid} = N \cdot \lambda_{fluid}$ where the N value increases with lower viscosity. In a case of a constant void thickness $d_{j,fluid}$ in the inner jacket, the inner

area of heat exchange $A_{j,inner}$ can be assumed to be proportional to the mass of fluid filled in the inner jacket. One can write:

$$A_{j,inner} = \frac{m_{fluid}}{d_{j,fluid}\rho_{fluid}} = C^{ste} \cdot m_{fluid} \qquad (8.11)$$

which means that for a fed-batch reactor, the area of heat exchange of the inner jacket changes proportionally with the amount of fluid added. The fluid amount (added or removed) is regulated according to the change of the reaction mass (e.g. due to a reactant feed). Fluid amount regulation, directly linked up with the term $U_2 A_2$ (see Chapter 5), results in achieving the same time constant τ_r and the heat loss similarity during the reaction for the scenario when a feed is added to the reactor. In addition, the temperature of the fluid which is added into the inner jacket can be adjusted to be identical to the external jacket temperature for avoiding perturbations in the system.
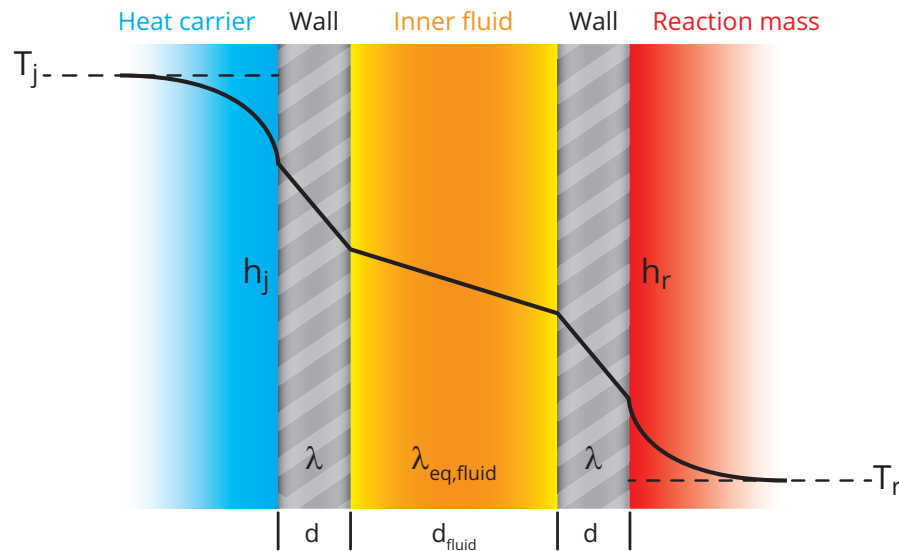
Figure 8.2 – Illustration of the overall heat transfer coefficient U in a triple wall reactor.

In order to mimic the thermal behaviour of the industrial reactor by applying the results obtained in the laboratory scale, one has to additionally correctly evaluate the thermal inertia of the heating (h) and cooling (c) system given by their time constants $\tau_{j,h}$ and $\tau_{j,c}$, respectively. Assuming, for simplification, the same time constants of the jacket in heating and cooling modes, we can write:

$$\tau_j = \tau_{j,h} = \tau_{j,c}, \qquad (8.12)$$

It is obvious that due to the significantly different sizes of the considered systems,

the values of the time constants of the jackets at large-scale are generally greater than those of the laboratory reactors i.e. $\tau_{j,1} > \tau_{j,2}$. Additionally, the temperature profile of the jacket as a function of time depends on the parameters of the temperature controlling systems. The temperature controllers, which can be denoted for simplification as PID_1 and PID_2, are different for the large- and laboratory-scale reactors.

As previously presented using the concept of heat loss similarity, if

$$\tau_r = \tau_{r,1} = \tau_{r,2} \tag{8.13}$$

it is necessary to fulfill the following equality

$$T_j = T_{j,1} = T_{j,2} \tag{8.14}$$

to have the same reaction temperature

$$T_r = T_{r,1} = T_{r,2} \tag{8.15}$$

for achieving at all reaction-time the same thermal behaviour and reaction rate in both, the large and laboratory scale reactors, respectively.

Under such conditions, the rate of change of T_j, in both reactors and during the overall process course, will be also equal. Referring to Chapter 5, equations 5.11 and 5.12, we have:

$$\frac{dT_j}{dt} = \frac{T_{j,set1} - T_j}{\tau_{j,1}} = \frac{T_{j,set2} - T_j}{\tau_{j,2}} \tag{8.16}$$

where $T_{j,set1}$ represents the set point of the jacket temperature that is imposed during heating or cooling in the large-scale reactor (see Chapter 5 and equation 5.9). After rearrangement of equation 8.16, we obtain:

$$T_{j,set2} = \frac{\tau_{j,2}}{\tau_{j,1}} \left(T_{j,set1} - T_j \right) + T_j \tag{8.17}$$

Equation 8.17 gives the correct temperature set point $T_{j,set2}$ of the laboratory jacket in T_j-mode so that both the small- and large-scale reactors have the same thermal behaviour i.e. the same temperature profiles T_j and T_r, which consequently results in

identical reaction rate per unit of the reaction mass.

Considering for example just one simple proportional temperature controller for a large-scale reactor in T_r-mode (see Chapter 5 and equation 5.9) we can write:

$$T_{j,set1} = T_{r,set} + K_1 \left(T_{r,set} - T_r\right) \tag{8.18}$$

where the parameter K_1 represents the proportional gain of the industrial reactor. For such a situation, after combining equations 8.17 and 8.18 for the initial temperatures $T_{r,0}$ and $T_{j,0}$, both reactors will have exactly the same thermal behaviour if the laboratory jacket temperature set point respects the following equation:

$$T_{j,set2} = \frac{\tau_{j,2}}{\tau_{j,1}} \left(T_{r,set} + K_1 \left(T_{r,set} - T_r\right) - T_j\right) + T_j \tag{8.19}$$

In such a case, the evolution of both temperature profiles T_r and T_j will be identical in both, the large-scale and the small-scale reactors. The perfect reproduction of the large-scale reactor thermal behaviour can be applied, using the above presented concept, in any correctly characterized computer-controlled jacketed reactor. It requires to measure T_r and T_j values and compute continuously the new set point of the jacket temperature $T_{j,set2}$ of the laboratory reactor.

The next figure depicts the scenario when the same reaction (Table A.7) takes place in:

A) An industrial reactor with $\tau_{r,1}$, $\tau_{j,1}$ and PID_1,

B) A laboratory reactor with $\tau_{r,2}$, $\tau_{j,2}$ and PID_2,

C) A laboratory reactor with $\tau_{r,2} = \tau_{r,1}$, $\tau_{j,2} \neq \tau_{j,1}$ and PID_1 instead of PID_2 and,

D) A laboratory reactor with $\tau_{r,2} = \tau_{r,1}$, $\tau_{j,2} \neq \tau_{j,1}$, PID_2 and $T_{j,set2}$ adjusted with PID_1 (equations 8.17 and 8.19).

It can be seen that in the cases (A) and (D) both reactors have the same thermal behaviour with $T_r = T_{r,1} = T_{r,2}$ and $T_j = T_{j,1} = T_{j,2}$. The kinetic parameters used to simulate the reaction as well as the parameters for determining the time constants of the reaction mass, jacket and the parameters for the controller of both, the large and small scale reactors are given in Table A.7 and A.8. All data were computed using AKTS-Reaction Calorimetry Software [134].
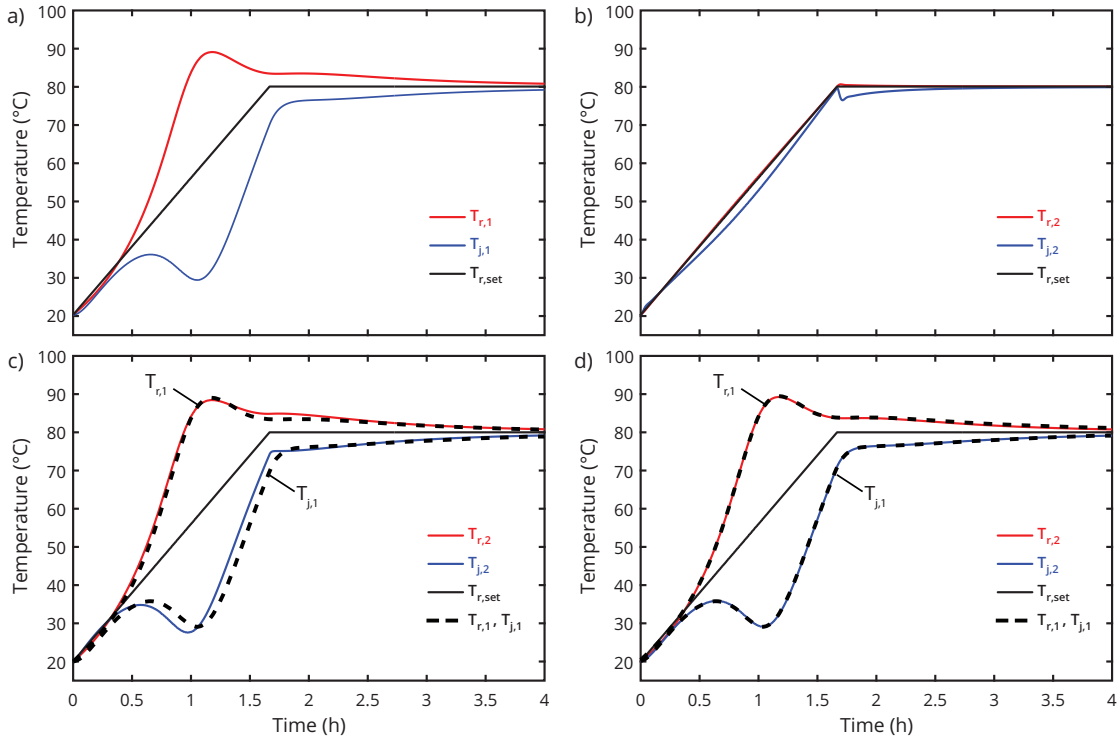
Figure 8.3 – Scenario when the same reaction takes place in a) an industrial reactor with $\tau_{r,1}$, $\tau_{j,1}$ and PID_1, b) a laboratory reactor with $\tau_{r,2}$, $\tau_{j,2}$ and PID_2, c) a laboratory reactor with $\tau_{r,2} = \tau_{r,1}$, $\tau_{j,2} \neq \tau_{j,1}$ and PID_1 instead of PID_2 and d) a laboratory reactor with $\tau_{r,2} = \tau_{r,1}$, $\tau_{j,2} \neq \tau_{j,1}$, PID_2 and $T_{j,set2}$ adjusted with PID_1 (equations 8.17 and 8.19). In the cases (A) and (D) both reactors have exactly the same thermal behaviour with $T_r = T_{r,1} = T_{r,2}$ and $T_j = T_{j,1} = T_{j,2}$. The parameters used for simulation reactors are given in Tables A.8 and A.7. All data were computed using AKTS-Reaction Calorimetry Software [134].

*The important thing is not to stop
questioning.*

Albert Einstein, 1879 - 1955

References

[1]   V. Ranade. *Computational flow modeling for chemical reactor engineering*. Academic Press, 2002, p. 480.

[2]   G. Donati and R. Paludetto. "Scale up of chemical reactors". In: *Catal. Today* 34.3 (1997), pp. 483–533. DOI: 10.1016/S0920-5861(96)00069-7.

[3]   E. Paul. "Design of reaction systems for specialty organic chemicals". In: *Chem. Eng. Sci.* 43.8 (1988), pp. 1773–1782. DOI: 10.1016/0009-2509(88)87041-6.

[4]   J. Harmsen. "Ideation and Research Stages". In: *Industrial Process Scale-up: A Practical Innovation Guide from Idea to Commercial Implementation*. Elsevier Science, 2013, pp. 15–44. DOI: 10.1016/B978-0-444-62726-1.00003-1.

[5]   T. Laird. "How to minimise scale up difficulties". In: *Chem. Ind. Dig.* (2010).

[6]   US Chemical Safety and Hazard Investigation Board. *Morton International Inc. Runaway Chemical Reaction*. Report. 2000.

[7]   O. Valdes, A. Pineda-Solano, V. Carreto, and S. Mannan. "Scale up of Stirred Batch and Semi-Batch Reactors-Gaps and Limitations of Current Methodologies". In: *9th Global Congress on Process Safety*. (San Antonio, Texas). American Institut of Chemical Engineers, 2013.

[8]   J. Verwijs, H. van den Berg, and K. Westerterp. "Start-up and safeguarding of an industrial adiabatic tubular reactor". In: *Chem. Eng. Sci.* 49.24, Part 2 (1994), pp. 5519–5532. DOI: 10.1016/0009-2509(94)00329-7.

[9]   K. Kidam and M. Hurme. "Analysis of equipment failures as contributors to chemical process accidents". In: *Process Saf. Environ. Prot.* 91.1 (2013), pp. 61–78. DOI: 10.1016/j.psep.2012.02.001.

[10] K. Kidam, M. Hurme, and M. Hassim. "Technical analysis of accident in chemical process industry and lessons learnt". In: *Chem. Eng. Trans.* 19 (2010), pp. 451–456.

References

[11]   P. Amyotte, D. MacDonald, and F. Khan. "An analysis of CSB investigation reports concerning the hierarchy of controls". In: *Process Saf. Prog.* 30.3 (2011), pp. 261–265. DOI: 10.1002/prs.10461.

[12]   G. Caygill, M. Zanfir, and A. Gavriilidis. "Scalable reactor design for pharmaceuticals and fine chemicals production. 1: Potential scale-up obstacles". In: *Org. Process Res. Dev.* 10.3 (2006), pp. 539–552. DOI: 10.1021/op050133a.

[13]   J. Atherton and A. Hall. "Scale-up - How do we get it right first time?" In: *Chemistry Today* 29.4 (2011), pp. 47–49.

[14]   M. Levin. *Pharmaceutical Process Scale-Up*. 3rd ed. CRC Press, 2001, p. 550. DOI: 10.1201/9780824741969.ch8.3.

[15]   E. Paul, V. Atiemo-Obeng, and S. Kresta. *Handbook of Industrial Mixing: Science and Practice*. John Wiley & Sons, 2004, p. 1440. DOI: 10.1002/0471451452.

[16]   L. Block. "Nonparenteral liquids and semisolids". In: *Pharmaceutical Process Scale-Up*. 3rd ed. Informa Healthcare, 2002, pp. 57–94. DOI: 10.1201/9780824741969.ch3.

[17]   M. Zlokarnik. *Scale-up in chemical engineering*. 2nd ed. Weinheim, Germany: Wiley-VCH Verlag GmbH & Co. KGaA, 2006, p. 296. DOI: 10.1002/352760815X.

[18]   M. Mannan, O. Reyes-Valdes, P. Jain, N. Tamim, and M. Ahammad. "The evolution of process safety: current status and future direction". In: *Annu. Rev. Chem. Biomol. Eng.* 7 (2016), pp. 135–162. DOI: 10.1146/annurev-chembioeng-080615-033640.

[19]   Council European Chemical Industry. *Landscape of European Chemical Industry*. Tech. rep. 2014.

[20]   Council European Chemical Industry. *Facts & figures of the European Chemical Industry*. Tech. rep. 2016.

[21]   S. Mathew. "Kinetic Approaches for Faster and Efficient Process Development". In: *Pharmaceutical Process Development*. Royal Society of Chemistry, 2011. Chap. 7, pp. 138–159. DOI: 10.1039/9781849733076-00138.

[22]   J. De Jong and P. Vermeulen. "Determinants of product innovation in small firms a comparison across industries". In: *Int. Small Bus. J.* 24.6 (2006), pp. 587–609. DOI: 10.1177/0266242606069268.

[23]   R. Van Bavel. "The annual digest of industrial R&D". In: *European Commission* 1 (2006).

[24]   A. Milewska and E. Molga. "Safety aspects in modelling and operating of batch and semibatch stirred tank chemical reactors". In: *Chem. Eng. Res. Des.* 88.3 (2010), pp. 304–319. DOI: 10.1016/j.cherd.2009.10.014.

[25]   S. Hoffenson, A. Dagman, and R. Söderberg. "Tolerance optimisation considering economic and environmental sustainability". In: *J. Eng. Des.* 25.10-12 (2014), pp. 367–390. DOI: 10.1080/09544828.2014.994481.

[26]   K. Ramani et al. "Integrated sustainable life cycle design: A review". In: *J. Mech. Des.* 132.9 (2010). 10.1115/1.4002308, pp. 091004–091004. DOI: 10.1115/1.4002308.

[27]   G. Vogel. "Process Development, 1. Fundamentals and Standard Course". In: *Ullmann's Encyclopedia of Industrial Chemistry*. Weinheim, Germany: Wiley-VCH Verlag GmbH & Co. KGaA, 2000, pp. 137–159. DOI: 10.1002/14356007.b04_437.pub2.

[28]   P. Bratley, B. Fox, and L. Schrage. *A guide to simulation*. Springer Science & Business Media, 1987, p. 397. DOI: 10.1007/978-1-4419-8724-2.

[29]   F. Neelamkavil. *Computer simulation and modelling*. John Wiley & Sons, 1987, p. 324. DOI: 10.1057/jors.1987.181.

[30]   F. Stoessel. *Thermal safety of chemical processes: Risk assessment and process design*. Weinheim, Germany: Wiley-VCH Verlag GmbH & Co. KGaA, 2008, p. 393. DOI: 10.1002/9783527621606.

[31]   J. Ingham, I. Dunn, E. Heinzle, J. Prenosil, and J. Snape. *Chemical engineering dynamics: An introduction to modelling and computer simulation*. Weinheim, Germany: Wiley-VCH Verlag GmbH & Co. KGaA, 2008, p. 640.

[32]   S. Copelli et al. "Classification and optimization of potentially runaway processes using topology tools". In: *Comput. Chem. Eng.* 56 (2013), pp. 114–127. DOI: 10.1016/j.compchemeng.2013.05.012.

[33]   J. Almquist, M. Cvijovic, V. Hatzimanikatis, J. Nielsen, and M. Jirstrand. "Kinetic models in industrial biotechnology – Improving cell factory performance". In: *Metab. Eng.* 24 (2014), pp. 38–60. DOI: 10.1016/j.ymben.2014.03.007.

[34]   R. Gani, I. Cameron, A. Lucia, G. Sin, and M. Georgiadis. "Process Systems Engineering, 2. Modeling and Simulation". In: *Ullmann's Encyclopedia of Industrial Chemistry*. Weinheim, Germany: Wiley-VCH Verlag GmbH & Co. KGaA, 2000, pp. 1–54. DOI: 10.1002/14356007.o22_o06.

[35]   G. Franceschini and S. Macchietto. "Model-based design of experiments for parameter precision: State of the art". In: *Chem. Eng. Sci.* 63.19 (2008), pp. 4846–4872. DOI: 10.1016/j.ces.2007.11.034.

References

[36] R. Hoffmann, V. Minkin, and B. Carpenter. "Ockham's razor and chemistry". In: *Hyle* 3 (1997), pp. 3–28.

[37] J. Billeter, Y. Neuhold, L. Simon, G. Puxty, and K. Hungerbühler. "Uncertainties and error propagation in kinetic hard-modelling of spectroscopic data". In: *Chemom. Intell. Lab. Syst.* 93.2 (2008), pp. 120–131. DOI: 10.1016/j.chemolab.2008.05.001.

[38] V. Hessel, S. Hardt, and H. Löwe. "Modeling and Simulation of Micro Reactors (Chapter 2)". In: *Chemical micro process engineering*. Weinheim, Germany: Wiley-VCH Verlag GmbH & Co. KGaA, 2005. Chap. 2, pp. 125–256. DOI: 10.1002/3527603042.ch2a.

[39] D. Gillespie. "Stochastic simulation of chemical kinetics". In: *Annu. Rev. Phys. Chem.* 58 (2007), pp. 35–55. DOI: 10.1146/annurev.physchem.58.032806.104637.

[40] R. Willson and A. Beezer. "A mathematical approach for the calculation of reaction order for common solution phase reactions". In: *Thermochim. Acta* 402.1–2 (2003), pp. 75–80. DOI: 10.1016/S0040-6031(02)00534-8.

[41] D. McQuarrie. "Stochastic approach to chemical kinetics". In: *J. Appl. Probab.* 4.3 (1967), pp. 413–478. DOI: 10.2307/3212214.

[42] T. Ozawa. "Kinetic analysis of derivative curves in thermal analysis". In: *J. Therm. Anal. Calorim.* 2.3 (1970), pp. 301–324. DOI: 10.1007/BF01911411.

[43] M. Brown et al. "Computational aspects of kinetic analysis: part A: the ICTAC kinetics project-data, methods and results". In: *Thermochim. Acta* 355.1 (2000), pp. 125–143. DOI: 10.1016/S0040-6031(00)00443-3.

[44] B. Roduit. *Advanced kinetics-based simulation method*. 2016, p. 136.

[45] B. Roduit et al. "Thermal decomposition of AIBN, Part B: Simulation of SADT value based on DSC results and large scale tests according to conventional and new kinetic merging approach". In: *Thermochim. Acta* 621 (2015), pp. 6–24. DOI: 10.1016/j.tca.2015.06.014.

[46] J. Mira, C. Fernández González, and J. Urreaga. "Two examples of deterministic versus stochastic modeling of chemical reactions". In: *J. Chem. Educ.* 80.12 (2003), p. 1488. DOI: 10.1021/ed080p1488.

[47] E. Radek, J. Chapman, and P. Maini. *A practical guide to stochastic simulations of reaction-diffusion processes*. 2007.

[48] A. Golightly and C. Gillespie. "Simulation of stochastic kinetic models". In: *In Silico Systems Biology*. London, UK: Humana Press, 2013, pp. 169–187. DOI: 10.1007/978-1-62703-450-0_9.

[49] K. Laidler. "Chemical kinetics and the origins of physical chemistry". In: *Arch. Hist. Exact Sci.* 32.1 (1985), pp. 43–75. DOI: 10.1007/BF00327865.

[50] M. Davis and R. Davis. *Fundamentals of chemical reaction engineering*. New York: McGraw-Hill Higher Education, 2012, p. 384.

[51] A. Coker. *Modeling of chemical kinetics and reactor design*. Houston, TX, USA: Gulf Professional Publishing, 2001, p. 1136.

[52] S. Vyazovkin et al. "ICTAC Kinetics Committee recommendations for performing kinetic computations on thermal analysis data". In: *Thermochim. Acta* 520.1–2 (2011), pp. 1–19. DOI: 10.1016/j.tca.2011.03.034.

[53] D. Magde. "Kinetic Measurements". In: *Kirk-Othmer Encyclopedia of Chemical Technology*. John Wiley & Sons, 2000, pp. 1–25. DOI: 10.1002/0471238961. 1109140513010704.a01.pub2.

[54] C. Hansen et al. "Correction for instrument time constant and baseline in determination of reaction kinetics". In: *Int. J. Chem. Kinet.* 43.2 (2011), pp. 53–61. DOI: 10.1002/kin.20530.

[55] M. O'Neill, A. Beezer, J. Tetteh, S. Gaisford, and M. Dhuna. "Application of chemometric analysis to complexity in isothermal calorimetric data". In: *J. Phys. Chem. B* 111.28 (2007), pp. 8145–8149. DOI: 10.1021/jp0700985.

[56] L. Almeida e Sousa et al. "Calorimetric determination of rate constants and enthalpy changes for zero-order reactions". In: *J. Phys. Chem. B* 116.22 (2012), pp. 6356–6360. DOI: 10.1021/jp302933f.

[57] K. Laidler. *Chemical kinetics*. 3rd ed. New York: Harper and Row, 1987, p. 531.

[58] J. van't Hoff. *Études de dynamique chimique*. University of California Libraries, 2012, p. 240.

[59] C. Capellos and B. Bielski. *Kinetic systems: Mathematical description of chemical kinetics in solution*. Krieger Pub Co., 1980, p. 138.

[60] J. Miller and J. Miller. *Statistics and chemometrics for analytical chemistry*. 6th ed. Pearson Education, 2005, p. 296.

[61] M. Adams. *Chemometrics in analytical spectroscopy*. Royal Society of Chemistry, 2004, p. 223. DOI: 10.1039/9781847550484.

[62] W. Ostwald. *Lehrbuch der Allgemeinen Chemie*. Vol. 2. Leipzig: University of California Libraries, 1896, p. 280. DOI: 10.1002/zaac.18970150136.

[63] S. Upadhyay. *Chemical kinetics and reaction dynamics*. London: Springer, 2006, p. 256. DOI: 10.1007/978-1-4020-4547-9.

[64] D. Blackmond. "Reaction Progress Kinetic Analysis: A Powerful Methodology for Mechanistic Studies of Complex Catalytic Reactions". In: *Angew. Chem. Int. Ed.* 44.28 (2005), pp. 4302–4320. DOI: 10.1002/anie.200462544.

References

[65] H. Jakobsen. *Chemical Reactor Modeling: Multiphase Reactive Flows*. 2nd ed. Springer International Publishing, 2014, p. 1535. DOI: 10.1007/978-3-319-05092-8.

[66] H. Fogler. *Elements of Chemical Reaction Engineering*. 5th ed. Prentice Hall, 2016, p. 992.

[67] K. Henkel. "Reactor types and their industrial applications". In: *Ullmann's Encyclopedia of Industrial Chemistry*. Weinheim, Germany: Wiley-VCH Verlag GmbH & Co. KGaA, 2000, pp. 1–49. DOI: 10.1002/14356007.b04_087.pub2.

[68] S. Nanda. *Reactors and fundamentals of reactors design for chemical reaction*. Lecture note. 2008.

[69] R. Felder and R. Rousseau. *Elementary Principles of Chemical Processes*. John Wiley & Sons, 2008, p. 688.

[70] A. de Lavoisier. *Traité élémentaire de chimie*. CreateSpace Independent, 2015, p. 140. DOI: 10.1086/347460.

[71] H. Piekarski. "Calorimetry - an important tool in solution chemistry". In: *Thermochim. Acta* 420.1 (2004), pp. 13–18. DOI: 10.1016/j.tca.2003.09.035.

[72] O. Ubrich. "Improving safety and productivity of isothermal semi-batch reactors by modulating the feed rate". Thesis. École Polytechnique Fédérale De Lausanne, 2000.

[73] B. Massey and J. Ward-Smith. *Mechanics of Fluids*. 7th ed. Taylor & Francis, 1998, p. 744.

[74] P. Novak, V. Guinot, A. Jeffrey, and D. Reeve. *Hydraulic modelling – An introduction: Principles, methods and applications*. CRC Press, 2010, p. 616.

[75] M. Usman. *Comprehensive dictionary of chemical engineering*. lulu.com, 2015, p. 588.

[76] L. Albright. *Albright's chemical engineering handbook*. Taylor & Francis, 2008, p. 1928.

[77] Ekato Ruehr- und Mischtechnik GmbH. *Handbook of Mixing Technology*. 2000.

[78] Z. Lazic. *Design of experiments in chemical engineering: A practical guide*. John Wiley & Sons, 2006, p. 620. DOI: 10.1002/3527604162.

[79] W. Tinsson. *Plans d'expérience: constructions et analyses statistiques*. Vol. 67. Springer Science & Business Media, 2010, p. 532. DOI: 10.1007/978-3-642-11472-4.

[80] O. Vasseur, A. Azarian, V. Jolivet, and P. Bourdon. "Capability of high intrinsic quality Space Filling Design for global sensitivity analysis and metamodelling of interference optical systems". In: *Chemom. Intell. Lab. Syst.* 113 (2012), pp. 10–18. DOI: 10.1016/j.chemolab.2011.05.008.

[81] P. Qian, M. Ai, and C. Wu. "Construction of nested space-filling designs". In: *Ann. Stat.* (2009), pp. 3616–3643. DOI: 10.1214/09-AOS690.

[82] J. Santiago, M. Claeys-Bruno, and M. Sergent. "Construction of space-filling designs using WSP algorithm for high dimensional spaces". In: *Chemom. Intell. Lab. Syst.* 113 (2012), pp. 26–31. DOI: 10.1016/j.chemolab.2013.11.009.

[83] J. Franco, O. Vasseur, B. Corre, and M. Sergent. "Minimum Spanning Tree: A new approach to assess the quality of the design of computer experiments". In: *Chemom. Intell. Lab. Syst.* 97.2 (2009), pp. 164–169. DOI: 10.1016/j.chemolab. 2009.03.011.

[84] S. Zaglauer. "Bayesian design of experiments for nonlinear dynamic system identification". In: *Proceedings of the 5th International ICST Conference on Simulation Tools and Techniques*. Institute for Computer Sciences, Social-Informatics and Telecommunications Engineering, 2012, pp. 85–92. DOI: 10.4108/icst.simutools.2012.247734.

[85] S. Boyd and L. Vandenberghe. *Convex optimization*. Cambridge University Press, 2004, p. 727. DOI: 10.2277/0521833787.

[86] M. Sergent. "Contribution de la Méthodologie de la Recherche Expérimentale à l'élaboration de matrices uniformes: Application aux effets de solvants et de substituants". Thesis. Université Paul Cézanne (Aix-Marseille), 1989.

[87] K. Madsen, H. Nielsen, and O. Tingleff. *Methods for Non-Linear Least Squares Problems*. Lecture note. Informatics and Mathematical Modelling, Technical University of Denmark, 2004.

[88] H. Gavin. *The Levenberg-Marquardt method for nonlinear least squares curve-fitting problems*. Report. 2016.

[89] H. Banks, M. Davidian, J. Samuels, and K. Sutton. "An inverse problem statistical methodology summary". In: *Mathematical and Statistical Estimation Approaches in Epidemiology*. Springer, Netherlands, 2009, pp. 249–302. DOI: 10.1007/978-90-481-2313-1_11.

[90] G. Casella and R. Berger. *Statistical Inference (Duxbury Advanced Series in Statistics and Decision Sciences)*. Thomson Learning, Pacific Grove, CA, 2002, p. 660.

[91] G. Seber and C. Wild. *Nonlinear Regression*. New York: John Wiley & Sons, 1989, p. 768. DOI: 10.1002/0471725315.

[92] A. Childers. "Parameter identification and the Design of Experiments for continuous non-linear dynamical systems". Thesis. Virginia Polytechnic Institute and State University, 2009.

References

[93] F. Anscombe. "Graphs in statistical analysis". In: *Am. Stat.* 27.1 (1973), pp. 17–21. DOI: 10.2307/2682899.

[94] K. A. P. McLean and K. B. McAuley. "Mathematical modelling of chemical processes—obtaining the best model predictions and parameter estimates using identifiability and estimability procedures". In: *Can. J. Chem. Eng.* 90.2 (2012), pp. 351–366. DOI: 10.1002/cjce.20660.

[95] R. Berk. *Statistical learning from a regression perspective*. New York: Springer, 2008, p. 360. DOI: 10.1007/978-0-387-77501-2.

[96] S. Konishi. *Introduction to multivariate analysis: Linear and nonlinear modeling*. Taylor & Francis, 2014, p. 338.

[97] G. Box and N. Draper. *Empirical model-building and response surfaces*. Vol. 424. Weinheim, Germany: Wiley-VCH Verlag GmbH & Co. KGaA, 1987, p. 688.

[98] P. Flom. *What is the meaning of "All models are wrong, but some are useful"*. https://goo.gl/FGC4jB. Accessed 02 March 2016.

[99] P. Velleman. "Truth, damn truth, and statistics". In: *J. Stat. Educ.* 16.2 (2008), pp. 1–14.

[100] N. Baati. "Predictive Models for Thermal Stability and Explosive Properties of Chemicals from Molecular Structure". Thesis. École Polytechnique Fédérale De Lausanne, 2016.

[101] R. Kohavi. "A study of cross-validation and bootstrap for accuracy estimation and model selection". In: *Ijcai*. Vol. 14. 1995, pp. 1137–1145.

[102] D. Wolpert. "Stacked generalization". In: *Neural Netw.* 5.2 (1992), pp. 241–259. DOI: 10.1016/S0893-6080(05)80023-1.

[103] J. De Leeuw, E. Meijer, and H. Goldstein. *Handbook of multilevel analysis*. New York: Springer Science & Business Media, 2008, p. 494. DOI: 10.1007/978-0-387-73186-5.

[104] J. Rouquerol and W. Zielenkiewicz. "Suggested practice for classification of calorimeters". In: *Thermochim. Acta* 109.1 (1986), pp. 121–137. DOI: 10.1016/0040-6031(86)85014-6.

[105] D. Haynie. *Biological thermodynamics.* Cambridge University Press, 2001, p. 438. DOI: 10.1017/CBO9780511802690.

[106] T. Lodwig and W. Smeaton. "The ice calorimeter of Lavoisier and Laplace and some of its critics". In: *Ann. Sci.* 31.1 (1974), pp. 1–18. DOI: 10.1080/00033797400200101.

[107] H. Callendar. *Calorimetry*. https://goo.gl/xxLCkH. Accessed 16 February 2016. 1910.

210

[108]   R. Landau. "Expanding the role of reaction calorimetry". In: *Thermochim. Acta* 289.2 (1996), pp. 101–126. DOI: 10.1016/S0040-6031(96)03081-X.

[109]   S. Gaisford. "Evaluation of analytical instrumentation. Part XXV: Differential Scanning Calorimetry". In: *Anal. Methods* 7.4 (2015), pp. 1240–1248. DOI: 10.1039/C4AY90087A.

[110]   G. Fonseca, M. Dubé, and A. Penlidis. "A critical overview of sensors for monitoring polymerizations". In: *Macromol. React. Eng.* 3.7 (2009), pp. 327–373. DOI: 10.1002/mren.200900024.

[111]   K. Westerterp and E. Molga. "Safety and runaway prevention in batch and semibatch reactors—a review". In: *Chem. Eng. Res. Des.* 84.7 (2006), pp. 543–552. DOI: 10.1205/cherd.05221.

[112]   S. Warrington and G. Höhne. "Thermal Analysis and Calorimetry". In: *Ullmann's Encyclopedia of Industrial Chemistry*. Weinheim, Germany: Wiley-VCH Verlag GmbH and Co. KGaA, 2008, pp. 415–439. DOI: 10.1002/14356007.b06_001.pub3.

[113]   P. Haines. *Thermal methods of analysis: Principles, applications and problems*. Netherlands: Springer, 2012, p. 286. DOI: 10.1007/978-94-011-1324-3.

[114]   M. Brown and P. Gallagher. *Handbook of thermal analysis and calorimetry: recent advances, techniques and applications*. Vol. 5. Elsevier, 2011, p. 780.

[115]   C. Schick, D. Lexa, and L. Leibowitz. "Differential Scanning Calorimetry and Differential Thermal Analysis". In: *Characterization of Materials*. John Wiley & Sons, Inc., 2012, pp. 483–495. DOI: 10.1002/0471266965.com030.pub2.

[116]   M. O'Neill, A. Beezer, J. Mitchell, J. Orchard, and J. Connor. "Determination of Michaelis–Menten parameters obtained from isothermal flow calorimetric data". In: *Thermochim. Acta* 417.2 (2004), pp. 187–192. DOI: 10.1016/j.tca.2003.07.019.

[117]   G. Höhne, W. Hemminger, and H. Flammersheim. *Differential scanning calorimetry*. Springer, 2003, p. 298. DOI: 10.1007/978-3-662-06710-9.

[118]   C. Schick. "Differential scanning calorimetry (DSC) of semicrystalline polymers". In: *Anal. Bioanal.Chem.* 395.6 (2009), pp. 1589–1611. DOI: 10.1007/s00216-009-3169-y.

[119]   A. Zogg, F. Stoessel, U. Fischer, and K. Hungerbühler. "Isothermal reaction calorimetry as a tool for kinetic analysis". In: *Thermochim. Acta* 419.1–2 (2004), pp. 1–17. DOI: 10.1016/j.tca.2004.01.015.

[120]   L. Karlsen and J. Villadsen. "Isothermal reaction calorimeters - I. A literature review". In: *Chem. Eng. Sci.* 42.5 (1987), pp. 1153–1164. DOI: 10.1016/0009-2509(87)80065-9.

References

[121]   Mettler-Toledo GmbH. *iControl RC1e Software*. Version 5.0.21. Accessed 1 Frebuary 2016.

[122]   R. Carloff, A. Pross, and K. Reichert. "Temperature oscillation calorimetry in stirred tank reactors with variable heat transfer". In: *Chem. Eng. Technol.* 17.6 (1994), pp. 406–413. DOI: 10.1002/ceat.270170608.

[123]   S. Krämer and R. Gesthuisen. "Simultaneous estimation of the heat of reaction and the heat transfer coefficient by calorimetry: estimation problems due to model simplification and high jacket flow rates - theoretical development". In: *Chem. Eng. Sci.* 60.15 (2005), pp. 4233–4248. DOI: 10.1016/j.ces.2005.02.060.

[124]   R. Gesthuisen, S. Krämer, G. Niggemann, J. Leiza, and J. Asua. "Determining the best reaction calorimetry technique: theoretical development". In: *Comput. Chem. Eng.* 29.2 (2005), pp. 349–365. DOI: 10.1016/j.compchemeng.2004.10.009.

[125]   J. Asua. "Emulsion polymerization: from fundamental mechanisms to process developments". In: *J. Polym. Sci., Part A: Polym. Chem.* 42.5 (2004), pp. 1025–1041. DOI: 10.1002/pola.11096.

[126]   S. Copelli, M. Derudi, R. Rota, A. Lunghi, and C. Pasturenzi. "Experimental design of topological curves to safely optimize highly exothermic complex reacting systems". In: *Ind. Eng. Chem. Res.* 50.17 (2011), pp. 9910–9917. DOI: 10.1021/ie200017f.

[127]   S. Copelli et al. "Synthesis of 4-Chloro-3-nitrobenzotrifluoride: Industrial thermal runaway simulation due to cooling system failure". In: *Process Saf. Environ. Prot.* 92.6 (2014), pp. 659–668. DOI: 10.1016/j.psep.2013.11.006.

[128]   F. Maestri et al. "Simple procedure for optimally scaling-up fine chemical processes. I. Practical tools". In: *Ind. Eng. Chem. Res.* 48.3 (2009), pp. 1307–1315. DOI: 10.1021/ie800465d.

[129]   C. Guinand, M. Dabros, B. Roduit, T. Meyer, and F. Stoessel. "Optimization of chemical reactor feed by simulations based on a kinetic approach". In: *Chimia* 68.10 (2014), pp. 746–747. DOI: 10.2533/chimia.2014.746.

[130]   O. Levenspiel. *Chemical reaction engineering*. 3rd ed. New York: John Wiley & Sons, 1999, p. 688. DOI: 10.1002/aic.690190143.

[131]   R. Chaudhari, A. Seayad, and S. Jayasree. "Kinetic modeling of homogeneous catalytic processes". In: *Catal. Today* 66.2 (2001), pp. 371–380. DOI: 10.1016/S0920-5861(00)00633-7.

[132] B. Roduit et al. "Determination of thermal hazard from DSC measurements. Investigation of self-accelerating decomposition temperature (SADT) of AIBN". In: *J. Therm. Anal. Calorim.* 117.3 (2014), pp. 1017–1026. DOI: 10.1007/s10973-014-3903-3.

[133] B. Hartmann, T. Ebert, and O. Nelles. "Model-based design of experiments based on local model networks for nonlinear processes with low noise levels". In: *Proceedings of the 2011 American Control Conference*. IEEE, 2011, pp. 5306–5311.

[134] AKTS SA. *AKTS-Reaction Calorimetry Software version 4.4*. http://www.akts.com. Accessed 10 February 2017.

[135] MathWorks. *Matlab Version R2015a (8.5.0.197613)*. http://www.mathworks.com. Accessed 28 August 2016.

[136] Y. Duh, C. Hsu, C. Kao, and S. Yu. "Applications of reaction calorimetry in reaction kinetics and thermal hazard evaluation". In: *Thermochim. Acta* 285.1 (1996), pp. 67–79. DOI: 10.1016/0040-6031(96)02899-7.

[137] R. Widell and H. Karlsson. "Autocatalytic behaviour in esterification between anhydrides and alcohols". In: *Thermochim. Acta* 447.1 (2006), pp. 57–63. DOI: 10.1016/j.tca.2006.05.003.

[138] L. Balland, N. Mouhab, J. Cosmao, and L. Estel. "Kinetic parameter estimation of solvent-free reactions: application to esterification of acetic anhydride by methanol". In: *Chem. Eng. Process. Process Intensif.* 41.5 (2002), pp. 395–402. DOI: 10.1016/S0255-2701(01)00164-7.

[139] L. Friedel and G. Wehmeier. "Modelling of the vented methanol/acetic anhydride runaway reaction using SAFIRE". In: *J. Loss Prev. Process Ind.* 4.2 (1991), pp. 110–119. DOI: 10.1016/0950-4230(91)80015-M.

[140] S. Bohm, G. Hessel, H. Kryk, H. Prasser, and W. Schmitt. *Auto-catalytic effect of acetic acid on the kinetics of the methanol/acetic anhydride esterification.* Report. Institute of Safety Research, 2005.

[141] G. Froment, K. Bischoff, and J. De Wilde. *Chemical reactor analysis and design*. Vol. 2. New York, USA: John Wiley & Sons, 1990, p. 900. DOI: 10.1002/cite.330630205.

[142] National Institute of Standards and Technology (NIST). http://webbook.nist.gov/chemistry. Accessed 02 March 2016.

[143] J. Johnson and K. Omland. "Model selection in ecology and evolution". In: *Trends Ecol. Evol.* 19.2 (2004), pp. 101–108. DOI: 10.1016/j.tree.2003.10.013.

References

[144] T. Bieringer, S. Buchholz, and N. Kockmann. "Future production concepts in the chemical industry: modular - small-scale - continuous". In: *Chem. Eng. Technol.* 36.6 (2013), pp. 900–910. DOI: 10.1002/ceat.201200631.

[145] P. Nolan and J. Barton. "Some lessons from thermal-runaway incidents". In: *J. Hazard. Mater.* 14.2 (1987), pp. 233–239. DOI: 10.1016/0304-3894(87)87015-2.

[146] G. Vogel. *Process development: from the initial idea to the chemical production plant.* Weinheim, Germany: Wiley-VCH Verlag GmbH & Co. KGaA, 2006, p. 492. DOI: 10.1002/3527605878.

[147] W. Dermaut. "Process safety and reaction hazard assessment". In: *Chemical engineering in the pharmaceutical industry: R&D to manufacturing.* Weinheim, Germany: Wiley-VCH Verlag GmbH & Co. KGaA, 2010, pp. 155–182. DOI: 10.1002/9780470882221.ch11.

[148] J. Rose. "Heat-transfer coefficients, Wilson plots and accuracy of thermal measurements". In: *Exp. Therm Fluid Sci.* 28.2–3 (2004), pp. 77–86. DOI: 10.1016/S0894-1777(03)00025-6.

[149] J. Fernandez-Seara, F. Uhía, J. Sieres, and A. Campo. "A general review of the Wilson plot method and its modifications to determine convection coefficients in heat exchange devices". In: *Appl. Therm. Eng.* 27.17 (2007), pp. 2745–2757. DOI: 10.1016/j.applthermaleng.2007.04.004.

[150] E. Kumpinsky. "A method to determine heat-transfer coefficients in a heat-flow reaction calorimeter". In: *Thermochim. Acta* 289.2 (1996), pp. 351–366. DOI: 10.1016/S0040-6031(96)03007-9.

[151] F. Caccavale, M. Iamarino, F. Pierri, and V. Tufano. *Control and monitoring of chemical batch reactors.* Springer Science & Business Media, 2010, p. 203. DOI: 10.1007/978-0-85729-195-0.

[152] R. Luus and O. Okongwu. "Towards practical optimal control of batch reactors". In: *Chem. Eng. J.* 75.1 (1999), pp. 1–9. DOI: 10.1016/S1385-8947(99)00019-4.

[153] B. Ogunnaike and W. Ray. *Process dynamics, modeling, and control.* United Kingdom: Oxford University Press, 1994, p. 260. DOI: 10.1002/aic.690440523.

[154] A. Datta, M. Ho, and S. Bhattacharyya. *Structure and synthesis of PID controllers.* Springer London, 2013, p. 252. DOI: 10.1007/978-1-4471-3651-4.

[155] B. Zufferey. "Scale-down approach: chemical process optimisation using reaction calorimetry for the experimental simulation of industrial reactors dynamics". Thesis. École Polytechnique Fédérale De Lausanne, 2006.

[156] R. Chylla and D. Haase. "Temperature control of semibatch polymerization reactors". In: *Comput. Chem. Eng.* 17.3 (1993), pp. 257–264. DOI: 10.1016/0098-1354(93)80019-J.

[157] A. Coker. "Appendix C - Physical Properties of Liquids and Gases". In: *Ludwig's Applied Process Design for Chemical and Petrochemical Plants (Fourth Edition)*. Boston: Gulf Professional Publishing, 2010, pp. 757–792. DOI: 10.1016/B978-0-7506-8366-1.10026-X.

[158] M. Johnson and M. Moradi. *PID control*. Springer, 2005, p. 544. DOI: 10.1007/1-84628-148-2.

[159] British Standards Institution. *BS EN 10088-1 Stainless steels - Part 1: List of stainless steels.* European Standard. 2005.

[160] M. Dupré and J. Le Coze. *Réactions à risque : regards croisés sur la sécurité dans la chimie*. Lavoisier, 2014, p. 192.

[161] US Chemical Safety and Hazard Investigation Board. *Synthron Chemical Explosion*. Report. 2007.

[162] US Chemical Safety and Hazard Investigation Board. *T2 Laboratories, Inc. Runaway Reaction*. Report. 2009.

[163] Dictionary.com. http:\www.dictionary.com. Accessed 29 September 2016.

[164] D. C. Hendershot. "A summary of inherently safer technology". In: *Process Safety Progress* 29.4 (2010), pp. 389–392. DOI: 10.1002/prs.10395.

[165] T. Kletz. "What you don't have, can't leak". In: *Chem. Ind. (London)* 6 (1978), pp. 287–292.

[166] T. Kletz and P. Amyotte. *Process plants: A handbook for inherently safer design*. CRC Press, 2010, p. 384. DOI: 10.1002/prs.10403.

[167] R. Gygax. "Chemical reaction engineering for safety". In: *Chem. Eng. Sci.* 43.8 (1988), pp. 1759–1771. DOI: 10.1016/0009-2509(88)87040-4.

[168] O. Ubrich, B. Srinivasan, P. Lerena, D. Bonvin, and F. Stoessel. "Optimal feed profile for a second order reaction in a semi-batch reactor under safety constraints: Experimental study". In: *J. Loss Prev. Process Ind.* 12.6 (1999), pp. 485–493. DOI: 10.1016/S0950-4230(99)00017-0.

[169] E. Serra, R. Nomen, and J. Sempere. "Maximum temperature attainable by runaway of synthesis reaction in semibatch processes". In: *J. Loss Prev. Process Ind.* 10.4 (1997), pp. 211–215. DOI: 10.1016/S0950-4230(97)00004-1.

[170] O. Ubrich, B. Srinivasan, P. Lerena, D. Bonvin, and F. Stoessel. "The use of calorimetry for on-line optimisation of isothermal semi-batch reactors". In: *Chem. Eng. Sci.* 56.17 (2001), pp. 5147–5156. DOI: 10.1016/S0009-2509(01)00183-X.

[171] K. Westerterp and E. Molga. "No More Runaways in Fine Chemical Reactors". In: *Ind. Eng. Chem. Res.* 43.16 (2004), pp. 4585–4594. DOI: 10.1021/ie030725m.

References

[172] K. Westerterp, M. Lewak, and E. Molga. "Boundary diagrams safety criterion for liquid phase homogeneous semibatch reactors". In: *Ind. Eng. Chem. Res.* 53.14 (2014), pp. 5778–5791. DOI: 10.1021/ie500028u.

[173] S. Copelli et al. "Emulsion polymerization of vinyl acetate: safe optimization of a hazardous complex process". In: *J. Hazard. Mater.* 192.1 (2011), pp. 8–17. DOI: 10.1016/j.jhazmat.2011.04.066.

[174] F. Maestri and R. Rota. "Kinetic-Free Safe Operation of Fine Chemical Runaway Reactions: A General Criterion". In: *Ind. Eng. Chem. Res.* 55.4 (2016), pp. 925–933. DOI: 10.1021/acs.iecr.5b04234.

[175] F. Maestri and R. Rota. "Kinetic-Free Safe Optimization of a Semibatch Runaway Reaction: Nitration of 4-Chloro Benzotrifluoride". In: *Ind. Eng. Chem. Res.* 55.50 (2016), pp. 12786–12794. DOI: 10.1021/acs.iecr.6b03590.

[176] P. Lerena, W. Wehner, H. Weber, and F. Stoessel. "Assessment of hazards linked to accumulation in semi-batch reactors". In: *Thermochim. Acta* 289.2 (1996), pp. 127–142. DOI: 10.1016/S0040-6031(96)03024-9.

[177] G. Maria and E. Heinzle. "Kinetic system identification by using short-cut techniques in early safety assessment of chemical processes". In: *J. Loss Prev. Process Ind.* 11.3 (1998), pp. 187–206. DOI: 10.1016/S0950-4230(97)00050-8.

[178] C. Venkateswarlu. "Perspectives of Process Systems Engineering". In: *Austin Chem Eng.* 3.1 (2016), p. 1022.

[179] F. McConville. *The pilot plant real book: A unique handbook for the chemical process industry*. 2nd ed. Worcester, MA: FXM Engineering and Design, 2002, p. 320. DOI: 10.1021/ed080p1260.

[180] M. Davis and S. Viswanath. "Heat transfer based scale-down of chemical reactions". In: *Org. Process Res. Dev.* 16.8 (2012), pp. 1360–1370. DOI: 10.1021/op300036p.

[181] United Nations. *UN Recommendations on the Transport of Dangerous Goods: Manual of tests and criteria*. 5th ed. New York and Geneva, 2009, pp. 297–316.

[182] Asahi Glassplant Inc. *Reaction Unit, Pilot-plant*. http://www.asahiglassplant.com/products/reactor/pilot-plant-en/. Accessed 30 January 2017.

A

Tables

A.1 Reaction Kinetic Investigation: Simulated example

Table A.1 – The retrieved parameters with their respective deviation to the real value (in percent) available in Table 4.3.

Reaction 1	units	value	errors (%)
$k_{0,1}$	$\left(g^{0.5} \cdot s^{-1} \cdot mol^{-0.5}\right)$	$9.95 \cdot 10^7$	-0.53
$E_{a,1}$	$\left(J \cdot mol^{-1}\right)$	64991	-0.01
$\Delta_r H_1$	$\left(J \cdot mol^{-1}\right)$	-50	0.01
Orders	$(-)$	$a1 = 1$	0.00
		$b1 = 0.5$	0.00
Reaction 2			
$k_{0,2}$	$\left(g^{0.2} \cdot s^{-1} \cdot mol^{-0.2}\right)$	$1 \cdot 10^9$	0.20
$E_{a,2}$	$\left(J \cdot mol^{-1}\right)$	75006	0.01
$\Delta_r H_2$	$\left(J \cdot mol^{-1}\right)$	-54	-0.01
Orders	$(-)$	$b2 = 1.195$	-0.42
		$c2 = 1.005$	0.50

Table A.2 – Correlation matrix generated after the regression on three simulated DSC experiments (Exp. 1-3). The regression results are: $RMSE = 0.03 mW \cdot g^{-1}$ and $R^2 = 1$; Number of correlated parameter relationships (red) = 15 (reaction 1: 5; reaction 2: 10) over 45.

	$k_{0,1}$	$E_{a,1}$	$\Delta_r H_1$	$m_{A,1}$	$b1$	$k_{0,2}$	$E_{a,2}$	$\Delta_r H_2$	$b2$	$c2$
$k_{0,1}$	1	0.99	-0.33	0.9	0.59	0.98	0.79	-0.03	0.42	-0.39
$E_{a,1}$	0.99	1	-0.43	0.84	0.54	0.97	0.76	-0.02	0.45	-0.41
$\Delta_r H_1$	-0.33	-0.43	1	-0.08	-0.09	-0.34	-0.19	-0.09	-0.23	0.22
$a1$	0.9	0.84	-0.08	1	0.33	0.88	0.72	-0.05	0.38	-0.35
$b1$	0.59	0.54	-0.09	0.33	1	0.57	0.45	0.00	0.29	-0.27
$k_{0,2}$	0.98	0.97	-0.34	0.88	0.57	1	0.78	-0.02	0.47	-0.44
$E_{a,2}$	0.79	0.76	-0.19	0.72	0.45	0.78	1	-0.53	0.09	-0.10
$\Delta_r H_2$	-0.03	-0.02	-0.09	-0.05	0.00	-0.02	-0.53	1	0.20	-0.13
$b2$	0.42	0.45	-0.23	0.38	0.29	0.47	0.09	0.20	1	-1
$c2$	-0.39	-0.41	0.22	-0.35	-0.27	-0.44	-0.10	-0.13	-1	1

Table A.3 – Correlation matrix generated after the regression on six simulated RC experiments (Regression $RMSE = 0.69W$; $R^2 = 0.9398$; Number of correlated parameter relationships (red) = 15 (reaction 1: 3; reaction 2: 12)).

	$k_{0,1}$	$E_{a,1}$	$\Delta_r H_2$	$a1$	$b1$	$k_{0,2}$	$E_{a,2}$	$\Delta_r H_2$	$b2$	$c2$
$k_{0,1}$	1	0.99	-0.41	-0.95	0.21	-0.04	0.19	-0.25	0.62	-0.71
$E_{a,1}$	0.99	1	-0.37	-0.93	0.09	-0.06	0.26	-0.32	0.64	-0.76
$\Delta_r H_1$	-0.41	-0.37	1	0.41	-0.17	0.04	0	0.03	-0.25	0.23
$a1$	-0.95	-0.93	0.41	1	-0.42	-0.06	0.08	-0.02	-0.51	0.5
$b1$	0.21	0.09	-0.17	-0.42	1	0.27	-0.72	0.7	-0.17	0.39
$k_{0,2}$	-0.04	-0.06	0.04	-0.06	0.27	1	-0.25	0.43	-0.1	0.17
$E_{a,2}$	0.19	0.26	0	0.08	-0.72	-0.25	1	-0.95	0.38	-0.8
$\Delta_r H_2$	-0.25	-0.32	0.03	-0.02	0.7	0.43	-0.95	1	-0.38	0.82
$b2$	0.62	0.64	-0.25	-0.51	-0.17	-0.1	0.38	-0.38	1	-0.7
$c2$	-0.71	-0.76	0.23	0.5	0.39	0.17	-0.8	0.82	-0.7	1

Table A.4 – Correlation matrix generated after the regression on three DSC and six RC simulated experiments (Regression $RMSE = 0.22W$; $R^2 = 0.9939$; Number of correlated parameter relationships (red) = 9 (reaction 1: 1; reaction 2: 8)).

	$k_{0,1}$	$E_{a,1}$	$\Delta_r H_2$	$a1$	$b1$	$k_{0,2}$	$E_{a,2}$	$\Delta_r H_2$	$b2$	$c2$
$k_{0,1}$	1	0.83	0.01	0.37	0.28	-0.26	-0.17	0.06	0.77	-0.83
$E_{a,1}$	0.83	1	-0.09	-0.01	0.02	-0.31	-0.21	0.1	0.65	-0.7
$\Delta_r H_1$	0.01	-0.09	1	0.23	0.07	0.15	0.15	-0.12	-0.05	0.02
$a1$	0.37	-0.01	0.23	1	-0.29	0.01	0.02	-0.04	0.26	-0.29
$b1$	0.28	0.02	0.07	-0.29	1	-0.05	-0.03	0	0.23	-0.25
$k_{0,2}$	-0.26	-0.31	0.15	0.01	-0.05	1	0.9	-0.67	-0.45	0.34
$E_{a,2}$	-0.17	-0.21	0.15	0.02	-0.03	0.9	1	-0.81	-0.44	0.16
$\Delta_r H_2$	0.06	0.1	-0.12	-0.04	0	-0.67	-0.81	1	0.29	-0.01
$b2$	0.77	0.65	-0.05	0.26	0.23	-0.45	-0.44	0.29	1	-0.9
$c2$	-0.83	-0.7	0.02	-0.29	-0.25	0.34	0.16	-0.01	-0.9	1

Table A.5 – Design of Experiment based on Space Filling methods for the generation of experiment simulations to apply the Reactor Dynamic Investigation over an industrial reactor model. Statistical parameters $MinDist$ and Cov are compared before and after the application of Space Filling methods (section 2.3).

Step	200kg		334 kg		412 kg	
1	0.16	0.84	0.87	0.74	0.19	0.51
2	0.64	0.21	0.47	0.87	0.67	0.75
3	0.58	0.99	0.19	0.56	0.93	0.15
4	0.79	0.62	0.92	0.31	0.03	0.11
5	0.26	0.01	0.34	0.17	0.49	0.03
6	0.28	0.43	0.06	0.99	0.27	0.95
	before	after	before	after	before	after
$MinDist$	0.42	0.00	0.42	0.00	0.44	0.00
Cov	**0.71**	**10.66**	**0.71**	**10.58**	**0.69**	**10.60**

A.2 Risk assessment and optimization

Table A.6 – Initial conditions for the definition of feed profile strategy considering the simulated example 6.16. * is the fed reactant.

	Temperature	MAT	A*	B	C	D	E	F
Units	$(°C)$	$(°C)$			(mol)			
Value	50	120	250	300	0	250	0	0

A.3 Conclusion & Perspectives

Table A.7 – Reaction kinetic parameters used for the simulations presented in Figure 8.3.

Reaction 1				
	k_0	E_a	$\Delta_r H$	**Orders**
Units	$(mol \cdot g^{-1} \cdot s^{-1})$	$(kJ \cdot mol^{-1})$	$(kJ \cdot mol^{-1})$	$(-)$
Value	$1 \cdot 10^7$	50	-100	$m_A = 1$ $m_B = 1$

Table A.8 – Parameters used for the simulations presented in Figure 8.3.

	m_r	U	A	τ_r	τ_j	K
Experiments	(kg)	$(W \cdot m^{-2} \cdot K^{-1})$	(m^2)	(s)	(s)	$(-)$
A	900	600	1.8	3677	300	1
B	0.9	180	0.0576	383	50	7
C	0.9	180	0.006	3677	50	1
D	0.9	180	0.006	3677	50	7

B

Copyright Credits

Chapter B: Copyright Credits

- Figure 2.13 reproduced from:

J. Santiago, M. Claeys-Bruno, and M. Sergent. "Construction of space-filling 1000 designs using WSP algorithm for high dimensional spaces". In: Chemom. Intell. Lab. Syst. 113 (2012), pp. 26–31. DOI: j.chemolab.2011.06.003.

Figure 1. Empirical repartition of different space-filling designs using *MinDist* and *Cov* criteria. The desirable designs have a high value of *MinDist*, corresponding to sufficiently distant points, and a low value of *Cov*, corresponding to a regular distribution.

Copyright ©2012 Elsevier.

- Figure 2.3 reproduced from:

B. Roduit. "Advanced kinetics-based simulation method". 2016, p. 136.

Figure 3.1 Relationship of the reaction progress α vs time for decelerating, autocatalytic and accelerating reaction models.

Copyright ©2016 AKTS.

- Figures 5.3, 5.4, 5.8, 5.9, 5.11, 5.15 and 5.17 reproduced from:

C. Guinand, M. Dabros, T. Meyer, F. Stoessel. "Reactor dynamics investigation based on calorimetric data". In: Can. J. Chem. Eng. 95 (2017), pp. 231-240 DOI: 10.1002/cjce.22700.

Copyright ©2016 John Wiley & Sons.

C

Curriculum Vitae

CG

Charles Guinand

Work Address
AKTS AG
TECHNOark 1
CH - 3960 Sierre
http://www.akts.com

Phone: +41 79 289 40 09

Email
charles.guinand@gmail.com

Work email
c.guinand@akts.com
charles.guinand@epfl.ch
charles.guinand@hefr.ch

LinkedIn
www.linkedin.com/in/cguinand

Personal status
29 years old (14/12/1987)

Soft Skills
Sociable
Competitive
Curious
Good listener

Education

2012 - 2017	**Ph.D. student in Chemical Process Safety**
	École Polytechnique Fédérale de Lausanne, EPFL (Switzerland)
2009 - 2011	**Master of Science in Chemical and Biochemical Engineering**
	École Polytechnique Fédérale de Lausanne, EPFL
2006 - 2009	**Bachelor of Science in Chemistry and Chemical Engineering**
	École Polytechnique Fédérale de Lausanne, EPFL
2003 - 2006	**High School Certificate in Sciences**,
	Lycée Denis-de-Rougemont, Neuchâtel (Switzerland)

Work Experience

2016 - 2017	**AKTS AG, Advanced Kinetics & Technology Solutions**
	Sierre, Switzerland
	Thermal process safety and software development
2012 - 2017	**EPFL - Doctoral Assistant**
	Supervised by Prof. F. Stoessel & MER T. Meyer
	Lausanne, Switzerland
	Accumulation in semi-batch reactors for multiple reaction schemes
2012 - 2017	**University of Applied Sciences and Arts Western Switzerland, Haute École d'Ingénierie et d'Architecture Fribourg**
	Lecturer:
	Bachelor 1st : *General Chemistry - Practical works*
	Bachelor 3rd : *Literature research and projects*
	Master 1st : *Chemometrics*
2011 - 2012	**Swiss military service,**
Spring 12	*Thun and Schwarzenburg, Switzerland*
	Electronic War and Driver C1/D1 (5 month)
Fall 11	**AKTS AG, Advanced Kinetics & Technology Solutions,**
	Process safety, simulation of polyvalent cases and software development (6 months)
Spring 11	**Group of Catalytic Reaction Engineering (GGRC), EPFL,**
	Lausanne, Switzerland
	Temperature management of very fast and exothermic reactions in Micro Structured Reactors (5 months)
Spring 11	**Teaching assistant in EPFL,**
	Lausanne, Switzerland
	Introduction to chemical engineering II (Bachelor 4st semester)
	Chemical engineering practice (Bachelor 6st semester)
2009 - 2011	**Swissi PS GmbH, Institute of Process Safety,**
Fall 10	*Basel, Switzerland*
	Analysis of polyvalent case (*5 months*)
2008 - 2009	**Petroplus, Oil refinery,**
Summer 09	*Cressier, Switzerland*
	Analysis of a separation process by distillation (*7 weeks*)
2003 - 2007	**Mandates in graphic design** (websites, pictures, etc.)

Publications

03.16 **Reactor Dynamic Investigation based on Calorimetric Data**
Can. J. Chem. Eng., 95(2),231-240

02.16 **Thermal process safety based on Reaction Kinetics and Reactor Dynamics**
Chem. Eng. Trans., 48

10.14 **Optimization of Chemical Reactor Feed by Simulations Based on a Kinetic Approach**
CHIMIA, *68*(10), 2014, 746-747

04.14 **Kinetic identification and risk assessment based on non-linear fitting of calorimetric data**
10th Global Congress on Process Safety, Proceedings (New Orleans, USA).

Conferences

08.16 **International Confederation for Thermal Analysis and Calorimetry 2016 (ICTAC)**
Oral presentation (Orlando, USA)
Control of process safety based on thermal dynamics of reactor and reaction kinetics

06.16 **15th International Symposium on Loss Prevention and Safety Promotion in the Process Industries**
Oral presentation (Freiburg, Germany)
Thermal process safety based on Reaction Kinetics and Reactor Dynamic

04.16 **41th Annual Meeting of Schweizerische Gesellschaft für Thermoanalyse und Kalorimetrie (STK)**
Oral presentation (Visp, Switzerland)
Thermal process safety based on Reaction Kinetics and Reactor Dynamic

09.15 **10th European Congress of Chemical Engineering (ECCE)**
Key-note presentation (Nice, France)
Reaction Kinetic Investigation and Scale-up evaluation based on calorimetric data

06.15 **40th Annual Meeting of Schweizerische Gesellschaft für Thermoanalyse und Kalorimetrie (STK)**
Oral presentation (Fribourg, Switzerland)
Reactor Dynamic Investigation applied to the Morton case

06.14 **39th Annual Meeting of Schweizerische Gesellschaft für Thermoanalyse und Kalorimetrie (STK)**
Oral presentation (Fribourg, Switzerland)
Feed optimization using kinetic model and scale-down approach

04.14 **10th Global Congress on Process Safety (GCPS)**
Electronic poster presentation and extended abstract (New Orleans, USA).
Kinetic identification and risk assessment based on non-linear fitting of calorimetric data

06.13 **38th Annual Meeting of Schweizerische Gesellschaft für Thermoanalyse und Kalorimetrie (STK)**
Oral presentation (Buchs, Switzerland)
Reaction kinetics investigation using Design Of Experiments and numerical simulation

Posters

08.15 **Summer School of Organic Chemistry (Villars, Switzerland)**
Study of reaction kinetics using Design of Experiments and Numerical Simulation

03.14 **Open doors at l'École d'Ingénieurs et d'Architectes de Fribourg (Switzerland)**
Identification de cinétique chimique et analyse de risque basées sur des données calorimétriques

09.11 **EPFL Master Poster session (Lausanne, Switzerland)**
Temperature management of very fast and exothermic reactions in Micro Structured Reactors

Computer skills

Advanced   Adobe Flash, Illustrator, InDesign and Photoshop
Microsoft Windows and Office Suite, OS
MatLab, Visual Basic Application and AKTS-Thermokinetics

Medium   Berkeley Madonna, ChemDraw, PRO/II

Languages

French   Native language
English   Fluent, ease in conversation and writing
German   Intermediate, long stay in German-speaking Switzerland

Interests

Interactive design (draw, animation, video editing ...)
Running, Crossfit and soccer
Multicultural experiences